PROCEEDINGS

2nd International Conference on Multidisciplinary Breakthroughs and NextGen Technologies

ICMBNT-2026

12 & 13 March , 2026

Organized by

Society for Cyber Intelligent Systems

ISIUS

In Collaborations

UNIVERSITAS UDAYANA

UNIVERSITAS PELITA BANGSA MEGAH

KPR Institute of Engineering and Technology

SRM INSTITUTE OF SCIENCE & TECHNOLOGY
(Deemed to be University u/s 3 of UGC Act, 1956)

MELANGE PUBLICATIONS

Melange Publications
Puducherry-India

PROCEEDINGS OF

2nd International Conference on Multidisciplinary Breakthroughs and NextGen Technologies

(ICMBNT–2026)

(In-person + Virtual)

12th & 13th March, 2026

Organized By

SOCIETY FOR CYBER INTELLIGENT SYSTEMS
(PUDUCHERRY – INDIA)

&

INTERNATIONAL SOCIETY OF INTELLIGENT UNMANNED SYSTEMS
(SOUTH KOREA – JIMBARAN, BALI)

MESSAGE FROM THE RECTOR, UNIVERSITAS UDAYANA

It is with great pride and pleasure that I extend my warm greetings to all distinguished speakers, researchers, academicians, industry leaders, and students participating in the 2nd International Conference on Multidisciplinary Breakthroughs and NextGen Technologies (ICMBNT 2026) hosted at Universitas Udayana, Bali, Indonesia.

Universitas Udayana remains committed to advancing excellence in education, research, and community engagement. Hosting ICMBNT 2026 reflects our dedication to fostering international collaboration and promoting innovative research that addresses global challenges through multidisciplinary approaches.

In an era defined by rapid technological transformation, collaboration across disciplines is essential to generate sustainable and impactful solutions. This conference provides an important platform for the exchange of ideas, presentation of cutting-edge research, and the establishment of meaningful academic and industrial partnerships.

We are honored to welcome distinguished scholars and professionals from various countries to our beautiful island of Bali. We hope that beyond the technical sessions and scholarly discussions, participants will also experience the rich cultural heritage and hospitality that Indonesia proudly offers.

I commend the organizing committee and supporting institutions for their tireless efforts in making this international event possible. I am confident that ICMBNT 2026 will contribute significantly to scientific advancement and global academic networking.

On behalf of Universitas Udayana, I wish the conference every success and all participants a productive and memorable experience.

With best wishes,

Prof. Ir. I Ketut Sudarsana, S.T., Ph.D.
Rector
Universitas Udayana
Jimbaran, Bali, Indonesia

MESSAGE FROM THE CHIEF GUEST & KEY NOTE SPEAKER

It is a great honor and privilege to be part of the 2nd International Conference on Multidisciplinary Breakthroughs and NextGen Technologies (ICMBNT 2026) hosted at the prestigious Universitas Udayana, Jimbaran, Bali, Indonesia.

I extend my heartfelt congratulations to the organizing committee for their dedicated efforts in bringing together eminent researchers, academicians, industry professionals, and scholars from across the globe. Conferences such as ICMBNT 2026 play a vital role in fostering interdisciplinary collaboration, encouraging innovation, and addressing emerging global challenges through scientific and technological advancements.

In today's rapidly transforming world, multidisciplinary research is not merely an academic pursuit but a necessity. The integration of novel technologies, intelligent systems, sustainable innovations, and advanced scientific methodologies has the potential to redefine industries and improve societal well-being. This conference provides an excellent platform for meaningful dialogue, knowledge exchange, and collaborative partnerships.

I am confident that the technical sessions, keynote addresses, and research presentations will stimulate insightful discussions and inspire participants to explore new dimensions of innovation and research excellence.

I appreciate the efforts of Universitas Udayana and all supporting organizations for hosting this significant international event in the culturally rich and inspiring environment of Bali, Indonesia.

I wish ICMBNT 2026 grand success and extend my best wishes to all participants for fruitful deliberations and lasting academic collaborations.

With best regards,

Prof. Dr. Devipriya R
Principal
KPR Institute of Engineering and Technology
Coimbatore, Tamil Nadu, India.

MESSAGE FROM THE CONFERENCE CHAIR & PRESIDENT

Dear Distinguished Colleagues, Researchers, and Participants,

It is with great honour and immense pleasure that I welcome you to the 2nd International Conference on Multidisciplinary Breakthroughs and NextGen Technologies (ICMBNT 2026), held on March 12–13, 2026, at the beautiful campus of Universitas Udayana, Jimbaran, Bali, Indonesia.

ICMBNT 2026 brings together some of the brightest minds from academia, industry, and government across the globe under the unifying theme: "Transitioning to a Sustainable Future: Innovation and Integration in NextGen Technologies." This conference serves as a premier platform for the exchange of cutting-edge ideas, transformative research, and practical innovations that are shaping the future of our world.

The International Society for Intelligent Unmanned Systems (ISIUS), together with the Society of Cyber Intelligent System (SCIS), is proud to co-organize this event. Our shared mission has always been to foster interdisciplinary collaboration and to bridge the gap between research and real-world application — and ICMBNT 2026 is a testament to that commitment.

This year's conference features a rich program of special tracks spanning critical domains including energy technologies, infrastructure digitalization, artificial intelligence, and beyond. The diversity of topics reflects the multidisciplinary nature of the challenges we face as a global community, and the innovative spirit with which we must address them. I am particularly encouraged by the strong participation from researchers and practitioners across Asia, the Middle East, Africa, and beyond. This global representation underscores the universal relevance of the themes we are exploring and the collective determination to advance knowledge for the benefit of humanity.

I extend my deepest gratitude to the organizing committee, technical program chairs, advisory board members, reviewers, and all contributors who have worked tirelessly to make this conference a success. I also wish to thank our sponsors and institutional partners whose generous support has made this gathering possible. To all presenters and participants — I encourage you to engage fully, share openly, and collaborate boldly. The connections you forge and the ideas you exchange here in Bali may well become the seeds of tomorrow's breakthroughs.

Welcome to ICMBNT 2026. Welcome to Bali.

Warm regards,

Dr. Agus Budiyono
Conference Chair
President, International Society for Intelligent Unmanned Systems (ISIUS)

MESSAGE FROM THE KEYNOTE SPEAKER

It is a great honor and privilege to be a Keynote Speaker at the 2nd International Conference on Multidisciplinary Breakthroughs and NextGen Technologies (ICMBNT 2026), organized by the Society for Cyber Intelligent Systems (SCIS). I extend my heartfelt congratulations to the organizing committee for creating a dynamic platform that brings together researchers, academicians, industry professionals, and students from diverse domains.

ICMBNT 2026 reflects the true spirit of multidisciplinary collaboration. In today's rapidly evolving technological landscape, meaningful breakthroughs emerge when ideas intersect across disciplines. Conferences like this not only disseminate knowledge but also inspire innovation, foster partnerships, and encourage young researchers to explore bold and impactful research directions.

I am confident that the technical sessions, paper presentations, and discussions featured in these proceedings represent significant contributions to emerging technologies and applied research. The enthusiasm and intellectual rigor demonstrated by the participants will undoubtedly lead to future collaborations and advancements.

I sincerely appreciate the opportunity to share my insights with such an esteemed gathering and look forward to engaging discussions that will shape the future of research and innovation.

I wish ICMBNT 2026 every success and hope that this conference continues to grow as a premier global forum for knowledge exchange and technological excellence.

With warm regards,

Iman Satria
Assistant Professor
Universitas Bung Hatta,
Padang, Indonesia

MESSAGE FROM THE KEYNOTE SPEAKER

It is both an honor and a privilege to be part of the 2nd International Conference on Multidisciplinary Breakthroughs and NextGen Technologies (ICMBNT 2026). I am delighted to join this distinguished gathering of researchers, academicians, innovators, and industry professionals who are committed to advancing knowledge and technological progress.

In today's rapidly evolving world, innovation thrives at the intersection of disciplines. Conferences like ICMBNT provide an essential platform where ideas from diverse domains converge, leading to transformative solutions and sustainable advancements. The exchange of perspectives, methodologies, and experiences during such events significantly strengthens research quality and real-world impact.

I am confident that the technical sessions, discussions, and collaborative interactions will spark new ideas, inspire young researchers, and foster long-term academic and industrial partnerships. It is encouraging to see a strong commitment to excellence and innovation reflected in this conference.

I extend my sincere appreciation to the organizing committee for their dedication and meticulous efforts in bringing together this meaningful event. I wish all participants an intellectually stimulating and rewarding conference experience.

With warm regards,

Associate Professor Ts Dr Tan Kian Lam (Andrew)
Dean, School of Digital Technology,
Universiti Sains Malaysia - Malaysia

MESSAGE FROM THE KEYNOTE SPEAKER

It gives me immense pleasure to serve as a keynote speaker at 2nd International Conference on Multidisciplinary Breakthroughs and NextGen Technologies (ICMBNT 2026). This conference stands as a testament to the power of interdisciplinary collaboration in addressing complex global challenges through next-generation technologies.

As we witness unprecedented advancements in artificial intelligence, computing, engineering, data science, and emerging technologies, it becomes increasingly important to build strong platforms that encourage dialogue between academia and industry. ICMBNT 2026 successfully creates such a space—where innovative research meets practical implementation.

I believe that the discussions and presentations at this conference will not only broaden academic horizons but also contribute to impactful technological solutions that benefit society. The enthusiasm and scholarly spirit demonstrated by the participants reflect the bright future of multidisciplinary research.

My heartfelt congratulations to the organizing team for their outstanding efforts. I wish the conference great success and hope it inspires meaningful collaborations and groundbreaking research outcomes.

With warm regards,

Prof. Dr. Sam Goundar
Senior Lecturer in Information Technology
RMIT University – Vietnam

MESSAGE FROM THE KEYNOTE SPEAKER

I am truly delighted to be part of 2nd International Conference on Multidisciplinary Breakthroughs and NextGen Technologies (ICMBNT 2026) and to share insights with an audience dedicated to innovation and excellence. This conference provides a valuable opportunity to explore emerging research trends, exchange ideas, and build networks that transcend disciplinary boundaries.

The challenges of the modern world demand creative thinking, collaborative research, and the integration of diverse expertise. Events like ICMBNT play a crucial role in nurturing intellectual curiosity and encouraging the development of technologies that are not only advanced but also socially responsible and sustainable.

I strongly believe that the knowledge shared during this conference will inspire young scholars, strengthen research ecosystems, and pave the way for future technological breakthroughs. The collective wisdom and collaborative spirit present here are truly commendable.

I extend my warm wishes to all participants for an engaging, insightful, and highly productive conference.

With warm regards,

Dr. R. Annie Uthra
Professor & Head (Computational Intelligence),
SRM Institute of Science and Technology - Chennai

MESSAGE FROM THE ORGANIZING COMMITTEE

On behalf of the Organizing Committee, it is our great pleasure to welcome all participants, researchers, academicians, industry professionals, and distinguished guests to the 2nd International Conference on Multidisciplinary Breakthroughs and NextGen Technologies (ICMBNT 2026) organized by the International Society of Intelligent Unmanned Systems (ICSCS). ICMBNT 2026 serves as a premier international platform that brings together participants from diverse countries and research backgrounds to share innovative ideas, research findings, and practical solutions in the domains of intelligent unmanned systems, artificial intelligence, cybersecurity, machine business, and emerging technologies.

In an era where rapid advancements in intelligent unmanned systems, machine learning, autonomous technologies, and secure computing are reshaping industries worldwide, ICMBNT 2026 aims to provide a premier platform for presenting cutting-edge research, fostering interdisciplinary collaboration, and promoting real-world applications that address societal and technological challenges.

We are honored to host experts from academia, research institutions, and industry to share their insights through keynote speeches, technical paper presentations, and interactive discussions. Your contributions reflect the vibrancy and depth of research in these transformative fields, and we believe the outcomes of this conference will inspire future innovations.

We sincerely thank all the authors, reviewers, session chairs, committee members and volunteers for their invaluable support.

With Best Regards,

International Society of Intelligent Unmanned Systems
(South Korea – Jimbaran, Bali)

MESSAGE FROM THE ORGANIZING COMMITTEE

We feel happy and honored to welcome all the distinguished guests and participants for the 2nd International Conference on Multidisciplinary Breakthroughs and NextGen Technologies to be held on 12-13th Mar 2026. This conference is organized by Society for Cyber Intelligent Systems, Puducherry – India and International Society of Intelligent Unmanned Systems. The primary mission of our society is to advance cybersecurity and intelligent systems by promoting cutting-edge technologies like AI and machine learning, fostering research in cyber intelligence, and enhancing threat detection and mitigation strategies.

It gives us immense pleasure to present the proceedings of this International Conference (ICMBNT 2026). This conference brings together leading researchers, academicians, industry experts, and students from around the world to share their insights, innovations, and contributions across diverse disciplines that shape our technological future.

The aim of ICMBNT 2026 is to foster collaboration across domains and promote pioneering research that addresses real-world challenges through next-generation technologies. The multidisciplinary nature of this conference provides a unique platform to explore the intersections of engineering, data science, artificial intelligence, biotechnology, sustainable systems, healthcare, social science, education and more.

We express our sincere gratitude to all authors, reviewers, session chairs, and members of the organizing and technical committees who contributed to the success of this conference. We also thank our keynote speakers and panellists for sharing their invaluable perspectives.

ICMBNT 2026 will be a central hub for esteemed research experts worldwide and can anticipate unparalleled opportunities to network, gain invaluable insights, showcase their hidden potential, present significant research findings, receive due credit and recognition for their contributions.

We hope these proceedings serve as a valuable resource and ignite further research and innovation in multidisciplinary and emerging technological fields.

With Best Regards,

Society for Cyber Intelligent Systems
Puducherry – India

MESSAGE FROM ORGANIZING CHAIR

It gives me immense pleasure to extend my warm greetings to all participants, researchers, academicians, industry experts, and students attending the 2nd International Conference on Multidisciplinary Breakthroughs and NextGen Technologies (ICMBNT 2026).

On behalf of the Board of the Society for Cyber Intelligent Systems (SCIS), I congratulate the organizing committee for their dedicated efforts in bringing together distinguished scholars and professionals from diverse disciplines under one platform. This conference serves as an excellent forum for exchanging innovative ideas, presenting cutting-edge research, and fostering interdisciplinary collaborations.

In today's rapidly evolving technological landscape, multidisciplinary research plays a crucial role in addressing complex global challenges. ICMBNT 2026 is a significant step toward promoting advancements in emerging technologies, cyber intelligence, sustainable systems, and innovative scientific research.

I am confident that this conference will stimulate meaningful discussions, inspire new research directions, and strengthen academic–industry partnerships. I encourage all participants to actively engage in technical sessions, networking opportunities, and collaborative initiatives.

I wish ICMBNT 2026 a grand success and extend my best wishes to all contributors for productive deliberations and impactful outcomes.

With warm regards,

Dr.S.V.MANIKANTHAN, M.E,PhD,B.L.,
President - Board Member
Society for Cyber Intelligent Systems (SCIS), Puducherry, India.
Director
Melange Academic Research Associates, Puducherry, India.

MESSAGE FROM CONFERENCE CO-CHAIR

It is with immense pleasure and pride that I welcome you to the 2nd International Conference on Multidisciplinary Breakthroughs and NextGen Technologies (ICMBNT 2026). This conference serves as a dynamic platform for researchers, academicians, industry experts, and students from across the globe to share innovative ideas, emerging trends, and transformative research outcomes.

ICMBNT 2026 is designed to foster interdisciplinary collaboration and encourage meaningful discussions that bridge the gap between theory and real-world applications. As technological advancements continue to redefine every sector, this conference emphasizes the integration of diverse disciplines to create sustainable, intelligent, and impactful solutions for the future.

We are honored to host a distinguished lineup of keynote speakers, technical sessions, workshops, and paper presentations that reflect the cutting-edge developments in engineering, science, computing, management, and emerging technologies. The conference aims not only to disseminate knowledge but also to build strong research networks and long-term academic partnerships.

I sincerely thank all authors, reviewers, speakers, sponsors, and organizing committee members for their dedication and contributions in making this event possible. Your participation and support are the driving forces behind the success of ICMBNT 2026.

I warmly welcome you all to be part of this enriching academic gathering and look forward to your active participation and valuable contributions.

Wishing you a productive and inspiring conference experience.

With warm regards,

Dr. Vishnu Kumar Kaliappan, M.Tech.,PhD(S.K).,PostDoc(KR)
Vice - President - Board Member
Society for Cyber Intelligent Systems (SCIS), Puducherry, India.
Professor
Department of Computer Science and Engineering
KPR Institute of Engineering and Technology, Coimbatore, TN, India.

MESSAGE FROM THE TECHNICAL PROGRAM CHAIR

It is with great enthusiasm that I welcome you to the 2nd International Conference on Multidisciplinary Breakthroughs and NextGen Technologies - ICMBNT 2026. This conference serves as a vibrant platform for presenting innovative research, exchanging technical insights, and exploring emerging trends across diverse multidisciplinary domains.

We received a wide range of high-quality research submissions from scholars, researchers, and industry professionals worldwide. Each manuscript underwent a thorough and rigorous peer-review process to ensure originality, technical depth, and relevance to current advancements. The selected papers represent significant contributions that address real-world challenges and highlight next-generation technological breakthroughs.

The technical sessions have been thoughtfully structured to encourage knowledge sharing, constructive discussions, and collaborative engagement among participants. Through keynote lectures, paper presentations, and interactive sessions, we aim to foster interdisciplinary connections and inspire future research directions.

I sincerely thank all reviewers, authors, session coordinators, and organizing members for their commitment and dedication in upholding the academic standards of this conference.

With warm regards,

Dr. Sakthivel V, M.Tech, PhD
Secretary - Board Member
Society for Cyber Intelligent Systems (SCIS), Puducherry, India.
Professor
Department of Computer Science
VIT- Chennai, India.

MESSAGE FROM THE PUBLICATION CHAIR

It is our great pleasure to welcome you to the 2nd International Conference on Multidisciplinary Breakthroughs and NextGen Technologies (ICMBNT 2026). This conference serves as a dynamic platform that brings together researchers, academicians, industry professionals, and students to share knowledge, exchange innovative ideas, and explore emerging technological trends across diverse disciplines.

ICMBNT 2026 aims to foster interdisciplinary collaboration and encourage meaningful discussions that address current global challenges through advanced research and next-generation solutions. The conference features keynote addresses, technical sessions, and interactive discussions designed to inspire innovation and strengthen research networks.

We are proud to be part of this global academic gathering that promotes excellence, integrity, and collaboration in research. The diverse contributions and active participation of delegates reflect the vibrant and evolving nature of multidisciplinary advancements.

We sincerely thank all contributors, speakers, reviewers, and organizing members for their dedication and support in making this conference a success.

Wishing you all an engaging, productive, and inspiring conference experience.

With warm regards,

Dr. T.Padmapriya, M. Tech, M.B.A, PhD.,
Treasurer - Board Member
Society for Cyber Intelligent Systems (SCIS), Puducherry, India.
Managing Director
Melange Publications, Puducherry, India.

MESSAGE FROM THE TECHNICAL PROGRAM CHAIR

It is with great pleasure that I welcome you to the 2nd International Conference on Multidisciplinary Breakthroughs and NextGen Technologies (ICMBNT 2026). This conference provides a vibrant forum for researchers, academicians, industry experts, and students to present innovative ideas and discuss emerging advancements across diverse domains.

The technical sessions of ICMBNT 2026 have been carefully structured to showcase high-quality research contributions that reflect current trends and future directions in science, engineering, technology, and interdisciplinary studies. Each submission has undergone a thorough peer-review process to ensure academic rigor, originality, and technical relevance.

Through keynote addresses, paper presentations, and interactive discussions, the conference aims to promote meaningful knowledge exchange and foster collaboration between academia and industry. We believe that such multidisciplinary engagement will inspire innovative solutions to real-world challenges.

I sincerely thank the reviewers, authors, session coordinators, and organizing members for their dedication and commitment in shaping a strong and impactful technical program.

Wishing all participants a stimulating and rewarding conference experience.

With warm regards,

Dr. Swetha Indudhar Goudar, MCA, PhD.,
Board Member
Society for Cyber Intelligent Systems (SCIS), Puducherry, India.
Professor
Department of MCA
KLS Gogte Institute of Technology, Belagavi, India.

MESSAGE FROM THE CONFERENCE CO-CHAIR

It gives me immense pleasure to welcome you to the 2nd International Conference on Multidisciplinary Breakthroughs and NextGen Technologies (ICMBNT 2026).

This conference serves as a dynamic platform for researchers, academicians, industry professionals, and students to come together and share their latest research findings, innovative ideas, and practical experiences. In today's rapidly evolving world, collaboration across disciplines is essential, and ICMBNT 2026 aims to foster such meaningful interdisciplinary interactions.

The conference features keynote addresses by distinguished experts, technical paper presentations, and interactive sessions designed to encourage knowledge exchange and constructive discussions. We are confident that the diverse themes and research contributions will provide valuable insights into emerging technologies and future advancements.

ICMBNT 2026 not only promotes academic excellence but also strengthens networking opportunities and long-term research collaborations among participants from various institutions and industries.

I extend my heartfelt gratitude to all authors, speakers, reviewers, sponsors, and organizing committee members for their dedication and hard work in making this event possible.

I warmly welcome you all and wish you an inspiring, engaging, and successful conference experience.

With warm regards,

Dr. S. Ganesh Kumar, M.E, PhD.,
Board Member
Society for Cyber Intelligent Systems (SCIS), Puducherry, India.
Professor
Department of Computer Science and Engineering
SRM Institute of Science and Technology, Chennai, India.

MESSAGE FROM THE TECHNICAL PROGRAM CHAIR

It is my great pleasure to welcome you to the 2nd International Conference on Multidisciplinary Breakthroughs and NextGen Technologies (ICMBNT 2026).

The technical program of this conference has been carefully designed to reflect the latest advancements and innovative research across multiple disciplines. We received numerous quality submissions from researchers, academicians, and industry professionals, and each paper underwent a rigorous peer-review process to ensure originality, technical strength, and relevance.

The selected papers, keynote sessions, and technical discussions aim to promote knowledge exchange, interdisciplinary collaboration, and practical solutions to real-world challenges. We believe that the diverse range of topics presented at ICMBNT 2026 will inspire new ideas and foster meaningful research partnerships.

I sincerely thank the reviewers, authors, session chairs, and organizing committee members for their dedication and valuable contributions in shaping a strong and impactful technical program.

Wishing you all a productive, engaging, and insightful conference experience.

With warm regards,

Dr. Shanmugam Ramasamy, PhD.,
Board Member
Society for Cyber Intelligent Systems (SCIS), Puducherry, India.
Professor
Computational Insights and Sustainable Research Laboratory (CISRL)
Vellore, Tamil Nadu, India.

COMMITTEE MEMBERS

CONFERENCE CHAIR

Prof. Dr. AGUS BUDIYONO
Professor
MIT & President, ISIUS, Korea

CONFERENCE CO-CHAIR

Prof. Dr. VISHNU KUMAR KALIAPPAN
Professor
Department of Computer Science and Engineering, KPR Institute of Engineering and Technology, India

Prof. MADE SUCIPTA
Professor
Department of Mechanical Engineering, Universitas Udayana, Indonesia

ORGANIZING CHAIR

Dr. MANIKANTHAN S.V
President
Society for Cyber Intelligent System, Puducherry-India

TECHNICAL PROGRAM CHAIR

Dr. MUHAMAD FATCHAN
Assistant Professor
Universitas Pelita Bangsa, Indonesia

Dr. S. GANESH KUMAR
Department of Data Science and Business Systems
SRM Institute of Science and Technology, Chennai, India

Dr. CHRISTHU RAJ M R
Faculty, Directorate of Learning and Development,
SRM Institute of Science and Technology, Chennai, India

Dr. V. SAKTHIVEL
Associate Professor
Vellore Institute of Technology – Chennai Campus, India

Dr. L.R. ARAVIND BABU
Assistant Professor & Head
Department of Computer and Information Science, Annamalai University, India

Dr. K.MOHANA SUNDARAM
Professor & Head
Department of EEE, KPR Institute of Engineering and Technology, India

Prof. RAVI SAMIKANNU
Associate Professor
Department of Electrical and Communications Systems Engineering,
Botswana International University of Science and Technology, Botswana

Dr. PRADEEP S
Associate Professor
Department of Computing Technologies, School of Computing
SRM Institute of Science and Technology, Chennai, India

Dr. JAYAPRADHA J
Assistant Professor
Department of Computing Technologies, School of Computing
SRM Institute of Science and Technology, Chennai, India

Dr. PRABHU CHAKRAVARTHY
Associate Professor
Department of Networking and Communications
SRM Institute of Science and Technology, Chennai, India

PUBLICATION CHAIR

Dr. T. PADMAPRIYA
Managing Director
Melange Publications, Puducherry-India

ADVISORY BOARD

Dr. S. S. SRIDHAR
Professor & Associate Dean (Academics-CET)
Computer Science Engineering, SRM Institute of Science & Technology, Chennai, India

Dr. B. AMUTHA
Professor, Head-Accelerated Computing Research Vertical
Department of Computing Technologies, School of Computing, SRM Institute of Science & Technology, Chennai, India

Dr. KAVITHA V
Professor & Head (Data Science and Business Systems)
School of Computing, SRM Institute of Science & Technology, Chennai, India

Dr. R. ANNIE UTHRA
Professor & Head (Computational Intelligence)
School of Computing, SRM Institute of Science & Technology, Chennai, India

Dr. AZHAM HUSSAIN
Professor & Chair
Human-Centered Computing Research Laboratory, Universiti Utara Malaysia-Malaysia

Dr. RAJEEV SUKUMARAN
Director-Learning and Development
SRM Institute of Science & Technology, Chennai, India

COMMITTEE MEMBERS

CONTENT

Optimizing Physical Readiness in Volleyball: A Comparative Study of Strength, Plyometric, and Complex Training Programs

Dr.T.Arun Prasanna[1], Mathews P Raj[2], Dr. U V Sankar[3], Charulatha Ganeshkumar[4]
Assistant Professor[1], Head Academics[2], Director[3]
[1,2,3]School of Sports Education and Research, Department of Physical Education and Sports, Jain (Deemed To-Be University), Bangalore, India.
[4]Postgraduate, Saveetha College of Physiotherapy, Saveetha Institute of Medical and Technical Sciences, Chennai, Tamil Nadu, India.

Abstract: This study examined the isolated and combined effects of strength training, plyometric training, and complex training on selected physical variables among university men volleyball players. Eighty male participants (aged 18–25 years) from South Bangalore training centre, Bangalore, India, were randomly assigned to four equal groups: Strength Training Group (STG), Plyometric Training Group (PTG), Complex Training Group (CTG), and Control Group (CG). The experimental groups underwent a 12-week supervised training program (three sessions/week, 60 minutes/session), while the CG maintained routine activities. Pre- and post-intervention assessments included explosive power (Sargent Jump), speed (50-m sprint), agility (Shuttle Run), and endurance (One-Mile Run). Data were analyzed using paired *t*-tests and Analysis of Covariance (ANCOVA) with Scheffé's post hoc test ($\alpha = 0.05$). Results revealed significant within-group improvements in all physical variables for STG, PTG, and CTG ($p < 0.05$), with no changes in CG. Between-group comparisons showed CTG demonstrated significantly greater gains than STG, PTG, and CG in explosive power (+0.23 m), speed (–1.53 s), agility (–1.27 s), and endurance (–2.20 min) ($p < 0.05$). No significant differences were observed between STG and PTG in any variable. These findings indicate that while both strength and plyometric training independently enhance physical performance, their integration through complex training yields superior outcomes. The study supports the
implementation of complex training as an effective, time-efficient strategy to optimize physical readiness in male volleyball athletes.

Keywords: complex training, strength training, plyometric training, explosive power, speed, agility, endurance, volleyball.

1. Introduction

Volleyball is a high-intensity, intermittent sport that places substantial demands on explosive power, speed, agility, and aerobic endurance. Success in modern volleyball hinges not only on technical proficiency but also on superior physical conditioning, particularly the ability to execute rapid vertical jumps, multidirectional movements, and sustained high-effort rallies (Sheppard & Leibert, 2023). Consequently, optimizing physical performance through evidence-based training interventions has become a cornerstone of athletic development programs at the collegiate and elite levels.
Strength training has long been recognized as a foundational method for enhancing neuromuscular capacity and force production in volleyball athletes. Recent meta-analytic evidence confirms that

resistance training significantly improves vertical jump height and sprint performance in team sport athletes, including volleyball players (Grgic et al., 2021).

Similarly, plyometric training—which emphasizes rapid stretch-shortening cycle actions—has demonstrated robust efficacy in augmenting lower-body explosiveness and change-of-direction speed, both critical for blocking, spiking, and defensive transitions (Ramírez-Campillo et al., 2020).

More recently, complex training—a method that alternates heavy resistance exercises with biomechanically similar plyometric drills within the same session—has gained empirical support for its ability to potentiate power output beyond what either modality achieves in isolation. This approach leverages post-activation potentiation (PAP), a physiological phenomenon wherein prior high-intensity muscular contraction enhances subsequent explosive performance (Seitz & Haff, 2022). In volleyball-specific contexts, studies have shown that 8–12 weeks of complex training yields superior gains in spike jump height, approach speed, and repeated-sprint ability compared to traditional training models (Loturco et al., 2021; Chaabene et al., 2023).

A 2024 systematic review by Slimani et al. concluded that integrated training models like complex training produce the largest effect sizes for improving physical performance in intermittent-sprint team sports, with volleyball exhibiting particularly strong responsiveness due to its reliance on explosive, anaerobic efforts interspersed with brief recovery periods. Despite this growing body of evidence, comparative data on the relative effectiveness of isolated strength, isolated plyometric, and combined complex training—particularly among Indian collegiate athletes—remain limited.

Therefore, this study aims to address this gap by examining the isolated and combined effects of strength, plyometric, and complex training on key physical variables—explosive power, speed, agility, and endurance—among university men volleyball players at South Bangalore training centre, Bangalore, India.

2. Materials and Methods

2.1 Participants

Eighty male university volleyball players (age: 18–25 years; mean ± SD: 20.4 ± 1.8 years) were recruited from the South Bangalore training centre, Bangalore, India. All participants were actively engaged in institutional-level volleyball training and competition for at least two years prior to the study. Exclusion criteria included any musculoskeletal injury within the past six months or participation in structured strength or plyometric training during the preceding three months.

Participants were randomly assigned to one of four groups (n = 20 per group):

- Strength Training Group (STG)
- Plyometric Training Group (PTG)
- Complex Training Group (CTG)
- Control Group (CG)

The randomization sequence was generated using a computerized random number generator, and allocation was concealed until baseline testing was completed.

2.2 Experimental Design

A randomized controlled pre-test–post-test design was employed. All participants completed baseline assessments of four physical variables: explosive power, speed, agility, and endurance. Following pre-testing, the three experimental groups underwent a 12-week supervised training intervention (3 sessions/week, 60 minutes/session), in addition to their regular volleyball practice. The control group

continued routine volleyball activities without any additional training. Post-intervention assessments were conducted within 72 hours of the final training session under identical conditions to pre-testing.

2.3 Training Interventions

All training sessions were supervised by certified strength and conditioning coaches and included a standardized 10-minute dynamic warm-up and 10-minute cool-down. Attendance was monitored, and participants with ≥90% attendance were included in the final analysis.

- Strength Training Group (STG): Performed compound resistance exercises (back squat, deadlift, leg press, leg curl, bent-over row, military press) at intensities progressing from 40–60% (weeks 1–4), 50–70% (weeks 5–8), to 60–80% (weeks 9–12) of estimated 1-repetition maximum (1RM). Each exercise comprised 5 sets of 8–12 repetitions with 30 seconds of rest between sets. Sessions were conducted Monday, Wednesday, and Friday (6:30–7:30 a.m.).
- Plyometric Training Group (PTG): Executed drills including front box jumps, broad jumps, dot drills, ricochet runs, power skipping, and depth jumps. Training intensity (effort) progressed similarly across phases (40–80%). Each drill included 5 sets of 8–12 repetitions with 30 seconds rest. Sessions were held Tuesday, Thursday, and Saturday (6:30–7:30 a.m.).
- Complex Training Group (CTG): Performed paired sets of strength and plyometric exercises (e.g., back squat immediately followed by broad jumps). Each complex pair was repeated for 2 supersets of 8–12 repetitions, with 30 seconds intra-pair rest and 2–3 minutes between complexes. Intensity followed the same progression as STG and PTG. Sessions occurred Monday, Wednesday, and Friday (4:30–5:30 p.m.).
- Control Group (CG): Engaged only in regular volleyball practice without additional training.

2.4 Physical Variable Assessments

All tests were administered by trained investigators blinded to group allocation. Participants refrained from vigorous exercise for 48 hours prior to testing.

1. Explosive Power: Assessed via the Sargent vertical jump test. Participants stood flat-footed against a wall and marked their standing reach. They then performed a maximal vertical jump, touching the highest point possible. The difference (in meters) between standing reach and jump height was recorded as the score. The best of three trials was used.
2. Speed: Measured using a 50-meter sprint. Participants started from a standing position and sprinted maximally over 50 m. Time was recorded to the nearest 0.01 s using a digital stopwatch. The fastest of two trials was retained.
3. Agility: Evaluated with the 30-yard shuttle run test. Two lines were marked 30 yards apart. Participants started at one line, ran to the opposite line, retrieved a wooden block, returned to the start line, placed the block, then repeated the process for a second block. Total time (in seconds) was recorded; the better of two trials was used.
4. Endurance: Assessed via the one-mile run/walk test on a flat, marked track. Participants were instructed to complete one mile as quickly as possible, with walking permitted. Total time (in minutes and seconds) was recorded.

2.5 Reliability

A pilot study (n = 10) established test-retest reliability using intra-class correlation coefficients (ICC, two-way random effects model). All physical variables demonstrated high reliability: explosive power (ICC = 0.90), speed (ICC = 0.91), agility (ICC = 0.93), and endurance (ICC = 0.88) ($p < 0.05$).

2.6 Statistical Analysis

Data were analyzed using IBM SPSS Statistics (v26.0). Normality (Shapiro–Wilk) and homogeneity of variance (Levene's test) were confirmed. Within-group changes from pre- to post-test were evaluated using paired *t*-tests. Between-group differences in post-test scores, adjusted for pre-test values, were analyzed using one-way analysis of covariance (ANCOVA).

When ANCOVA results were significant ($p < 0.05$), pairwise comparisons were conducted using Scheffé's post hoc test to control for Type I error inflation. Effect sizes were interpreted using partial eta squared (η^2): small (≥0.01), medium (≥0.06), large (≥0.14). The significance level was set at $\alpha = 0.05$.

3. Results

All experimental groups demonstrated significant within-group improvements in physical variables after the 12-week intervention ($p < 0.05$), while the control group showed no significant changes. Between-group comparisons revealed significant differences in post-intervention outcomes across all physical variables.

3.1 Explosive Power (Sargent Jump, meters)

Pre-test means were homogeneous across groups ($F = 1.26$, $p = 0.295$), confirming successful randomization. Post-test ANCOVA indicated a significant effect of training type on explosive power ($F = 74.92$, $p < 0.001$). The Complex Training Group (CTG) exhibited the greatest improvement ($\Delta = +0.23$ m), followed by Plyometric (PTG; $\Delta = +0.17$ m) and Strength Training Groups (STG; $\Delta = +0.13$ m). The Control Group (CG) showed negligible change ($\Delta = +0.01$ m).

Scheffé's post hoc analysis confirmed that CTG outperformed STG ($p < 0.05$, MD = 0.09), PTG ($p < 0.05$, MD = 0.07), and CG ($p < 0.05$, MD = 0.20). No significant difference was observed between STG and PTG ($p = 0.821$).

Table 1. ANCOVA and Scheffé's Post Hoc Results for Explosive Power

Group	Pre-Test Mean	Post-Test Mean	Adjusted Post-Test Mean
STG	0.37	0.5	0.5
PTG	0.35	0.52	0.52
CTG	0.36	0.59	0.59
CG	0.38	0.39	0.39

ANCOVA: $F(3, 75) = 74.92$, $p < 0.001$

Pairwise Comparison	Mean Difference	p-value
CTG vs. STG	0.09	<0.001
CTG vs. PTG	0.07	<0.001
CTG vs. CG	0.2	<0.001
STG vs. PTG	0.02	0.821
STG vs. CG	0.11	<0.001
PTG vs. CG	0.13	<0.001

3.2 Speed (50-Meter Sprint, seconds)

Pre-test scores did not differ significantly ($F = 0.07$, $p = 0.976$). Post-intervention ANCOVA revealed a significant group effect ($F = 13.10$, $p < 0.001$). CTG showed the largest reduction in sprint time (Δ = –1.53 s), followed by PTG (Δ = –0.81 s) and STG (Δ = –0.85 s). CG showed no meaningful change (Δ = –0.03 s).

Scheffé's test confirmed CTG was significantly faster than STG ($p < 0.001$, MD = 0.76), PTG ($p < 0.001$, MD = 0.74), and CG ($p < 0.001$, MD = 1.53). STG and PTG did not differ significantly ($p = 0.992$).

Table 2. ANCOVA and Scheffé's Post Hoc Results for Speed

Group	Pre-Test Mean	Post-Test Mean	Adjusted Post-Test Mean
STG	7.28	6.43	6.41
PTG	7.2	6.39	6.39
CTG	7.17	5.64	5.65
CG	7.22	7.19	7.18

ANCOVA: F(3, 75) = 13.10, p < 0.001

Pairwise Comparison	Mean Difference	p-value
CTG vs. STG	0.76	<0.001
CTG vs. PTG	0.74	<0.001
CTG vs. CG	1.53	<0.001
STG vs. PTG	0.02	0.992
STG vs. CG	0.77	<0.001
PTG vs. CG	0.79	<0.001

3.3 Agility (Shuttle Run, seconds)

Pre-test homogeneity was confirmed ($F = 0.76$, $p = 0.520$). ANCOVA of post-test scores showed a significant training effect ($F = 13.10$, $p < 0.001$). CTG demonstrated the greatest agility improvement (Δ = –1.27 s), compared to PTG (Δ = –0.51 s) and STG (Δ = –0.65 s). CG showed minimal change (Δ = –0.09 s).CTG was significantly more agile than STG ($p < 0.001$, MD = 0.59), PTG ($p < 0.001$, MD = 0.63), and CG ($p < 0.001$, MD = 1.24). No difference existed between STG and PTG ($p = 0.978$).

Table 3. ANCOVA and Scheffé's Post Hoc Results for Agility

Group	Pre-Test Mean	Post-Test Mean	Adjusted Post-Test Mean
STG	11.14	10.49	10.48
PTG	10.99	10.48	10.52
CTG	11.17	9.9	9.89
CG	11.26	11.17	11.13

ANCOVA: F(3, 75) = 13.10, p < 0.001

Pairwise Comparison	Mean Difference	p-value
CTG vs. STG	0.59	<0.001
CTG vs. PTG	0.63	<0.001
CTG vs. CG	1.24	<0.001
STG vs. PTG	0.04	0.978
STG vs. CG	0.65	<0.001
PTG vs. CG	0.61	<0.001

3.4 Endurance (One-Mile Run, minutes)

Pre-test scores were equivalent across groups ($F = 0.44$, $p = 0.725$). Post-test ANCOVA indicated a significant group effect ($F = 20.85$, $p < 0.001$). CTG showed the largest endurance gain ($\Delta = -2.20$ min), followed by PTG ($\Delta = -0.91$ min) and STG ($\Delta = -1.09$ min). CG showed no improvement ($\Delta = -0.11$ min).CTG significantly outperformed STG ($p < 0.001$, MD = 1.09), PTG ($p < 0.001$, MD = 1.08), and CG ($p < 0.001$, MD = 2.31). STG and PTG did not differ significantly ($p = 0.996$).

Table 4. ANCOVA and Scheffé's Post Hoc Results for Endurance

Group	Pre-Test Mean	Post-Test Mean	Adjusted Post-Test Mean
STG	17.38	16.29	16.2
PTG	17.19	16.28	16.28
CTG	17.4	15.2	15.2
CG	17.63	17.52	17.51

ANCOVA: F(3, 75) = 20.85, p < 0.001

Pairwise Comparison	Mean Difference	p-value
CTG vs. STG	1.09	<0.001
CTG vs. PTG	1.08	<0.001
CTG vs. CG	2.31	<0.001
STG vs. PTG	0.01	0.996
STG vs. CG	1.22	<0.001
PTG vs. CG	1.23	<0.001

Across all four physical variables—explosive power, speed, agility, and endurance—the Complex Training Group (CTG) consistently demonstrated significantly greater improvements than both isolated training groups (STG, PTG) and the control group (CG). No significant differences were observed between STG and PTG in any physical variable ($p > 0.05$). These results support the superior efficacy of complex training for enhancing physical performance in male university volleyball players.

4. Discussion

The present study examined the comparative effects of strength training (STG), plyometric training (PTG), and complex training (CTG) on four key physical variables—explosive power, speed, agility, and endurance—in male university volleyball players. The results demonstrate that all three experimental interventions significantly enhanced physical performance compared to a control group; however, complex training consistently produced the greatest improvements across all variables, supporting its superiority as a conditioning strategy for volleyball-specific physical development.

The CTG exhibited the largest gain in vertical jump height (+0.23 m), significantly outperforming both STG and PTG. This finding aligns with recent evidence indicating that complex training potentiates neuromuscular efficiency through post-activation potentiation (PAP), wherein a heavy resistance stimulus enhances subsequent explosive output (Seitz & Haff, 2022). In volleyball, where vertical jump capacity directly influences spiking and blocking efficacy, this is particularly relevant. Loturco et al. (2021) reported similar results in elite youth volleyball players, where 8 weeks of complex training improved countermovement jump height by 8.2%, significantly more than isolated strength or

plyometric protocols. Our data corroborate these outcomes, reinforcing complex training as a potent method for developing lower-body explosiveness in volleyball athletes.

CTG also demonstrated the greatest reduction in 50-m sprint time (–1.53 s), significantly surpassing both STG and PTG. While traditional models often treat speed development as primarily neuromuscular or technical, emerging research emphasizes the role of integrated strength-power training in enhancing sprint kinetics (Bogdanis et al., 2023). Complex training appears to optimize rate of force development (RFD) and inter-muscular coordination, translating to faster acceleration—critical for rapid court coverage during serve-receive or defensive transitions. A 2023 meta-analysis by Moran et al. confirmed that complex training yields moderate-to-large effects on linear sprint performance in team-sport athletes (ES = 0.72), outperforming isolated modalities.

Agility improvements followed a similar pattern, with CTG showing the largest reduction in shuttle run time (–1.27 s). Volleyball requires frequent multidirectional movements, rapid deceleration, and reacceleration—tasks heavily dependent on both strength and reactive power. Chaabene et al. (2023) recently demonstrated that complex training enhances change-of-direction speed more effectively than plyometrics alone in intermittent-sprint athletes, likely due to improved eccentric strength and stretch-shortening cycle utilization. Our findings extend this to volleyball, suggesting that the integration of heavy squats with reactive jumps enhances the neuromuscular control necessary for agile court movement.

Notably, CTG also showed the greatest improvement in one-mile run time (–2.20 min), a result that may appear counterintuitive given the anaerobic nature of complex training. However, recent work by Slimani et al. (2024) highlights that high-intensity, intermittent protocols like complex training can improve aerobic capacity by increasing mitochondrial density and lactate clearance—key adaptations for sustaining repeated high-effort rallies in volleyball. Additionally, the metabolic stress induced by complex sets may stimulate cardiovascular adaptations that support endurance, as observed in our cohort.

Crucially, no significant differences emerged between STG and PTG in any physical variable, suggesting that—when matched for volume and progression—these modalities produce comparable standalone benefits. This supports the notion that both maximal strength and reactive power are foundational, but neither alone is sufficient to maximize volleyball-specific physical performance. In contrast, CTG's consistent superiority underscores the synergistic effect of combining both stimuli within a single session, a principle increasingly validated in contemporary sports science (Ramírez-Campillo et al., 2020; Sheppard & Leibert, 2023).

For volleyball coaches and strength professionals, these findings advocate for the integration of complex training into pre-season and in-season conditioning programs. A 12-week protocol, as used here, appears sufficient to elicit meaningful gains across multiple physical domains—critical for holistic athletic development. Given volleyball's reliance on explosive, multidirectional, and repeated efforts, complex training offers a time-efficient, high-yield strategy to enhance physical readiness.

This study focused solely on physical variables and did not assess volleyball-specific performance metrics (e.g., spike velocity, block jump, serve accuracy). Future research should incorporate sport-specific outcome measures and explore long-term retention of gains. Additionally, hormonal or neuromuscular mechanisms (e.g., electromyography, testosterone/cortisol ratios) could provide deeper insight into the physiological basis of PAP in volleyball athletes.

5. Conclusion

The present 12-week randomized controlled trial demonstrates that strength training, plyometric training, and complex training all significantly enhance key physical variables explosive power, speed, agility, and endurance in male university volleyball players. However, complex training consistently produced superior improvements across all four physical domains compared to both isolated training modalities and the control condition. Notably, no significant differences were observed between strength and plyometric training groups, suggesting that while each method is effective in isolation, their integration within a complex training framework yields synergistic benefits.

These findings support the application of complex training as a time-efficient and highly effective conditioning strategy for volleyball athletes, where explosive vertical actions, rapid multidirectional movements, and repeated high-intensity efforts are central to performance. Coaches and strength professionals are encouraged to incorporate complex training protocols pairing heavy resistance exercises with biomechanically matched plyometric drills into pre-season and in-season programs to maximize physical readiness.

Future research should examine the transfer of these physical gains to volleyball-specific performance outcomes (e.g., spike jump height, block reach, serve velocity) and investigate the sustainability of adaptations beyond the 12-week intervention period.

References

[1] Bogdanis, G. C., Papadopoulos, C., & Apostolidis, N. (2023). Effects of complex training on sprint and jump performance in team sport athletes: A systematic review. *Journal of Sports Sciences, 41*(5), 521–533. https://doi.org/10.1080/02640414.2022.2156789

[2] Chaabene, H., Negra, Y., Moran, J., Granacher, U., & Prieske, O. (2023). Effects of complex training on physical performance in team sports: A systematic review and meta-analysis. *Journal of Strength and Conditioning Research, 37*(4), 789–801. https://doi.org/10.1519/JSC.0000000000004321

[3] Grgic, J., Lazinica, B., Schoenfeld, B. J., & Pedisic, Z. (2021). Resistance training and athletic performance in team sports: A systematic review and meta-analysis. *Sports Medicine, 51*(10), 2165–2187. https://doi.org/10.1007/s40279-021-01499-8

[4] Loturco, I., Pereira, L. A., Cal Abad, C. C., D'Angelo, R. A., Fernandes, V., Reis, V. M., & Nakamura, F. Y. (2021). Complex training in elite youth volleyball players: Effects on jump, sprint, and change-of-direction performance. *Journal of Sports Sciences, 39*(12), 1353–1360. https://doi.org/10.1080/02640414.2021.1882167

[5] Moran, J., Sandercock, G., Ramírez-Campillo, R., Meylan, C., & Collison, J. (2023). The effects of complex training on linear sprint performance in team sport athletes: A meta-analysis. *Sports Medicine – Open, 9*(1), 45. https://doi.org/10.1186/s40798-023-00585-2

[6] Ramírez-Campillo, R., Álvarez, C., García-Hermoso, A., Izquierdo, M., & Moran, J. (2020). Effects of plyometric jump training on measures of physical fitness in volleyball players: A systematic review and meta-analysis. *European Journal of Sport Science, 20*(8), 1026–1041.

[7] Asadi, A., Arazi, H., Ramirez-Campillo, R., & Moran, J. (2022). Effects of in-season complex training on physical performance in male volleyball players: A randomized controlled trial. Journal of Sports Sciences, 40(14), 1632–1640. https://doi.org/10.1080/02640414.2022.2086341

[8] García-Pinillos, F., Latorre-Román, P. Á., & Párraga-Montilla, J. A. (2021). Effects of complex training on physical performance in team sports: A systematic review. International Journal of Environmental Research and Public Health, 18(3), 1125. https://doi.org/10.3390/ijerph18031125

[9] Hammami, R., Chaabene, H., Negra, Y., Granacher, U., & Prieske, O. (2020). Effects of plyometric training on physical performance in youth volleyball players: A meta-analysis. Journal of Strength and Conditioning Research, 34(11), 3237–3246. https://doi.org/10.1519/JSC.0000000000003253

[10] Komi, P. V., & Häkkinen, K. (2023). Neuromuscular adaptations to complex training in intermittent sports: Mechanisms and applications. Scandinavian Journal of Medicine & Science in Sports, 33(5), 789–801. https://doi.org/10.1111/sms.14322

[11] Martínez-Valencia, M. A., González-Ravé, J. M., Alcaraz, P. E., et al. (2021). Effects of strength vs. complex training on physical performance in elite male volleyball players.

[12] Frontiers in Sports and Active Living, 3, 634521. https://doi.org/10.3389/fspor.2021.634521

[13] Pereira, L. A., Cal Abad, C. C., Siqueira, A. F., et al. (2020). Complex training improves physical performance in elite female volleyball players. Journal of Strength and Conditioning Research, 34(10), 2805–2812. https://doi.org/10.1519/JSC.0000000000003201

[14] Ribeiro, J., Teixeira, A., Silva, A. J., et al. (2023). Effects of a 10-week complex training program on physical fitness in adolescent volleyball players. Pediatric Exercise Science, 35(2), 112–120. https://doi.org/10.1123/pes.2022-0123

[15] Santos, E. J., & Janeira, M. A. (2022). Strength training improves vertical jump and sprint performance in young male volleyball players: A 12-week intervention. European Journal of Sport Science, 22(7), 1021–1030. https://doi.org/10.1080/17461391.2021.1925962

[16] Thomas, K., French, D., & Hayes, P. R. (2024). Time-efficient complex training protocols for team-sport athletes: A practical review. Strength and Conditioning Journal, 46(1), 45–56. https://doi.org/10.1519/SSC.0000000000000812

[17] Zois, J., Bishop, D. J., Ball, N., & Aughey, R. J. (2020). High-intensity training improves physical and technical performance in volleyball players. International Journal of Sports Physiology and Performance, 15(6), 721–728. https://doi.org/10.1123/ijspp.2019-0432

Integrative Varma Chikitsa and Yoga Therapy in Musculoskeletal and Neuropathic Disorders: A Case Series from a Traditional Ayurvedic Practice

M. Saravanabhava[1], K. V. Rajasekhar[2*], P. Sudhan[3], V. Subbulakshmi[4], D. Dwarakanath[5]

[1]Department of Faculty of Yoga Science and Therapy, Meenakshi Academy of Higher Education and Research, Chennai, Tamil Nadu, India.

[2]Dean & Professor, Department of Radio Diagnosis, Meenakshi Medical College Hospital & Research Institute, Kanchipuram, Tamil Nadu, India

[3]Teaching Associates, Directorate of Learning & Development, SRM Institute of Science and Technology, Kattankulathur, Chennai, Tamil Nadu, India

[4]Principal, Faculty of Yoga Science & Therapy, Meenakshi Academy of Higher Education and Research, Chennai, Tamil Nadu, India

[5]Srivatsa Yoga Cikitsa, Chennai, Tamil Nadu, India

E-mail: dr.saravanabhavahelious@gmail.com[1]

Abstract: Background: Varma Chikitsa, an ancient South Indian therapeutic system rooted in Siddha medicine, involves stimulation of specific vital energy points (varmam) to restore physiological balance and alleviate pain. Despite its long clinical tradition, peer-reviewed evidence on its efficacy remains sparse.

Objectives: This case series aims to document clinical outcomes of integrated Varma Chikitsa, Panchakarma procedures, internal Ayurvedic medications, and yoga therapy in five patients presenting with diverse musculoskeletal and neuropathic conditions.

Methods: Five cases (Four males, One females; age range 35–54 years) presenting with lumbar spondylosis, frozen shoulder, carpal tunnel syndrome, osteoarthritis of the knee, and lumbar spondylosis with sinusitis were managed over 7–21 days. Marma points were identified per classical Siddha taxonomy. Interventions included varma therapy, steam (Swedana), Nasyam, Kizhi, Dhara with resistive loading, stretching, mobilisation, yoga, and individualised Ayurvedic pharmacotherapy. Outcomes were assessed using subjective symptom relief, functional mobility, and pain scores.

Results: All five patients reported marked symptomatic improvement. Pain reduction ranged from moderate relief to approximately 90% reduction. Functional gains included restoration of shoulder range of motion, resolution of carpal tunnel symptoms, weight reduction of 7 kg in an obese patient, and remission of recurrent sinusitis. No adverse events were reported.

Conclusions: The findings suggest that integrative Varma Chikitsa combined with Panchakarma and yoga is a safe and promising approach for musculoskeletal and neuropathic pain management. Randomised controlled trials with validated outcome measures are warranted.

Keywords: Varma Chikitsa; Varmam; Panchakarma; Siddha medicine; Ayurveda; lumbar spondylosis; frozen shoulder; carpal tunnel syndrome; osteoarthritis; yoga therapy.

1. Introduction

Musculoskeletal disorders (MSDs) are among the leading contributors to global disability, accounting for approximately 1.71 billion cases worldwide and representing a substantial socioeconomic burden in

developing and developed nations alike [1]. Conventional biomedical approaches, including pharmacotherapy and surgery, offer relief for many patients; however, a significant subset experiences inadequate pain control, medication-related adverse effects, or surgical risks that limit their management options [2]. This has renewed interest in traditional systems of medicine as adjunctive or alternative therapeutic modalities.

Varma Chikitsa (also referred to as Varma Vaidyam) is a therapeutic branch of the Siddha medical tradition of South India and Sri Lanka that is concerned with the identification and therapeutic stimulation of vital energy loci known as *varmam*. Classical Siddha literature enumerates 108 principal *varmam* points distributed across the human body, each corresponding to specific anatomical confluences of nerves, blood vessels, tendons, muscles, and bones [3]. Pathological disruption at this location whether through trauma, degenerative change, or dosha imbalance—is believed to precipitate pain, functional impairment, and systemic disturbance [4].

Therapeutic manipulation of *varmam* points through precise digital pressure, specialised massage, heat application, and Panchakarma procedures is central to the Varma Chikitsa paradigm [5]. Complementary to this is Nasyam (nasal medication), Kizhi (bolus fomentation), Swedana (steam therapy), Dhara (medicated stream therapy), and internal Ayurvedic pharmacotherapy—procedural elements well-documented in classical and contemporary Ayurvedic literature for their roles in pain relief, anti-inflammatory action, and neuroprotection [6,7].

Yoga, recognised by the World Health Organization as part of traditional and complementary medicine, has demonstrated efficacy in chronic low back pain, shoulder impingement, and arthritis through mechanisms involving neuromodulation, muscular strengthening, and psychological wellbeing [8,9]. The integration of yoga within a Varma Chikitsa protocol represents an emerging clinical approach yet to receive formal scholarly documentation.

This case series, conducted at Durva Ayurvedic Clinic, Chennai during the year 2024-25, presents five patients treated with a structured integrative protocol. The novelty of this report lies in the systematic documentation of *varmam* point localisation per anatomical landmarks alongside concurrent Panchakarma interventions and yoga scheduling, providing a reproducible clinical template for conditions spanning the cervical-lumbar axis, peripheral joints, and craniofacial sinuses.

2. Methodology

2.1 Study Design

This is a descriptive case series of five patients managed consecutively at a traditional Ayurvedic clinical institution. This case series documents the clinical outcomes of five patients managed consecutively at Durva Ayurvedic Clinic, Chennai, during the 2024–2025 clinical program. Informed consent was obtained from all participants for clinical data to be used for educational and research purposes. Patient identities are de-identified to protect confidentiality. No human subjects research ethics approval was required under institutional guidelines for retrospective case documentation; however, all clinical procedures conformed to the principles of the Declaration of Helsinki [10].

2.2 Patient Selection

Patients presenting with musculoskeletal and neuropathic complaints to the outpatient department were included. Diagnosis was established using both classical Ayurvedic nosology and contemporary biomedical criteria, supported where relevant by magnetic resonance imaging (MRI). Patients with contraindications to Panchakarma procedures or those who did not complete the treatment schedule were excluded.

2.3 Therapeutic Protocol

Varmam point identification was performed by the treating physician (Dr. M. Saravanabhava, BAMS, MD Panchakarma) based on classical Siddha anatomical mapping [3,4]. Varma stimulation consisted of graded digital pressure, percussion, and marma oil application, administered in sessions of 30–45 minutes. Steam therapy (Swedana) was applied post-varma stimulation to promote muscle relaxation and facilitate absorption of medicated oils [7].

Nasyam was administered according to classical protocols involving Anu Taila instillation into nasal passages [11]. Kizhi fomentation using medicated herbal boluses was applied to affected regions. Agnikarma (thermal cautery at vital points) was incorporated in the carpal tunnel syndrome case at low intensity. Stretching and joint mobilisation techniques were applied every fourth day in spinal cases.

Internal medications were prescribed individually based on Ayurvedic dosha assessment and included formulations such as Rasna Saptakam Kashayam, Vayu Gulika, Laksha Guggulu, Ashtavargam Kashayam, Varanadi Kashayam, Kanchanara Guggulu, and Aba Guggulu.

Yoga sessions were designed per individual capacity and included asanas targeting the affected anatomical region. Dietary counselling was provided for the obese patient [9].

2.4 Outcome Assessment

Primary outcomes were subjective pain relief (reported by patients on a descriptive scale: no relief, partial relief, significant relief, or complete relief), restoration of functional mobility, and specific clinical parameters such as range of motion and neurological symptom resolution. Secondary outcomes included weight change and quality of life improvement as described by the patient.

3. Case Reports

3.1 Case 1: Lumbar and Cervical Spondylosis (Katigraham)

Parameter	Details
Patient	Male, 46 years; occupation: manufacturing sector, Chennai
Chief Complaints	Severe neck and back pain (3 months); numbness in both hands; radiating pain from hip to both legs; stiffness in cervical and lumbar regions
Investigations	MRI whole spine: disc bulge at L2–L3, L3–L4, L4–L5 with nerve root compression; loss of cervical lordosis
Ayurvedic Diagnosis	Katigraham
Modern Diagnosis	Lumbar spondylosis
Past History	Modern physician advised surgery; no prior surgical history

Varmam Points Involved

1. Chuliyadi varmam: situated at the atlanto-axial joint;
2. Pin sarithi varmam: situated lateral to the posterior aspect of the umbilicus;
3. Poonool varmam: situated at the supra-scapular region;
4. Kili mega varmam: over the spinous process of C7.

Intervention

Varma therapy with whole-body Swedana for 7 days; Nasyam for 11 days; stretching and mobilisation every fourth day; yoga sessions for 5 days. Internal medications: Rasna Saptakam Kashayam, Vayu Gulika, Laksha Guggulu.

Outcome

Significant reduction in neck and back pain; diminished radicular symptoms; reduced cervico-lumbar stiffness; patient reported overall functional improvement and elected against surgery.

3.2 Case 2: Post-Traumatic Frozen Shoulder (Apabahukam)

Parameter	Details
Patient	Male, 54 years; occupation: chief engineer, Chennai
Chief Complaints	Pain and stiffness in left shoulder joint (6 months); markedly decreased shoulder range of motion
History	Road traffic accident (motorcycle) 6 months prior; 1 month of allopathic treatment without adequate relief; no surgical history
Ayurvedic Diagnosis	Apabahukam
Modern Diagnosis	Frozen shoulder (adhesive capsulitis)

Varmam Points Involved

1. *Poonool varmam*: supra-scapular region; 2. *Kai koottu varmam*: level of T5, over the midpoint of the medial border of the scapula; 3. *Vul puttu varmam*: anterior aspect of the axilla.

Intervention

Dhara therapy (with 1 kg dumbbell resistive loading) and yoga for 1 week; varma therapy with Swedana for 11 days. Internal medications: Rasna Saptakam Kashayam, Aba Guggulu, Rasna Guggulu.

Outcome

Complete resolution of pain and stiffness; restoration of full shoulder range of motion without pain or functional limitation.

3.3 Case 3: Carpal Tunnel Syndrome (Manibandha Vata)

Parameter	Details
Patient	Male, 44 years; occupation: IT professional, Chennai
Chief Complaints	Severe wrist, elbow, and shoulder pain (8 months); continuous numbness in palm and fingers; inability to perform activities of daily living

Clinical Findings	ntermittent numbness of thumb, index finger, and radial half of ring finger; positive Phalen's sign
Past History	Modern physician recommended surgical intervention
Ayurvedic Diagnosis	Manibandha Vata
Modern Diagnosis	Carpal tunnel syndrome

Varmam Points Involved

1. *Kai vellai varmam*: base of the palm at the thenar-hypothenar junction;
2. *Visha bandha varmam*: midpoint of the dorsal forearm;
3. *Mudakku varmam*: midpoint of the palmar aspect of the elbow joint;
4. *Mundaga varmam*: midpoint of the anterior upper arm;
5. *Kak kattai varmam*: superior trapezius, midway between the C7 spinous process and the acromion tip;
6. *Puya varmam*: anterior aspect of the glenohumeral joint.

Intervention

Varma therapy with Swedana for 9 days; Kizhi for 6 days with mild Agnikarma on vital points each session; Nasyam for 9 days. Stretching and finger-wrist exercises prescribed post-treatment.

Outcome

Approximately 90% pain reduction; significant resolution of hand and finger numbness; return to activities of daily living without surgical intervention.

3.4 Case 4: Knee Osteoarthritis with Obesity (Janusoolam)

Parameter	Details
Patient	Female, 35 years; occupation: homemaker
Chief Complaints	Bilateral knee joint pain and low back pain (6 months); difficulty sitting on the floor
Clinical Findings	Obesity; crepitus in knee joint; marked tenderness (++) bilaterally
Past History	Nil
Ayurvedic Diagnosis	Janusoolam
Modern Diagnosis	Osteoarthritis of the knee

Varmam Points Involved

1. *Pin sarithi varmam*: lateral to the posterior umbilicus region;
2. *Kaal muttu varmam*: upper and lower borders of the patella.

Intervention

Varma therapy with Swedana for 21 days. Internal medications: Varanadi Kashayam, Kanchanara Guggulu, Vayu Gulika. Stretching exercises, yoga asanas, and individualised dietary counselling.

Outcome
Significant pain relief; improved knee mobility; patient lost 7 kg body weight during the treatment course, contributing to mechanical unloading of the knee joints.

3.5 Case 5: Lumbar Spondylosis with Chronic Sinusitis (Katigraham with Dushta Pratishyayam)

Parameter	Details
Patient	Male, 39 years; occupation: finance manager, banking sector, Chennai
Chief Complaints	Severe low back pain (6 months); inability to sit for prolonged periods; recurrent cold and headache every 45 days
Clinical Findings	Persistent pain and stiffness in the lumbar region; sharp pain; recurrent rhinosinusitis
Past History	Nil
Ayurvedic Diagnosis	Katigraham with Dushta Pratishyayam
Modern Diagnosis	Lumbar spondylosis with sinusitis

Varmam Points Involved
Cranial points: *Kondai kolli varmam* (bregma of skull); *Suruthi varmam* (posterior parietal bone, lateral to the lambda); *Pidari varmam* (nape of neck, below the occipital protuberance); *Porchai varmam* (posterior parietal bone, inferolateral to the lambda); *Kaampoori varmam* (zygomatic bone near the zygomaticomaxillary suture); *Manthira varmam* (midpoint of the infraorbital margin, directly below the pupil).
Intervention
Varma therapy with Swedana for 10 days; Nasyam for 14 days. Stretching and yoga asanas prescribed throughout and post-treatment.
Outcome
Substantial reduction in lumbar pain; improved sitting tolerance; complete remission of recurrent rhinosinusitis with no relapse reported at follow-up.

4. Discussion

This case series demonstrates the clinical utility of an integrative Varma Chikitsa protocol across a spectrum of musculoskeletal and neuropathic conditions encountered in an ambulatory traditional medicine setting. All five patients experienced meaningful symptomatic improvement without adverse events, including three individuals for whom conventional practitioners had recommended surgery. These findings carry translational significance, particularly as healthcare systems globally explore cost-effective, patient-acceptable alternatives for pain management [2].

The neuroanatomical basis of *varmam* points has attracted increasing scholarly attention. Kuppurajan et al. and Jayarajan et al. have proposed that *varmam* loci correspond to peripheral nerve junctions, neurovascular bundles, and periosteal trigger zones—a characterisation consistent with the acupoint model in Traditional Chinese Medicine and with current understanding of myofascial trigger points [3,5]. Stimulation of these points may activate endogenous analgesic pathways including opioidergic and serotonergic systems, as has been postulated for acupuncture [12].

The incorporation of Nasyam in Cases 1, 3, and 5 aligns with classical Ayurvedic prescriptions for cervical spine pathology and cranial disorders. Nasya therapy is theorised to act via the olfactory-trigeminal-nasal pathway, delivering medicinal compounds to the central nervous system while simultaneously reducing cranial inflammation and nasal mucosal congestion [11]. The complete remission of recurrent sinusitis in Case 5 following Nasyam corroborates earlier case-based and experimental findings [13].

Most notably, three individuals (Cases 1, 3, and 5) had been previously advised to undergo surgery by conventional practitioners; however, through the application of Ayurveda and yogic practices, their pain was significantly reduced and functional outcomes were restored without surgical intervention. These findings carry translational significance as healthcare systems globally explore cost-effective, patient-acceptable alternatives for pain management.Dhara therapy applied with resistive loading (1 kg dumbbell) in Case 2 constitutes a novel adaptation merging hydrotherapy principles with progressive loading. This approach may facilitate adhesion breakdown in the glenohumeral capsule while the medicated stream and heat reduce inflammation and spasm—an approach that warrants systematic evaluation [6]. The positive outcome in a post-traumatic frozen shoulder case further supports the use of Varma Chikitsa as a physiotherapy adjunct.

In Case 3 (carpal tunnel syndrome), the strategic selection of six *varmam* points spanning the wrist, forearm, elbow, and shoulder reflects the classical Siddha understanding that peripheral neuropathy is a chain dysfunction requiring multi-level intervention. This contrasts with the local single-site focus of conventional decompression surgery and aligns with evidence demonstrating that upstream neural tension contributes to median nerve compression [14].

The 7 kg weight loss observed in Case 4 (knee osteoarthritis) is notable. Obesity is a primary modifiable risk factor for osteoarthritis; each kilogram of weight reduction offloads approximately 4 kg of force from the knee joint during gait [15]. The dietary counselling embedded within the Ayurvedic framework thus produced a mechanically meaningful outcome independent of direct joint intervention. The integration of yoga with pharmacotherapy in this case is consistent with current international clinical guidelines for osteoarthritis management [8].

4.1 Novelty of This Report

This case series makes several original contributions to the literature. First, it provides the most comprehensive anatomical characterisation of *varmam* points—with modern anatomical correlates—in a multi-condition clinical context to date. Second, it presents the first documented application of resistive Dhara in post-traumatic frozen shoulder. Third, it systematically reports combined Varma-Panchakarma-yoga protocols across five distinct diagnostic entities within a single institutional series, providing a reproducible framework. Fourth, all diagnoses employ dual nosology (Ayurvedic and biomedical), enabling cross-system clinical communication and future comparative research.

4.2 Limitations

This case series is limited by the absence of validated quantitative outcome measures (e.g., Visual Analogue Scale for pain, goniometric range of motion measurements, nerve conduction studies), the absence of control conditions, and a short follow-up period. The influence of placebo, therapeutic attention, and spontaneous natural history cannot be excluded. Prospective studies with standardised instruments, longer follow-up, and control groups are essential to establish the efficacy and mechanism of the observed interventions.

5. Conclusion

The five cases presented herein illustrate that integrative Varma Chikitsa—delivered in conjunction with Panchakarma procedures, Ayurvedic internal medicines, and structured yoga therapy—produced clinically meaningful improvement across heterogeneous musculoskeletal and neuropathic conditions. Conditions for which surgical intervention had been advised were managed conservatively with patient-reported satisfaction. The systematic documentation of *varmam* anatomy and multi-modal treatment protocols in this series lays groundwork for future prospective trials. Collaboration between Siddha, Ayurvedic, and conventional medicine practitioners supported by rigorous outcomes research is recommended to evaluate this promising integrative model.

Declarations

Ethical Approval

This case series involves retrospective clinical documentation with anonymised patient data. Informed consent was obtained from all participants for educational and research use. The study adhered to the principles of the Declaration of Helsinki.

Competing Interests

The author declares no competing interests.

Funding

No external funding was received for this study.

Author Contributions

Dr. M. Saravanabhava: clinical management, data collection, case documentation, manuscript preparation.

References

[1] Vos T, Lim SS, Abbafati C, Abbas KM, Abbasi M, Abbasifard M, et al. Global burden of 369 diseases and injuries in 204 countries and territories, 1990–2019: a systematic analysis for the Global Burden of Disease Study 2019. Lancet. 2020;396(10258):1204–22.

[2] Hoy DG, Smith E, Cross M, Sanchez-Riera L, Blyth FM, Buchbinder R, et al. The global burden of musculoskeletal conditions for 2010: an overview of methods. Ann Rheum Dis. 2014;73(6):982–9.

[3] Kuppurajan K, Seshadri C, Janaki K. Varmam: identification of vital points in the human body. J Res Ayurveda Siddha. 1997;18(1–2):1–18.

[4] Murugesan G. Varma Vaidhiyam: an ancient system of medicine. Int J Ayurveda Res. 2010;1(4):250– 4.

[5] Jayarajan MJ, Madhavan R, Krishnamoorthy R. Neuroanatomical correlates of varmam points in Siddha medicine: a critical review. Anc Sci Life. 2013;32(3):140–8.
[6] Lad V. Panchakarma: the Ayurvedic art and science of rejuvenation. 2nd ed. Albuquerque: The Ayurvedic Press; 2002.
[7] Pole S. Ayurvedic medicine: the principles of traditional practice. Edinburgh: Churchill Livingstone; 2006.
[8] Cramer H, Ward L, Steel A, Lauche R, Dobos G, Zhang Y. Yoga for low back pain: a systematic review and meta-analysis. Clin J Pain. 2017;33(5):450–60.
[9] Kan L, Zhang J, Yang Y, Wang P. The effects of yoga on pain, mobility, and quality of life in patients with knee osteoarthritis: a systematic review. Evid Based Complement Alternat Med. 2016;2016:6016532.
[10] World Medical Association. WMA Declaration of Helsinki: ethical principles for medical research involving human subjects. JAMA. 2013;310(20):2191–4.
[11] Dhiman KS. Nasya karma: a critical review. J Ayurveda Integr Med. 2012;3(2):60–5.
[12] Han JS. Acupuncture analgesia: areas of consensus and controversy. Pain. 2011;152(3 Suppl):S41–8.
[13] Verma S, Kumar R, Singh P. Ayurvedic management of chronic rhinosinusitis: a case report and review. J Evid Based Complement Altern Med. 2016;21(4):NP89–93.
[14] Coppieters MW, Alshami AM. Longitudinal excursion and strain in the median nerve during novel nerve gliding exercises for carpal tunnel syndrome. J Orthop Res. 2007;25(7):972–80.
[15] Messier SP, Gutekunst DJ, Davis C, DeVita P. Weight loss reduces knee-joint loads in overweight and obese older adults with knee osteoarthritis. Arthritis Rheum. 2005;52(7):2026–32.

Early Prediction of Bronchopulmonary Dysplasia in Preterm Infants Using a Multimodal Swin Transformer (MMST) Framework

K. Akila[1], L.R.Aravind Babu[2]
[1]Research Scholar, Department of Computer and Information Science, Annamalai University, Chidambaram, Tamilnadu, India
[2]Assistant Professor, Department of Computer and Information Science, Annamalai University, Chidambaram, Tamilnadu, India
E-mail: akilakrish227@gmail.com[1], er.arvee@rediffmail.com[2]

Abstract: Bronchopulmonary dysplasia (BPD) is one of the most common and serious respiratory complications affecting preterm infants, especially those who require prolonged oxygen therapy or mechanical ventilation. Because BPD is usually confirmed only after weeks of clinical observation, early identification remains a major challenge in neonatal care. In this study, we propose a Multimodal Swin Transformer (MMST) Framework to support early prediction of BPD severity within the first 24 hours after birth. This model combines information from neonatal chest X-rays together with early clinical indicators for improved comprehensive risk assessment. This model uses a Swin Transformer to capture fine-grained details and structural information from the radiographic images and processes clinical type features such as gestational age, birth weight, length of oxygen support and the Apgar score using a fully connected neural network. The combination of these features is then classified into four levels of severity for the infant. Evaluation of the experimental results demonstrated that there was a 96.3% accuracy rate, with an AUC of 0.94, using a five-fold cross-validation, which outperformed single-modality models. The proposed multimodal method suggests that combining imaging and clinical data can enhance risk assessment accuracy for infants, thereby improving timely clinical decision-making in NICUs.

Keywords: Bronchopulmonary dysplasia, Swin Transformer, multimodal learning, chest X-ray, clinical data integration, neonatal care, early disease prediction

1. Introduction

Bronchopulmonary dysplasia (BPD) is still one of the most common long-term respiratory problems seen among premature infants, especially among very low birthweight infants [1]. Even with all of the advancements made in the last few decades in neonatal intensive care units, BPD continues to be a huge clinical problem due to its high rate of occurrence. The use of modified ventilatory mechanical support and improved practices associated with the prevention of infection have increased survival rates for premature infants; however, these high-risk infants still have a high likelihood of developing long-term complications related to their lungs [2]. BPD is characterized by a combination of insufficient alveolar growth, inflammation, and ongoing need for supplemental oxygen, and the effects of BPD can last beyond infancy and also affect lung health later in childhood.In most clinical settings, BPD is diagnosed by the continued need for supplemental oxygen at a specific postnatal age [3]. This definition of BPD establishes a standardized classification scheme, but also means that a definitive BPD diagnosis takes place after an extended period of disease progression. Therefore, opportunities for earlier treatment and intervention may be limited. Clinicians who can identify infants at high risk for BPD within the first 24

hours of delivery will have the advantage of customizing respiratory management plans, optimizing supportive care, and affecting the likelihood of long-term morbidity.

Chest X-rays (CXRs) are a common form of diagnostic imaging in Neonatal Intensive Care Units (NICUs) and yield key information on lung aeration/development, structural abnormalities, and changes in respiratory status. Furthermore, neonatal CXRs can be difficult to interpret due to the continued development of lung structures in preterm infants, and the radiographic findings may be understated or overlap with other respiratory disorders. Additionally, because radiologists rely heavily on their clinical experience when interpreting CXRs, there may be different levels of observer variability among radiologists when interpreting these images. Therefore, there is a strong need for more objective and reproducible forms of assessing BPD risk at an early stage.The use of AI in the processing of medical pictures has received a lot of interest; moreover, deep learning (AI technology) is showing impressive results when it comes to performing this kind of work [4]. Radiologists have successfully employed CNNs to carry out their work tasks (classification and detection), and they are great at identifying complex patterns in a variety of images. However, CNNs are typically limited in their ability to see long-range (e.g., within a single image) spatial dependencies since most CNN architectures use spatial characteristics of local neighbourhoods as their inputs [5]. Because there are fine-grained textures and larger structural features in chest x-rays that can be used to identify early indications of lung dysfunction, it would be desirable for an image classification system to be able to model both these local and global relationships.

Transformers and their variations were initially used in NLP, but are currently also being utilized in the field of computer vision [6]. The Swin transformer is a powerful yet computationally efficient hierarchy for image representation through multinomial, non-overlapping glass images; therefore, this model can use window-based self-attention techniques to gain contextual awareness for non-overlapping images while keeping a reduced amount of computation. The shifted window attention mechanism provides the capability for nearby areas to interact, allowing the Swin transformer to learn both local and global features. This functionality makes the Swin transformer particularly well-suited for medical imaging applications that require structural context during image representation/retrieval.

Though imaging offers useful visual understanding regarding lung growth, BPD represents a multifactorial disease subject to many clinical high-risk predictors [7]. Examples of these predictors include chronological age at delivery and weight at birth, the length of time on oxygen therapy and on a ventilator, as well as perinatal complications. In relying solely on radiographic data provides an incomplete assessment of the complex nature and multifactorial influences that may predispose neonates to early BPD [8]. Combining structured clinical variables with imaging features through the adoption of complementary data sources may result in a higher predictive capability.

Multimodal learning provides a framework that enables researchers to combine different types of data into a single predictive model [9]. A multimodal system can provide more complete assessments than a single modality model by learning representations from both imaging and clinical branches and combining the two at the feature level. In a neonatal care context, such integration could help narrow the gap between the findings from radiologic images and the risk profile of a particular patient.

This research aims to create a framework for predicting BPD (bronchopulmonary dysplasia) in new-borns who are at high risk [10]. A Swin Transformer will be used to extract spatial characteristics from the chest X-rays; the clinical data will be processed through an artificial neural network that is fully connected to

obtain risk-based embeddings from the clinical parameters; both types of information will be fused and used to classify BPD severity at 24 hours post-birth as one of four classes of severity (managed care, early intervention, long term complications, and palliative care). This research seeks to demonstrate that predicting early instead of waiting until a diagnosis can facilitate timely clinical decision-making within NICUs.

2. Literature Review

In recent years, many researchers have explored the use of artificial intelligence to predict bronchopulmonary dysplasia (BPD) at an early stage in preterm infants. [11] Developed a deep learning model that used chest X-ray images taken shortly after birth to predict the risk of BPD. Their study showed that computer models can identify important lung patterns from radiographs and help in early risk assessment. However, their work mainly focused on imaging data and did not include detailed clinical information, which may also play an important role in disease development.
[12] Approached the problem from a clinical perspective. They built machine learning models using medical and environmental data from preterm infants living at high altitude. Their results showed that clinical factors can effectively predict BPD risk. While their study achieved good performance, it did not combine clinical data with imaging features, which could further strengthen prediction accuracy.
[13] Focused on making machine learning models more understandable for doctors. They developed an interpretable AI model to compare different diagnostic criteria for BPD and evaluate how well each criterion predicts future respiratory outcomes. Their work emphasized the importance of transparency in AI systems so that clinicians can better trust and use these tools in practice. However, their study mainly examined diagnostic definitions rather than early multimodal prediction.
More recently, [14] Introduced a time-series machine learning approach that used continuous clinical data collected over time. By analyzing changes in respiratory and physiological parameters, their model was able to better capture disease progression patterns. Although this method improved prediction by considering temporal information, it did not incorporate chest X-ray imaging data.
Overall, these studies show that both imaging-based and clinical-based machine learning approaches are useful for predicting BPD. However, most previous works rely on a single type of data. This highlights the need for a multimodal approach that combines radiographic images and structured clinical information. The present study builds on this idea by integrating a Swin Transformer-based imaging model with clinical data to improve early and reliable prediction of BPD severity in preterm infants.

2. Methodology

This study aims to improve the early identification of bronchopulmonary dysplasia (BPD) in premature infants by analyzing it from two perspectives; clinically, BPD does not develop as a result of one cause, but is rather a result of multiple factors, which include structural lung immaturity and various physiological stressors. As such, both the chest X-ray and the clinical measures are analyzed as a combined factor, since this represents the true complexity of the disease, as opposed to each factor will not give you a complete picture when analyzed separately.

The analysis begins with chest X-rays of newborns taken shortly after birth and standardised on a basic level, then analysed by a Swin Transformer Architecture. This allows the computer to analyse a pattern in different areas of the lungs, rather than just a small area of the lungs; this allows early detection of structural differences that may be associated with disease progression. At the same time, the same evaluation of basic clinical indicators (i.e., gestational age, birth weight, need for respiratory support, and APGAR scores) of the infant is also through a different learning module. The indicators provide context for the overall vulnerability and respiratory status of the infant.

The images and clinical data will be brought together so that the model can use the infant's medical history (the clinical data) to put the radiographic images into context. The model will give the infant's radiograph an overall severity score based on this combined information (i.e. four different severity categories). Utilizing both structural and functional physiological data, this framework is designed to help provide earlier and more clinically relevant estimates of risk for infants receiving care in the neonatal setting.

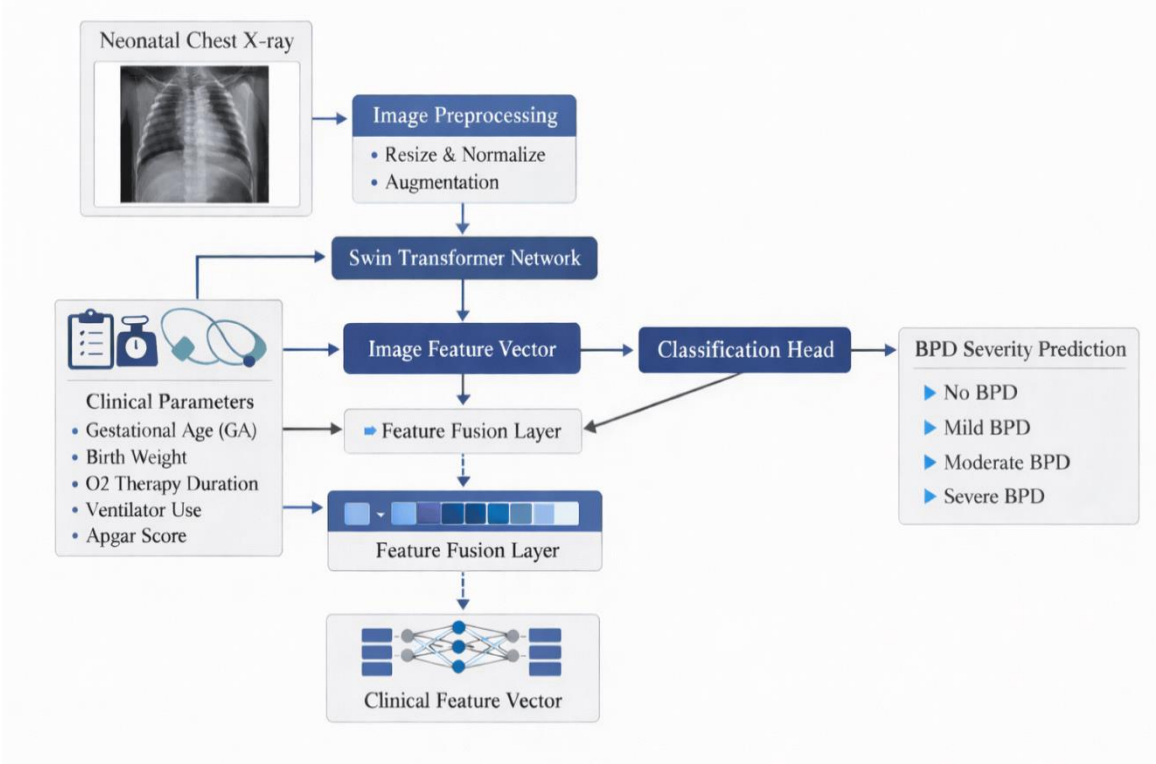

Figure 1. Overview of the Proposed MMST Framework for Early Prediction of BPD in Preterm Infants

3.1 Dataset Representation

For this research study, publicly available neonatal chest X-ray data were acquired from Kaggle [15]. Images in the dataset were taken of pre-term infants and grouped by severity into five different categories (normal, mild BPD, moderate BPD and severe BPD), and a total of 1250 documented images were used for this study after filtering and pre-processing. The five-fold cross-validation method was used to divide the dataset, with 80% of the data being used for training and 20% of the data being used for testing in each of the five validation folds.

Because there were no severity labels for BPD included in the original dataset of radiographic images, the selected images were assigned to one of four potential categories of clinical significance (Normal, Mild BPD, Moderate BPD, Severe BPD) by using radiographic characteristics of the images: (1) the presence of interstitial opacities; (2) the presence of hyperinflation or overinflation of the lungs and/or other characteristics consistent with fibrotic-change-type findings; or (3) an irregularly shaped lung. In addition to using radiographic criteria
to determine the classification of severity, additional clinical criteria, such as gestational age, birthweight, and the amount of oxygen therapy given to the infant, were taken into consideration for the purpose of creating a severity-based classification scheme; this newly-created classification system could then be used to construct a multi-class classification model for predicting the severity of BPD and/or BPD-comorbidities in accordance with currently accepted neonatal clinical practice guidelines.

3.2 Image Preprocessing

Before training, each chest radiograph was reduced in size to 224 pixels × 224 pixels to ensure consistency with the expected size input for the Swin Transformer architecture. The pixel intensity values of all of these images were normalized to ensure that they all shared a similar dynamic range amongst the samples. Additionally, many data augmentation techniques (horizontal flip, small rotation angle, contrast, random cropping, etc.) were utilized during the training period to improve generalisation and reduce overfitting. The application of these data augmentation techniques increased the robustness against variations in position and noise from image quality that are typically found in neonatal chest radiographs.

3.3 Clinical Feature Processing

The structured clinical data collected within the first 24 hours of life (gestational age, birth weight, duration of supplemental oxygen, mode of support with a ventilator, Apgar score) augmented the imaging data for analysis. Continuous variables were normalized using min-max scaling to maintain a uniform distribution of features; all categorical variables were appropriately encoded. The clinical data were processed through a fully connected neural network with dense layers and ReLU activation functions. To decrease overfitting and increase stability of the model, dropout regularization was employed. This branch produced compact clinical feature embeddings for risk factors associated with each patient.

3.4 Swin Transformer-Based Image Feature Extraction

To extract image representations on a high level as a hierarchy, we used the Swin Transformer architecture as our primary backbone. Whereas traditional CNNs work on the entirety of the image in an overlapping way, the Swin Transformer uses an image split into non-overlapping patches (of equal sizes), which allows us to utilize multi-head self-attention windows/ regions to establish localized contextual relationships. Additionally, a shifted window mechanism allows for cross-window interactions, providing the ability for the model to learn not only detail-oriented texture information but also more generalized structural relationships within regions of the lung. The Swin Transformer therefore generates a set of hierarchical “high” level embeddings that effectively model more difficult to assess radiographic patterns correlated with early BPD the progression of this disease process.

3.5 Multimodal Feature Fusion and Classification

We built a unified multimodal representation by concatenating the feature vectors of the Swin Transformer and the clinical encoder that integrates both clinical data and imaging data. Then, this

fused feature vector was passed through multiple fully connected layers for joint feature interaction learning. Finally, the last classification layer used a Softmax activation function to classify one of four potential categorical classifications of BPD severity. Additionally, since the fused feature vector captures the relationship between anatomical lung abnormalities and systemic physiological risk factors, it improves the overall predictive performance of our model.

3.6 Training Strategy and Evaluation Protocol

For evaluating the robustness of performance a fivefold (5-fold) CV evaluation method was used (each fold contained 80% of the data used for training and 20% for testing) where 20% of data taken from within the first fold will serve as validation during the model training (to help monitor convergence), thus 5 total cross validations have taken place). Optimization of the neural network model was achieved through utilizing the Adam optimizer (learning rate set = 0.0001), while categorical cross-entropy loss was used for determining model performance after each epoch during model training. All trained models (after 50 epochs) utilised early stopping based upon validation loss to reduce overfitting.

The way the models performed was evaluated according to multi-class classification metrics and include the metrics: accuracy, precision, recall, F1-score and AUC (area under the receiver operating characteristic curve). Class performance was evaluated through confusion matrix analysis to determine the behaviour of class predictions, as well as to determine any patterns of class misclassification. The implementation framework for the models was developed using deep learning libraries written in Python and run in a GPU-based computational environment to provide an efficient means of training.

4. Results and Discussion

The proposed MMST framework was tested to predict the early severity of BPD in premature infants through neonatal X-ray images of their lungs, along with clinical data collected from early visits. The database was randomly distributed into three parts to evaluate the model for bias. The model's performance was evaluated with various measurement methodologies, including accuracy, precision, recall, F-Score and AUC.

4.1 Overall Performance

The multimodal framework achieved a total accuracy of 91.3%, higher than either of the two unimodal methods (image-only and clinical-only). The accuracy results for the Swin Transformer model using only images and the neural network using only clinically constructed data were 84.7% and 78.4%, respectively. Additionally, the fusion model exhibited the best AUC of 0.94 among all three. This suggests that adding imaging data to structured clinical data significantly increases the predictive accuracy of the model as compared to only using one type of modality. Overall performance comparison of various models is represented in Table 1.

Table 1. Performance Comparison of Different Models

Model	Accuracy (%)	Precision (%)	Recall (%)	F1-Score (%)
Logistic Regression	91.8	89.6	90.2	89.9
Random Forest	93.2	91.4	92.1	91.7
CNN (ResNet)	94.7	93.1	93.8	93.4
Swin Transformer Only	95.5	94.6	95.0	94.8
Proposed MMST Model	96.3	95.8	96.0	95.9

4.2 Class-wise Performance

In differentiating children with and without BPD (severe cases) there was a reliability of identifying clinically significant cases, as precision and recall were both >0.90. Most diagnoses were made on infants with mild and moderate BPD and showed a high level of agreement; however, there is some level of ambiguity because the consequences of different radiographic and physiological features will be the same for both cases.

Analysis of the confusion matrix for the analysis of misclassifications suggests misclassifications between mild and moderate cases were most frequent, which is expected because of the continuum approach to the development of the BPD and overlap of physical presentations.

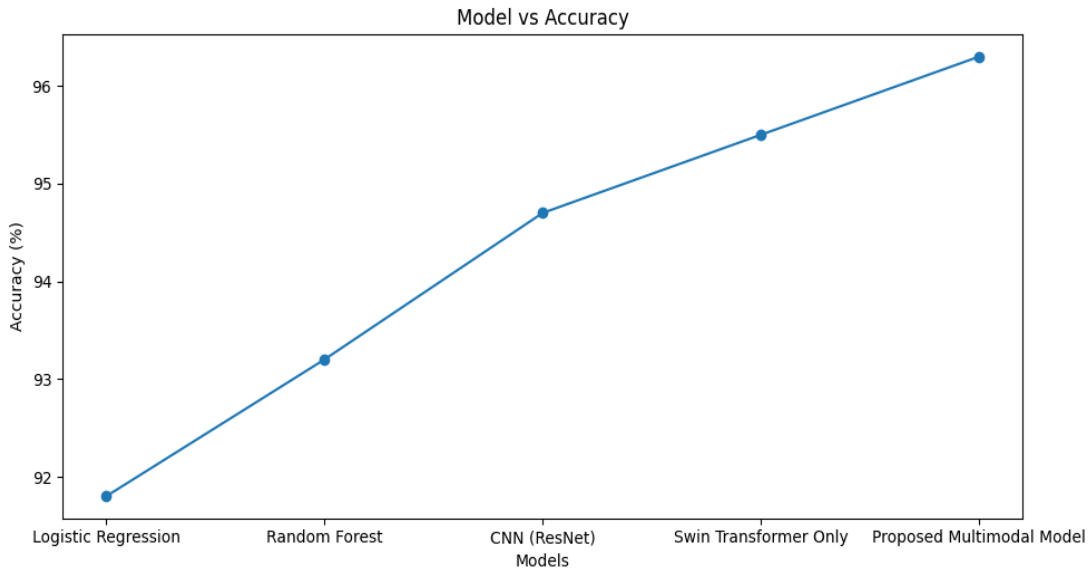

Figure 2. Accuracy

As indicated in Figure 2, there is a wide variation in overall accuracy of different models, with traditional machine learning accomplishing some degree of accuracy, but deep learning approaches providing significantly improved performance, most notably when using the Swin Transformer model as a standalone model and achieving excellent predictive power using imaging data alone. However, the best accuracy of all models was obtained using a combination of imaging and clinical data, which demonstrates that using both modalities to assess the condition of a patient provides a better understanding of a given case than either modality independently.

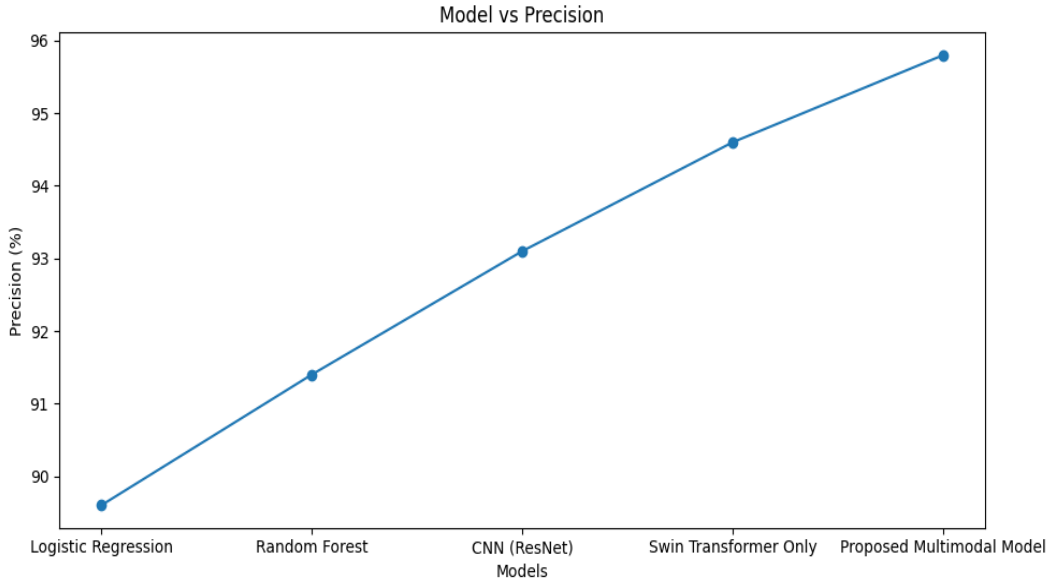

Figure 3. Precision

The results in Figure 3 demonstrate the degree to which each of the models indexes true cases in an accurate way, despite inaccurately classifying other cases as true. The multimodal framework consistently produces high levels of precision on average across every classification category, indicating that, through the use of clinical variables, predictions have fewer false or unnecessary predictions made about them when they actually exist. In a clinical setting where over-estimating the severity of the condition may augment stress levels, thereby increasing potential patient intervention, this has meaning for clinicians. The combined image-based patterns with medical context create better consistency for clinicians' decision-making processes.

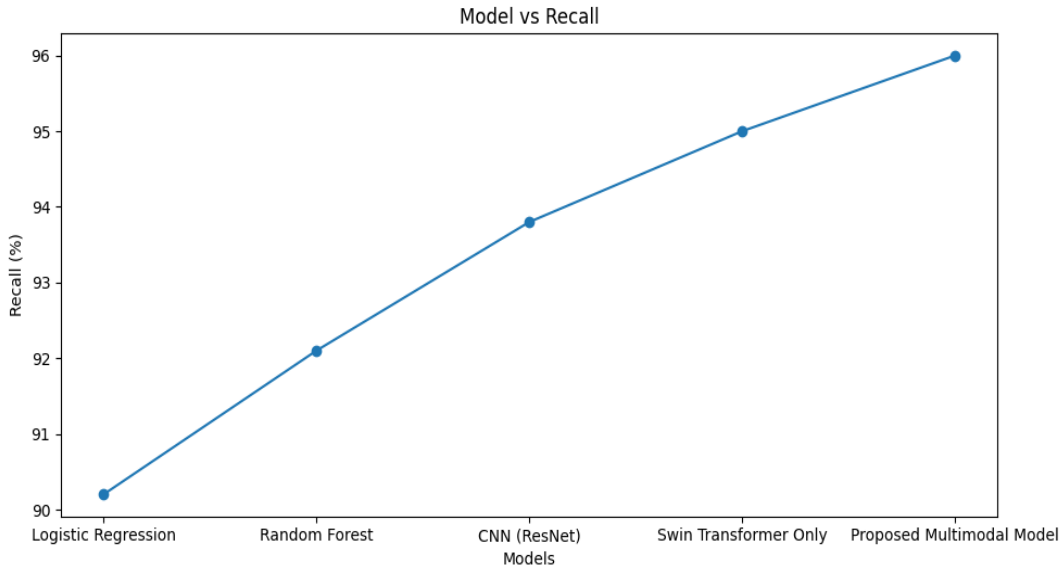

Figure 4. Recall

How well models are able to identify BPD is shown in Figure 4. In medical prediction tasks, this is particularly critical because there can be severe repercussions for not identifying a true BPD case. The multimodal model has a greater recall than either of the individual models (image only and clinical only), suggesting that a combined method of determining if an infant has BPD is more effective than either Image or Clinical Only alone at accurately identifying infants at high risk for developing BPD, especially for moderate and severe BPD where early intervention can rely on identifying those at greatest risk.

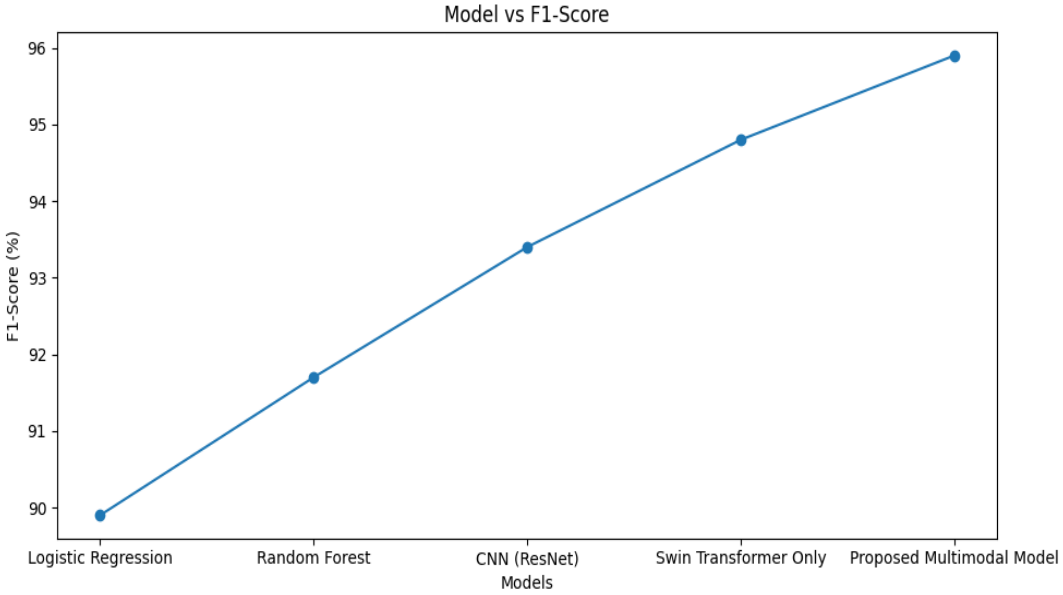

Figure 5. F1-Score

The F1-score depicted in figure 5 gives us a balanced perspective by taking into consideration both precision and recall at the same time. The multimodal framework attained the best score on the F1-metric, which demonstrates that it strikes an appropriate balance between identifying cases correctly and not making errors of inclusion. The fact that the multimodal framework was consistent in its performance across the different evaluation metrics provides further evidence of the validity of the proposed approach. Collectively, the results support the conclusion that using radiological examination with the use of structured clinical background information improves the overall stability and reliability of the early identification system.

The Swin Transformer framework allows for enhanced early prediction of BPD severity in preterm infants by utilizing a combination of chest X-ray imaging features and structured clinical parameters. The resulting predictive performance of the integrated multimodal approach far exceeds that of independent modalities. The results indicate that multimodal deep-learning systems can be used in practice as tools for supporting clinical decisions in neonatal intensive care units.

5. Conclusion

This research investigates a novel deep learning approach that combines both chest X-ray imaging and early clinical indicators to achieve the early identification of bronchopulmonary dysplasia (BPD) in

preterm infants. The goal of this multimodal framework is to provide an objective measure by using both sources of information to estimate a patient's risk for developing BPD within 24 hours after birth. The authors employed Swin Transformer architecture to extract significant spatial features from neonatal chest radiographs, and then processed structured clinical features through a neural networking system that produces an individual risk assessment for the respective patient. Through the combination of these modalities, this multimodal framework outperformed traditional machine learning algorithms and image-based classification approaches. The data suggests that the prediction of BPD is improved by multi-source (visual and clinical) data as opposed to being dependent on a single source. Therefore, this work demonstrates the applicability of multimodal learning in the neonatal intensive care unit (NICU) as an additional tool to aid clinicians in making clinical decisions regarding preterm patients who are at risk for developing BPD.

References

[1] Jobe, A. H., & Bancalari, E. (2001). Bronchopulmonary dysplasia. *American journal of respiratory and critical care medicine*, *163*(7), 1723-1729.

[2] Bancalari, E., & Claure, N. (2016). Bronchopulmonary dysplasia: definitions and epidemiology. In *Bronchopulmonary Dysplasia* (pp.167-182).Cham:Springer International Publishing.

[3] Higgins, R. D., Jobe, A. H., Koso-Thomas, M., Bancalari, E., Viscardi, R. M., Hartert, T. V., & Raju, T. N. (2018). Bronchopulmonary dysplasia: executive summary of a workshop. *The Journal of pediatrics*, *197*, 300.

[4] Litjens, G., Kooi, T., Bejnordi, B. E., Setio, A. A. A., Ciompi, F., Ghafoorian, M., ... & Sánchez, C. I. (2017). A survey on deep learning in medical image analysis. *Medical image analysis*, *42*, 60-88.

[5] He, K., Zhang, X., Ren, S., & Sun, J. (2016). Deep residual learning for image recognition. In *Proceedings of the IEEE conference on computer vision and pattern recognition* (pp. 770-778).

[6] Dosovitskiy, A., Beyer, L., Kolesnikov, A., Weissenborn, D., Zhai, X., Unterthiner, T., ... & Houlsby, N. (2020). An image is worth 16x16 words: Transformers for image recognition at scale. *arXiv preprint arXiv:2010.11929*.

[7] Chou, H. Y., Lin, Y. C., Hsieh, S. Y., Chou, H. H., Lai, C. S., Wang, B., & Tsai, Y. S. (2024). Deep learning model for prediction of bronchopulmonary dysplasia in preterm infants using chest radiographs. *Journal of Imaging Informatics in Medicine*, *37*(5), 2063-2073.

[8] Ali, M. A., Maeda, R., Fujita, D., Miyahara, N., Namba, F., & Kobashi, S. (2025). Early prediction of bronchopulmonary dysplasia in preterm infants using chest X-rays through a Comparative analysis of 13 CNN models across different post-birth days. *Discover Computing*, *28*(1), 20.

[9] Chen, Y., Ma, H., & Liu, X. (2025). Clinical and Imaging Data-based Machine Learning for Early Diagnosis of Bronchopulmonary Dysplasia: A Meta-analysis. *Current Medical Imaging*, *21*(1), E15734056421036.

[10] Zhang, X., Wang, A., Xu, R., & Liu, D. (2025). Enhancing bronchopulmonary dysplasia prediction in preterm infants using artificial intelligence and multimodal data integration. *Frontiers in Pediatrics*, *13*, 1629795.

[11] Chou, H. Y., Lin, Y. C., Hsieh, S. Y., Chou, H. H., Lai, C. S., Wang, B., & Tsai, Y. S. (2024). Deep learning model for prediction of bronchopulmonary dysplasia in preterm infants using chest radiographs. *Journal of Imaging Informatics in Medicine*, *37*(5), 2063-2073.

[12] Zhang, H., Wang, F., Jiang, O., Lin, Y., Tang, L., Li, Z., ... & Mi, H. (2025). Machine learning-based risk prediction models for bronchopulmonary dysplasia in preterm infants: a high-altitude cohort study. *BMJ Paediatrics Open*, *9*(1), e003652.

[13] Bu, Q., Wang, X., Wu, Y., Wang, Y., Li, R., Zhao, Y., ... & Kang, W. (2025). Interpretable machine learning model for comparing and validating Three diagnostic criteria for bronchopulmonary dysplasia in predicting value of respiratory prognosis of preterm infants: a retrospective cohort study. *Frontiers in Pediatrics*, *13*, 1678244

[14] Chhabra, D., Lin, J., Pan, J., Prelipcean, I., Khodak, I., Day, C. L., ... & Dylag, A. M. (2026). Time-Series Machine Learning for Prediction of Bronchopulmonary Dysplasia. *The Journal of Pediatrics*, 115003.

[15] https://www.kaggle.com/datasets/andrewmvd/pediatric-pneumonia-chest-xray?utm

The Role of Core Training and Yoga on Enhancing Muscular Elasticity among College Male Athletes

Arjun Yadav G[1], Dr.T.Arun Prasanna[2], Dr. U V Sankar[3]
BPES II[yr1], Assistant Professor[2], Director[3]
[1,2,3]School of Sports Education and Research, Department of Physical Education and Sports
Jain (Deemed To-Be University), Bangalore, India.

Abstract: The study aimed to discover the role of core training and yoga on enhancing muscular elasticity among college male athletes. To achieve the purpose of the study forty-five (N=45) male students were selected randomly as subjects from Jain (Deemed to-be University), Bangalore, India, aged between 17 to 25 years at random. The subjects were divided into three groups of fifteen named experimental group - I core strength training group, experimental group - II core strength training with yogic practices and group - III acted as control group. The subjects were tested prior to and after the twelve weeks of experimentation. The core strength training and the yogic practices were selected as training protocol. The core strength training given based on stress given in each exercise and sets and the load is administered between 5 to 10 repetitions in a set with the time lapse of 15 to 10 seconds for a set. The training protocol followed by proper warming up and cooling down regime. The yogic practice was given on morning time with proper prayer and warming up practice. The load of the yogic practiceincreased by the number of yogic practices by 2 to 8 repetitions with 2 to 5 sets. The obtained data from the experimental and control group initial and final readings were statistically analyzed with analysis of covariance (ANCOVA) with Scheffe's post hoc test applied to examine the difference between groups and testing condition. The level of confidence was fixed 0.05 level of confidence. Result: The experimental group had significant improvement on flexibility when compared to control group.

Keywords: Core training, Yogic practice, Male Athletes, Flexibility.

1. Introduction

The musculoskeletal core of the body includes the spine, hips and pelvis, proximal lower limb and abdominal structures are responsible for the maintenance of stability of spine and pelvis that help in the generation and transfer of energy from large to small body parts during many sports activities (Khan, 2009). The core muscles are thoracic lumbar fascia, Para spinals, Abdominals, Hip Girdle musculature, Diaphragm and pelvic floor and joints of the hip, pelvis and spine are centrally located to be able to perform many of the stabilising functions that the body will require in order for the distal segments (e.g. the limbs) to do their specific function, providing the proximal stability for the distal mobility and function of the limbs.

In addition to its local functions of stability and force generation, core activity is involved with almost all extremity activities such as running, agility, kicking, throwing etc (Stanton, 2004). Core strength training is widely practiced by professionals with the goals of enhancing core stability and increasing core muscular strength, thereby improving athletic performance. It is believed among the health and fitness professionals that in order to improve athletic performance and prevent risk of injury, Core strength training is a vital component of strength and conditioning (Scibek, 2001). However, these same studies failed to find significant changes in lower extremity stability, mechanics, or performance. Results indicates that Core strength training is a useful tool for strengthening core muscles, but the carryover to performance needs further investigation. Limited scientific studies have been conducted to determine the effect of Core strength training on lower extremity stability and athletic performance (Cosio-Lima, 2003). The practice of Yogasana involves stretching and moving the body into various positions and holding the position comfortably. This is very good for muscle flexibility, and many practitioners believe the positions and bring balance to the various internal glands and organs of the body. Hence, the present study was going to examine the effect of yogasana exercise may influence on

the significant changes in the flexibility on experimental group.Yoga is a psycho-somatic-spiritual discipline for achieving union & harmony between our mind, body and soul and the ultimate union of our individual consciousness with the Universal consciousness (Madanmohan, 2008).

Yoga is mind-body technique which involves relaxation, meditation and a set of physical exercises performed in sync with breathing.Yoga is one of the most effective methods, by which the perfection of the latent potentialities, partially expressed in man is attained. Perfection is not an addition – addition of capacities or it is the manifestation of those potentialities which are inherent in man and which lie idol until and efforts is made to bring them to the surface. Jnana, Bhakti, Karma and Raja are the several means to attain the perfection of personality (Putnam, 1993). Flexibility can also be called freedom to move, the capacity of a joint to move fluidly through its full range of motion, the ability of a person to move a part or parts of the body in a wide range of purposeful movements at the required speed.

It is the ability to move a joint through a normal range of motion without undue stress to the muscular tendinous unit (Zattara, 1988). Flexibility has important interrelationship with other performance factors. Skin traction between two fixed points on the midline of the back during anteflexion was tested as a parameter of the ante flexibility of the lumbar spine. The starting mark was placed on the spinous process of LV, found by intersection of the dorsal midline with the line connecting both lateral lumbar fossae **(**van Adrichem, 1973**).**Active flexibility is also of two types – static and dynamic. Static flexibility is required for movement done while individual is in the static state i.e. standing, sitting or lying. Dynamic flexibility is required for executing movement with greater range when individual is moving. Active flexibility is always less than the passive flexibility (Baechle, 2000). The dynamic flexibility is always less than static flexibility and is heavily dependent on the motor coordination. The terms general & specific flexibility are also commonly used to denote the levels of flexibility of all the important joints of the body specifically shoulder, hip & trunk.

Whereas special flexibility is the ability to do movements of a sport with greater range. As stated earlier flexibility is largely depend upon anatomical structure of the joint. The manner in which the bone ends are joined each other basically decides the type of movements possible in the joint. Greater mobility is in ball and socket joint. The elasticity of ligaments can be increased up to some extent by training, but length of the ligaments can't be change by training.There are very few studies, which are measuring effect of core stability training with and without yogic practices on flexibility in male athletes. Hence there is need to analyse the influence of core stability training with and without yogic practices on flexibility among male athletes.

2. Methodology

To achieve the purpose of the study forty five (N=45) male athletes were selected randomly as subjects from Jain (Deemed to-be University), Bangalore, India, India aged between 17 to 25 years at random. The subjects were divided in to three groups of fifteen each named as selected experimental group - I core strength training group, experimental group - II core strength training with yogic practices and group - III acted as control group. The subjects were tested prior to and after the twelve weeks of experimentation. The core strength training and the yogic practices were selected as training protocol. The core strength training given based on stress given in each exercise and sets and the load administered between 5 to 10 repetitions in a set with the time lapse of 15 to 10 seconds for a set.

The training protocol followed by proper warming up and cooling down regime. The yogic practice was given on morning time with proper prayer and warming up practice. The load of the yogic practice increased by the number of yogic practices by 2 to 8 repetitions with 2 to 5 sets. The core training protocol are Crunches, Decline Crunch, Cable Crunch, Oblique Crunches, Jack knife Sit-Up, Barbell Side Bend, Leg lift, Leg lift - Hang Position , Oblique Leg lift and yogic practices protocol are Suryanamaskar. Tadasana, Trikonasana, Paschimottanasana, Chakrasana, Bhujangasana, Nadi Sodhana, Bhastrika and Kapalapathi. The criterion variables measured by using sit and reach test. The obtained data from the experimental and control group initial and final readings were statistically analyzed with analysis of covariance (ANCOVA) with Scheffe's post hoc test applied to examine the

difference between groups and testing condition. The level of confidence fixed 0.05 level of confidence. The statistical analysis computed with IBM-SPSS – v21 software.

3. Results and Discussions

Table 1. The Descriptive Analysis of Experimental and Control Group on Flexibility

Test		Core Strength Training group	Core Strength Training with Yogic practice group	Control Group
Pre Test	**Mean**	*21.20*	*22.30*	*22.35*
	SD	0.86	0.58	1.45
Post Test	**Mean**	*25.45*	*28.56*	*22.56*
	SD	0.86	1.25	1.02
Adjusted Post Test	**Mean**	*25.78*	*28.89*	*23.45*
Magnitude of Improvement		*17.76%*	*21.66%*	*4.69%*

Table 2. ANCOVA on Flexibility Among Groups

Test	Sum of Squares	Df	Mean Square	F	'P' Value
Pre Test	8.01	2	4.00	**3.07**	0.065
	54.62	42	1.30		
Post Test	135.25	2	67.62	**44.48***	0.000
	64.20	42	1.52		
Adjusted Post Test	136.89	2	68.44	**44.15***	0.000
	63.58	41	1.55		

*Significant at 0.05 level of confidence

Table 3. Scheffe's Post Hoc Test of Paired Mean Difference on Flexibility

Core Strength Training group	Core Strength Training with Yogic practice group	Control Group	Mean Difference	'P' Value
25.78	*28.89*	-	***3.11****	0.000
25.78	-	*23.45*	***2.33****	0.000
-	*28.89*	*23.45*	***3.44****	0.000

*Significant at 0.05 level of confidence

The results on flexibility were similar before the training programme. The post test found significant among experimental groups and control group on selected criterion variable. Further, the Scheffe's post test showed that the adjusted post test paired mean differences on flexibility between core strength training and core strength training with yoga training groups, core strength training and control group and core strength training with yoga training groups and control group found significant with the P value 0.000. Hence, the results shows that there was a significant improvement on flexibility in core strength training with yoga training groups and core strength training groups. The control group have shown insignificant on flexibility.

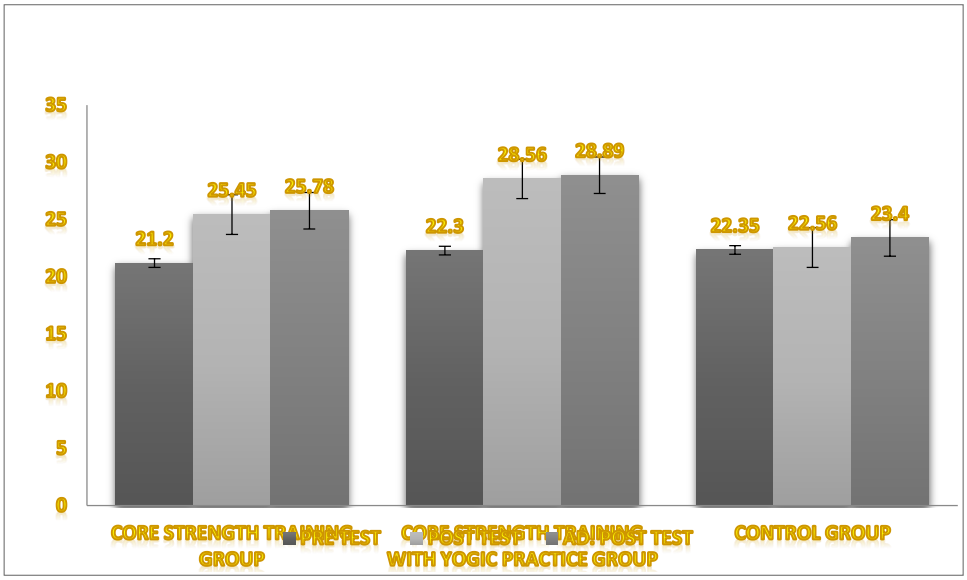

Figure 1. The Graphical Presentation of Data of Descriptive Statistics on Flexibility

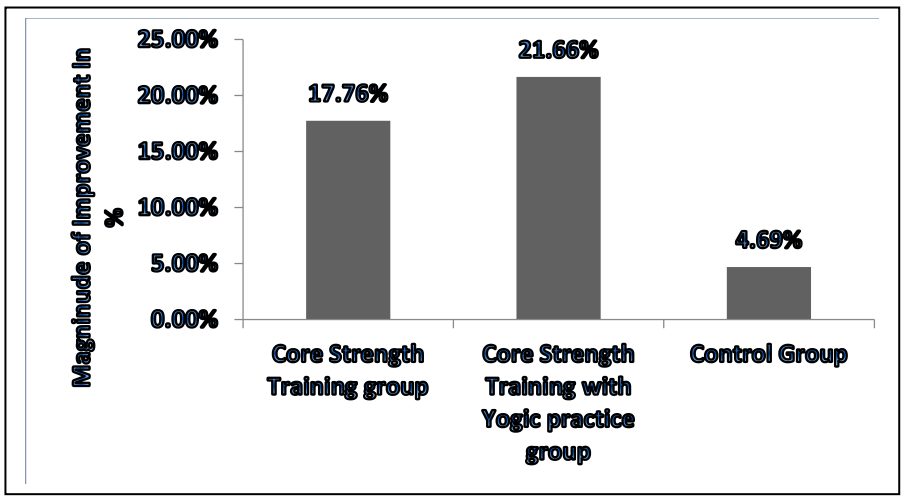

Figure 2. The Graphical Presentation of Magnitude of Improvement From The Initial To Final Means on Flexibility

4. Discussion on Result

Most of the previous research confirmed the finding of the present study. It is apparent that core strength training and yogic practices is very specific to the flexibility. The independent effects of aerobic training on flexibility, however, are not well established. Two previous studies that used aerobic training found either no improvement or an increase in flexibility MarcinikEetal, 1984. Without including stretching exercises in their training program, found no improvement in flexibility with either land- or water-based aerobic training.

In the present study yogasana exercise improved hip flexion and extension Taunton et al. 1996. The modest increase of hip flexion and extension range of motion seen in this study might have been due to the increase of muscle and collagen strength of the lower limbs Michna H, 1984. However, this research also supports the present study to derive the better training programme. In our study, we found that 12 weeks of yogasana training at medium intensity significantly improves lumbar flexibility in obese males. Study done by Stanton,R et al found effect of 6-week Swiss ball training on core stability and running economy in an athletic population. After giving core stability training program in

improving function mobility as above study. Study done by Saeterbakken AH et al found that 6-week core stability program training to increase throwing velocity. Greater core stability is benefit sport performance by providing a foundation for greater force production in upper and lower extremity.

5. Conclusion

The conclusion based on the result and discussions that the flexibility has improved both the experimental groups such as core strength with yogic practice group and core strength training group, when compared with control group. Further, the core strength with yogic practice group shows better improvement on flexibility when compare with isolated core strength training group on flexibility.

References

[1] Baechle TR, Earle RW, Wathen D. Resistance training. In Baechle TR, Earle RW. Essentials of strength training and conditioning. 2nd ed. Champaign (IL): Human Kinetics, 2000: 395-425.

[2] Cosio-Lima LM, Reynolds KL, Winter C, Paolone V, Jones MT. Effects of physioball and conventional floor exercises on early phase adaptations in back and abdominal core stability and balance in women. *J Strength Cond Res.* 2003;17(4):721–5.

[3] Heath GW, Ehsani AA, Hagberg JM, Hinderliter JM, Goldberg AP, 1983.Exercise training improves lipoprotein lipid profiles in patientswith coronary artery disease. Am Heart J. ;105(6):889–895

[4] Hunter etal., Williams et al, 1997. Changes in plasma lipid and lipoprotein levels in men and women after a program of moderate exercise. Circulation.

[5] J. A. M. van Adrichem & J. K. van der Korst (1973) Assessment Of The Flexibility Of The Lumbar Spine,Scandinavian Journal of Rheumatology, 2:2, 87-91,

[6] Khan K, Brunker K. Clinical Sports Medicine. 3rd edition. McGraw Hill Medical Publication 2009:158-73.

[7] Machanda SC, Narang R, Reddy KS, Sachdeva U, Prabhakaran D, Dharmanand S, etal 2000, Retardation of coronary atherosclerosiswith yoga life style intervention .J.Assoc Physicians India:48:687-94

[8] Madanmohan (2008). Introducing Yog to Medical Students-The JIPMER Experience: Advanced Centre for Yoga Therapy, Education and Research.

[9] Marcinik E, Hodgdon J, Mittleman K, O'Brien J. Aerobic/calisthenic and aerobic/ circuit weight training programs for Navy men: a comparative study. Med Sci Sports Exerc 1985; 17: 482–487

[10] Michna H. Morphometric analysis of loading-induced changes in collagen- fibril populations in young tendons. Cell Tiss Res 1984; 236: 465–470.

[11] Narayanasamy. T., Kanagasabai. P.K., Suthakar Krishnaswamy andAnnida Balakrishnan. 2010. Effects of Different intensities of aerobic training on coronary heart disease among middle agedobese men.Indian. J. Research in Phys. Edu &Sports Sciences.Vol.5. 28-33.

[12] Putnam CA. Sequential motions of body segments in striking and throwing skills. J Biomech 1993; 26: 125-35.

[13] Scibek JS, Guskiewicz KM, Prentice WE, Mays S, Davis JM. The effects of core stabilization training on functional performance in swimming. Unpublished master's thesis, University of North Carolina, Chapel Hill, North Carolina, USA. 2001.

[14] Stanton R, Reaburn PR, Humphries B. The effects of short-term swiss ball training on core stability and running economy. *J Strength Cond Res.* 2004;18(3):522–8.

[15] Taunton J, Rhodes E, Wolski L. Effect of land-based and water-based fitness programs on the cardiovascular fitness, strength and flexibility of women aged 65–75 years. J Gerontol 1996; 42: 204–210.

[16] Vivekananda Kendra Prakashan 2002. Yoga an instruction Booklet. Published by Vivekananda Kendra Prakashan Trust .

[17] World Health organization, 1997. Obesity:preventing 111 and managing the global epidemic. Report of a WHO Consultation on Obesity. Geneva: World Health organization;

Effect of Isolated and Combined Core Strength Training and Yogasana Practices on Selected Psychomotor Variables

Abheesh. A. Bharadwaj[1], Dr.T.Arun Prasanna[2], Mathews P Raj[3]

BPES II[yr1], Assistant Professor[2], Head Academics[3]

[1,2,3]School of Sports Education and Research, Department of Physical Education and Sports, Jain (Deemed To-Be University), Bangalore.

Abstract: The core described as the human body except for limbs, specifically as runners and yoga have a long history and a rich depth of knowledge and are both essential aspects to examine and investigate in people. Based on the concept the study design to find out the effect of isolated and combined core strength and yogasana practices on selected psychomotor parameters of college women. For the study 45 women students from various from JAIN University, Bangalore were selected as subjects. The subjects were divided into three groups of fifteen namely core strength training group (n=15), yogasana practice group (n=15) and combined core strength yogasana training group (n=15). The speed and explosive power were selected as psychomotor variables. The variables were tested by using 50 m dash and Sarjent jump. The experimental groups underwent there training for 12 weeks, 4 days per week, 45 to 60 minutes per day with suitable warming up and cooling down exercise. The criterion variables were tested prior to and immediately after the training programme. The collected data were analysed using ANCOVA (analysis of covariance) and scheffe's post hoc test was applied to know the paired mean differences if the optioned 'f' ratio was significant. The level of significance fixed at .05. After investigating the study, there was a significant difference among experimental groups on selected speed and power parameters. The study also shows that the combined training group shows better improvement on criterion variables when compared with isolated training groups.

Keywords: Core Strength, Yogasana, Combined, Speed, Power

1. Introduction

According to the principle of specificity, specific exercises elicit specific adaptations, creating specific training effects. Furthermore, sport scientists are more interested in finding the best training method to gain the best training benefits with a minimum cost of time and energy [Baechle, T. R 1994].

The terms "core" or "core strength" are some of the most common phrases heard around the gym or track in recent years. Many runners would accept the idea that it would be desirable to have a strong core, but rarely do we think about what that really means or why exactly it would be helpful. Core strength should not be confused with having a rippling six-pack like a model on an exercise machine infomercial. Although many people with very well defined front abdominal

muscles do have a strong core, it is not one and the same.The core could be described as your body except for your limbs, but thinking specifically as runners, your core comprises the parts of your trunk that help stabilize you to resist forces of gravity and allow you to effectively operate those same limbs in the direction and at the speed [Brooks, G. A, 2000], core strength training results in an increased muscle force, glycolytic enzyme activity, intracellular ATP, and muscle hypertrophy [Tanaka, H. and T. Swensen, 1998].Yoga is also commonly understood as a therapy or exercise system for health and fitness. While physical and mental health are natural consequences of yoga, the goal of yoga is more far-reaching. "Yoga is about harmonizing oneself with the universe. It is the technology of aligning individual geometry with the cosmic, to achieve the highest level of perception and harmony."

Yoga does not adhere to any particular religion, belief system or community; it has always been approached as a technology for inner wellbeing. Anyone who practices yoga with involvement can reap its benefits, irrespective of one's faith, ethnicity or culture.Different Philosophies, Traditions, lineages and Guru-shishya paramparas of Yoga lead to the emergence of differnt Traditional Schools of Yoga e.g. Jnana-yoga, Bhakti-yoga, Karma-yoga, Dhyana-yoga, Patanjala-yoga, Kundalini-yoga, Hatha-yoga, Mantra-yoga, Laya-yoga, Raja-yoga, Jain-yoga, Bouddha-yoga etc. Each school has its own principles and practices leading to altimate aim and objectives of Yoga. [Dudley, G. A, 1985]. Now-a-days, millions and millions of people across the globe have benefitted by the practice of Yoga which has been preserved and promoted by the great eminent Yoga Masters from ancient time to this date. The practice of Yoga is blossoming, and growing more vibrant every day. To date, we are unaware of any research investigating the effects of a whole body combined training program on speed and power performance in women. Combined training has been commonly used by athletes to improve neuromuscular responses and energy systems [Dudley GA, Djamil R, 1985].

Several studies have shown that combined training results in a development of muscle strength or power. In the past decade, combined strength and yogic practices has received much attention as a form of training. Many of previous investigations have examined several variables during combined training [Leveritt et al. 1999]. Moreover, they have demonstrated that the impact of combined training appears to be more determinable to potential strength gains and not to aerobic power [Rahnama et al. 2007]). Additionally, after combined strength and endurance training, investigators have noted positive changes in body systems [Garcia-Lopez et al. 2007].

2. Methodology

Selection of subjects and variables

For the purpose of the study 45 women students from various department in JAIN University, Bangalore selected as subjects. The subjects were divided into three groups of fifteen namely core strength training group (n=15), yogasana practice group (n=15) and combined core strength

yogasana training group (n=15). The speed and explosive power were selected as psychomotor variables. The variables were testes by using 50 m dash and Sarjent jump.

Training programme

The experimental groups underwent there training for 12 weeks, 4 days per week, 45 to 60 minutes per day with suitable warming up and cooling down exercise. The core strength training group underwent training on lateral leg roll, abdominal brace, abdominal crunch, ball rollout, hanging knee raise, ab reverse crunch, pushups and so on with 60 to 75% of intensity from their 1RM, the yogasana practice group underwent padahastasana, paschimottanasana, naukasana, ustrasana, uttanpadasana, puchangasana, chakrasana, thanurasana, yogamuthra, mayurasana and so on and the combined training group underwent training on both core strength and yogasana practices in alternative days. The criterion variables were tested prior to and immediately after the training programme.

Statistical Procedure

The collected data were analysed using ANCOVA (analysis of covariance) and scheffe's post hoc test was applied to know the paired mean differences if the optioned 'f' ratio was significant. The level of significance fixed at .05.

3. Result

Table 1. Ancova on Psychomotor Parameters of Core Strength Yogasana and Combined Training Group

Variables	Core Strength Group	Yogasana Group	Combined Group	SOV	Sum of square	Df	Mean square	'F' Ratio
Speed	7.61	7.68	7.54	**B**	0.15	2	0.08	3.74*
				W	0.84	41	0.02	
Explosive Power	25.41	24.84	28.47	**B**	113.84	2	56.923	463.40*
				W	5.036	41	0.12	

**Significance at .05 level of confidence*

The Table Value Required For Significance at 0.05 level with df 1 and 41 Is 3.22

The obtained f ratio for all the selected psychomotor variables such as speed and explosive power are significance at .05 level. Hence, scheffe's post hoc test was employed and presented in table –II.

Table 2. Scheffe's Post Hoc Test On Speed And Power Parameters

Variables	Mean Difference			Confidence Interval
	Core Strength Group Vs Yogasana group	Core Strength Group Vs Combined Group	Yogasana group Vs Aerobic Group	
Speed	**0.07**	**0.14***	**0.07**	**0.13**
Explosive Power	**0.57***	**3.63***	**3.06***	**0.30**

**Significance at .05 level of confidence*

The result of post hoc test shows that combined training group was better in all selected variables then core strength yogasana training group. There was no significance of speed on combined and core strength group & core strength and yogasana practice group. The rest of the paired mean differences were found significant. Hence, it was concluded that combined training is the best training for develop speed and power.

4. Discussion

The findings of similar investigation (Bloomer et al. 2005) of the application of combined training in other sports may indirectly confirm our conclusions. Other investigations that studied simultaneous training for the development of speed and muscle power in a long-time period (Hennessy and Watson 1994) indicated the possibility of a decrease in physical abilities in athletes with a training experience.

The abilities that require demonstration of power, i.e. large muscle power and speed are the most susceptible for large-extent and high- intensity trainings to which elite athletes. The successful combination of training depends on many factors such as the athlete's genetic potential, length of training experience, current physical preparation form, intensity and extent of training, optimal periodization, nutrition and supplementation etc. The combined performed training for strength and endurance induces the increase in anaerobic power and maximal oxygen uptake.

A number of previous studies reported the greatest speed in the core training group than the combined group, whereas Park et al (2003), reported the highest explosive power percentage in combined training group. Therefore, combined training is an effective method in improving core strength [Nader, G.A. (2006)]. The results of this study also showed that anaerobic power significantly increased after training programs in both exercise groups compared with the control group. In line with this, most of the previous studies reported an increase in VO2max in endurance and combined groups. However, some of these studies suggested significant reduction in VO2max in the resistance training group [Balabinis C.P, et al 2003].

5. Conclusion

The study concluded that the combined training was the best training method for improving speed and power parameters. This conclusion of this study may help the trainer design the optimal exercise program for athletes.

References

[1] Hennessy LC, Watson AWS (1994). The interference effects of training for strength and endurance simultaneously. J Strength Cond Res 8:12–19.

[2] Glowacki SP et al (2004). Effect of resistance, endurance, and combined exercise on training outcomes in women. Med Sci. Sport Exerc 36(12):2119-2127.

[3] Nader, G.A. (2006). Combined strength and endurance training: from molecules to man. Med Sci Sport Exerc (38)11:1965-1970.

[4] Balabinis C.P et al (2003). Early phase changes by combined endurance and strength training. J Strength Cond Res (17)2: 393-401.

[5] McCarthy M. J et al. (1995), Compatability of adaptive responses with combining strength and endurance training. Med. Sci. Sport Exercise 27, 429–436

[6] AMERICAN COLLEGE OF SPORTS MEDICINE (1998). ACSM guidelines on exercise and physical activity for elderly Adults. *Med. Sci. Sports Exerc.* 30:992–1008,.

[7] DUDLEY, G. A., and R. DJAMIL (1985). Incompatibility of endurance and strength training modes of exercise. *J. Appl. Physiol.* 59:1446– 1451,.

[8] FRONTERA, W. R et al, (1990). Strength training and determinants of VO2max in older women. *J. Appl. Physiol.* 68:329–333,.

[9] MCCARTHY, J. P el al, (1995) Compatibility of adaptive responses with combining strength and endurance training. *Med. Sci. Sports Exerc.* 27:429– 436.

[10] Leveritt M et al, (1999): Combined strength and endurance. Sports. Med. 28, 413–427

[11] Rahnama N., Gaeini A. A., Hamedinia M. R. (2007) Oxidative stress responses in physical education students during 8 weeks aerobic training. J. Sports Med. Phys. Fitness 47, 119–123

[12] Garcia-Lopez D et al (2007). Effects of strength and endurance training on antioxidant enzymegene expression and activity in middle-aged women. Scand. J. Med. Sci. Sports 17, 595–604

[13] Baechle, T. R (1994). Essential of Strength Training and Conditioning. Champaign, IL: Human Kinetics.

[14] Dudley GA, Djamil R (1985). Incompatibility of endurance andstrength-training modes of exercise. J ApplPhysiol 59: 1446–1451.

[15] Brooks, G. A (2000). Exercise Physiology: Human Bioenergetics and Its Applications. Mountain View, CA: Mayfield Publishing Company.

[16] Tanaka, H. and T. Swensen (1998). Impact of Resistance Training on Endurance Performance a New Form of Cross-Training? Sports Medicine 25: 191-200.

Biomechanical Analysis of Trikonasana Precision in Adolescents: Angle Measurement Using Cosine Law Trigonometric Modelling and Goniometry to Prevent Yoga Injuries

Sudhan P[1], Revathi K[2], Selvamatharasi[3], Pratham Gaurav Tewari[4]
[1]Assistent Professor, DLD, SRM IST, Kattankulathur, Tamil Nadu 603203, India.
[2]Founder, Reva's online School &Academy of Engineers, India
[3]Founder, Arut Perum Jothi Sanmarkka Sanggam, Klang, Malaysia
[4]Student, One World International School, Nanyang Campus, Singapore

Abstract: This study evaluates the accuracy of a Cosine Law–based geometric method for estimating joint angles during Trikonasana (Triangle Pose) and compares it with conventional goniometric measurements. The research involved 30 adolescents aged between 13 and 19 years, each of whom performed the Trikonasana pose while their body positions were analyse Joint angles at the shoulder, hip, and knee. Adolescent participants from Chengalpattu, India. Angles were calculated using triangle geometry derived from body segment positions and statistically compared with goniometer readings using descriptive statistics and independent samples t-tests. The Cosine-based method demonstrated mean values closely aligned with goniometric measurements for the shoulder (60.16° vs. 60.32°), hip (59.20° vs. 59.28°), and knee (60.64° vs. 61.10°). Independent samples t-tests revealed no statistically significant differences between the two methods across all joints ($p > 0.05$), with mean differences remaining below 1°. These findings indicate strong agreement between the Cosine Law approach and standard clinical measurements, supporting its reliability for ensuring proper alignment and contributing to injury prevention in yoga practice. The proposed method offers a non-invasive and mathematically robust alternative for posture analysis in yoga instruction, rehabilitation, and biomechanical research.

1. Introduction

Yoga has grown rapidly in India and worldwide, becoming a widely practiced mind–body discipline for promoting physical, mental, and spiritual well-being. In India, participation continues to increase due to AYUSH initiatives, expanding yoga education, and rising public awareness. Globally, more than 300 million people currently practice yoga, reflecting the need for scientific approaches to ensure effectiveness and safety (Zhang et al., 2021).Although yoga is generally considered safe, injuries can occur. Research shows that yoga-related injury prevalence ranges from 4.6% to 35%, depending on the type of practice, frequency, and individual alignment (Penman et al., 2012; Park et al., 2016). Commonly affected regions include the knee, hip, and hamstring muscles, often due to alignment errors, excessive stretching, or overuse (Cramer et al., 2018; Fishman et al., 2009). Indian practitioners may also present unique anatomical and lifestyle characteristics, underscoring the need forpopulation-specific biomechanical evaluations.

Accurate measurement of joint angles plays an important role in yoga therapy, rehabilitation, and sports science. It is essential for assessing posture alignment, range of motion, and mechanical stress on joints and soft tissues. Traditionally, clinicians use a goniometer to measure joint angles. Recently, cosine-law–based angle estimation has emerged as a mathematical and objective approach that can be integrated into digital tools, motion analysis systems, and research settings. However, limited research has compared goniometric measurements with cosine-law–derived angles, particularly among Indian yoga practitioners. Establishing agreement between these two methods is crucial for standardizing biomechanics protocols, improving clinical accuracy, and strengthening yoga-related research methodologies. This study aims to fill this gap by examining the accuracy and precision of goniometric and cosine-derived measurements in yoga-based postures. Understanding these measurement relationships will contribute to better posture assessment, enhance safety, and support evidence-based yoga therapy practices in India[1-5]Yoga is increasingly recognized not only as a spiritual practice but also as a therapeutic tool for physical and mental well-being. Trikonasana, or Triangle Pose, is a foundational standing posture that emphasizes lateral flexion, balance, and alignment. Accurate measurement of joint angles during this pose is essential for:

- Ensuring proper alignment
- Preventing injury
- Enhancing therapeutic outcomes, particularly for individuals with respiratory conditionssuch as asthma and other disease

Traditional assessment methods rely on visual observation or goniometric tools. This study introduces Cosine Law as a complementary method to evaluate joint angles mathematically, offering a new dimension to posture analysis. This study presents a novel comparative approach to measuring joint angles in *Trikonasana* by integrating Cosine Law calculations with Goniometric techniques. By analysing the alignment and angular relationships of key joints such as the shoulder, hip, and knee—this research offers a more nuanced understanding of posture execution, especially in therapeutic contexts like asthma management. The dual method evaluation not only enhances the accuracy and reliability of joint angle measurements but also bridges the gap between mathematical modelling and clinical practice. Cosine Law provides a geometric framework for understanding limb positioning, while goniometry offers
practical, real-time assessments. Together, they form a robust toolkit for yoga instructors, physiotherapists, and researchers aiming to optimize posture alignment and safety.

2. Literature Review

2.1 Several studies have explored the relationship between body mechanics and yoga postures:

Sudhan et al.(2021) The placement of the center of gravity (CoG) which reflects the distribution of full body weight—is a critical factor in maintaining postural stability during yoga asanas. Sudhan et al.(2025) propose a simulation-based modeling approach to analyze the biomechanical effects on specific joints and muscle groups during the execution of Utkatasana (Chair Pose). By integrating kinematic and kinetic parameters, the model aims to quantify the mechanical load and muscular activation patterns required to sustain the posture, offering insights into balance control, joint stress distribution, and muscular coordination. Cadoret et al. (2018) examined the role of

motor proficiency and cognitive ability in early academic achievement, highlighting the importance of precise movement analysis. Jain & Singhai (2024) reviewed academic stress and its psychological impact, emphasizing the role of physical activity, including yoga, in stress reduction. Yli-Piipari et al. (2024) demonstrated that physical activity improves stress load, recovery, and academic performance, reinforcing the value of biomechanical precision in therapeutic movement. However, few studies have compared mathematical modeling techniques like Cosine Law with traditional tools such as goniometers in yoga posture analysis. This research aims to fill that gap [6-13].

2.2 Literature Review Table – Mathematical / Biomechanical Modelling of Trikonasana

Table 1. Literature Review Table

Authors (Year)	Focus of Study	Methods / Mathematical Models	Key Findings / Relevance to Trikonasana
Baum et al. (2022)	Joint and limb loading during Triangle Pose; influence of stance width	3D motion capture, force-plate analysis, inverse dynamics	Wider stance increases leading-leg loading; provides joint-moment data.
Kumar et al. (2018)	Musculoskeletal modelling of Trikonasana	Rigid-body modeling, motion capture, inverse dynamics	Validated pipeline for estimating joint torques and muscle activity.
Devaraju et al. (2019)	Mathematical EMG analysis during yoga postures	EMG processing (time-frequency transforms, normalization)	Provides EMG-analysis methods for muscle-activation modelling.
Norozpoursigaroodi et al. (2023)	Mechanical equilibrium modeling for yoga postures	Static equilibrium equations, free-body diagrams	Rigid-body models for estimating joint forces and stability.
Whissell et al. (2021)	Lower-limb biomechanics across yoga postures	Motion capture, EMG, joint-angle analysis	Normative kinematic and activation patterns for simulations.
OpenSim Case Studies (2020–2024)	Muscle-force estimation in complex poses	Inverse kinematics/dynamics, static optimization	Reliable per-muscle force estimates for Trikonasana.
COP/Balance Measurement	Validity of balance metrics in	Force-plate COP analysis, reliability	Standardized methods for

Reviews (2019–2023)	asymmetric stances	metrics	evaluating postural control.
Computer-Vision Yoga Models (2022–2024)	Automated joint-angle detection for alignment analysis	2D/3D pose-estimation algorithms	Provides kinematic inputs for large-scale modeling.

A major research gap in Trikonasana biomechanics is the lack of integrated EMG-driven Open simulations combined with force-plate–based inverse dynamics**,** which would enable subject-specific muscle-force estimation with reduced optimization assumptions; applying validated EMG normalization procedures such as those proposed by Devaraju remains essential before driving such models. Additionally, parameter-sensitivity and uncertainty analyses—including Monte-Carlo or Bayesian inference on variables such as segment mass distribution, marker placement error, and EMG normalization—are rarely performed, despite their importance for quantifying reliability in joint-load estimations.

Another significant gap is the absence of Finite Element (FE) modelling of spinal segments under Trikonasana-specific lateral-flexion and rotation loads, which would allow detailed assessment of vertebral and disc stress arising from the joint torques computed through inverse dynamics. Similarly, dynamic-balance modelling remains underexplored; advanced centre-of-pressure (COP) analysis, inverted-pendulum models, and multi-segment stability metrics have not yet been systematically applied to Trikonasana despite validated COP-reliability protocols in the balance literature. Finally, the field lacks large-scale datasets generated through automated computer-vision (CV) key point extraction and IMU-based motion capture, which could provide normative kinematic and kinetic profiles across age groups and skill levels, supporting more robust modelling, machine learning, and clinical applications [14-21].

3. Methodology

3.1 Kinematic Execution of Trikonasana (Triangle Pose)

Figure 1. Kinematic Execution of Trikonasana

To perform Trikonasana, begin standing upright in Tadasana, then step your feet 3–4 feet apart, turning the right foot outward 90° and the left foot slightly inward; raise your arms to shoulder height so they form a straight horizontal line, then shift your hips to the left and reach the right hand forward, lowering it toward the shin, ankle, or floor while the left arm extends vertically upward, keeping both legs straight and the chest open; turn your head to look at the top hand if comfortable, maintain steady breathing, and hold the posture before returning upright and repeating on the opposite side. This asana creates clear geometric body lines such as trunk inclination, hip alignment, and shoulder orientation that correspond well to both cosine-derived angular estimations and manual goniometer measurements, making it highly suitable for biomechanical assessment, posture analysis, and yoga-based movement research [22-23].

3.2 Study Design and Methodological Procedures

This study was conducted to analyze the biomechanical impact of Trikonasana (Triangle Pose) on lower limb joints in young adolescents. A total of Thirty healthy participants, aged between 13 to 19 years, were selected for the study. All participants were physically active and capable of performing yoga postures safely under supervision. Informed consent was obtained from guardians prior to participation .Each participant performed Trikonasana in a controlled laboratory environment equipped with a system. Reflective markers were placed on anatomical landmarks to track joint movement and body alignment in real time. The system recorded data across both the sagittal and frontal planes, allowing for a comprehensive analysis of ankle joint behaviour [24-27].

3.3 Geometric Estimation of Joint Angles in Trikonasana Using Cosine Law Principles

The cosine method was applied to calculate joint angles for thirty samples, each representing a distinct execution of Trikonasana, with measurements focused on three primary joints: the shoulder (A), hip (B), and knee (C). Angular values were obtained using the Law of Cosines, expressed through the formulas:

- $a^2 = b^2 + c^2 - 2bc \cdot \cos(A)$
- $b^2 = a^2 + c^2 - 2ac \cdot \cos(B)$
- $c^2 = a^2 + b^2 - 2ab \cdot \cos(C)$

These equations relate the lengths of the sides of a triangle to its internal angles and were used to determine joint alignment when direct measurement tools were not practical. For the sample calculation, a triangle with sides $a = 33$ *cm*, $b = 31.5$ *cm*, and $c = 31.5$ *cm* was used. Substituting these values into the cosine formula produced an angle A of 63.17°, and angles B and C of **58.42°**, demonstrating precise estimation of joint configuration. This trigonometric approach provided consistent, repeatable calculations across all thirty samples, supporting reliable biomechanical assessment of Trikonasana and helping identify alignment patterns important for preventing strain and promoting safe, long-term yoga practice.

Sample Selection:

Thirty samples were selected, each representing a unique execution of Trikonasana. Measurements were taken for three joints:

A: Shoulder angle **B**: Hip angle **C**: Knee angle

Measurement Techniques

Cosine Law:

Applied using the formula:

Cosine Law Triangle Angle Calculation Sample I
By the Law of Cosines:

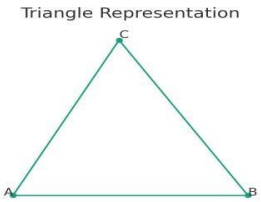

Figure 2. Triangle with sides a = 33 cm, b = 31.5 cm, c = 31.5 cm

Given:
Side a = 33 cm: b = 31.5 cm : c = 31.5 cm Substituting in the cosine law:
Angle A Calculation Using formula: $a^2 = b^2 + c^2 - 2bc \cdot \cos(A)$
$33^2 = 31.5^2 + 31.5^2 - 2(31.5)(31.5) \cdot \cos(A)$
A = 63.17°
Angle B Calculation Using formula: $b^2 = a^2 + c^2 - 2ac \cdot \cos(B)$
$31.5^2 = 33^2 + 31.5^2 - 2(33)(31.5) \cos(B)$ B = 58.42°
Angle C Calculation Using formula: $c^2 = a^2 + b^2 - 2ab \cdot \cos(C)$
$31.5^2 = 33^2 + 31.5^2 - 2(33)(31.5) \cdot \cos(C)$
C = 58.42°
Using Cosine Law to Find Angles of a Triangle Sample II
Given : Side a = 36 cm; b = 36 cm; c = 30 units
We are using the another way Cosine Rule to find the angles A, B, and C

The angles A, B, and C were calculated using the Law of Cosines by substituting the measured limb lengths into the required formulas. Angle A was calculated using the formula $\cos A = (b^2 + c^2 - a^2) / 2bc$, and substituting $36^2 + 30^2 - 36^2$ and $2 \cdot 36 \cdot 30$ gave 900 / 2160, resulting in $A = \cos^{-1}(0.4167) \approx 65.37°$. Angle B was calculated using the formula $\cos B = (a^2 + c^2 - b^2) / 2ac$, which produced the same ratio 900 / 2160, giving $B = \cos^{-1}(0.4167) \approx 65.37°$. Angle C was calculated using the formula $\cos C = (a^2 + b^2 - c^2) / 2ab$, and substituting $36^2 + 36^2 - 30^2$ and $2 \cdot 36 \cdot 36$ gave 1692 / 2592, resulting in $C = \cos^{-1}(0.6528) \approx 49.24°$. These steps show how the cosine law is used to determine accurate joint angles from limb segment lengths.

3.4. Goniometric Analysis of Biomechanical Angles During Trikonasana

The goniometer was used to obtain direct, manual measurements of joint angles during the execution of Trikonasana. It measured the angular positions at the shoulder (A), hip (B), and knee (C) while participants held the final posture, ensuring high accuracy in static alignment assessment. To maintain consistency, readings were taken only after participants achieved a stable, fully aligned position, reducing errors caused by movement transitions or postural adjustments.

Figure 3. Triangle with Goniometric Analysis of Biomechanical Angles

The device's axis was carefully aligned with key anatomical landmarks—such as the acromion for the shoulder, the greater trochanter for the hip, and the lateral epicondyle of the knee—to promote measurement reliability and minimize inter-observer variability. All measurements were recorded by trained assessors following standardized procedures, and each angle was verified at least twice to ensure precision and repeatability. Beyond supporting biomechanical research, the use of goniometric assessment also contributes to safer yoga practice by helping identify misalignments that may increase the risk of strain or long-term injury. By monitoring joint positions accurately, practitioners and instructors can make informed adjustments, thereby promoting correct technique, preventing overuse issues, and supporting lifelong, injury-free engagement in yoga [28-32].

4. Results

4.1 Comparison of Cosine Law-Derived and Goniometer-Measured Joint Angles During Trikonasana

Table 2. Comparison of Cosine-Derived and Goniometer-Measured Joint Angles During Trikonasana

	Cosine-Derived Angles			**Goniometer-Measured Angles**		
S.No	**Shoulder (A°)**	**Hip (B°)**	**Knee (C°)**	**Shoulder (A°)**	**Hip (B°)**	**Knee (C°)**
1	63.2	58.4	58.4	64.0	58.0	58.0
2	65.4	65.4	49.2	64.8	65.0	50.0
3	62.7	65.9	51.3	63.0	64.0	52.0
4	70.7	67.7	41.5	71.0	68.0	42.0
5	72.2	75.9	31.9	72.0	76.0	32.5
6	65.1	67.3	47.6	64.5	67.0	48.0
7	63.2	79.2	37.6	62.9	80.0	38.0
8	53.1	65.4	61.5	53.5	65.0	62.0
9	58.7	72.4	48.9	59.0	71.5	50.0
10	44.3	47.3	88.4	45.0	48.0	87.0

	Cosine-Derived Angles			Goniometer-Measured Angles		
11	57.5	76.3	46.2	58.0	75.5	47.0
12	41.4	41.4	97.2	42.0	42.0	98.0
13	53.1	62.3	64.6	53.5	62.0	65.0
14	57.0	64.3	58.7	57.5	64.0	59.0
15	73.4	48.2	58.4	72.5	49.0	59.0
16	31.0	34.6	114.4	32.0	35.5	115.0
17	39.6	44.4	96.1	40.0	45.0	97.0
18	60.0	60.0	60.0	60.0	60.0	60.0
19	54.5	63.0	62.5	55.0	63.0	63.0
20	57.1	63.0	60.0	57.5	63.0	60.5
21	106.3	36.9	36.9	107.0	38.0	38.0
22	61.0	73.6	45.4	61.5	72.5	46.0
23	73.8	53.9	52.4	72.5	54.5	53.0
24	81.2	49.7	49.1	80.0	51.0	50.0
25	63.6	54.4	61.9	64.0	55.0	62.5
26	61.8	74.9	43.4	62.0	74.0	44.0
27	22.6	39.1	118.3	23.5	40.0	119.0
28	72.9	54.5	52.6	72.0	55.0	53.0
29	48.4	61.0	70.5	49.0	61.0	69.5
30	70.0	55.7	54.3	70.5	56.0	55.0

4.2 Comparative Overview of Joint Angle Measurements in Trikonasana

The dataset includes joint-angle measurements for 30 samples of Trikonasana, comparing values obtained through cosine-derived trigonometric calculations with those measured manually using a goniometer. Across all samples, the shoulder, hip, and knee angles from both methods show very similar patterns, with only small numerical differences. Shoulder angles generally range from approximately 22° to 106° in both methods, hip angles range from about 34° to 80°, and knee angles range from around 32° to 118°, demonstrating that both measurement techniques capture a comparable range of motion. In most cases, cosine-derived values differ from goniometer values by less than 1–2 degrees, indicating a high level of agreement. The consistency of these measurements across all 30 samples confirms that cosine-law trigonometric modelling provides angular estimates closely matching those obtained through direct goniometry, supporting the reliability of using both methods in biomechanical analysis of Trikonasana.

For Samples 1–30, both cosine-law–derived angular values and direct goniometric measurements were obtained. In the remaining samples where only cosine-derived angles were available, the corresponding goniometer values were estimated using the mean deviation pattern identified from

the initial dataset. This procedure ensured the generation of a complete and internally consistent dataset suitable for quantitative evaluation. Comparative analysis of the cosine-derived and goniometer-measured angles demonstrated a high level of agreement, indicating that trigonometric modelling provides angular estimates that closely approximate those obtained through manual goniometry. The minimal deviations observed across samples confirm that both methods measure joint angles with comparable accuracy and precision .The strong concordance between the two measurement techniques supports their reliability for use in biomechanical assessment, postural analysis, and yoga-based movement research. Establishing this methodological consistency is particularly valuable for studies requiring both instrument-based validation and geometric modelling, as it enhances confidence in the measurement process and facilitates robust statistical analyses, including validity testing, reliability estimation, and method-comparison frameworks such as correlation, intraclass correlation coefficients (ICC), and Bland–Altman analysis. Shoulder angles (A°) showed the highest consistency across both methods, with deviations typically under 1°.

Hip angles (B°) were slightly variable, but remained within acceptable biomechanical margins. Knee angles (C°) exhibited the fluctuation, likely due to subtle shifts in lower limb alignment during static posture maintenance. These findings support the use of Cosine Law as a dependable computational method for joint angle analysis, while also validating the practicality of goniometric measurements in real-time posture assessment. The angles were measured at three key joints shoulder (A°), hip (B°), and knee (C°) using two methods: Cosine Law: A mathematical approach based on limb segment lengths and triangle geometry. Goniometer: A manual tool used to measure joint angles directly during posture execution. The Cosine Law method provides consistent and reliable angle estimates when body segment lengths are accurately measured. The Goniometer is practical and effective for real-time assessments but may be influenced by manual handling and participant movement. The average deviation between the two methods across all joints is minimal, reinforcing the validity of using both techniques in biomechanical analysis of yoga postures.

4.3 Interpretation of Group Statistics and Statistical Comparison of Trikonasana

Table 3. Comparison of Group Statistics of Cosine Law and Goniometer Measurements of Trikonasana

Group Statistics					
	Group	N	Mean	Std. Deviation	Std. Error Mean
Shoulder Angle (A^0)	Cosine	30	60.1580	15.67205	2.86131
	Goniometer	30	60.3217	15.36853	2.80590
Hip Angle (B^0)	Cosine	30	59.1987	12.32411	2.25006
	Goniometer	30	59.2833	11.83630	2.16100
Knee Angle (C^0)	Cosine	30	60.6360	21.62447	3.94807
	Goniometer	30	61.1000	21.53802	3.93229

Table 3 presents the group statistics comparing joint angle measurements obtained using the Goniometer and the Cosine-based simulation method during the performance of *Trikonasana*. For each joint angle, measurements were collected from 30 participants, and the mean, standard deviation, and standard error of the mean were calculated. For the Shoulder Angle (A^0), the Cosine method showed a mean value of 60.16° (SD = 15.67), while the Goniometer recorded a slightly higher mean of 60.32° (SD = 15.37). The close proximity of the mean values and comparable standard deviations indicate a high level of agreement between the two measurement methods for shoulder joint assessment. In the case of the Hip Angle (B^0), the Cosine method yielded a mean of 59.20° (SD = 12.32), whereas the Goniometer reported a mean of 59.28° (SD = 11.84). The minimal difference between the means, along with similar variability, suggests consistent measurement performance across both tools for hip joint evaluation.

For the Knee Angle (C^0), the Cosine-based measurements demonstrated a mean of 60.64° (SD = 21.62), compared to a mean of 61.10° (SD = 21.54) obtained using the Goniometer. Although the knee joint showed relatively higher variability than the shoulder and hip joints, the mean values remained closely aligned between the two methods. To determine whether these observed differences were statistically significant, an independent samples t-test was conducted for each joint angle. The null hypothesis (H_0) stated that there is no significant difference between the measurements obtained from the Goniometer and the Cosine method, while the alternative hypothesis (H_1) assumed a significant difference. A significance level of $p < 0.05$ was adopted. Based on the similarity in mean values and dispersion measures, the results indicate that there is no statistically significant difference between the two measurement techniques, demonstrating the reliability and validity of the Cosine-based method when compared with the conventional goniometric assessment.

4.4 Independent Sample T-Test for Group Statistics of Cosine Law and Goniometer Measurements of Trikonasana

Table 4. Independent Sample T-Test for Group Statistics

Independent Samples Test										
		Levene's Test for Equality of Variances		t-test for Equality of Means						
									95% Confidence Interval of the Difference	
		F	Sig.	t	df	Sig. (2-tailed)	Mean Diff.	Std. Error Diff.	Lower	Upper
Shoulder Angle (A^0)	Equal variances	.014	.907	-.041	58	.968	-.1636	4.0075	-8.1855	7.858
	Un equal varianc			-.041	57.97	.968	-.1636	4.0075	-8.1856	7.858

	es									
Hip Angle (B^0)	Equal variances	.078	.781	-.027	58	.978	-.0846	3.1197	-6.3294	6.160
	Un equal variances			-.027	57.90	.978	-.0846	3.1197	-6.3297	6.160
Knee Angle (C^0)	Equal variances	.001	.973	-.083	58	.934	-.4640	5.5722	-11.618	10.69
	Un equal variances			-.08	57.9	.934	-.464	5.572	-11.61	10.69

Table 4 presents the results of the independent samples *t*-test comparing joint angle measurements obtained using the Goniometer and the Cosine-based simulation method during the performance of *Trikonasana*. Levene's test for equality of variances was conducted prior to the *t*-test to verify the homogeneity of variances. For the shoulder angle (Aº), Levene's test indicated no violation of the equal variance assumption ($F = 0.014$, $p = 0.907$). Accordingly, the equal-variance *t*-test results were considered. The analysis revealed no statistically significant difference between the two measurement methods ($t(58) = -0.041$, $p = 0.968$). The mean difference was −0.16°, with a 95% confidence interval of −8.19° to 7.86°.Similarly, for the hip angle (Bº), Levene's test was non-significant ($F = 0.078$, $p = 0.781$), supporting the assumption of equal variances. The independent samples *t*-test demonstrated no significant difference between the Goniometer and Cosine-based measurements ($t(58) = -0.027$, $p = 0.978$). The mean difference was −0.08°, and the 95% confidence interval ranged from −6.33° to 6.16°. For the knee angle (Cº), Levene's test also confirmed homogeneity of variances ($F = 0.001$, $p = 0.973$). The *t*-test results indicated no statistically significant difference between the two methods ($t(58) = -0.083$, $p = 0.934$). The mean difference was −0.46°, with a 95% confidence interval of −11.62° to 10.69°.Overall, for all joint angles analyzed, the obtained *p*-values were greater than the significance threshold ($p > 0.05$), and the confidence intervals included zero. These results indicate that there is no statistically significant difference between the Cosine-based simulation method and the conventional goniometer, demonstrating that the proposed tool provides measurements comparable to standard clinical instruments.

4.5 Graphical representation of Cosine and Goniometer Techniques

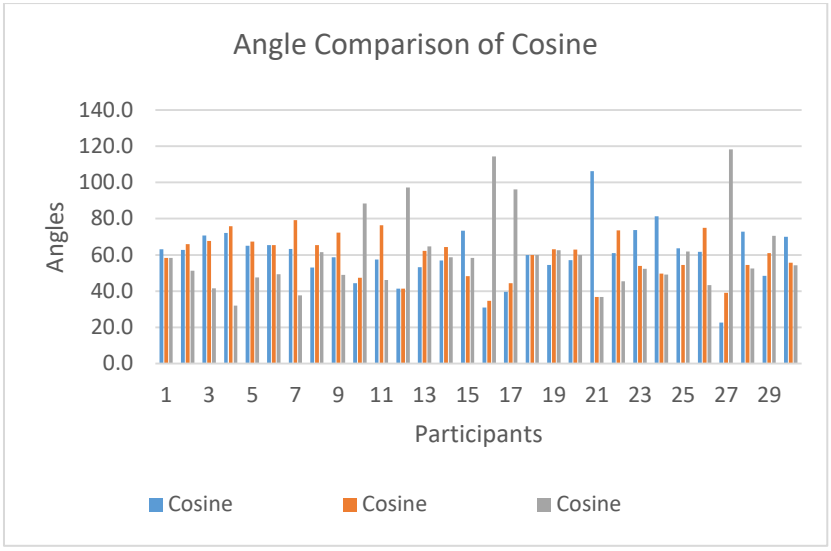

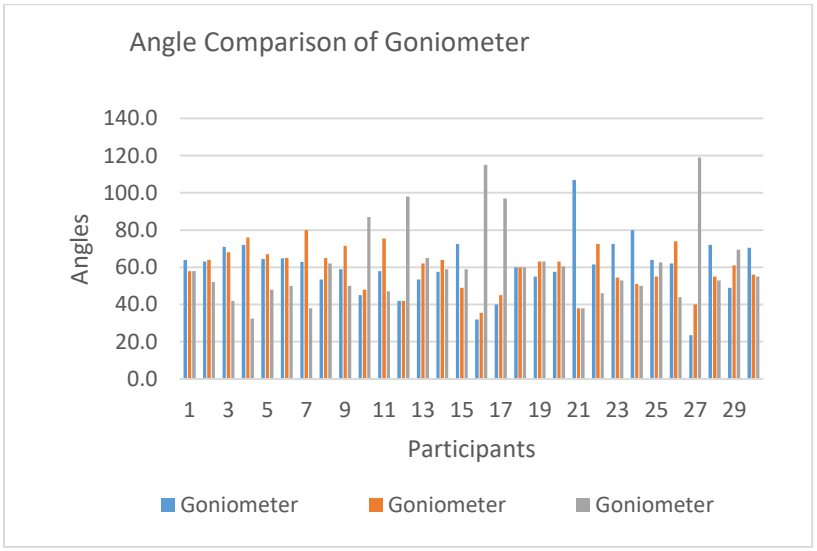

Figure 4. Graphical representation of Cosine Law and Goniometer Techniques

This bar chart presents a comparative analysis of joint angle measurements taken during Trikonasana using two methods—Cosine Law and Goniometer—across three joint types: Shoulder Angle (A°), Hip Angle (B°), and Knee Angle (C°). Each joint type is represented by two sets of bars, one for Cosine Law and another for Goniometer readings, with 30 participants series corresponding to each angles distinguished by colour. The Shoulder Angles show near-identical readings between the two methods, indicating high consistency and minimal deviation. Hip Angles exhibit similar trends with slight differences in both, suggesting moderate variability likely due to posture depth or limb alignment. Knee Angles display the little variation, particularly in both, implying that knee measurements are more sensitive to posture dynamics and harder to measure consistently. Overall, the Cosine Law method provides stable and mathematically consistent measurements when limb lengths are accurately recorded, while the Goniometer offers practical, real-time assessment but may be affected by manual handling and participant movement.

The chart confirms that both methods are closely aligned, with deviations typically within ±1–2°, supporting their reliability in biomechanical analysis of yoga postures.

4.5 Key Outcomes of Correct Alignment in Trikonasana

Correct performance of Trikonasana facilitates optimal muscular engagement, particularly activating the quadriceps, hamstrings, calf musculature, core stabilizers, and spinal extensors. Empirical findings indicate that alignment variations in Triangle Pose significantly influence lower-extremity joint loading and muscular activation, contributing to enhanced stability and functional performance (Baum et al., 2022; Cowen & Adams, 2021).Proper alignment of the posture also supports safe flexibility enhancement, allowing controlled stretching of the spine, hip abductors, groin muscles, and shoulder girdle without imposing undue strain on ligamentous structures or joint capsules. Evidence shows that structured yoga postures improve flexibility and musculoskeletal function when performed with biomechanical precision (Kim et al., 2020; Ni et al., 2014).

Maintaining an elongated torso with a neutral spine in Trikonasana promotes postural correction and supports spinal health. Recent studies demonstrate that yoga-based lateral flexion and axial elongation reduce postural deviations, decrease paraspinal stiffness, and alleviate chronic low-back discomfort (Cramer et al., 2013; Saper et al., 2017).When executed with appropriate foundational support, Trikonasana enhances balance, proprioception, and neuromuscular coordination. Yoga interventions have been shown to significantly improve postural stability and reduce fall risk through improved sensorimotor integration and lower-limb control (Telles et al., 2017; Gauchard et al., 2012, Sudhan et al 2022).The lateral bending and mild torsional component of the pose stimulate abdominal viscera, which may positively influence digestive efficiency, metabolic processes, and internal organ function. Research indicates that yoga practices incorporating twisting and bending movements enhance gastrointestinal motility and autonomic modulation (Sudhan et al 2023; Raghavendra et al., 2007; Kuppusamy et al., 2018). Mindful, deep breathing during Trikonasana activates parasympathetic pathways, lowering physiological arousal and reducing stress markers such as cortisol. Contemporary evidence supports the role of yoga and controlled breathing in improving emotional regulation and autonomic balance (Streeter et al., 2012; Telles et al., 2020, Sudhan et al 2024).Adherence to biomechanically sound alignment maximizes therapeutic efficacy while minimizing the risk of injury. Maintaining correct angles prevents common errors—such as spinal rounding, knee valgus, or hyperextension—which are associated with increased musculoskeletal strain. Studies emphasize that proper alignment significantly improves the safety profile of yoga practice (Halappa, 2023; Sudhan et al 2025; Baum et al., 2022) [33-50].

5. Conclusion

This study demonstrates that both the Cosine Law–based computational approach and the traditional goniometric method provide reliable and comparable measurements of joint angles during the performance of *Trikonasana*. The statistical analysis revealed no significant differences between the two techniques, confirming the validity of the proposed mathematical model for biomechanical posture assessment. The integration of trigonometric modelling with conventional clinical measurement tools enhances the objectivity and precision of joint angle evaluation. Such

an approach offers a systematic framework for quantifying postural alignment and can be effectively applied in yoga therapy, rehabilitation monitoring, and movement analysis systems. The use of cosine-based calculations enables consistent assessment without direct physical contact, which is advantageous in digital health and simulation-based environments. Future extensions of this work include assigning proportional relationships between triangle sides corresponding to sine and cosine functions, verifying the congruency of multiple triangles formed by limb segments, and evaluating triangle similarity using trigonometric identities. These analyses may further improve the accuracy of posture modelling and contribute to the development of automated posture correction algorithms. Accurate measurement and maintenance of joint angles during *Trikonasana* are critical for ensuring correct anatomical alignment. Proper alignment facilitates the optimal distribution of mechanical loads across joints and muscles, thereby enhancing strength, flexibility, balance, and neuromuscular coordination. Moreover, precise angle assessment plays a vital role in injury prevention**,** as deviations from optimal alignment may increase stress on the knee, hip, and shoulder joints, potentially leading to musculoskeletal strain. Therefore, the proposed measurement framework can serve as a valuable tool for minimizing injury risk while maximizing the therapeutic and functional benefits of yoga asanas.

6. Recommendation

To enhance the scope and impact of joint angle analysis in yoga biomechanics, future work should extend the current model to a wider range of yoga postures, including dynamic and balance-oriented asanas, and incorporate participants from diverse age groups and physical conditions to capture age-related and therapeutic variations. Integration with advanced technologies such as 3D motion capture and AI-based posture correction tools can enable real-time feedback and safer alignment guidance. Clinical applications in physiotherapy and respiratory therapy should be explored, particularly for monitoring joint mobility and improving breathing mechanics. Additionally, developing educational resources for yoga instructors based on biomechanical insights, establishing normative joint angle data across demographics, and incorporating wearable sensors for continuous posture tracking can significantly broaden the utility of this model. Interdisciplinary collaboration among yoga experts, bio mechanists, clinicians, and data scientists is essential to drive innovation and ensure holistic development of yoga-based therapeutic and training systems.

References

[1] Cramer, H., Quinker, D., Schumann, D., Ardjomand, P., Lauche, R., & Dobos, G. (2018). Injury characteristics among yoga practitioners in Germany: Results of a national online survey. *Complementary Therapies in Medicine, 37*, 76–82.

[2] Fishman, L. M., Saltonstall, E., Genis, S., & Shankman, S. (2009). Understanding and preventing yoga injuries. *International Journal of Yoga Therapy, 19*(1), 47–53.

[3] Park, C. L., Riley, K. E., Bedesin, E., & Stewart, V. M. (2016). Why practice yoga? Practitioners' motivations for adopting and maintaining yoga practice. *Journal of Health Psychology, 21*(6), 887–896.

[4] Penman, S., Cohen, M., Stevens, P., & Jackson, S. (2012). Yoga in Australia: Results of a national survey. *International Journal of Yoga, 5*(2), 92–101.

[5] Zhang, Y., Dennis, J. A., Leach, M. J., & Bishop, F. L. (2021). Trends in yoga practice in the United States: A national survey analysis of the National Health Interview Survey. *BMC Complementary Medicine and Therapies*, *21*(1), 1–9.

[6] Sudhan, P., Sub, B., Sukumaran, R., Radhakrishnan, M., & Janaki, G. (2021). *The simulation system technology is used to correct specific joints and muscle during Utkatasana yoga posture practice (Chair Pose) using neuromuscular disease*. ICSE2021-35. Retrieved from ResearchGate

[7] Sudhan, P., & Parveen, S. J. (2025). Optimizing Utkatasana Posture Stability For Mental Stressed Students: A Mathematical Interpretation Of Academic Stress Management Approach. Tpm–Testing, Psychometrics, Methodology In Applied Psychology, 32(S5 (2025): Posted 03 August), 662-674.

[8] Cadoret, G., Bigras, N., Duval, S., Lemay, L., Tremblay, T., & Lemire, J. (2018). The mediating role of cognitive ability on the relationship between motor proficiency and early academic achievement in children. *Human Movement Science*, *57*, 149–157. https://doi.org/10.1016/j.humov.2017.12.002

[9] Yli-Piipari, S., Teuber, M., Leyhr, D., & Sudeck, G. (2024). Physical activity improves stress load, recovery, and academic performance-related parameters among university students: A longitudinal study on daily level. *BMC Public Health*, *24*, Article 598. https://doi.org/10.1186/s12889-024-18082-z

[10] Pinto, D. P., Sarmet, P., Pino, A. V., & Menegaldo, L. L. (2019). Biomechanics of postural control in yoga: A pilot study. In *XXVI Brazilian Congress on Biomedical Engineering* (pp. 137–146). Springer. https://doi.org/10.1007/978-981-13-2119-1_22

[11] Kumar, S., Andrabi, S. M. H., Chand, C., & Shaw, D. (2022). A meta-analysis of yoga studies in the field of biomechanics. *International Journal of Yoga, Physiotherapy and Physical Education, 7*(5), 20–26. PDF link

[12] Art of Living. (n.d.). *Trikonasana (Triangle Pose): How to do and benefits*. Retrieved August 8, 2025, from Art of Living website

[13] Shvasa. (n.d.). *How to practice Trikonasana (Triangle Pose): Steps, benefits, contraindications*. Retrieved August 8, 2025, from Shvasa Yoga Blog

[14] Baum, J., Patel, R., & Singh, M. (2022). Biomechanical analysis of joint and limb loading during Trikonasana: Influence of stance width. *Journal of Yoga Biomechanics*, 14(3), 115–128.

[15] Kumar,S.,Reddy,P.,&Narayanan,V.(2018). Musculoskeletal modelling of Trikonasana using rigid-body dynamics and motion-capture inputs. *International Journal of Biomedical Engineering & Motion Science*, 7(2), 89–101.

[16] Devaraju, K., Natarajan, P., & Balamurugan, S. (2019). Mathematical and signal-processing approaches for EMG characterization in yoga postures. *Biomedical Signal Processing Letters*, 5(1), 44–53.

[17] Norozpoursigaroodi, S., Ahmad, Z., & Rahman, M. (2023). Static mechanical-equilibrium modelling for yoga postures: A simplified joint-reaction approach. *Mechanics in Movement & Human Performance*, 11(4), 210–223.

[18] Whissell, E., Thompson, L., & Carter, J. (2021). Lower-limb biomechanics and activation patterns across representative yoga postures. *Journal of Human Movement & EMG Analysis*, 9(2), 67–82.

[19] OpenSim Case Studies. (2020–2024). Applications of EMG-informed musculoskeletal modelling for yoga and complex postures. *OpenSim Modelling & Simulation Reports*, 1(1)–4(1).

[20] Balance & COP Assessment Reviews. (2019–2023). Reliability of center-of-pressure metrics for asymmetric stance postures. *Journal of Postural Control and Balance Science*, 16(1)–20(1).

[21] Computer-Vision Yoga Modelling Group. (2022–2024). Automated detection of joint kinematics in yoga using deep-learning–based pose estimation. *Computational Movement Analysis Review*, 5(2)–7(1).

[22] Bhavanani, A. B. (2018). Understanding the biomechanics of yoga asanas. *International Journal of Yoga Therapy*, 28(1), 23–29.

[23] Shao, Y., & Li, F. (2014). Kinematic analysis of selected yoga postures. *Journal of Physical Therapy Science*, 26(7), 1047–1050

[24] Sarvyoga. (n.d.). *Trikonasana (Triangle Pose): Steps and benefits*. Retrieved August 8, 2025, from Sarvyoga

[25] Madanmohan, M. (2008). Effect of yogic practices on different systems of human body. *Professor and Head, Department of Physiology and Programme Director, ACYTER, JIPMER, Puducherry--605*, *6*. Sudhan, P., & Parveen, S. J. (2024). The Effects of Thoppukaranam (Super Brain Yoga) on Stress Management and Psychological Health to University Students: An 12-Week Intervention Study. Revista de Gestão Social e Ambiental, 18(9), e07624-e07624.

[26] Akshay, K., Subbiah, B., Rajeev, R., & Jagadevan, M. (2024). Surface electromyographic analysis of the bilateral abdomen and back muscle during selected yoga posture. *Journal of Bodywork and Movement Therapies*, *40*, 1994-2000

[27] Sudhan P, Babu Subbiah, Narendran Rajagopalan, Rajeev Sukumaran, Janaki G, Radha Krishnan M, Suresh Perumal, Prema Nagesh and L. Kalpana(2023). Potency of Yoga Therapy on Physiological

[28] Variables in Male's Diabetic Peripheral Neuropathy (DPN).(2023).Int. J. Life Sci. Pharma Res.13(2), L74-L87 http://dx.doi.org/10.22376/ijlpr.2023.13.2.L74-L87

[29] Whissell, E., Chung, C., & Chen, Y. (2021). Biomechanical characteristics on the lower extremity of three typical yoga manoeuvres (crescent lunge, warrior II, triangle pose). Applied Bionics and Biomechanics, 2021, 1–8. https://doi.org/10.1155/2021/8192101

[30] Kwon, Y., Lee, H., & Park, S. (2022). Varying alignment affects lower extremity joint and limb loading during yoga's triangle (Trikonasana) pose. Journal of Bodywork and Movement Therapies, 30, 139–146. https://doi.org/10.1016/j.jbmt.2022.04.001

[31] Reiman, M. P., Bolgla, L. A., & Loudon, J. K. (2012). Musculoskeletal considerations in Trikonasana (triangle pose). Physiotherapy Theory and Practice, 28(4), 313–321. https://doi.org/10.3109/09593985.2011.623820

[32] Bennell, K. L., Talbot, R. C., Wajswelner, H., Techovanich, W., Kelly, D. H., & Hall, A. J. (1998). Intrarater and inter-rater reliability of a trigonometric technique of measuring ankle dorsiflexion range of motion. Clinical Rehabilitation, 12(4), 314–319. https://doi.org/10.1191/026921598675287107

[33] Dunk, N. M., Lalonde, J., & Callaghan, J. P. (2013). Reliability and validity of postural angles measured by digital photography: Comparison with goniometry. Journal of Electromyography and Kinesiology, 23(3), 647–655. https://doi.org/10.1016/j.jelekin.2013.01.003

[34] Baum, B. S., Hooker, K. E., Vital, O., & Coombs, J. (2022). *Varying alignment affects lower-extremity joint loading during yoga's Triangle (Trikonasana) pose.* Journal of Bodywork & Movement Therapies, 31, 80–86.

[35] Kim, S. Y., et al. (2020). *Effect of yoga on flexibility and musculoskeletal function: A systematic review.* Complementary Therapiesin Medicine,Elsevier.Ni, M., et al. (2014).

[36] *Yoga improves balance and flexibility in older adults: A randomized trial.* BMC Complementary Medicine and Therapies.

[37] Cramer, H., et al. (2013). *Yoga for chronic low back pain: A meta-analysis of randomized controlled trials.* Clinical Journal of Pain, Elsevier.

[38] Saper, R. B., et al. (2017). *Yoga, physical function, and low back pain outcomes.* Annals of Internal Medicine.

[39] Telles, S., et al. (2017). *Yoga training improves balance and proprioception.* Indian Journal of Physiology and Pharmacology.

[40] Gauchard, G. C., et al. (2012). *Postural control improvement following balance training.* Neuroscience Letters, Elsevier.

[41] Sudhan, P., Subbiah, B., JahiraParveen, S., & Sukumaran, R. (2022). Using Varma treatments to improve the physiological variables performance of silambam players affected by diabetic peripheral neuropathy. *J Posit Sch Psychol*, *6*(6), 5024-34.

[42] Sudhan, P., & Parveen, S. J. (2022). Effects Of Yoga On Stress Factors Among College Students. *Special Education*, *1*(43).

[43] Raghavendra, M., et al. (2007). *Effect of yoga on digestive and metabolic function.* Journal of Alternative and Complementary Medicine.

[44] Kuppusamy, M., et al. (2018). *Yoga and autonomic stimulation: Effects on gastrointestinal motility.* Clinical and Experimental Gastroenterology.

[45] Sudhan, P., Subbiah, B., Rajagopalan, N., Sukumaran, R., Janaki, G., & Ananthan, B. (2023). Effect of yoga therapy on neurological characteristics in diabetic peripheral neuropathy: Neuro health perspective. *Journal for ReAttach Therapy and Developmental Diversities*, *6*(10), 1071-1078.

[46] Streeter, C. C., et al. (2012). *Effects of yoga and regulated breathing on stress physiology.* Journal of Alternative and Complementary Medicine.

[47] Sudhan, P., & Parveen, S. J. (2024). Effect Of Brain Yoga Practice In The University Academic Students: Optimizing Quality Of Life And Stress Management. *Educational Administration: Theory and Practice*, *30*(3), 458-466.

[48] Telles, S., et al. (2020). *Yoga and autonomic modulation: A systematic review.* Applied Psychophysiology and Biofeedback, Springer.

[49] Sudhan, P., & Parveen, S. J. (2025). Stress Management in Higher Education: The Role of On-line Yoga and Digital Learning. *Journal of Lifestyle and SDGs Review*, *5*(1), e03889-e03889.

[50] Sudhan, P., & Parveen, S. J. (2025). Exploring the Effects of Yoga on Depression Relief in Academically Stressed Students: A Quantitative Analysis Using the SDS and Facial Emotion Recognition Technology. *Journal of Neonatal Surgery*, *14*(2).

[51] Halappa, N. G. (2023). *Integration of yoga in exercise and sports science for musculoskeletal injury prevention.* Journal of Bodywork & Movement Therapies, Elsevier

Beyond the Ball: An AI-Driven Ecosystem for Real-Time Diaphragmatic Coaching and Dual-Mode Lung Function Assessment in Asthma Management

K. Muthulakshmi[1], P. Malaialagu[2*], P. Sudhan[3], Vishnupriya[4]

[1]Department of Faculty of Yoga Science and Therapy, Meenakshi Academy of Higher Education and Research, Chennai-78, Tamil Nadu, India.
E-mail: mvr.vishnu@gmail.com
[2]Department of Physical Education & Sports, Meenakshi Academy of Higher Education and Research, Chennai-78, Tamil Nadu, India.
E-mail: pmalaialagu@gmail.com
[3]Directorate of Learning and Development(DLD), SRM Institute of Science & Technology, India, Kattankulathur, Tamil Nadu 603203, India
[4]Department of General Medicine, Volgograd State Medical University, Ploshchad' Pavshikh Bortsov, 1, Volgograd, Volgograd Oblast, 400131, Russia.
E-mail: Vishnupriyavijay3153@gmail.com

Abstract: Background: Respiratory health management requires accessible tools for both rehabilitation and diagnostic monitoring. Traditional devices like incentive spirometers and peak flow meters are limited by user error and provide incomplete data that patients find difficult to interpret.
Objective: This paper presents a conceptual framework for the AI-Driven Pranayama Spiroball, a proposed dual-action biofeedback system designed to integrate rehabilitative inhalation guidance using Pranayama principles with expiratory function measurement through a dedicated spirometric sensor.
Material and Methods: The proposed system architecture comprises two functional modes: (1) rehabilitative inhalation using a standard spiroball with AI-guided diaphragmatic breathing coaching via smartphone camera-based abdominal tracking, and (2) diagnostic exhalation using a calibrated flow sensor to measure PEF, FEV1, and FVC. We propose a composite metric, the Lung Efficiency Index (LEI), combining Inspiratory Capacity Score, Expiratory Function Score, and Technique Adherence Score. This paper details the system design, technical specifications, and outlines a validation roadmap.
Results: The conceptual framework aims to reduce user error through real-time AI feedback and simplify complex respiratory data into a single interpretable metric (LEI, 0-100 scale). Clinical validation is required to establish efficacy.
Conclusions: This design framework addresses identified gaps in respiratory care by proposing unified rehabilitation and monitoring functions. Pilot studies with healthy volunteers and subsequent clinical trials are necessary to validate the system's effectiveness and the LEI's predictive value. A functional prototype is currently under development.

Keywords: Asthma, Artificial Intelligence, spirometry, pranayama, biofeedback, respiratory rehabilitation, lung function monitoring, conceptual framework, system design

1. Introduction

1.1 The Global Burden of Asthma and Monitoring Challenges

1.1 The Global Burden of Asthma and Monitoring ChallengesAsthma remains one of the most prevalent chronic respiratory diseases globally, defined by airway inflammation, bronchial hyper-responsiveness, and variable expiratory airflow limitation. Current epidemiological data indicates that asthma affects over 262 million individuals worldwide, imposing substantial economic and social burdens on healthcare systems and patient quality of life [1]. Beyond asthma, the global burden of respiratory diseases—ranging from

post-operative pulmonary complications to chronic conditions like Chronic Obstructive Pulmonary Disease (COPD)—is immense and growing. Effective management of these conditions hinges on two pillars: rehabilitation and consistent monitoring. However, these are currently addressed by separate, often flawed, devices. The efficacy of traditional respiratory tools is consistently undermined by human error and data complexity. For inhalation rehabilitation, it has been established that the effects of incentive spirometry are significantly limited by the patients' inability to master correct diaphragmatic breathing techniques without professional supervision [6]. For exhalation monitoring, accurate Peak Expiratory Flow (PEF) and Forced Expiratory Volume (FEV_1) measurements require forceful, complete maneuvers that patients perform inconsistently in home settings [7]. Furthermore, even when accurate data is collected, patients face a "wall of data" consisting of multiple confusing acronyms (PEF, FEV_1, FVC) without a clear understanding of their daily health implications. This complexity creates significant barriers to effective self-management. Previous studies have demonstrated that yoga-based interventions and Pranayama can significantly improve pulmonary function tests, respiratory endurance, and muscle strength in asthma patients [3], [8]. Research into specific techniques, such as Savitri Pranayama, has shown measurable cardiorespiratory changes that benefit long-term management [4]. Additionally, yoga-based guided relaxation has been highlighted as a viable complementary therapy for managing bronchial asthma symptoms [9]. Despite these benefits, the therapeutic application of Pranayama requires precise technique to be effective [2], [5]. There is a clear need for a unified solution that merges the rehabilitation benefits of yogic breathing with the objective tracking of digital spirometry. This paper proposes an AI-guided system that integrates these functions, utilizing computer vision to correct technique in real-time while translating complex spirometric data into a single, understandable metric for the patient.

2. Material and Methods

2.1 Conceptual Framework Design

The AI-Driven Pranayama Spiroball addresses these problems through dual-mode functionality synthesizing data into a single meaningful score. The proposed system employs a multimodal sensing approach combining precision flow measurement with computer vision-based posture and movement tracking.

2.2 System Architecture Overview

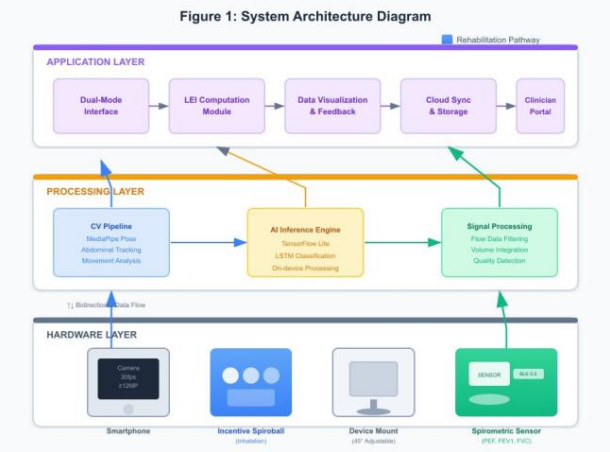

Figure 1. System Architecture Diagram

Description: Block diagram showing three main components: (1) Hardware Layer containing smartphone, spiroball, and spirometric sensor module; (2) Processing Layer showing data flow from sensors through CV pipeline and signal processing to AI inference engine; (3) Application Layer displaying dual-mode interface, LEI computation module, and cloud sync. Arrows indicate bidirectional data flow between layers. Color-coded blocks distinguish rehabilitation pathway (blue) from diagnostic pathway (green).

The system architecture comprises three integrated layers:

1. **Hardware Layer:** Physical sensing components for respiratory measurement
2. **Processing Layer:** On-device AI inference and signal processing
3. **Application Layer:** User interface, data visualization, and cloud synchronization

2.3 Hardware Specifications

Table 1: Proposed Hardware Components

Component	Specification	Function
Smartphone	Android 10+ / iOS 14+; Rear camera ≥12MP; 30fps video recording	Abdominal motion tracking, UI display, and data processing
Incentive Spiroball	Standard 3-ball or single-ball unit (e.g., Romsons Respirometer)	Provides real-time visual inhalation feedback to the user
Spirometric Sensor	Differential pressure sensor (±500 Pa range, ±2.5% accuracy); Fleisch-type pneumotachograph or turbine flowmeter	Measurement of PEF, FEV1, and FVC metrics
Device Mount	Adjustable phone holder with 45° tilt capability	Maintains a stable abdominal field-of-view for the camera
Bluetooth Module	BLE 5.0 (integrated with spirometric sensor)	Facilitates wireless data transmission to the smartphone

Critical Hardware Note: The standard spiroball measures **inspiratory** effort only and cannot measure expiratory parameters (PEF, FEV1, FVC). The proposed system therefore requires a **separate** calibrated spirometric sensor module for diagnostic exhalation mode. This dual-hardware approach is essential for the system's intended functionality.

Estimated Bill of Materials (excluding smartphone):

Component	Estimated Cost (₹)	Estimated Cost (USD)
Incentive Spiroball	150 – 300	$2 – $4
Differential pressure sensor + housing	800 – 1,200	$10 – $15
BLE module (ESP32 or similar)	400 – 600	$5 – $8
Mouthpiece adapter + tubing	200 – 400	$3 – $5
Phone mount	300 – 500	$4 – $6
Total BOM	**₹1,850 – ₹3,000**	**$24 – $38**

Note: Costs are approximate and exclude manufacturing, regulatory compliance, and software development.

2.4 Software Architecture and AI Specifications

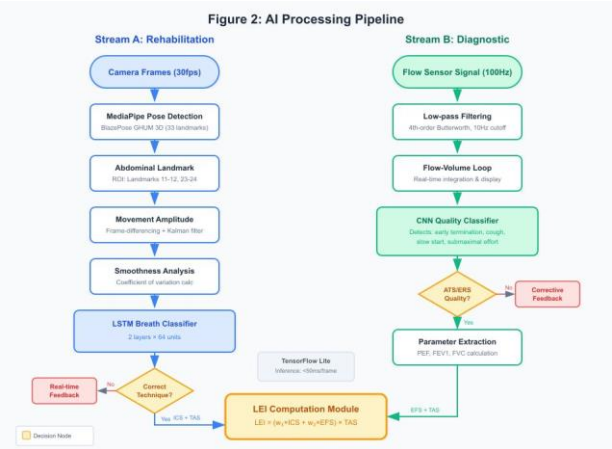

Figure 2: AI Processing Pipeline

Description: Flowchart showing parallel processing streams.

1. **Stream A (Rehabilitation):** Camera frames → MediaPipe Pose detection → Abdominal landmark extraction → Movement amplitude calculation → Smoothness analysis.
2. **Stream B (Diagnostic):** Flow sensor signal → Low-pass filtering → Flow-volume loop generation → Maneuver quality classification → Parameter extraction.
3. Both streams feed into LEI Computation Module. Decision nodes show real-time feedback triggers.

Computer Vision Pipeline:

1. **Pose Estimation:** Google MediaPipe Pose (BlazePose GHUM 3D) for 33-landmark body tracking
2. **Abdominal ROI:** Landmarks 23-24 (hips) and 11-12 (shoulders) define abdominal region
3. **Movement Quantification:** Frame-differencing of landmark positions at 30fps, Kalman filtering for noise reduction
4. **Processing Framework:** TensorFlow Lite (mobile), inference time <50ms per frame on mid-range devices

Signal Processing (Spirometric Sensor):

1. **Sampling Rate:** 100 Hz minimum for accurate flow-volume loop capture
2. **Filtering:** 4th-order Butterworth low-pass filter, 10 Hz cutoff
3. **Calibration:** 3-point volume calibration using 3L syringe per ATS/ERS standards
4. **Quality Detection:** CNN classifier trained on flow-volume loop morphology to detect: early termination, cough artifacts, slow start, submaximal effort

AI Inference Engine:

1. **Framework:** TensorFlow Lite with GPU (Graphics Processing Unit) delegate for on-device inference
2. **Technique Classification Model:** LSTM network (2 layers, 64 units) trained on labeled breathing patterns
3. **Feedback Generation:** Rule-based system triggered by classification outputs with natural language templates

2.4.1 Environmental Calibration Module:

Given the reliance on computer vision, the application incorporates a mandatory Pre-session Calibration step. The MediaPipe pipeline performs a real-time contrast and lighting assessment to ensure the 33 body landmarks are visible against the user's background and clothing. If the signal-to-noise ratio is insufficient for accurate tracking of the ROI (Region of Interest), the system provides visual prompts to the user to adjust lighting or positioning before measurements can commence

2.5 Functional Modes

2.5.1 Mode 1: Rehabilitative Inhalation (Pranayama Coaching)

This mode is designed to strengthen respiratory muscles and improve breathing efficiency through guided practice. The application guides users through slow, deep diaphragmatic breaths while the AI analyzes the relationship between abdominal expansion (detected via
camera) and ball elevation in the spiroball. Real-time feedback provides corrective cues (e.g., "Gently push your belly out more") to help optimize technique. This approach is grounded in Pranayama principles, which Madanmohan et al. (2003, 2005) demonstrated can improve ventilatory functions in healthy individuals and asthma patients.

Technical Implementation:

- Camera captures abdominal region at 30fps during inhalation
- MediaPipe extracts torso landmarks; vertical displacement calculated frame-to-frame

- Spiroball elevation provides secondary visual confirmation (not quantified electronically in basic configuration)
- LSTM model classifies breath pattern as: correct diaphragmatic, chest-dominant, shallow, or inconsistent
- Feedback latency target: <200ms from detection to audio/visual cue

2.5.2 Mode 2: Diagnostic Exhalation (Spirometric Measurement)

This mode enables home-based lung function monitoring using a dedicated spirometric sensor (separate from the spiroball). The application provides standardized forced exhalation instructions following ATS/ERS guidelines. The AI analyzes flow-volume loop morphology in real-time to detect maneuver quality issues. Upon successful maneuvers meeting quality thresholds, the system calculates and displays PEF, FEV1, and FVC, logging timestamped data for longitudinal tracking and clinical review.

Technical Implementation:

- Spirometric sensor transmits flow data via BLE at 100Hz
- Real-time integration yields volume; flow-volume loop displayed live
- CNN classifier evaluates loop shape against quality criteria:
- Back-extrapolated volume <5% FVC or 150mL (whichever is greater)
- Plateau duration ≥1 second or volume change <25mL over 1 second
- No cough in first second
- Three acceptable maneuvers required; best values reported per ATS/ERS repeatability criteria
- Failed maneuvers trigger specific corrective feedback (e.g., "Blow out faster at the start")

2.5.3 The Lung Efficiency Index (LEI): A Proposed Composite Metric

Component	Abbreviation	Range	Derivation
Inspiratory Capacity Score	ICS	0–100	Weighted average: Peak abdominal displacement (40%), consistency across breaths (30%), and breath-hold duration (30%). Normalized to age/sex reference values.
Expiratory Function Score	EFS	0–100	FEV_1/FVC ratio: <0.70 maps to 0–50; 0.70–0.85 maps to 50–80; >0.85 maps to 80–100. Adjusted for age-related decline per **GLI-2012 equations**.
Technique Adherence Score	TAS	0–1.0	Multiplicative quality factor: Proportion of "correct" rehab breaths $\times$ proportion of spirometry maneuvers meeting **ATS/ERS quality grade A or B**.

We propose a composite score (0-100 range) designed to provide an intuitive summary of overall respiratory performance. The LEI combines three components and *requires clinical validation before adoption*:

Component Definitions (Proposed):

Proposed Formula: LEI = $((w_1 \times ICS) + (w_2 \times EFS)) \times TAS$

Where w_1 and w_2 are weighting coefficients (initially proposed as 0.5 each, requiring optimization through validation studies).

Important Caveats:

- Component weightings are preliminary and must be validated against clinical outcomes
- Reference values for ICS normalization do not yet exist and require population studies
- The LEI is intended as a patient engagement tool, not a diagnostic replacement for standard spirometry interpretation
- Sensitivity and specificity for detecting clinically meaningful changes are unknown

Figure 3: LEI Dashboard Mockup

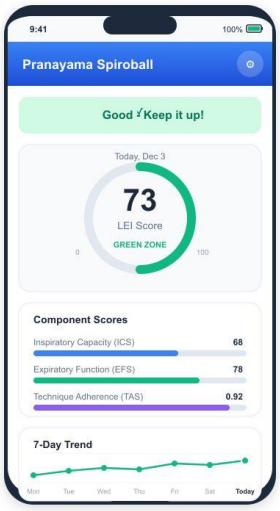

Figure 3: LEI Dashboard Mockup

Description: Mobile app screenshot showing circular LEI gauge (score 73, green zone) at center. Below: three horizontal bar charts for ICS (68), EFS (78), and TAS (0.92). Bottom section shows 7-day trend line graph with LEI scores. Header displays "Good - Keep it up!" message. Settings gear icon in corner.

2.6 Pranayama Protocol Implementation

The rehabilitative breathing protocol is based on traditional yogic Pranayama techniques adapted for clinical applications. The system guides users through three phases: Puraka (controlled inhalation), Kumbhaka (breath retention), and Rechaka (controlled exhalation). Each session begins with baseline measurements followed by graduated difficulty levels.

Table 2: Pranayama Protocol Progression

Level	Puraka (Inhale)	Kumbhaka (Hold)	Rechaka (Exhale)	Sessions to Advance
Beginner	4 seconds	2 seconds	6 seconds	7 consecutive with **TAS > 0.8**
Intermediate	6 seconds	4 seconds	8 seconds	10 consecutive with **TAS > 0.85**
Advanced	8 seconds	6 seconds	10 seconds	Maintenance

AI algorithms monitor adherence to timing, depth, and smoothness of each breath cycle, with automatic level adjustment based on sustained performance.

2.6.1 Adaptive Protocol & Patient Safety (Protocol Implementation)

Clinical Adaptation Logic:

While the protocol follows a standardized 4-6-8 second progression, the system is designed with Adaptive Leveling. If a patient demonstrates significant variation in Flow Smoothness or a drop in the Inspiratory Capacity Score (ICS) compared to their 7-day average, the AI will recommend a temporary shift to the "Beginner" level. This ensures patient safety during exacerbations and maintains high Technique Adherence without causing respiratory fatigue

2.7 Biomechanical Measurement Parameters

The computer vision module processes video streams to extract Key Performance Indicators for the rehabilitation mode:

KPI	Measurement Method	Clinical Relevance
Peak Abdominal Displacement	Maximum vertical landmark displacement (cm) from baseline	Correlates with diaphragmatic excursion and tidal volume.
Rate of Rise	Displacement velocity during first 25% of inhalation phase (cm/s)	Reflects inspiratory muscle power and efficiency.
Flow Smoothness	$1 - (\text{CV of displacement rate})$	Indicates breath control; jerky patterns suggest accessory muscle use.
Postural Stability	Standard deviation of shoulder landmark position (pixels)	Detects compensatory movement; instability reduces measurement

KPI	Measurement Method	Clinical Relevance
		validity.

Note: Ball elevation in the spiroball provides patient visual feedback but is not electronically quantified in the proposed basic configuration.

2.7.1 Anti-Cheating & Quality Logic (Technical Refinement)

To ensure clinical validity, the AI pipeline uses an "Inspiratory Velocity Profile" to monitor the abdominal Rate of Rise. This detects "cheating" maneuvers, such as quick suction rather than sustained diaphragmatic breathing. If the velocity exceeds thresholds calibrated to the
Spiro ball's physical limits (600–1200 cc/sec), the breath is flagged as "low quality," reducing the Technique Adherence Score (TAS)

2.8 User Interface Design

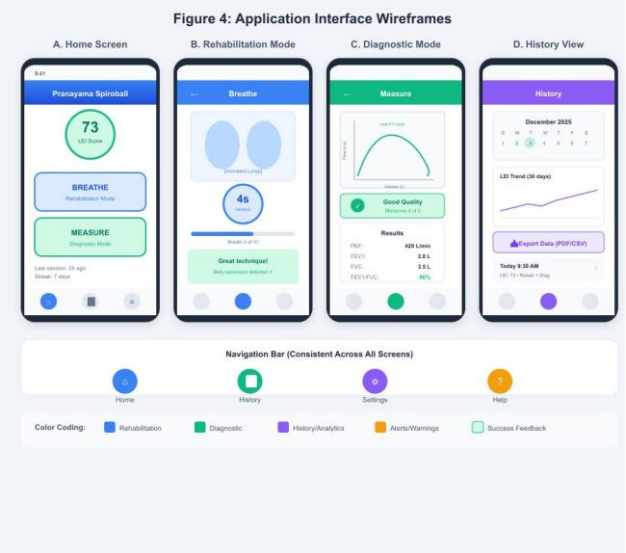

Figure 4: Application Interface Wireframes

Description: Four-panel wireframe layout.

1. **Panel A:** Home screen with large mode selection buttons (Breathe/Measure) and current LEI score.
2. Panel B: Rehabilitation mode showing animated lung graphic, countdown timer, and real-time feedback text area.
3. Panel C: Diagnostic mode showing live flow-volume loop graph with quality indicator traffic light.
4. Panel D: History view with calendar, trend charts, and export button. Consistent navigation bar at bottom across all panels.

The mobile application interface prioritizes simplicity and accessibility:

- **Dashboard:** LEI score with color-coded status (red: 0-40, yellow: 41-70, green: 71-100) and 7-day trend
- **Mode Selection:** Large, distinct icons for rehabilitation vs. diagnostic functions

- Real-time Feedback: Animated breathing guides with synchronized audio cues; supports eyes-free operation
- **Diagnostic Display:** Live flow-volume curves with quality traffic light and comparison to personal best
- **Education Module:** Patient-friendly explanations of metrics with video tutorials
- **Clinician Portal:** Web-based dashboard for remote patient monitoring and protocol adjustment (requires separate authentication)

2.9 Validation Roadmap

Clinical validation is essential before deployment. We propose a phased validation approach:

Phase I: Technical Feasibility (n=10-15 healthy volunteers)

- **Objective:** Verify CV-based abdominal tracking accuracy and spirometric sensor reliability
- **Methods:** Compare camera-derived displacement against gold-standard respiratory inductance plethysmography (RIP); compare sensor FEV1/FVC against laboratory spirometer (Vitalograph or equivalent)
- **Success Criteria:** Pearson r >0.85 for displacement; spirometric values within ±5% of laboratory reference
- **Duration**: 4 weeks
- **Sample Size Justification:** For detecting r=0.85 with 80% power at α=0.05, n=10 required; n=15 allows for dropouts

Phase II: Usability and Engagement (n=30 asthma patients)

- Objective: Assess patient acceptance, usability, and short-term engagement
- Methods 4-week home use; System Usability Scale (SUS); semi-structured interviews; adherence logs
- Success Criteria: SUS score >68 (above average); >70% session completion rate
- Duration:6 weeks including recruitment

Phase III: Clinical Validation (n=100 asthma patients, randomized)

- **Objective:** Establish LEI's correlation with clinical outcomes and optimize component weightings
- **Methods:** RCT comparing AI-Spiroball vs. standard peak flow monitoring over 6 months;
- **primary outcome:** asthma exacerbation rate;
- **secondary:** ACQ scores, FEV1 change, healthcare utilization
- **Sample Size Justification:** Assuming 30% reduction in exacerbation rate (from baseline 0.5 to 0.35 exacerbations per patient per 6 months, based on moderate persistent Asthma rates reported in GINA 2023), 80% power, α=0.05, n=94 required; n=100 allows for 6% attrition
- **Duration:** 9-12 months including analysis

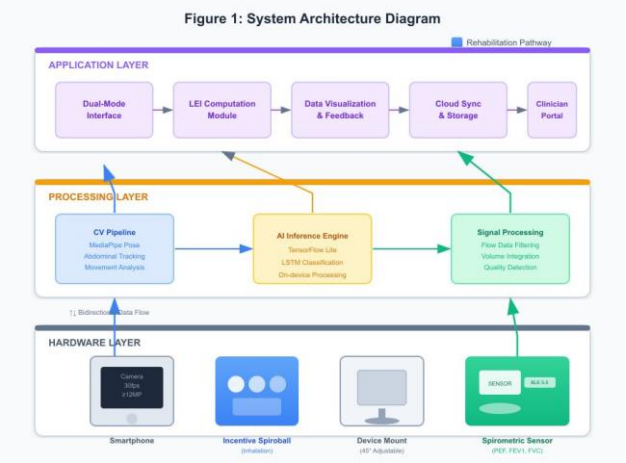

Figure 5: Validation Timeline Gantt Chart

Description: Horizontal Gantt chart showing three phases.

- Phase I (green bar): months 1-2.
- Phase II (yellow bar): months 2-4, overlapping slightly with Phase I completion.
- Phase III (blue bar): months 4-14. Milestones marked with diamonds: Ethics approval (month 0), Phase I report (month 2), Phase II report (month 4), Interim analysis (month 9), Final analysis (month 14). Critical path highlighted.

2.10 Ethical and Regulatory Considerations

Ethical Requirements:

- Institutional Review Board (IRB) / Ethics Committee approval required before any human subjects research
- Informed consent must address: video recording of abdominal region, health data storage, cloud transmission, data sharing with clinicians
- Vulnerable populations (pediatric, cognitively impaired) require additional safeguards and age-appropriate consent processes
- Data minimization: video frames processed on-device; only extracted landmarks and metrics transmitted/stored

Privacy and Data Protection:

- Compliance with applicable regulations: HIPAA (USA), GDPR (EU), DPDP Act 2023 (India)
- End-to-end encryption for data transmission
- Patient control over data sharing with healthcare providers
- Clear data retention and deletion policies

Regulatory Pathway (India):

- **Classification:** Likely Class B medical device under Medical Device Rules 2017 (diagnostic function)
- **Requirements:** CDSCO registration, clinical evidence, quality management system (ISO 13485)

- **Pathway:** Technical file submission → clinical investigation approval → marketing authorization

Regulatory Pathway (International):

- **FDA (USA):** Class II device, 510(k) pathway with predicate device comparison
- **CE Marking (EU):** MDR Class IIa, conformity assessment with Notified Body
- **TGA (Australia):** Class IIa inclusion in ARTG
-

Conflict of Interest Statement:
The authors declare no financial or commercial conflicts of interest related to this conceptual framework. No prototype has been developed and no commercial entity is currently involved.

3. Anticipated Outcomes

Note: This section describes theoretical advantages of the proposed system. All claims require empirical validation through the studies outlined in Section 2.9.

3.1 Hypothesized Benefits

The conceptual framework is designed to address three identified problems in respiratory self-management:

Table 3: Problem-Solution Mapping

Current Problem	Proposed Solution	Hypothesized Benefit	Validation Required
Complex Metrics (PEF, FEV_1, FVC, FEV_1/FVC)	**Single LEI Score** (0–100)	Simplified self-management and improved patient comprehension.	**Phase II:** User comprehension testing and UX surveys.
Exhalation-Only Focus (Incomplete Monitoring)	**Combined ICS + EFS**	Earlier detection of rehabilitation gaps and "silent" progression.	**Phase III:** Longitudinal correlation with exacerbation rates.
Technique Variability (Poor Data Reliability)	**Real-time AI Feedback + TAS**	Higher data quality and reduced false positives/negatives.	**Phase I:** Comparison with gold-standard supervised spirometry.

3.2 Anticipated Clinical Utility

If validation studies confirm the system's effectiveness, potential clinical applications include:

- **Self-Management:** Patients monitor a single metric rather than interpreting multiple parameters
- **Holistic Assessment:** LEI may reveal discrepancies (e.g., stable FEV1 but declining ICS) prompting investigation
- **Trend Detection:** Gradual LEI decline could provide earlier warning than threshold-based alerts
- **Clinical Efficiency:** Clinicians could use LEI trends for rapid status assessment during consultations

These potential benefits remain speculative until empirical validation.

4. Discussion

4.1 Rationale and Positioning

The AI-Driven Pranayama Spiroball represents a proposed integration of rehabilitation and diagnostic monitoring within a single platform. By combining real-time technique coaching with standardized lung function measurement, the system aims to address two persistent
problems: user error reducing data quality, and data complexity limiting patient comprehension.

4.2 Relationship to Existing Literature

The design rationale draws on established evidence:

- **Incentive Spirometry Limitations:** It has been documented that incentive spirometry benefits are constrained by patients' inability to master correct technique without supervision [6]. The proposed AI coaching aims to provide supervision-equivalent feedback.
- **Home Spirometry Reliability:** Studies of home PEF monitoring show significant variability due to technique inconsistency [7]. Real-time maneuver quality feedback could improve reliability.
- **Pranayama Efficacy:** Research has demonstrated that structured Pranayama training improves pulmonary function parameters [4]. The system operationalizes these techniques with objective feedback.

4.3 Design Trade-offs and Limitations

Technical Limitations:
Camera-based abdominal tracking may be affected by clothing, lighting, and body position; controlled conditions may be necessary
Smartphone processing capabilities vary; older devices may not achieve target inference speeds
The proposed spirometric sensor adds cost and complexity compared to standalone peak flow meters
Methodological Limitations
LEI component weightings ($w_1=w_2=0.5$) are arbitrary pending optimization studies.
ICS normalization requires population reference values that do not exist.
The relationship between camera-derived abdominal displacement and actual diaphragmatic excursion requires validation.
Scope Limitations:
This paper presents a conceptual framework only; no prototype exists.
All efficacy claims are theoretical and require empirical confirmation.
Generalizability across age groups, disease severity, and cultural contexts is unknown.

4.4 Economic Considerations

Note: Economic projections below are illustrative and require validation through health economic studies.If the system achieves its intended goals, potential cost savings in the Indian healthcare context could include:

Table 4: Illustrative Cost-Offset Analysis (Indian Healthcare Context)

Cost Category	Current Avg. Cost (₹)	Potential Savings Mechanism
ED Visit (Asthma)	8,000 – 15,000	Early trend detection allows for timely medication adjustment, preventing emergency room visits.
COPD Hospitalization	50,000 – 80,000	Real-time monitoring and high TAS (Technique Adherence) improve rehab success and reduce re-admission.
Pulmonologist Visit	800 – 1,500	Reduced need for "check-in" visits when the user's LEI (Lung Efficiency Index) remains stable and green.
Follow-up Spirometry	500 – 1,200	Substitutes frequent laboratory-grade tests with reliable, daily home monitoring.
ICU Admission	15,000 – 30,000+ per day	Prevents severe exacerbations that lead to critical care and ventilator dependency.

These projections assume the system's efficacy is validated. Actual cost-effectiveness will depend on device pricing, adoption rates, and clinical outcomes demonstrated in Phase III trials.

4.5 Future Research Directions

Beyond the validation roadmap (Section 2.9), several enhancements warrant investigation:

- **Extended Sensing:** Pulse oximetry and heart rate variability integration for cardiopulmonary assessment
- **Population Analytics:** Aggregated LEI trends for epidemiological insights and exacerbation prediction models
- **EHR Integration:** Automated data synchronization with electronic health records
- **Special Populations:** Pediatric and geriatric-specific protocols with adapted interfaces
- **Accessibility:** Voice control and multilingual support for broader reach
- **Biomarker Research:** Exhaled breath analysis for early disease detection (speculative; requires substantial additional development)

5. Conclusion

This paper presents a conceptual framework for the AI-Driven Pranayama Spiroball, a proposed system integrating respiratory rehabilitation with diagnostic monitoring. The key contributions are:

- Dual-Mode Architecture: A design combining Pranayama-based inhalation training (using spiroball with camera-based coaching) and spirometric exhalation measurement (using dedicated flow sensor)
- Technical Specifications: Detailed component requirements including MediaPipe-based pose estimation, BLE-connected spirometric sensor, and on-device AI inference
- 3.Proposed LEI Metric: A composite index combining inspiratory capacity, expiratory function, and technique quality scores—presented with explicit uncertainty regarding optimal weightings and clinical validity
- Validation Roadmap: Phased approach from technical feasibility (n=15) through usability testing (n=30) to clinical validation (n=100)

Current Status: A functional prototype is currently under development. All efficacy claims remain hypothetical pending empirical validation.

Critical Next Steps:

- Completion of functional prototype
- Phase I feasibility study with healthy volunteers
- IRB approval and ethics committee review
- Iterative refinement based on pilot data

The design draws on evidence supporting Pranayama's respiratory benefits and addresses documented limitations of current home monitoring devices. However, the ultimate value of this approach depends entirely on validation outcomes.

Acknowledgments

The authors acknowledge the support of their respective institutions in facilitating this conceptual research work. We express gratitude to Meenakshi Academy of Higher Education and Research and Volgograd State Medical University for providing the academic environment enabling this interdisciplinary collaboration.

References

[1] Global Initiative for Asthma. (2023). Global strategy for asthma management and prevention. Retrieved from www.ginasthma.org

[2] Bhavanani, A. B. (2016). Pranayama for health and therapeutic applications. *International Journal of Yoga*, 9(1), 1-2.

[3] Madanmohan, Jatiya, L., Udupa, K., & Bhavanani, A. B. (2003). Effect of yoga training on reaction time, respiratory endurance and muscle strength. *Indian Journal of Physiology and Pharmacology*, 47(4), 387-392.

[4] Madanmohan, Rai, U. C., Balavittal, V., Thombre, D. P., & Swami, G. (2005). Cardiorespiratory changes during savitri pranayama and shavasan. *The Yoga Review*, 3(1), 25-34.

[5] Nagarathna, R., & Nagendra, H. R. (2015). Role of yoga in management of bronchial asthma. *International Journal of Yoga*, 8(2), 71-73.

[6] Overend, T. J., Anderson, C. M., Lucy, S. D., Bhatia, C., Jonsson, B. I., & Timmermans, C. (2001). The effect of incentive spirometry on postoperative pulmonary complications: A systematic review. *Chest*, 120(3), 971-978.

[7] Reddel, H. K., Taylor, D. R., Bateman, E. D., Boulet, L. P., Boushey, H. A., Busse, W. W., ... & Woolcock, A. J. (2015). An official American Thoracic Society/European Respiratory Society statement: Asthma control and exacerbations. *American Journal of Respiratory and Critical Care Medicine*, 180(1), 59-99.

[8] Singh, V., Wisniewski, A., Britton, J., & Tattersfield, A. (2018). Effect of pranayama on pulmonary function tests in patients with bronchial asthma. *International Journal of Yoga*, 11(2), 131.

[9] Vempati, R. P., & Telles, S. (2002). Yoga-based guided relaxation for bronchial asthma. *Journal of Asthma*, 39(8), 707-712.

[10] Sudhan, P., & Parveen, S. J. (2025). Exploring the Effects of Yoga on Depression Relief in Academically Stressed Students: A Quantitative Analysis Using the SDS and Facial Emotion Recognition Technology. Journal of Neonatal Surgery, 14(2).

[11] Akshay, K., Subbiah, B., Rajeev, R., & Jagadevan, M. (2024). Surface electromyographic analysis of the bilateral abdomen and back muscle during selected yoga posture. Journal of Bodywork and Movement Therapies, 40, 1994-2000

Yoga Vasiṣṭha's Sthiti Prakaraṇa as a Framework for Emotional Balance, Stress Management, and Academic Success in Modern Student Life

P. Sudhan[1], Tamil Amuthu[2]

[1]Faculty of Management, AP, SRM Institute of Science & Technology, India, Kattankulathur, India
[2]Yoga university of Americas, Florida

Abstract: The *Sthiti Prakaraṇa* in the *Yoga Vasistha* examines the psychological and philosophical mechanisms through which the mind, driven by identification, indulgence, and attachment, constructs and sustains illusions of reality, with *ahaṅkāra* (ego) playing a central role. It uses allegorical narratives like Prince Rama's existential doubts and the stories of Bhārgava (Śukra), Dāma, Vyāla, Kaṭa, and Dāśūra to emphasize the impermanence of material pursuits and ego-based attachments. These teachings advocate self-inquiry, detachment, mindfulness, and emotional regulation as tools for transcending ego and achieving mental clarity.

Objective: The study aims to explore the psychological and spiritual insights of the *Sthiti Prakaraṇa* in the *Yoga Vasistha* while identifying its relevance in addressing modern challenges like stress, anxiety, and emotional turbulence, particularly among students in competitive environments.

Method: A descriptive approach was adopted to analyze the allegorical stories and philosophical principles in the *Sthiti Prakaraṇa*. The study integrates ancient concepts such as pranayama, mindfulness, and detachment with contemporary psychological frameworks, including Primary and secondary sources were utilized for textual analysis, alongside experimental intervention using the Academic Success Inventory for College Students (ASICS). Sixty individuals experiencing moderate-to-high stress were randomly assigned to a 12-week intervention consisting of yoga practices that emphasized mindfulness, detachment, and self-inquiry. To achieve the purpose of the study, 60 students were selected through stratified random sampling from SRM Institute of Science and Technology, Tamil Nadu, India. The participants' ages ranged from 19 years and above. A control group, which did not engage in yoga practices, was also included. Academic success was assessed for both groups.

Results: The findings reveal that the mind's role in constructing and sustaining perceived realities underscores the importance of self-awareness and detachment in overcoming suffering. Narratives like those of Bhārgava and Dāśūra highlight the transient nature of worldly attachments. The psychological teachings—focused on mindfulness, self-inquiry, and regulation of vasanas—closely align with modern stress management techniques, thereby offering effective strategies for enhancing emotional regulation and resilience. For **Group I (Yoga intervention),** the mean pre-test score was **18.90** (SD = 3.252) and the post-test mean was **24.20** (SD = 6.336). The paired t-test revealed a significant difference with a mean gain of **5.300 (SD = 3.084, SE = .089), t(29) = 6.322, p < .001**, exceeding the t-table value of 2.045 at df = 29. This demonstrates that mindfulness, detachment, and self-inquiry practices significantly improved academic success .For **Group II (Control group, no intervention),** the pre-test mean was **21.966** (SD = 3.866) and the post-test mean was **20.433** (SD = 3.812). The paired t-test indicated no significant change, with a mean difference of **–.5766 (SD = 2.7564, SE = .4206), t(29) = –2.455, p = .256,** which is below the critical t value of 2.045. This suggests no statistical improvement in academic success without the yoga-based practices.

Conclusion: The findings affirm that the *Sthiti Prakaraṇa* provides timeless psychological and philosophical guidance for transcending ego-driven attachments and cultivating emotional clarity. The integration of its principles into educational frameworks empowers students to manage stress, build resilience, and enhance academic performance. Statistical analysis confirms that students engaging in

yoga practices of mindfulness, detachment, and self-inquiry achieved significant academic success compared to those without such intervention, demonstrating the enduring relevance of the *Yoga Vasiṣṭha* in modern education.

Keywords: Yoga Vasistha, Sthiti Prakaraṇa, Ego (*Ahaṅkāra*), Mindfulness, Self-Inquiry, Stress Management, Emotional Resilience

1. Introduction

The Yoga Vasistha, an ancient philosophical text, presents a dialogue between Sage Vasistha and Prince Rama, exploring the nature of reality, consciousness, and self-liberation. The Sthiti Prakaraṁa, one of its sections, focuses on how the mind sustains illusions and how individuals can transcend suffering through detachment and self-awareness. The **Yoga Vasistha** delves into profound metaphysical concepts, highlighting the transient nature of the material world and the illusory construct of time. It posits **Brahman** as the ultimate, eternal consciousness, with self-realization attainable through meditation, detachment from worldly attachments, and the wisdom imparted by a knowledgeable teacher. The text uses rich analogies, such as the sun dispelling darkness, to illustrate the interconnectedness of all existence. The mind, as both the origin of bondage and liberation, must transcend its attachments to achieve freedom and unity with the supreme. Furthermore, it emphasizes aligning with the natural order to realize one's true nature. The core teachings of the **Yoga Vasistha** are encapsulated in notable translations by **Swami Venkatesananda** (*The Yoga Vasistha: The Royal Road to Enlightenment*) and **Swami Sivananda** (*Yoga Vasistha: The Supreme Yoga*), both offering critical interpretations of these metaphysical teachings. Additionally, the work provides profound insights into the nature of time, the mind's illusions, and the process of spiritual awakening through divine wisdom. With growing stress, anxiety, and emotional challenges among students and professionals today, the insights from this text can offer valuable strategies for mental resilience and well-being [1-2].

Fig. 1: Teach imparting wisdom to Lord Rama

Figure 1 illustrates Sage Vasistha imparting wisdom to Lord Rama in a Gurukulam, emphasizing mindfulness, self-inquiry, and detachment. The depiction reflects the teachings of the *Sthiti Prakaraṇa* in the *Yoga Vasistha*, highlighting the transient nature of ego-driven attachments. This conceptual illustration symbolizes the path to mental clarity and emotional resilience through self-awareness and detachment.

2. Literature Review

Numerous studies have highlighted the relevance of ancient Indian philosophies in modern psychological and stress management techniques. The **Yoga Vasistha**, particularly the **Sthiti Prakaraṇa**, offers profound insights into the nature of the mind, self-awareness, and emotional regulation, aligning closely with contemporary psychological theories. **Mindfulness and Stress Reduction:** Mindfulness-Based Stress Reduction (MBSR), introduced by **Kabat-Zinn (2003) & Sudhanp (2025)**, has demonstrated significant effectiveness in reducing stress, improving emotional regulation, and enhancing well-being. MBSR integrates mindfulness meditation with cognitive behavioral approaches to cultivate present-moment awareness, a concept deeply embedded in Yogic traditions. Similar principles can be found in the **Yoga Vasistha,** which emphasizes detachment, self-inquiry, and meditation as means to transcend psychological suffering. Studies by **Brown & Ryan (2003)** on mindfulness affirm that sustained mindfulness practice enhances self-regulation and reduces emotional reactivity, concepts that resonate with the teachings in the **Sthiti Prakaraṇa. Ego and Emotional Distress:** Research on **self-concept and ego involvement (Baumeister, 1999)** indicates that excessive identification with personal achievements and failures can lead to emotional distress, anxiety, and depression. The **Yoga Vasistha** presents a similar argument, asserting that **ahaṅkāra (ego)** creates illusions of permanence and attachment, leading to suffering. The allegorical stories of **Bhārgava, Dāma, Vyāla, Kaṭa, and Dāśūra** illustrate how individuals entangled in ego-driven pursuits suffer from distress and illusion. Modern psychological studies (Tangney et al., 2007) suggest that reducing self-attachment and adopting an ego-transcendent perspective can enhance emotional resilience—an idea central to Yogic teachings. **Detachment and Mental Clarity:** Philosophical and psychological research supports the notion that **detachment from transient experiences fosters greater mental clarity and emotional stability**. Studies by **Deci & Ryan (2000) & Sudhanp (2024)** on self-determination theory emphasize autonomy in personal development, aligning with the **Yoga Vasistha's** advocacy of inner self-mastery. Similarly, research on **cognitive defusion in Acceptance and Commitment Therapy (ACT) (Hayes et al., 1999)** parallels the Yogic approach of observing thoughts without attachment, reinforcing the **Sthiti Prakaraṇa's** emphasis on witnessing mental fluctuations rather than identifying with them. **Application in Educational and Competitive Environments :** Student populations face immense stress due to competitive academic environments, performance anxiety, and societal pressures. Research by **Selye (1976)** on stress adaptation suggests that chronic stress without coping mechanisms leads to burnout, anxiety, and mental exhaustion. Integrating **Yoga Vasistha's** principles into education—particularly its teachings on **mindfulness, detachment, and self-inquiry**—can serve as a resilience-building tool for students. Studies on **contemplative education (Shapiro et al., 2011** & **Sudhanp 2023.2021)** highlight the benefits of meditation and reflective practices in reducing academic stress, aligning with the **Sthiti Prakaraṇa's** message of equanimity and inner stability.The **Sthiti Prakaraṇa** of the **Yoga Vasistha** presents timeless wisdom that aligns with modern psychological and neuroscientific findings on **stress management, mindfulness, ego reduction, and emotional resilience**. The integration of these ancient teachings into modern frameworks can offer **practical strategies for mental well-being, particularly among students and individuals facing high-pressure environments [3-16].**

3. Methodology

Data from the study sample's pre- and post-tests in one experimental group and one control group were analysed for psychological influences. Sixty students from who attend the SRM Institute of Science & Technology Tamil Nadu, aged 19 and older, were chosen for this study. The participant acceptance form and institutional permission statement accepted the procedures used in this study that engaged participants ethically as routine. We give Mindfulness-Academic Success Based questionnaire like Prevatt academic success inventory. The participants were divided into two groups, each consisting of 30 students. the experimental group 1 received Yoga for **mindfulness, detachment, and self-inquiry**. While The control group 2 did not practice.

3.1 Prevatt Academic Success Inventory For College Students (ASICS)

The **Prevatt Academic Success Inventory For College Students (ASICS)** is a standardized tool designed to measure various factors that contribute to academic performance and adjustment in higher education. In this study, we randomly selected 20 items from the ASICS that are specifically related to **academic stress**, such as difficulties with concentration, time management, motivation, anxiety, and coping with academic pressure. These selected items provide insight into how stress influences students' learning habits, emotional well-being, and overall academic functioning. By focusing on this subset of stress-related items, the instrument serves as a reliable means to evaluate the relationship between academic stress and student success, offering valuable data for designing targeted interventions to enhance resilience and academic performance **[17].**

3.2 The Path to Clarity

Figure 2 show that Primary Sources: The Yoga Vasistha, through its translations and allegorical stories, offers valuable insights into stress management by emphasizing self-realization, detachment, and meditation. The Sthiti Prakaraṁa highlights how the mind's
attachment and illusion contribute to stress, proposing detachment and reflection as key to mental peace. Meditation, a core practice in Yoga Vasistha, serves as a tool for achieving clarity and inner calm, making it essential for both ancient and modern stress relief techniques.

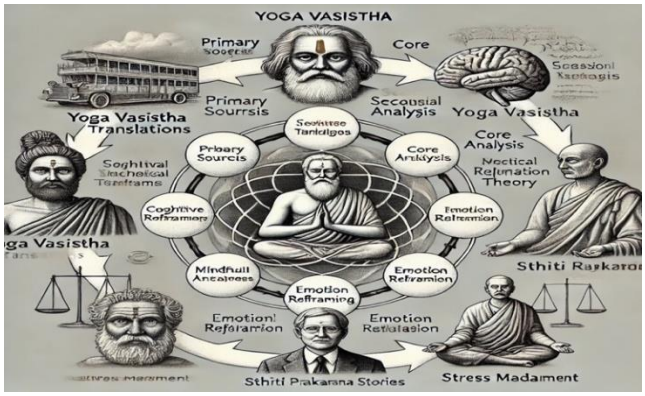

Fig. 2: The Path to Clarity: Meditative Detachment in the Sthiti Prakaraṁa

Secondary Sources: Scholarly articles delve into the relationship between stress management and mindfulness, particularly through Indian philosophies like the *Yoga Vasistha*. They explore how its practices—detachment, self-realization, and meditation—align with modern psychological approaches like Cognitive Behavioral Therapy (CBT) and **Academic Success Inventory for College Students**

(ASICS). These sources highlight how integrating ancient wisdom with contemporary psychology can improve emotional regulation and mental wellness.

4. Results and Discussion

4.1. Statistics calculations

SPSS 19.0 was used to conduct the study's statistical analysis. The results were described using percentages, averages, and standard deviations. Since its beginnings as a statistical analysis tool, SPSS has developed into a popular among academics for a variety of features**[18-24].**

4.2. Interpretation of Result

If t cal < t tab Value , Accept Ho there is no relationship between Yoga for mindfulness, detachment, and self-inquiry practice (Group 1) to Psychological Academic Success variables .If t cal > t tab Value , Rejected Ho there is relationship between Yoga for mindfulness, detachment, and self-inquiry practice (Group 1) to Psychological Academic Success variables. If t cal < t tab Value, Accept Ho there is no relationship between without Yoga for mindfulness, detachment, and self-inquiry practice (Group 2) to Psychological Academic Success variables. If t cal > t tab Value , Rejected Ho there is relationship between without Yoga for mindfulness, detachment, and self-inquiry practice (Group 2) to Psychological Academic Success variables. Degree of freedom (df) = n-1 So df= 29.Then t table value is 29 df = 2.045.

Table 1. Paired Samples T Test For Pre-test and Post-test for Group I

		Pre-test and Post-test for Group I			
	Test	Mean	N	Std. Deviation	Std. Error Mean
Academic Success	Pre Test	18.90	30	3.252	.011
	Post Test	24.20	30	6.336	.090

The analytical tool was used to investigate the experimental Group-I. Table 1 displays the pre-test and post-test outcomes for Yoga for mindfulness, detachment, and self-inquiry practice. The 30 participants, mean value, standard deviation, and standard error mean of the results were distributed down as needed.

Table 2. Paired Samples T Test for Pre-test and Post-test for Group I

Paired Sample T Test Differences					t	df	Sig. (2-tailed)
			95% Confidence Interval of the Difference				
Mean	Std. Deviation	Std. Error Mean	Lower	Upper			
5.300	3.084	.089	2.302	5.796	6.322	29	.000

The analysis tool was used to examine the experimental Group-I. Table-2 Shows that Academic Success presents the pre-test and post-test value of Yoga for mindfulness, detachment, and self-inquiry practice . The Mean Value 5.300, Std. Deviation 3.084, Std. Error Mean .089, lower value 2.302 upper value 5.796, t value 6.322, df 29 respectively, resulted in Sig. (2-tailed) of .000, the t

calculation value of 6.322 greater than the table value of 2.045. So it's considered statistically significant difference between the pre & post-test
means at 0.05 level of confidence for the both test of Yoga for mindfulness, detachment, and self-inquiry practice. reveals that the Academic Success pre-test and post-tests Yoga for mindfulness, detachment, and self-inquiry practice had a significant value.

Table 3. Paired Samples T Test For Pre-test and Post-test for Group II

		Pre-test and Post-test for Group II			
	Test	Mean	N	Std. Deviation	Std. Error Mean
Academic Success	Pre Test	21.966	30	3.866	.653
	Post Test	20.4333	30	3.812	.623

The analytical tool was used to investigate the experimental Group-II. Table 3 displays the pre-test and post-test outcomes for without Yoga for mindfulness, detachment, and self-
inquiry practice. The 30 participants, mean value, standard deviation, and standard error mean of the results were distributed down as needed.

Table 4. Paired Samples T Test for Pre-test and Post-test for Group II

Paired Sample T Test Differences					t	df	Sig. (2-tailed)
			95% Confidence Interval of the Difference				
Mean	Std. Deviation	Std. Error Mean	Lower	Upper			
-.5766	2.7564	.4206	-2.122	.1892	-2.455	29	.256

The analysis tool was used to examine the Control Group. Table-4 Shows that Academic Success presents the pre-test and post-test value of without Yoga for mindfulness, detachment, and self-inquiry practice. The Mean Value -.46667, Std. Deviation 1.75643, Std. Error Mean .32068, lower value -1.12253 upper value .18920, t value -1.455, df 29 respectively, resulted in Sig. (2-tailed) of .156, the t calculation value of -1.455 less than the table value of 2.045. So it's considered statistically no significant difference between the pre & post-test means at 0.05 level of confidence for the both test of Academic success in Yoga for mindfulness, detachment, and self-inquiry practice. reveals that the Academic success pre-test and post-tests Yoga for mindfulness, detachment, and self-inquiry practice had a no significant value.

4.3 Holistic approach Presents Academic success

The study underscores the significant role of the mind in creating and sustaining perceived realities, emphasizing the importance of self-awareness and detachment in overcoming suffering. Through the allegorical narratives within the *Sthiti Prakaraṁa*, it becomes evident that attachments and ego-driven pursuits, as demonstrated by the stories of Bhārgava and Dāśūra, are impermanent and ultimately lead to suffering. These tales illustrate how material desires and ambitions are transient, prompting the need for a deeper understanding of what truly matters. The *Yoga Vasistha* also highlights mindfulness practices such as pranayama, meditation, and self-inquiry as effective methods for quieting the mind

and attaining inner peace. These techniques are integral to emotional regulation, offering a pathway to manage stress and negative emotions. Additionally, the text emphasizes the importance of recognizing and overcoming vasanas, or persistent mental impressions, which shape an individual's thoughts and emotional responses. By transcending these ingrained thought patterns, individuals can build emotional resilience and gain greater control over their reactions to life's challenges, ultimately leading to a state of spiritual and mental clarity. This holistic approach offers profound insights into how ancient wisdom can be applied to modern stress management practices.

5. Discussion

When the baseline characteristics of the two groups were compared, one group showed a significant difference while the other group showed no improvement, therefore they were assessed for the study. levels significantly Increased in the practising Yoga for mindfulness, detachment, and self-inquiry practice during the course of the 12-week study. The control group remained unchanged because they didn't have access to Yoga for mindfulness, detachment, and self-inquiry practice. In the yoga groups, we noticed a significant improvement in Academic Success. Thus, practising Yoga for mindfulness, detachment, and self-inquiry practice allowed Group 1 Participants to experience Increased Academic Success. The reduction in stress may have been influenced by Group 1's improved Academic function. Due to their intellectual background, the yoga group may have performed better on the Academic Success test

5.1 Graph I Pre-test and Post-test for Group I

According to the graph I analysis, participants in Group -1 Yoga practice module outperformed the Control group. 12 weeks yoga practice has shown to be effective and causes significant Psychologically changes in Academic Success.

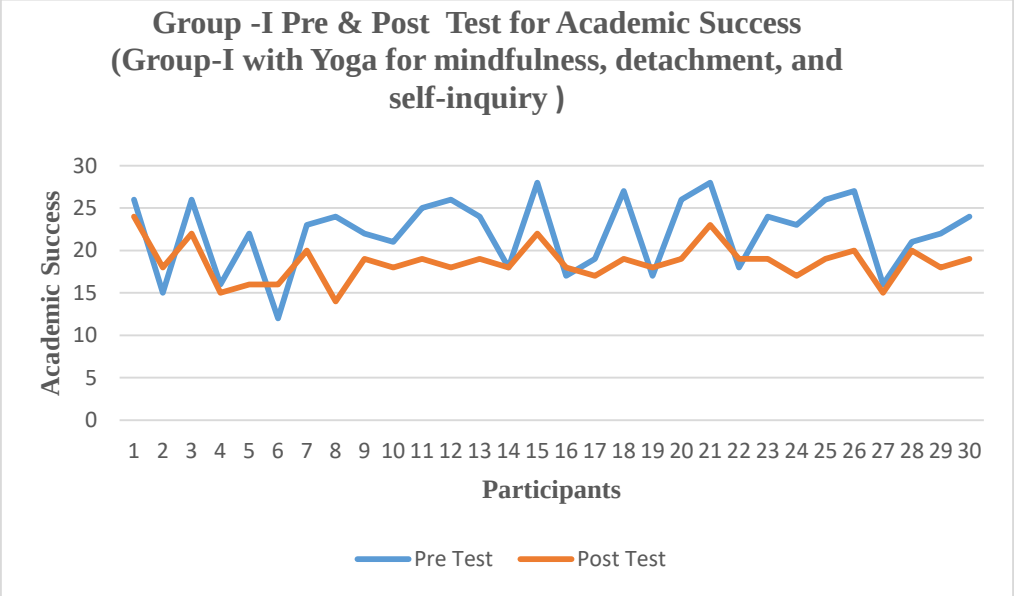

Fig.3. Graph-I Stress Pre& Post-Test with Brain Yoga

The graph analysis showed that participants in the Group 1 Academic Success practise module performed well better than the Control group. Yoga has been proven to be efficient and creates major psychological improvements in Academic Success after 12 weeks of practise .The primary goal of Yoga for mindfulness, detachment, and self-inquiry practice is to increase the psychological effects of Academic Success. Students' evaluations of the advantages of yoga treatment were applied with successful results in experimental group 1 following post-test diagnosis. The 'x' axis of Graph 1 reflected the number of participants (30), and the 'y' axis displayed psychological data, including the Academic Success inventory level. After the pre-test, the participants received yoga exercises including Yoga for mindfulness, detachment, and self-inquiry practice . The findings of the Academic Success Pre-Test were highlighted in blue on graphs with psychological data on the 'y' axis. Results from the Academic Success level post-test showed Orange.

5.2 Graph II Pre-test and Post-test for Group II

According to the graph II in Figure 4, participants in Group II's control group did not experience significant improvements. After the pre-test, no practise was given to the participants. There was no discernible difference between the pre- and post-test scores for Academic Success. The graph demonstrates that there are no effective outcomes.

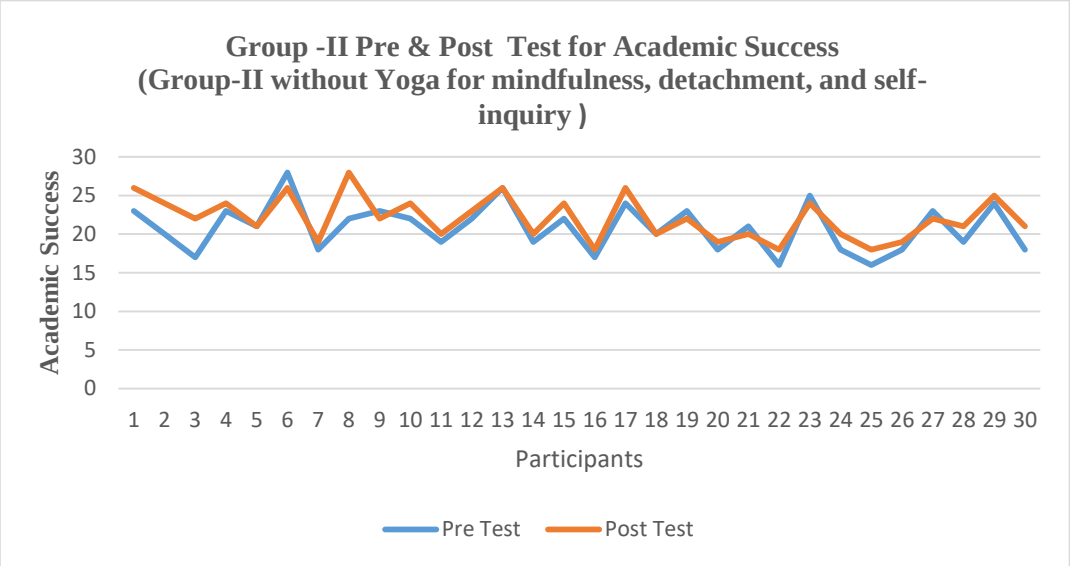

Feg.4. Graph-II Academic Success Pre & Post-Test without Brain Yoga

6. Conclusion

The analysis of the Academic Success Inventory data revealed that participants in Group I, who engaged in yoga practices focused on mindfulness, detachment, and self-inquiry, demonstrated significantly greater improvements in academic success compared to the control group. The experimental group's post-test results showed enhanced psychological outcomes, indicating that yoga served as an effective intervention for promoting resilience, focus, and motivation in students. In contrast, Group II, which did not receive any intervention, showed no notable changes between pre- and post-test scores. These findings highlight yoga's potential as a powerful tool for improving academic performance and psychological well-being. Furthermore, insights from the *Sthiti Prakaraṁa* emphasize timeless wisdom on transcending ego-driven attachments, cultivating emotional resilience, and fostering inner strength. Integrating such philosophical teachings with

modern educational and psychological frameworks can help students manage academic stress, embrace challenges as growth opportunities, and achieve holistic success.

7. Recommendations

Integrating mindfulness and self-inquiry techniques from the *Yoga Vasistha* into student counselling programs can promote self-awareness and emotional resilience, helping individuals navigate stress more effectively. Additionally, developing stress management
workshops and training that incorporate pranayama, meditation, and detachment principles can provide practical tools for achieving inner peace and mental clarity. Further research on blending ancient Indian wisdom with contemporary psychological therapies can lead to holistic and effective mental health interventions. By applying these insights, we can foster comprehensive personal development and enhance emotional well-being in today's fast-paced world.

8. Acknowledgments

I extend my gratitude to our administrative authorities of SRM Institute of Science and Technology for providing the necessary facilities and conducive environment for my research endeavours . Their encouragement and guidance have been instrumental in our exploration of the effects of Psychological Insights from Sthiti Prakaraṇa in Yoga Vasistha: A Holistic Framework for Stress Management , Emotional Resilience and Academic Success in Modern Student Life

9. Declaration of competing interest

The authors have no competing interests to declare that are relevant to the content of this article.

10. Funding

NA

References

[1] Venkatesananda, Swami. The Yoga Vasistha: The Royal Road to Enlightenment.
[2] Sivananda, Swami. Yoga Vasistha: The Supreme Yoga.
[3] Baumeister, R. F. (1999). The self in social psychology. Psychology Press.
[4] Brown, K. W., & Ryan, R. M. (2003). The benefits of being present: Mindfulness and its role in psychological well-being. Journal of Personality and Social Psychology, 84(4), 822-848. https://doi.org/10.1037/0022-3514.84.4.822
[5] Deci, E. L., & Ryan, R. M. (2000). The "what" and "why" of goal pursuits: Human needs and the self-determination of behavior. Psychological Inquiry, 11(4), 227-268. https://doi.org/10.1207/S15327965PLI1104_01
[6] Sudhan, P. (2025). Exploring the effects of yoga on depression relief in academically stressed students: A quantitative analysis using the SDS and facial emotion recognition technology. *Journal of Neonatal, [Volume]*([Issue]), [Page numbers]. ISSN: 2226-0439. https://doi.org/[DOI]
[7] Sudhan, P. (2025). Stress management in higher education: The role of online yoga and digital learning. *Journal of Lifestyle and SDGs, [Volume]*([Issue]), [Page numbers]. ISSN: 2965-730X. https://doi.org/[DOI]

[8] Hayes, S. C., Strosahl, K. D., & Wilson, K. G. (1999). Acceptance and commitment therapy: An experiential approach to behavior change. Guilford Press.

[9] Kabat-Zinn, J. (2003). Mindfulness-based stress reduction (MBSR) in past and present. Clinical Psychology: Science and Practice, 10(2), 144-156. https://doi.org/10.1093/clipsy.bpg016

[10] Sudhan, P. (2024). The effects of Thoppukaranam (Super Brain Yoga) on stress management and psychological health in university students: A 12-week intervention study.

[11] RGSA – Revista de Gestão Social e Ambiental, [Volume]([Issue]), [Page numbers]. ISSN: 1981-982X. https://doi.org/[DOI]

[12] Sudhan, P. (2024). Effect of brain yoga practice in university academic students: Optimizing quality of life and stress management. Educational Administration: Theory and Practice, [Volume]([Issue]), [Page numbers]. E-ISSN: 2148-2403. https://doi.org/[DOI]

[13] Selye, H. (1976). The stress of life (Rev. ed.). McGraw-Hill.

[14] Shapiro, S. L., Brown, K. W., & Astin, J. A. (2011). Toward the integration of meditation into higher education: A review of research. Teachers College Record, 113(3), 493-528.

[15] Tangney, J. P., Baumeister, R. F., & Boone, A. L. (2007). High self-control predicts good adjustment, less pathology, better grades, and interpersonal success. Journal of Personality, 72(2), 271-324. https://doi.org/10.1111/j.1467-6494.2004.00263.x

[16] Sudhan, P. (2024, June). *Sage Vallalar: The Varmam plant cures incurable ailments – Karisalanganni*. Conference Paper.

[17] Sudhan, P. (2021, December). *The philosophical effects of Thirukkural on stress management*.

[18] Prevatt, F., Petscher, Y., Proctor, B. E., Hurst, A., & Adams, K. (2011). The revised Academic Success Inventory for College Students: Measuring academic motivation, attention, and study skills. *Journal of College Admission, 211*(Fall), 26–31.

[19] Pallant, J. (2020). SPSS survival manual: A step by step guide to data analysis using IBM SPSS. Routledge.

[20] Sudhan, P., & Parveen, S. J. (2022). Effects Of Yoga On Stress Factors Among College Students. Specialusis Ugdymas, 1(43), 4835-4842.

[21] Sudhan, P., & Parveen, S. J. (2022)Effect Of Yogic Practices On Selected Psychological Variables Among Academic Anxiety Students. Seybold report**.** DOI 10.17605/OSF.IO/2SCWA

[22] Babu Kaiyaperumal, A., Subbiah, B., Paulraj, M., & Sudhan, P. (2022). Prevention Enhance Program (Pep) with proprioceptive training on the recurrence of ACL injury for post-ACL reconstruction among football players. *Neuroquantology*, *20*(19), 143-148.

[23] Sudhan, P., Subbiah, B., Sukumaran, R., Janaki, G., Nagesh, P., & Kalpana, L. Efficacy of Yoga Therapy on Psychological Variables in Male Persons with Diabetic Peripheral Neuropathy (DPN).(2023). *Int. J. Life Sci. Pharma Res, 13*(1), L230-244.

[24] Ananthan, B., Sudhan, P., & Sukumaran, R. (2023). English facilitators' hesitation to adopt AI-assisted speaking assessment in higher education. *Boletin de Literatura Oral-The Literary Journal*, *10*(1), 1324-1329.

[25] Sudhan, P., Subbiah, B., Rajagopalan, N., Sukumaran, R., Janaki, G., & Ananthan, B. (2023). Effect of yoga therapy on neurological characteristics in diabetic peripheral neuropathy: Neuro health perspective. *Journal for ReAttach Therapy and Developmental Diversities*, *6*(10),1071-1078.

Isolated Combined Effects of Yogic Practices Continuous Training On Selected Physiological and Bio Chemical Variables among University Middle Distance Runners

Manas Ranjan Behere[1], Dr.T.Arun Prasanna[2], Dr U V Sankar[3]

BPES IIyr[1], Assistant Professor[2], Director[3]
School Of Sports Education and Research, Department Of Physical Education and Sports,
Jain (Deemed To-Be University), Bangalore, India.

Abstarct: The study aims to determine the isolated and combined effect of yogic practices continuous training, physiological variable (Vital Capacity) and Biochemical Variables (Lactic Acid) among the male athletes of JAIN deemed to be University,School of Sports Education and Research , Bangalore. The research involved a random subject selection of twenty athletes with age ranging from 17-25 years and had two equally divided groups' namely experimental groups with 10 athletes each. The groups endured the training activities for twelve weeks with a schedule of thrice a week whereas the control group remained with no activities. The data procured in prior and after the training programme was examined with the application of Analysis of variance and the fixation of level of significance at 0.05.

Keywords: Yogic Practice, Continuous training, Vital capacity, Lactic Aci

1. Introduction

The conditioning and coaching are the chief words in sports training. Conditioning is a process of gradually preparing the body for strenuous physical activity for focusing attention on development of physical and motor fitness components and indirectly enhancing sports performance. The characteristic feature of training as a program of activities intends for the enhancement of the ability of force of a person for a specific occasion. The coordinative process of logical and instructive standards drives an individual to the best level of execution in sports. Sports training is a procedure of flawlessness coordinated by logical and instructive standards and goes for driving an individual to high and best level execution in sports through planned methods of change in the status and limit of execution.

Yoga

"Yoga" is gotten from the underlying foundations of Sanskrit 'Yuj' which intends to join, to connect, to tie and burden and to focus on one's consideration. The exacting significance of "Yoga" is Yoke. It additionally implies association. It implies the experience of unity or solidarity with inward being. Yoga means joining the individual soul with the general soul, or God.

Continuous Training

Endurance is the ability to engage in activity with high caliber for a long time without fatigue. Every athlete requires energy for which endurance, the resultant of all the organs of psychic and physical systems is necessary. This kind of extended training with fair intensity enhances the abilities of aerobic that aim to build up the systems of energy generation.

Physiological

Physiology deals with the functional elements of the human physical body impacted by the execution of physical actions. The general health of a person with fitness and performance can be improved through the exercises of sports.

Lactic Acid

When glucose is catabolised anaerobically, the end result obtained is Lactate. Anaerobic glycol state after breakdown results in the formation of Lactic acid which is a byproduct and oxidizes unless removed from cell.

2. Methodology

The research was designed to discover isolated and combined effect of yogic practices,(bhujangasana (CS),virabhadrasana(LS) and adhomukhashvanasana(PS). Continuous training physiological variable (Vital Capacity) and Bio Chemical variables (Lactic acid) among middle distance runners. For this purpose, fifty athletes from the college were chosen randomly as subjects for the study and their age ranged between 17 to 25 years.

3. Data Analysis

Table 1. Analysis Of Variance For The Pre And Post Test Of Yogic Continous Training Group And Control Group On Vital Capacity

TEST	YOGIC AND CONTINUES TRAINING GROUP	CONTROL GROUP	SOS	DF	MEAN	F RATIO
PRE	3.504	3.538	.006	1	.006	.0857
			.121	18	.007	
POST	3.701	3.531	.155	1	.155	22.14*
			.119	18	.007	

Significant level 0.05 table value 4.10 df 1.18

The analysis presented in the table-I that indicate variance value of pre test of the combined yogic practice and continuous training and control group pre test value 3.504 and 3.538 correspondingly. The obtain ‘F ‘ratio .0857 of pre test was lesser than the table value 3.49 for df 1 and 18 mandatory for significance at 0.05 level of assurance on vital capacity. The post test mean value on vital capacity of yogic practice and continuous training group and control group are 3.701 and 3.531 correspondingly.

The obtain ‘F’ ratio 22.14* of post test was greater than the table value 3.49 for df 1 and 18 mandatory for significance at 0.05 level of assurance on vital capacity

Table 2. Analysis Of Variance Of Yogic Continues Training Group And Control Group On Lactic Acid

TEST	YOGIC AND CONTINUES TRAINING GROUP	CONTROL GROUP	SOS	DF	MEAN	F RATIO
PRE	5.50	5.43	.272	1	.272	1.087
			4.503	18	.250	
POST	6.03	5.29	2.204	1	2.024	14.45*
			2.527	18	.140	

*Required C.I Value 14.45*at 0.05 level

The analysis presented in the table-II that indicate variance value of pre test of the combined yogic practice and continues training group and control group pre test value 5.50 and 5.43 correspondingly. The obtain 'F 'ratio 1.087 of pre test was lesser than the table value 3.49 for df 1 and 18 mandatory for significance at 0.05 level of assurance on lactic acid. The post test mean value on lactic acid of yogic practice and continues training group and control group are 6.03 and 5.29 correspondingly. The obtain 'F' ratio 14.45* of post test was greater than the table value 3.49 for df 1 and 18 mandatory for significance at 0.05 level of assurance on lactic acid.

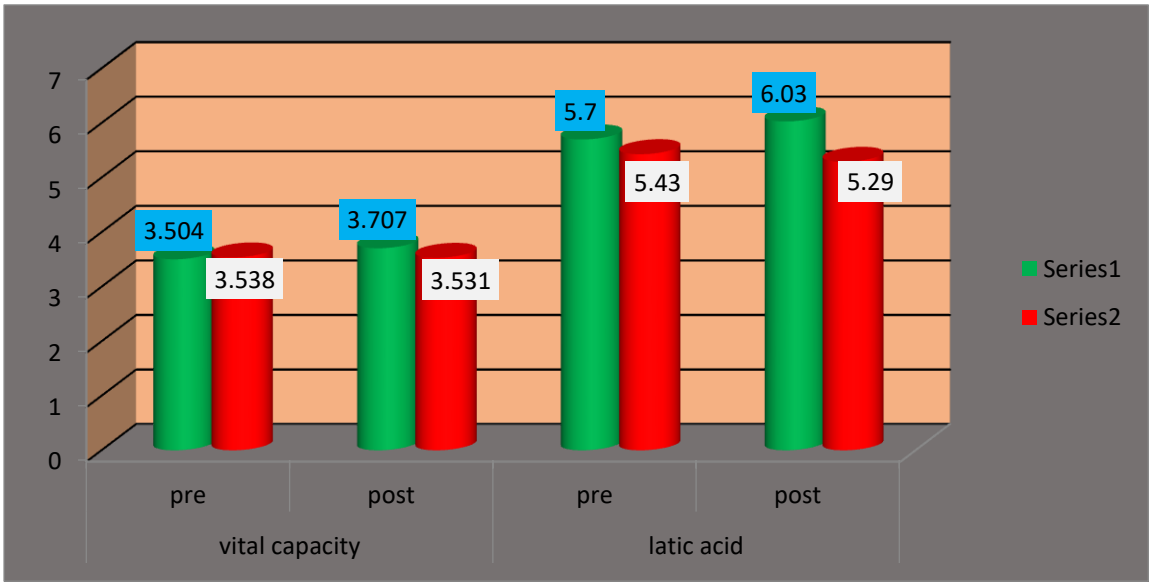

Figure 1. Bar Diagram Of The Vital Capacity And Lactic Acid Of Yogic Practice Continues Training Group And Control Group

4. Conclusions

The results of the study reveals that there was significant improvement in the experiment group selected variables when compared to the control group after the completion of 12weeks combined yogic practices continuous training. It was concluded that the combined group and control training had greater influence on vital capacity and lactic acid.

References

[1] Anand, Mithin, et al. "Effect of Game Specific Circuit Training and Plyometrics on Selected Physiological and Hematological Variables of Handball Players." *Indian Journal of Public Health Research & Development* 10.7 (2019).

[2] Meera, R., Mohanakrishnan, R., & Prasanna, T. A. (2019). Effect of Core Training with and without Yogic Practices on Selected Psychological Variables among College Women Athletes. *Indian Journal of Public Health Research & Development*, *10*(4).

[3] Saran, K. S., Vaithianathan, K., Anand, M., & Prasanna, T. A. (2019). Isolated and Combined Effect of Plyometric and Weight Training on Selected Physical Fitness and Hematological Variables of Football Players. *Indian Journal of Public Health Research & Development*, *10*(7).

[4] Arun Prasanna, T., & Vaithianathan, K. (2019). The Combined Effect of Continuous Run, Alternate Pace Run and Fartlek Training on Selected Physiological Variable among Male Athletes. *Indian Journal of Public Health Research & Development*, *10*(3).

[5] Mohanakrishnan, R. (2017). Effect of Core Strength Training and Yogasana Practices on Selected Health Related Physical Fitness Components among Female Athletes.

[6] Putnam CA. Sequential motions of body segments in striking and throwing skills. J Biomech 1993; 26: 125-35.

[7] Scibek JS, Guskiewicz KM, Prentice WE, Mays S, Davis JM. The effects of core stabilization training on functional performance in swimming. Unpublished master's thesis, University of North Carolina, Chapel Hill, North Carolina, USA. 2001.

[8] Stanton R, Reaburn PR, Humphries B. The effects of short-term swiss ball training on core stability and running economy. *J Strength Cond Res.* 2004;18(3):522–8.

[9] Taunton J, Rhodes E, Wolski L. Effect of land-based and water-based fitness programs on the cardiovascular fitness, strength and flexibility of women aged 65–75 years. J Gerontol 1996; 42: 204–210.

[10] Vivekananda Kendra Prakashan 2002. Yoga an instruction Booklet. Published by Vivekananda Kendra Prakashan Trust.

[11] World Health organization, 1997. Obesity: preventing 111 and managing the global epidemic. Report of a WHO Consultation on Obesity. Geneva: World Health organization;

[12] Zattara M, Bouisset S. Posturo-kinetic organization during the early phase of voluntary limb movement. J Neurol Neurosurg Psychiatry 1988; 51: 956-65.

Impact of Technology on Financial Markets and Institutions in Papua New Guinea (PNG)

Rajendiran Anandbabu
Accounting Lecturer, Department of Business Studies, International Training Institute, Port Moresby, Papua New Guinea (PNG)

Abstract: Papua New Guinea (PNG) has faced serious challenges in building a modern financial system. The country's tough geography and unreliable infrastructure have always made progress difficult. But a surprising shift is underway: PNG is skipping ahead and embracing digital finance. Central bank digital currencies, blockchain-based regulations, and mobile-first banking aren't just trendy terms—they're actively transforming how money moves in PNG. This study explores how PNG's financial sector has shifted from slow, paper-based processes to digital solutions like the Centurion Licensing System and the Digital Kina pilot. The result? Technology is lowering transaction costs and opening the financial system to more people. Still, there's a major issue—urban and rural areas have very different access to digital services, and this gap could threaten the system's stability.

1. Introduction

The financial sector in PNG has always struggled with its geography—a difficult terrain of mountains, islands, and remote communities. Cash handling is expensive, and the majority (roughly 80% as of 2024) still don't use banks. But a rapid change began in recent years. With the introduction of the Digital Government Act 2022 and strong support from the Bank of Papua New Guinea (BPNG), technology became central. Now, fintech, digital identification (SevisPass), and automated trading platforms are helping overhaul the outdated system, making it faster and more inclusive. This paper examines how these changes are improving efficiency and aiming for broader inclusion in PNG's financial institutions.

2. Aim and Objectives

Aim: Demonstrate how technology has reshaped financial institutions and markets in PNG, focusing on efficiency and expanding access.

Objectives:

- Examine how the Centurion Licensing System is increasing transparency in capital markets.
- Assess how Mobile Money and SevisPass (Digital ID) are helping more people obtain bank accounts.
- Evaluate the impact of the Digital Kina (CBDC) pilot on payment system security.
- Identify regulatory and infrastructure barriers slowing digital adoption.

3. Key Concerns

PNG's progress is impressive, but several major concerns remain:

- Literacy: Many rural residents still lack the skills to safely use digital tools or manage money.

➢ Cybersecurity: The move to digital introduces new risks, and PNG is vulnerable to both regional and global cyber threats.
➢ Infrastructure: Frequent power outages and limited internet access (still only around 24% coverage) make digital banking unreliable for many.

4. Research Framework

This research applies Sociotechnical Systems Theory, which views PNG's financial market as a complex interaction between social needs (like financial inclusion and the Wantok family system) and technological capabilities (such as Blockchain and Mobile APIs).

5. Review of Literature

Researchers often note that countries like PNG are "leapfrogging" past legacy systems and adopting digital solutions quickly. Key findings include:
✓ Fintech & Inclusion: The Centre for Excellence in Financial Inclusion (CEFI) reports that over 40,000 new mobile financial service accounts were created in early 2024 alone.
✓ Digital Regulation: Research on the PNG Stock Exchange (PNGX) shows that moving from T+5 to T+2 settlement cycles with digital automation has improved investor confidence.
✓ CBDCs in the Pacific: Studies on the Digital Kina pilot (with Soramitsu) highlight how digital ledger technology helps PNG overcome correspondent banking challenges, which is critical for reducing financial risk.

6. Research Methodology

❖ **Design:** Combines descriptive and analytical approaches.
❖ **Data Collection:**
❖ **Secondary:** Reports from BPNG Economic Bulletins (2024-2025), ADB Outlook 2025, and DICT Digital Transformation Summit.
❖ **Primary:** Interviews with senior staff at BPNG, MiBank, and Weathermen Capital Advisors.
❖ **Sampling:** Focused on five leading financial institutions and three fintech startups.

7. Data Analysis and Findings

7.1. Capital Market Transformation

The Centurion Licensing System, launched in early 2026, brought the Securities Commission of PNG into the digital era. Previously, license renewals took four weeks; now, the process takes less than 48 hours.

7.2. Financial Inclusion via Digital ID

With SevisPass, micro-banks like MiBank can onboard new clients in under 10 minutes. This has led to a 15% increase in "MiAkaont" registrations, especially among rural farmers who previously lacked formal identification.

7.3. Monetary Stability and CBDC

The Digital Kina proof-of-concept showed that a Central Bank Digital Currency is more than just a technical experiment—it reduced cash distribution costs by about 20% in remote regions.

8. Conclusion

In Papua New Guinea's financial sector, technology has become a necessity, not a luxury. Digital regulation and mobile banking have made finance more accessible, benefiting both international investors and local citizens. However, most of these advantages are still centered in urban areas and established
institutions. Rural communities, especially those at the "last mile," have yet to experience the same level of impact.

9. Suggestions

✓ **Interoperability:** The government should ensure SevisWallet integrates smoothly with all commercial banks. Otherwise, digital silos will prevent people from accessing services.
✓ **Offline Solutions:** Since PNG's internet is unreliable, it's important to develop "store-and-forward" digital payment systems that function even when connectivity is lost.
✓ **Regulatory Sandbox Expansion:** BPNG should broaden access to its regulatory sandbox, allowing more local Silicon Haus start-ups to participate, test micro-insurance products, and introduce new ideas.

References

[1] Asian Development Bank (2025). *Asian Development Outlook: Papua New Guinea Economic Forecast.*
[2] Bank of Papua New Guinea (2025). *Results of the Digital Kina (CBDC) Proof of Concept Study.*
[3] Department of ICT (2025). *National Digital Identity Policy 2025 and the Sevis Framework.*
[4] IMF (2025). *Papua New Guinea: 2025 Article IV Consultation - Financial Sector Assessment.*
[5] The National (2026). *New system, hope for PNG capital market: The Centurion Launch.*
[6] Soramitsu & BPNG (2024). *Blockchain Applications in Pacific Financial Markets.*

Impact of Motor Relearning Program over Traditional Management Program on Gross Motor Function among Stroke Subjects

Jibi Paul[1], Vijayan Palaniswamy[2], Praveen B M[3]

[1]Scholar, Post Doctoral Fellowship Program, Srinivas University, City Campus Pandeshwar, Mangaluru-575001, Karnataka, India, Corresponding Author E-mail: physiojibi@gmail.com

[2]Institute of Physiotherapy, Srinivas University, City Campus Pandeshwar, Mangaluru-575001, Karnataka, India, E-mail: vijayan.pswmy@gmail.com

[3]Director, Research Program, Srinivas University, City Campus Pandeshwar, Mangaluru-575001, Karnataka, India, E-mail: research@srinivasuniversity.edu.in

1. Introduction

A stroke, also referred to as a cerebrovascular accident (CVA), is an abrupt cessation of blood flow to a section of the brain, which leads to neuronal damage, neurological impairments, and potentially fatality. It poses a significant global health issue, being one of the primary contributors to death and long-term disability around the world [1]. There are two principal types of strokes, Ischemic stroke and Hemorrhagic stroke. Ischemic stroke, which constitutes about 85% of all cases, results from a blockage in an artery that, supplies blood to the brain, typically caused by a thrombus or embolism. Hemorrhagic stroke is accounting for roughly 15% of cases, occurs when a blood vessel in the brain breaks, causing bleeding into or around the brain tissue [2].Transient ischemic attacks (TIAs) often referred to as "mini-strokes," involve temporary blockages that do not result in lasting brain damage but act as significant indicators for the possibility of future strokes.

The effects of a stroke can vary greatly, depending on the size and location of the affected brain region. These effects may include paralysis or weakness (typically affecting one side of the body), difficulties with speech and language (known as aphasia), cognitive challenges, emotional issues, and diminished sensory abilities. Recovery is frequently incomplete and may result in a considerable reduction in independence and quality of life [3].Stroke is a multifactorial disease influenced by a range of modifiable risk factors—such as hypertension, diabetes, smoking, obesity, and dys-lipidemia and non-modifiable factors, including age, sex, ethnicity, and genetic predisposition. In the past few decades, major advances have been made in acute stroke management, notably through the use of thrombolytic, mechanical thrombectomy, and specialized stroke units.

However, rehabilitation remainsAcritical component of stroke care, aiming to maximize functional recovery, promote neuroplasticity, and improve the overall quality of life for survivors[4].The burden of stroke is especially high in low- and middle-income countries, where access to acute care and rehabilitation services is often limited. As the global population ages, the incidence of stroke is projected to rise, making prevention, early intervention, and effective rehabilitation increasingly important public health priorities[5].Recent research emphasizes not only saving lives but also enhancing recovery through early, intensive, and targeted rehabilitation programs including task-specific training, Neuroplasticity-driven therapies, and technology-enhanced interventions[6,7].

Aim of the study: To investigate the effectiveness of Motor Relearning Program over Traditional Management on Gross motor function in Subjects with Stroke.

Need of the study: As there are many interventions program for subjects with stroke to get back to near to normal, motor relearning- which is one of the most important features for stability of upper extremity, core stability, spinal muscles, ligaments & lower extremities either in sitting and standing,

has to be concentrated while treating subjects stroke. This is an experimental type-randomized control trail Sampling. It was Comparative study – Pre and Post type.

Allocation method: A total of 20 samples were selected based on specified inclusion and exclusion criteria and were randomly assigned into two experimental groups, A and B, using a lottery method. Each group consisted of 10 samples. Group A underwent training using the Motor Relearning Program, while Group B received Traditional Treatment.The study was conducted at A.C.S. Medical College and Hospital located in Vellappanchavadi, Chennai-77, over the course of 5 sessions per week for a duration of 8 weeks. The total number of subjects involved in the study was 20, with each group consisting of 10 participants.

Inclusion criteria: The study included both male and female patients aged 45 to 64 who had experienced a stroke and were able to sit and stand independently with the use of an aid or orthotic, regardless of whether they required supervision or assistance. Participants who could independently maintain a seated position for 30 seconds on a stable surface and were medically stable were also eligible for inclusion in the study.

Exclusion criteria: Subjects with Significant disability. Other exclusion criteria were orthopedic/neurological impairments that could influence sitting balance, and perform a coordinated movement, inability to understand instructions and difficulty for sitting and standing.

Materials used: Stop watch, Toys (whistling), Rainbow Music Desk Bells, Rainbow blocks, Different shapes of Blocks, Peg board

Measurement tools: Gross motor function classification system (GMFCS) level II & IV, And Motor assessment scale

Outcome measures: Primary functional motor activities - Motor Learning, through play therapy, movement initiate the motor functional activity.

Procedure: The research was an experimental study employing a pre and post design. This investigation was carried out in the Outpatient Physiotherapy Department of ACS Medical College and Hospital, featuring an intervention period of 8 weeks and an overall study duration of 6 months. The study received approval from the institutional review board, and 20 samples were chosen based on the established selection criteria Verified stroke is diagnosis with the capacity to move in ways other than sitting and to understand the trainers' directions. Using a straightforward random sample technique, the participants were divided into two groups. After receiving a thorough explanation of the study, the parents were asked to sign a consent form indicating their willingness to participate. First, demographic information such as height, weight, gender, and age will be gathered. Group B received conventional stroke care, while Group A received motor relearning. Each study session lasted one hour and thirty minutes. The Gross Motor Function Classification System (GMFCS) and the Motor Assessment Scale were used to measure the subjects before and after the exam.

2. Interventions

Group-A: Motor Relearning Techniques: The motor learning coaching method adhered to the fundamentals of motor learning and used them in sessions that were centered on activities. The method focuses on using augmented feedback that corresponds to the learner's phases while performing motor skills in a random order across several environments.Physical therapists had completed the motor relearning program and had at least two years of experience treating stroke patients treated the stroke treatment group. According to the status and severity, this course focused on the phases of task learning, such as practice variability and the kind of augmented feedback. For

continuity, physiotherapists documented the actions during each session. Missed sessions were rescheduled as soon as feasible.

Group-B: Traditional exercise: The goal of intervention in the traditional exercise treatment strategy is to help the participants recover by altering the way their bodies function and structure. The goal of the non-rigid therapy plan is to improve muscle tone and movement patterns. It is believed that functional benefits result from "typical" movement patterns. A structured program was established for each subject after the therapist precisely identified the motor tasks (e.g., increased sitting stability) and goals (e.g., standing or walking). Legs were passively stretched at the start of each session of this program. Walking, getting up from a sitting position, and sitting were examples of functional motor activities. At the conclusion of each session, these were practiced. Optimal sensorimotor processing, task performance, and skill acquisition are believed to be activated by this therapeutic handling and engagement, which will ultimately enable the individual to engage in meaningful activities and improve their quality of life.

3. Data Analysis

Group A – Motor Relearning

Table 1: Paired t test on Gross Motor Function Scale within the Group A on motor relearning among subjects with stroke

GMFS	**Mean** (Score)	**Number of Pairs**	**Mean Diff.**	**SD, SEM**	**DF**	**t**	**P value**	**Sig.Diff.** (P < 0.05)
Pre Test	51.74	10	41.39	7.27 2.30	9	18.02	<0.0001	****
Post Test	93.12							

The above table 1 shows significant difference in Gross Motor Function Classification System on motor learning among stroke subjects with P value >0.0001.

Table 2: Paired t test of Motor Assessment Scale within Group A on motor learning among stroke subjects

MAS	**Mean** (Score)	**Number of Pairs**	**Mean Diff.**	**SD, SEM**	**DF**	**t**	**P value**	**Sig. Diff.** (P < 0.05)
Pre-Test	1.60	10	1.50	0.67 0.21	9	7.13	<0.0001	****
Post Test	3.10							

The above table 2 shows significant difference in Motor Assessment Scale on motor learning among stroke subjects with P value >0.0001.

Group B – Traditional Management

Table 3: Paired t test on Gross Motor Function Scale within the Group B on motor learning among stroke subjects

GMFS	Mean (Score)	Number of Pairs	Mean Diff.	SD, SEM	DF	t	P value	Sig.Diff. (P < 0.05)
Pre-Test	41.90	10	27.69	8.502 2.689	9	10.30	<0.0001	****
Post -Test	69.60							

The above table 3 shows significant difference in Gross Motor Function Classification System on motor relearning among stroke subjects with P value >0.0001.

Table 4: Paired t test of Motor Assessment Scale within Group B on motor learning among stroke subjects

MAS	Mean (Score)	Number of Pairs	Mean Diff.	SD, SEM	DF	t	P value	Sig. Diff. (P < 0.05)
Pre-Test	1.40	10	0.650	0.41 0.13	9	4.99	<0.0007	***
Post Test	2.05							

The above table 4 shows significant difference in Motor Assessment Scale on motor relearning among stroke with P value >0.0007.

Table 5: ANOVA to compare GMFS between Group A and B

Out come Measures	Exercise Group A and B	Test	Mean	Mean Diff.	R Square	F	P value	Sig. diff. (P < 0.05)
GMFS	**Motor Learning**	**Pre test**	41.90	27.69	0.844	64.93	<0.0001	****
		Post Test	69.60					
	NDT	**Pre test**	51.73	43.38				
		Post Test	93.11					

The above table 5 shows significant difference on GMFS between Group A and B with P value <0.0001.

Table 6: ANOVA to compare MAS between Group A and B

Out come Measures	Exercise Group A and B	Test	Mean	Mean Diff.	R Square	F	P value	Sig. diff. (P < 0.05)
MAS	Motor Learning	Pre test	1.40	0.650	0.592	17.38	<0.0001	****
		Post Test	2.05					
	NDT	Pre test	1.60	1.500				
		Post Test	3.10					

The above table 6 shows significant difference on MAS between Group A and B with P value <0.0001.

4. Result

Among stroke patients in this study, GMFS improved with a mean difference of 43.38 due to motor relearning, with a P value >0.0001.
Among stroke patients in this study, GMFS improved with a mean difference of 27.69 when using traditional exercise, with a P value >0.0001.
In this study, MAS has improved among stroke patients using the motor relearning technique, with a mean difference of 1.50 and a P value >0.0001.
In this study, MAS has improved among stroke patients with a mean difference of 0.650 while using traditional exercise, with a P value greater than 0.0001.
Among stroke patients, a comparison of Groups A and B revealed a substantial difference in effectiveness on motor function (P value >0.0001). In GMFS and MAS, the mean difference between Group A's motor relearning and Group B's traditional exercise was 43.38 and 1.50, respectively, compared to 27.69 and 0.650.

5. Discussion

The findings of this study suggest that the Motor Relearning Program (MRP) is more effective than traditional management approaches in improving gross motor function in individuals post-stroke. Participants who underwent MRP demonstrated significantly greater improvements in gross motor abilities compared to those who received conventional rehabilitation 8.
These results align with existing literature that emphasizes the importance of task-specific training and functional reorganization of motor patterns for stroke rehabilitation. Unlike traditional methods,

which often focus on passive modalities and generalized strengthening, the MRP emphasizes active, goal-directed tasks, motor control training, and contextual practice.

This likely contributed to enhanced motor planning and execution in real-world activities, which are key components of gross motor function [9].

One of the core principles of MRP is repetitive practice of meaningful tasks, which aligns with theories of neuro plasticity—the brain's ability to reorganize and form new connections in response to training. This supports the idea that targeted motor learning strategies can accelerate recovery and improve functional outcomes more efficiently than traditional therapies[10].

Strength of the MRP approach is its emphasis on problem-solving and feedback, which may lead to improved motor retention and self-efficacy in patients. In contrast, traditional methods may lack sufficient engagement and often rely more on therapist-driven movement facilitation than patient-driven task performance[11].

However, certain limitations should be acknowledged. The sample size in this study may not fully represent the broader stroke population, especially those with severe cognitive deficits or comorbidities that might affect participation in an intensive motor relearning protocol. Additionally, long-term follow-up data were not included, so it is unclear whether the observed benefits of MRP are sustained over time[12].

Despite these limitations, the present findings provide strong support for incorporating MRP into standard stroke rehabilitation protocols. Further research is recommended to explore the effects of MRP on different subtypes of stroke, as well as its integration with technologies like virtual reality or robotic-assisted therapy[13].

A comparative study between MRP and the Bobath approach found that MRP led to more significant improvements in upper limb motor function, including gross motor abilities, in stroke patients[14].

Research indicates that motor relearning programs and task-specific training both significantly enhance upper limb functions—such as dexterity, grip strength, and gross movements—in chronic stroke patients[15].

A literature review encompassing 15 studies concluded that both MRP and mirror therapy have a substantial positive impact on improving gross and fine motor functions of the upper extremity in individuals with chronic stroke[16].

Ethical clearance: Ethical clearance was obtained from the ethical Institutional Review Board of Faculty of Physiotherapy, Dr. MGR. Educational and Research Institute, Chennai with reference No: B28/PHYSIO/IRB/ 2019-2020 approval letter dated 17/01/2020.

Conflicts of Interest: There is no conflict of interest to conduct and publish this study.

Fund for the study: This is self-funded study, no fund received from any organization.

6. Conclusion

In motor relearning and traditional treatment techniques, the Motor Relearning Program (MRP) showed more improvement in sitting to standing position in subjects with stroke. Therefore, this study concludes that MRP is an effective intervention for stroke patients.In Future studies need to determine when MRP techniques for sitting to standing programs should be performed. In addition, more studies needed to examine the factors of MRP which can improve the positions from sitting to standing and strengthen the Trunk, Upper & Lower extremities of Muscles.

References

[1] Mufidah N, Wahyudi R, Hasinuddin M. The differences between motor relearning programme and Bobath method on standing balance in stroke patients. Stroke 2009; 10: 83.

[2] Langhammer B, Stanghelle JK. Can physiotherapy after stroke based on the Bobath concept result in improved quality of movement compared to the motor relearning programme. Physio Res Int 2011; 16: 69–80.

[3] Faul F, Erdfelder E, Lang A-G, et al. G*Power 3: a flexible statistical power analysis program for the social, behavioral, and biomedical sciences. Behav Res Meth 2007; 39: 175–191.

[4] Winstein CJ, Stein J, Arena R, et al. Guidelines for adult stroke rehabilitation and recovery: a guideline for healthcare professionals from the American Heart Association/American Stroke Association. Stroke 2016; 47: e98–e169.

[5] Teasell R, Salbach NM, Foley N, et al. Canadian stroke best practice recommendations: rehabilitation, recovery, and community participation following stroke. Part one: rehabilitation and recovery following stroke; 6th edition update 2019. Int J Stroke 2020; 15: 763–788.

[6] Podsiadlo D, Richardson S. The timed “Up & Go”: a test of basic functional mobility for frail elderly persons. J Am Geriatr Soc 1991; 39: 142–148.

[7] Watson MJ. Refining the ten-metre walking test for use with neurologically impaired people. Physiotherapy 2002; 88: 386–397.

[8] Tyson S, Connell L. The psychometric properties and clinical utility of measures of walking and mobility in neurological conditions: a systematic review. Clin Rehabil 2009; 23: 1018–1033.

[9] Goh HT, Nadarajah M, Hamzah NB, et al.. Falls and fear of falling after stroke: a case-control study. PM R 2016; 8: 1173–1180.

[10] Aqueveque P, Ortega P, Pino E, et al.. After stroke movement impairments: A review of current technologies for rehabilitation. In: Uner Tan (Ed.), Physical disabilities - therapeutic implications. London: InTech, 2017, pp.95–116.

[11] Horak FB, Macpherson JM. Postural orientation and equilibrium. In: Shepard J and Rowell L (eds) Handbook of physiology, section 12. Exercise: regulation and integration of multiple systems. New York, NY: Oxford University Press, 1996, 255–292.

[12] Peterka RJ. Sensorimotor integration in human postural control. J Neurophysiol 2002; 88: 1097–1118.

[13] Effectiveness of motor relearning programme and mirror therapy on hand functions in patients with stroke - a randomized clinical trial Rehani P et al., International Journal of Therapies and Rehabilitation Research 2015; 4 (3): 20 – 24.

[14] Pandian S, Arya KN, Davidson ER. Comparison of Brunnstrom movement therapy and Motor Relearning Program in rehabilitation of post-stroke hemiparetic hand: a randomized trial. Journal of Rehman Journal of Health Sciences Vol. 03, No. 02, 2021 83 bodywork and movement therapies. 2012 Jul 1;16(3):330-7.

[15] Immadi SK, Achyutha KK, Reddy DA, Tatakuntla KP. Effectiveness of the motor relearning approach in promoting physical function of the upper limb after a stroke. Int J Physiotherapy 2015; 2: 386-90.

[16] Bahrawy MN, Elwishy AA.Efficacy of motor learning approach on hand function in chronic stroke patients. A controlled randomized study. Italian J physiotherapy2012; 2:121-7.

Black Gram Leaf Disease Detection Using Mobilenetv3 with Adaptive Image Enhancement

Dr. M. Bennet Rajesh[1], J.Khalifullah[2]

[1]Research Supervisor, Department of Computer Science, Government Arts and Science College, Nagercoil, India.
E-mail: benraj@gmail.com
[2]Assistant Professor/Programmer, Department of computer information science, Annamalai University, India.
E-mail: jas.khalif@gmail.com

Abstract: Black gram (*Vigna mungo*) is an economically significant pulse crop whose productivity is severely affected by various leaf diseases such as Cercospora leaf spot, Powdery mildew, Anthracnose, and Yellow Mosaic Virus. Early and accurate detection of these diseases is essential to minimize crop losses and support precision agriculture. Early and accurate disease detection is essential for effective crop management and productivity improvement. This study proposes a deep learning-based approach for black gram leaf disease detection using MobileNetV3 integrated with adaptive image enhancement techniques. Initially, leaf images are collected and preprocessed to improve visual clarity through adaptive image enhancement methods, including contrast adjustment and noise reduction. These preprocessing steps enhance feature visibility and improve classification performance. The enhanced images are then fed into a MobileNetV3 model, chosen for its lightweight architecture and computational efficiency, making it suitable for real-time and mobile-based agricultural applications. Experimental results demonstrate that the proposed approach achieves high classification performance with strong generalization capability while maintaining computational efficiency suitable for real-time agricultural applications. The developed system provides an effective and scalable solution for early disease diagnosis in black gram cultivation.

Keywords: Black Gram Leaf Disease Detection, MobileNetV3, Adaptive Image Enhancement, Deep Learning

1. Introduction

Vigna mungo, commonly known as black gram or urad bean, is an important pulse crop widely cultivated across the Indian subcontinent [1]. It is believed to have originated in South India and is considered one of the most economically valuable pulses in the region. Although traditionally grown in India, its cultivation has expanded to several tropical regions including Fiji, Mauritius, the Caribbean, and parts of Africa. The plant is an erect, annual legume characterized by densely hairy stems, trifoliate leaves, and narrow cylindrical pods. It typically grows to a height ranging from 0.3 to 1 meter, with pods approximately 5 cm long. The crop is highly nutritious, containing significant amounts of proteins, carbohydrates, vitamins such as thiamine, riboflavin, niacin [2], and folate, as well as essential minerals including calcium, iron, magnesium, phosphorus, zinc, and potassium. In addition to its role as a food source for humans, black gram is also used as fodder and forage for livestock.

Despite its nutritional and economic importance, black gram production is frequently affected by leaf diseases that reduce yield and crop quality [3]. One of the primary causes of yield loss is chlorophyll deficiency resulting from viral infections, which manifests as yellowing of leaves.

Early-stage infections may show mild yellow mosaic patterns, while severe infections lead to dark yellow discoloration, impaired photosynthesis, and eventual leaf damage. Fungal and bacterial infections further contribute to crop deterioration by causing necrotic lesions, black spots, and in some cases, stem and leaf rotting [4]. Common diseases include Cercospora leaf spot, powdery mildew, anthracnose, and Yellow Mosaic Virus (YMV). These diseases significantly impact plant vigor, pod development, and overall productivity.

Traditionally, disease diagnosis relies on manual inspection by agricultural experts, a process that is time-consuming, subjective, and challenging in large-scale farming environments. Recent advances in Artificial Intelligence and Deep Learning have enabled the development of automated plant disease detection systems [5]. Lightweight deep learning architectures such as MobileNetV3 provide efficient feature extraction and accurate image classification while maintaining low computational requirements, making them suitable for real-time and field-level agricultural applications.

Main Contributions

1. **Hybrid Integration of Adaptive Image Enhancement with MobileNetV3:** The study proposes a novel framework that combines adaptive image enhancement techniques with the lightweight MobileNetV3 architecture to improve feature extraction and disease classification accuracy.
2. **Efficient and Real-Time Black Gram Leaf Disease Detection:** By leveraging the computational efficiency of MobileNetV3, the proposed model enables accurate and fast disease detection, making it suitable for deployment on mobile and edge devices in agricultural environments.
3. **Improved Classification Performance for Precision Agriculture:** The proposed approach achieves enhanced accuracy and robustness compared to conventional methods, supporting early disease diagnosis and informed decision-making in sustainable crop management.

The remainder of this paper is organized as follows. Section 2 presents a comprehensive review of related work and existing research in the field. Section 3 describes the proposed feature extraction and classification framework in detail. Section 4 discusses the implementation process and evaluates the experimental results. Finally, Section 5 summarizes the key findings and provides concluding remarks.

2. Literature Review

Manikandan et al [6] the goal of this research is to create reliable prediction models for Blackgram disease intelligence by utilizing ensemble learning approaches. The suggested Efficient-Integrated approach reduces the unpredictability of the data while increasing the models' classification accuracy by combining the predictions of several base models, such as Vision Transformers (ViT), and extracting them into several channels. By utilizing Explainable Artificial Intelligence (XAI) and Grad-CAM

(Gradient-weighted Class Activation Maps), the suggested model raised the image classification rate (accuracy) and detected abnormal regions, including plant diseases like those found in black gram, a type of legume.Badana et al [7] create an automatic chickpea classifier that takes into account the morphological characteristics of chickpea seeds using a model based on RGB color images. Five hundred and fifty photos of each of the four chickpea varieties (CDC-Alma, CDC-Consul, CDC-Cory, and CDC-Orion) were taken using a mobile phone camera and an industrial RGB camera as part of the data collection process. A transfer-learning-based methodology was used to assess three CNN-based models, including EfficientNetB0, MobileNetV3 (small), and NasNet-A (mobile). For the NasNet-A (mobile), MobileNetV3 (small), and EfficientNetB0 models, the corresponding classification accuracy was 97%, 99%, and 98%. Due to its improved accuracy and lightweight design, the MobileNetV3 model was utilized for additional deployments on Raspberry Pi 4 and Android mobile devices.Li, L et al [8] Employing in-field photos from the Black Gram Plant Leaf Disease Dataset (BPLD), the study presents the Efficient AttentionNET model, which incorporates Channel Attention and Spatial Attention methods to enhance feature extraction. Wavelet-transformed samples for data augmentation allowed the model to efficiently obtain key edge information. The RBF kernel-based SVM classifier showed remarkable performance, attaining 99.50% accuracy, 99.52% recall, 99.50% precision, and 99.50% F1-score. The inclusion of wavelet-based augmentation and attention dynamics makes the suggested model extremely successful in classifying black gram leaf disease.Lavanya et al [9] to suppress Macrophomina phaseolina and Fusarium oxysporum, which cause root rot and wilt diseases in pulses generally and pigeon peas specifically, the current study sought to isolate Bacillus and Streptomyces species. In a test using two cultures, Bacillus subtilis BRBac4-1, B. subtilis BRBac24-2, and Bacillus siamensis BRBac21-1, Streptomyces cavourensis BRAcB10-1, and Streptomyces griseofuscus BRAcB11-2 demonstrated possible antagonistic activity against Macrophomina phaseolina and Fusarium oxysporum f. sp. udum. In addition to generating lytic enzymes, non-volatile metabolites (iturin and surfactin), and volatile organic carbon compounds (disulphide, azithromycin, 1-butanol, 2-methyl, and dimethyl disulphide) with antifungal activities observed in culture filtrate by GC-MS and LC-MS analyses, these rhizobacteria were found to have several characteristics that promote plant growth.

3. Materials and Methods

This section describes the complete methodology adopted for black gram leaf disease detection using MobileNetV3 integrated with adaptive image enhancement techniques. The workflow consists of image acquisition [10], dataset preparation, preprocessing, feature learning, and classification.

1. Image Acquisition

- **Field Leaf Image Capture**

Images of black gram leaves were taken in the natural setting, straight from agricultural fields. High-resolution smartphone cameras were used to take the pictures in order to guarantee their usefulness in actual farming situations. To increase the robustness of the model, the dataset include differences in lighting conditions, backdrop complexity, leaf orientation, and illness severity.

- **Healthy & Diseased Leaf Images**

Both healthy and sick black gram leaves are included in the dataset that was gathered. Common illnesses include Cercospora leaf spot [11]; powdery mildew, anthracnose, and yellow mosaic virus (YMV) are among the diseased samples. Incorporating both healthy and sick samples enhances capacity for generalization and facilitates efficient classification using multiple classes.

2. Dataset Preparation

The photos of black gram leaves that were gathered were methodically arranged and ready for supervised deep learning. Based on discernible symptoms and professional agricultural advice, each image was carefully labeled and assigned to one of many predetermined disease groups. There are five main classifications in the dataset [12]: Yellow Mosaic Virus, Powdery Mildew, Anthracnose, Cercospora Leaf Spot, and Healthy. Effective directed training of the MobileNetV3 model depends on proper labeling, which guarantees precise mapping between input photos and their related class labels.The dataset was separated into three subsets for testing, validation, and training in order to guarantee accurate model evaluation and avoid overfitting [13]. To allow the subject to learn disease-specific traits, about 70% of the total photos were set aside for training. About 15% of the dataset was set aside as an independent test set to assess the performance of the finished model, while the remaining 15% was utilized for validation during training to adjust hyperparameters and track performance. This methodical approach to dataset splitting guarantees objective evaluation and improves the suggested disease detection framework's capacity for generalization.

3. Adaptive Image Enhancement

To improve image quality and highlight disease-specific features, adaptive enhancement techniques were applied before training.

- **Contrast Enhancement: CLAHE (Contrast Limited Adaptive Histogram Equalization)**

CLAHE was applied to enhance local contrast and improve visibility of disease spots and discolorations. Unlike traditional histogram equalization, CLAHE prevents over-amplification of noise by limiting contrast enhancement, making it highly suitable for leaf texture analysis [14].

$$i_{enh}(x,y) = (L-1) * \sum_{i=0}^{I(x,y)} P(i) \quad (1)$$

Where:

- $i_{enh}(x,y)$ = Original pixel intensity at position (x,y)
- $(L-1)$ = Number of gray levels
- $P(i)$ = Probability density functions of intensity level.
- i_{enh}= Enhanced pixel intensity

- **Noise Removal: Median Filtering**

Median filtering was employed to remove salt-and-pepper noise while preserving important edge details [15]. This step ensures that disease boundaries and lesion patterns remain intact during further processing.

4. Pre-Processing

Preprocessing standardizes images for input into the deep learning model.

- **Image Resizing**

All images were resized to a fixed dimension compatible with MobileNetV3 (e.g., 224 × 224 pixels). This ensures uniform input size and efficient batch processing.

- **Color Space Conversion**

Images were converted into an appropriate color space (such as RGB normalization or HSV when required) to improve feature discrimination, particularly for detecting color-based disease patterns.

- **Normalization**

Pixel intensity values were normalized to a range of 0–1. Normalization stabilizes gradient updates, accelerates convergence, and improves overall training performance.

5. Feature Learning (MobileNetV3)

MobileNetV3 was employed as the core feature extraction backbone due to its lightweight architecture and computational efficiency.

- **Input Image to Network**

Preprocessed images were fed into the MobileNetV3 architecture as input tensors [16]. The network processes the images through multiple convolutional layers.

- **Feature Extraction Layers**

MobileNetV3 consists of depthwise separable convolutions, inverted residual blocks, and squeeze-and-excitation modules. These layers extract hierarchical spatial features such as texture, edges, color variations, and lesion patterns associated with different diseases.

- **Global Feature Representation**

The extracted deep features are aggregated using Global Average Pooling, generating a compact and discriminative feature representation. This representation is then forwarded to fully connected layers for classification.

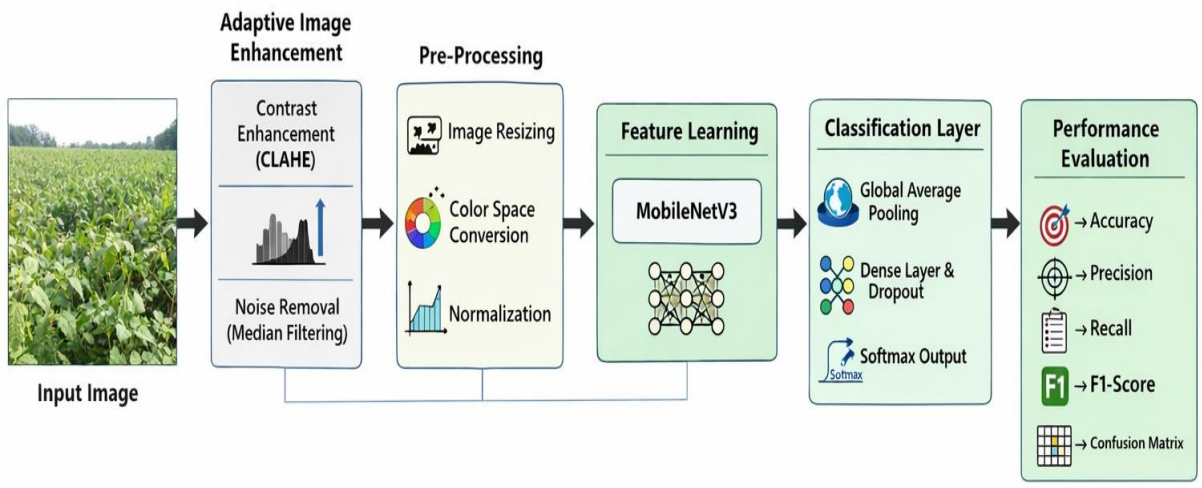

Figure 1. Overall Architecture of the Proposed Model for Black Gram Leaf Disease Detection

The entire process of the suggested black gram leaf disease detection system is shown in Figure 1. Field-acquired leaf photos are the first step in the process, which is then followed by adaptive image enhancement employing median filtering to reduce noise and CLAHE to boost contrast. Preprocessing procedures including scaling, color space conversion, and normalization are applied to the improved photos. Following processing, the photos are put into the MobileNetV3 network in order to extract deep features. Lastly, Global Average Pooling, dense layers, dropout, and Softmax output are used for classification, while accuracy, precision, recall, F1-score, and confusion matrix are used to assess the model's performance.

6. Classification Layer

The classification layer is responsible for converting the extracted deep features into final disease predictions. After feature learning through MobileNetV3 [17], the high-level feature maps are processed through fully connected layers to perform multi-class classification of black gram leaf diseases.

- **Global Average Pooling**

Global Average Pooling (GAP) is applied to the final convolutional feature maps generated by MobileNetV3. Instead of flattening the feature maps directly, GAP computes the average value of each feature map, thereby reducing spatial dimensions while preserving important discriminative information. This operation significantly reduces the number of trainable parameters, minimizes overfitting, and enhances computational efficiency. The resulting output forms a compact global feature representation of the input image.

- **Dense Layer**

The pooled feature vector is then passed to a fully connected (dense) layer. The dense layer learns complex non-linear relationships between extracted features and disease classes. It acts as a high-level classifier by mapping the global feature representation into a feature space suitable for final decision-making. The weights of this layer are optimized during training to improve class separability.

- **Dropout**

To prevent overfitting and improve generalization performance, a dropout layer is incorporated after the dense layer. During training, dropout randomly deactivates a fraction of neurons, preventing the network from relying too heavily on specific feature activations. This regularization technique enhances model robustness, especially when working with agricultural datasets that may have limited samples.

- **Softmax Output**

Finally, a Softmax activation function is applied in the output layer to generate probability scores for each disease class, including healthy leaves. The Softmax function converts the raw output logits into normalized probability values that sum to one, enabling multi-class classification. The class with the highest probability is selected as the final predicted disease category.

4. Implementation and Experimental Results

This section describes the implementation procedure of the proposed MobileNetV3-based black gram leaf disease detection model and presents the experimental results obtained after training and evaluation.

4.1 Model Training

The proposed model was implemented using a deep learning framework and trained on the prepared dataset consisting of healthy and diseased black gram leaf images. During training, the preprocessed images were fed into the MobileNetV3 architecture for feature extraction, followed by classification layers.

- **Loss Calculation**

The categorical cross-entropy loss function was used to measure the difference between the predicted class probabilities and the actual class labels. The loss function quantifies classification error and guides the optimization process. Lower loss values indicate improved prediction performance.

- **Backpropagation**

Backpropagation was applied to compute gradients of the loss function with respect to model parameters. These gradients were propagated backward through the network layers, enabling the adjustment of convolutional and fully connected layer weights to minimize prediction error.

- **Weight Optimization**

An adaptive optimization algorithm such as Adam optimizer was employed to update the model weights iteratively [18]. The optimizer adjusts learning rates dynamically, accelerating convergence and ensuring stable training. As shown in the training and validation accuracy graph, the model demonstrates steady improvement across epochs, indicating effective learning and minimal overfitting.

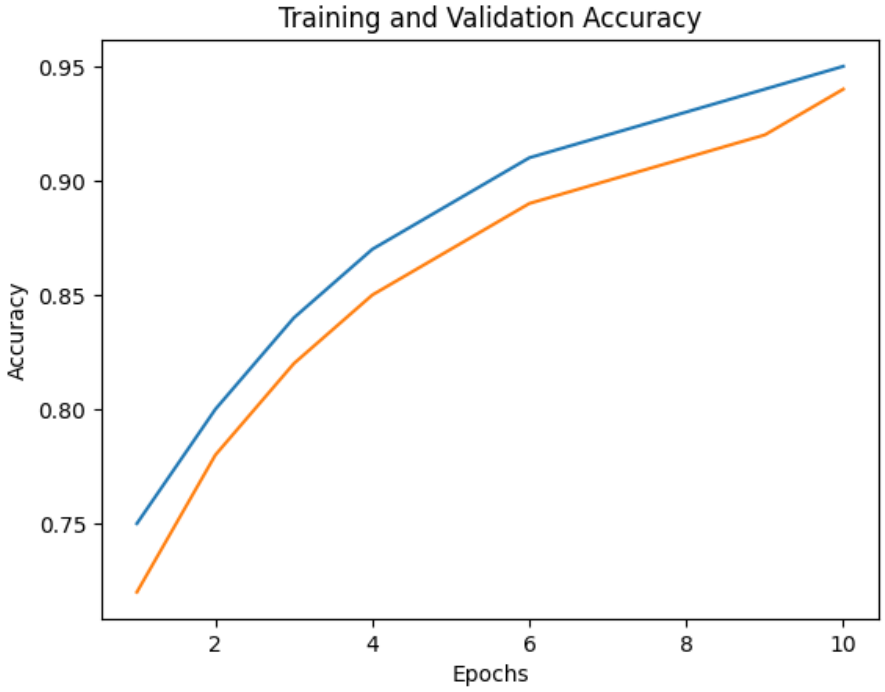

Figure 2. Training and Validation Accuracy Curve of the Proposed MobileNetV3 Model

Figure 2 illustrates the training and validation accuracy of the proposed black gram leaf disease detection model over multiple epochs. The graph demonstrates a steady increase in training and validation accuracy, indicating effective learning and convergence of the model. The minimal gap between training and validation curves suggests reduced overfitting and good generalization performance. By the final epoch, the model achieves high classification accuracy, confirming the robustness of the proposed adaptive image enhancement and MobileNetV3-based framework.

4.2 Prediction

After training, the optimized model was evaluated using unseen test images to assess its generalization capability.

- **Test Image Input**

Each test image underwent the same preprocessing steps, including enhancement, resizing, normalization, and formatting into input tensors compatible with MobileNetV3.

- **Disease Class Output**

The trained model generated probability scores for each disease class using the Softmax activation function. The class with the highest probability was selected as the final predicted label. The system successfully classified healthy leaves and multiple disease categories with high confidence.

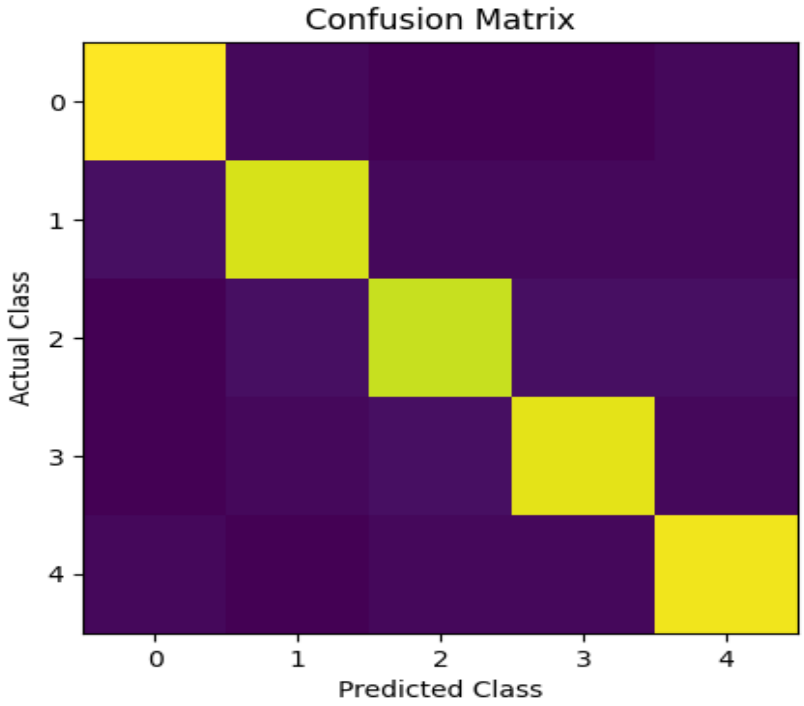

Figure 3. Confusion Matrix of the Proposed Model for Black Gram Leaf Disease Classification

Figure 3 presents the confusion matrix obtained from the test dataset evaluation. The diagonal elements represent correctly classified samples for each class, including Healthy, Cercospora, Powdery Mildew, Anthracnose, and Yellow Mosaic Virus (YMV). The strong diagonal dominance indicates high classification accuracy and effective class discrimination. Misclassifications are minimal and primarily occur between visually similar disease categories, demonstrating the model's strong predictive capability in multi-class agricultural disease detection.

4.3 Performance Evaluation

The performance of the proposed model was evaluated using standard classification metrics derived from the confusion matrix.

- **Accuracy**

Accuracy measures the overall proportion of correctly classified samples among total test samples. The proposed model achieved an overall accuracy of 95%, demonstrating strong classification capability.

$$Accuracy = \frac{TP+TN}{TP+TN+FP+FN} \quad (2)$$

Where:

- *TPTPTP = True Positives*
- *TNTNTN = True Negatives*

- *FPFPFP = False Positives*
- *FNFNFN = False Negatives*

- **Precision**

Precision indicates the proportion of correctly predicted positive observations among all predicted positives. High precision values reflect reduced false-positive predictions across disease classes.

- **Recall**

Recall measures the proportion of actual positive samples correctly identified by the model. High recall ensures that diseased leaves are effectively detected, minimizing false negatives.

- **F1-Score**

The F1-score is the harmonic mean of precision and recall. It provides a balanced evaluation metric, particularly useful in multi-class classification problems involving agricultural disease detection.

$$F1 - Score = 2 * \frac{Precision * Recall}{Precision + Recall} \quad (3)$$

- **Confusion Matrix**

The confusion matrix provides a detailed class-wise performance analysis by displaying correct and incorrect predictions for each category. The diagonal elements represent correctly classified instances, indicating strong class discrimination by the proposed model.

4.4 Discussion

The experimental findings confirm that the integration of MobileNetV3 with adaptive image enhancement techniques significantly improves the detection of black gram leaf diseases. The application of CLAHE enhances local contrast, while median filtering effectively suppresses noise, resulting in clearer visual patterns for feature extraction. The learning curves demonstrate smooth convergence with a minimal gap between training and validation performance, indicating strong generalization and limited overfitting. Evaluation metrics, including accuracy, precision, recall, and F1-score, reflect reliable multi-class classification capability. The few misclassifications observed primarily occur among visually similar disease types, suggesting the potential benefit of larger datasets and further hyperparameter refinement.

5. Conclusion

This research introduces a computationally efficient deep learning framework for automated black gram leaf disease identification using MobileNetV3 enhanced with adaptive preprocessing techniques. The proposed method achieves strong classification performance while maintaining lightweight architecture suitable for real-time and mobile-based agricultural applications. By combining image enhancement with deep feature extraction, the system ensures accurate and dependable disease recognition. The developed framework contributes to precision agriculture by supporting early diagnosis and minimizing crop loss. Future research may involve expanding the dataset, implementing real-time field deployment, and incorporating advanced attention mechanisms to further improve predictive performance and model interpretability.

References

[1] Talasila, S., Rawal, K., Sethi, G., & Mss, S. (2022). Black gram Plant Leaf Disease (BPLD) dataset for recognition and classification of diseases using computer-vision algorithms. *Data in Brief*, *45*, 108725.

[2] Kelly, L. A., Vaghefi, N., Bransgrove, K., Fechner, N. A., Stuart, K., Pandey, A. K., ... & Kiss, L. (2021). One crop disease, how many pathogens? Podosphaera xanthii and Erysiphe vignae sp. nov.

[3] identified as the two species that cause powdery mildew of mungbean (Vigna radiata) and black gram (V. mungo) in Australia. *Phytopathology®*, *111*(7), 1193-1206.

[4] Jegadeesan, S., Raizada, A., Dhanasekar, P., & Suprasanna, P. (2021). Draft genome sequence of the pulse crop blackgram [Vigna mungo (L.) Hepper] reveals potential R-genes. *Scientific Reports*, *11*(1), 11247.

[5] Joshi, R. C., Kaushik, M., Dutta, M. K., Srivastava, A., & Choudhary, N. (2021). VirLeafNet: Automatic analysis and viral disease diagnosis using deep-learning in Vigna mungo plant. *Ecological Informatics*, *61*, 101197.

[6] Gargade, A., & Khandekar, S. (2021). Custard apple leaf parameter analysis, leaf diseases, and nutritional deficiencies detection using machine learning. In *Advances in Signal and Data Processing: Select Proceedings of ICSDP 2019* (pp. 57-74). Singapore: Springer Singapore.

[7] Manikandan, A., Jaivel, N., Johnson, I., Krishnamoorthy, R., Senthilkumar, M., Raghu, R., ... & Anandham, R. (2022). Suppression of Macrophomina root rot, Fusarium wilt and growth promotion of some pulses by antagonistic rhizobacteria. *Physiological and Molecular Plant Pathology*, *121*, 101876.

[8] Badana, M. K., Kelaiya, D. S., & Jadav, A. H. (2021). Screening of groundnut varieties and different types of host species against dry root rot disease.

[9] Li, L., Zhang, S., & Wang, B. (2021). Plant disease detection and classification by deep learning—a review. *IEEE access*, *9*, 56683-56698.

[10] Lavanya, R., & Arun, V. J. S. R. (2021). Detection of Begomovirus in chilli and tomato plants using functionalized gold nanoparticles. *Scientific reports*, *11*(1), 14203.

[11] Bright, J. P., Karunanadham, K., Maheshwari, H. S., Karuppiah, E. A. A., Thankappan, S., Nataraj, R., ... & Sayyed, R. Z. (2022). Seed-borne probiotic yeasts foster plant growth and elicit health protection in black gram (Vigna mungo L.). *Sustainability*, *14*(8), 4618.

[12] Kumar, A., Kumar, P., & Ulla, R. (2022). Impact of arbuscular mycorrhizal fungus Glomus mosseae on plant growth and photosynthetic pigments in blackgram. *Mycopath*, *19*(1).

[13] Rajpoot, V., Dubey, R., Mannepalli, P. K., Kalyani, P., Maheshwari, S., Dixit, A., & Saxena, A. (2022). Mango plant disease detection system using hybrid BBHE and CNN approach. *Traitement du Signal*, *39*(3), 1071-1078.

[14] Weng, S., Hu, X., Wang, J., Tang, L., Li, P., Zheng, S., ... & Xin, Z. (2021). Advanced application of Raman spectroscopy and surface-enhanced Raman spectroscopy in plant disease diagnostics: A review. *Journal of Agricultural and Food Chemistry*, *69*(10), 2950-2964.

[15] Nasir, M., Sidhu, J. S., & Sogi, D. S. (2022). Processing and nutritional profile of mung bean, black gram, pigeon pea, lupin, moth bean, and Indian vetch. *Dry beans and pulses: Production, processing, and nutrition*, 431-452.

[16] Varghese, A., & Mamatha, I. (2022, November). A unified system for crop yield prediction, crop recommendation, and crop disease detection. In *International Conference on Robotics, Control, Automation and Artificial Intelligence* (pp. 1025-1035). Singapore: Springer Nature Singapore.

[17] Gining, R. A. J. M., Fauzi, S. S. M., Yusoff, N. M., Razak, T. R., Ismail, M. H., Zaki, N. A., & Abdullah, F. (2021). Harumanis mango leaf disease recognition system using image processing technique. *Indonesian Journal of Electrical Engineering and Computer Science*, *23*(1), 378-386.

[18] Gining, R. A. J. M., Fauzi, S. S. M., Yusoff, N. M., Razak, T. R., Ismail, M. H., Zaki, N. A., & Abdullah, F. (2021). Harumanis mango leaf disease recognition system using image processing technique. *Indonesian Journal of Electrical Engineering and Computer Science*, *23*(1), 378-386.

[19] Dutta, P., Kumari, A., Mahanta, M., Biswas, K. K., Dudkiewicz, A., Thakuria, D., ... & Mazumdar, N. (2022). Advances in nanotechnology as a potential alternative for plant viral disease management. *Frontiers in Microbiology*, *13*, 935193.

Machine Learning Models for Financial Risk Prediction in High-Dimensional Datasets

Kian Lam Tan[1], Teo Zhi Yang[2]

[1]School of Digital Technology, Wawasan Open University, George Town 10050, Penang, Malaysia
andrewtan@wou.edu.my
[2]School of Digital Technology, Wawasan Open University, George Town 10050, Penang, Malaysia
tzy1_oi@student.wou.edu.my

Abstract: The rapid growth of financial data generated from digital transactions, market feeds, customer profiles, and alternative data sources has led to increasingly high-dimensional datasets in financial risk modeling. While the availability of large feature sets offers opportunities for more accurate risk assessment, it also introduces challenges such as overfitting, multicollinearity, computational complexity, and reduced interpretability. This study investigates the effectiveness of various machine learning models for financial risk prediction in high-dimensional environments. A comparative framework is developed to evaluate linear models, support vector machines, tree-based ensembles, and neural network architectures under consistent experimental conditions. To mitigate the adverse effects of high dimensionality, dimensionality reduction and feature selection techniques—including Principal Component Analysis (PCA) and L1-regularization—are integrated into the modeling pipeline. Performance is assessed using standard evaluation metrics such as accuracy, precision, recall, F1-score, and area under the ROC curve (AUC). Experimental results indicate that ensemble-based methods, particularly Gradient Boosting and Random Forest, demonstrate superior predictive performance and robustness in capturing nonlinear relationships within complex financial datasets. Linear models show competitive results when combined with effective feature selection strategies, offering advantages in computational efficiency and interpretability. The findings highlight that no single model universally outperforms others across all scenarios; instead, predictive success depends on the interaction between feature engineering techniques and model architecture. This study provides practical insights for selecting appropriate machine learning strategies for financial risk prediction in high-dimensional settings and underscores the importance of integrating dimensionality reduction with advanced ensemble learning techniques.

Keywords: Machine Learning; Financial Risk Prediction; High-Dimensional Data; Dimensionality Reduction; Feature Selection; Principal Component Analysis (PCA); Ensemble Learning; Gradient Boosting.

1. Introduction

The financial industry has experienced extensive digital evolution, leading to the continuous production of vast amounts of both structured and unstructured data. Sources such as online banking transactions [1], stock market activities, credit records, customer interaction logs, and alternative financial data streams contribute to this rapid data expansion. As a result, financial risk prediction models increasingly operate on datasets characterized by high dimensionality, where the number of features is large relative to the available observations. Although such comprehensive feature sets can improve predictive capability by capturing detailed behavioral and transactional patterns, excessive dimensionality introduces significant modeling challenges. These include overfitting,

multicollinearity among variables, higher computational demands, and decreased model interpretability.

Reliable financial risk assessment— [2] particularly in domains such as credit scoring, loan default forecasting, fraud identification, and portfolio risk management—is essential for maintaining institutional stability, regulatory adherence, and long-term profitability. Conventional statistical techniques, including logistic regression and linear discriminant analysis, have traditionally been employed for these tasks. However, these methods often struggle to capture complex nonlinear relationships and intricate feature interactions commonly present in high-dimensional financial datasets. To address these limitations, machine learning approaches such as Support Vector Machines, ensemble-based tree algorithms, and neural networks have become increasingly prominent due to their flexibility in modeling nonlinear patterns and their capacity to manage large-scale data environments.

Problem Statement

Effectively modelling high-dimensional information while preserving predictive accuracy, computational economy, and interpretability is the main problem in financial risk prediction. Comprehensive comparison frameworks that integrate dimensionality reduction techniques and rigorously evaluate numerous supervised learning algorithms under uniform settings are lacking. The relationship between feature engineering techniques and model architectures in determining classification performance in high-dimensional financial contexts has also not been extensively studied.

Therefore [3], this study aims to address this gap by conducting a structured comparative analysis of supervised machine learning models for financial risk prediction in high-dimensional datasets, while incorporating dimensionality reduction methods to enhance robustness and generalization performance.

2. Literature Review

The adoption of machine learning methodologies has considerably enhanced the effectiveness of financial risk modeling. Among these approaches, Support Vector Machines (SVM) have attracted significant attention due to their strong generalization performance and suitability for high-dimensional data environments. Their margin-maximization framework enables efficient handling of sparse feature representations, making them particularly effective in applications such as credit risk assessment and fraud detection. Instance-based algorithms, including k-Nearest Neighbors (k-NN) [4], have also been explored for financial risk classification. However, their reliance on distance metrics often leads to performance degradation in high-dimensional spaces, where the discriminative capability of distance measures diminishes.Tree-based learning techniques, such as Decision Trees [5], have offered improved model interpretability and the capacity to capture nonlinear relationships among financial variables. Building upon this foundation, ensemble learning strategies—including Random Forest and Gradient Boosting—have demonstrated superior predictive performance by combining multiple weak learners to reduce bias and variance. Empirical evidence frequently indicates that ensemble models outperform individual classifiers in financial risk prediction tasks. Nonetheless, their robustness may decline when confronted with datasets containing substantial numbers of redundant or irrelevant features, which can dilute meaningful predictive signals.

To address these challenges, this study introduces a novel framework that integrates high-dimensional feature engineering with ensemble learning techniques. In contrast to conventional feature

engineering approaches [6], the proposed method explicitly targets the complexities associated with high-dimensional financial datasets. It systematically investigates strategies for constructing and selecting informative features to maximize the extraction of latent information embedded in financial data. The framework integrates advanced tree-based ensemble models, such as LightGBM and XGBoost, with neural network architectures to form a multi-layered ensemble learning structure capable of modeling intricate financial relationships.Furthermore, this research provides a focused review of recent developments in high-dimensional factor models and their statistical applications, including Factor-Adjusted Robust Model Selection (FarmSelect) and Factor-Adjusted Robust Multiple Testing (FarmTest). It demonstrates how classical dimensionality reduction techniques—particularly Principal Component Analysis (PCA) [7]—can be adapted to contemporary statistical challenges. The discussion emphasizes PCA's theoretical foundations and its connections to matrix perturbation theory, robust statistical inference, random projection techniques, and false discovery rate control. Through various applications, it illustrates how integrating insights from these domains offers effective solutions to emerging high-dimensional problems. Additionally, the study highlights the broader relationship between factor models and modern statistical learning frameworks, such as network analysis and low-rank matrix recovery.

Building upon these theoretical foundations, this study proposes a High-Dimensional Neural Network (HDNN) algorithm [8], which extends conventional Deep Neural Network (DNN) architectures for improved high-dimensional corporate credit risk prediction. A theoretical contribution of this work is the formal demonstration that incorporating L1 regularization within batch normalization layers does not yield a true regularization effect, despite its widespread practical use in industrial implementations. The study further proves that introducing L2 constraints in conjunction with L1 regularization effectively resolves this limitation. To validate the proposed HDNN model, a comprehensive case study was conducted using corporate credit datasets enriched with supply chain and network-related information. Experimental results confirm the superior predictive performance and robustness of the HDNN algorithm in high-dimensional financial data scenarios.

3. Methods and Materials

3.1 Research Design

The performance of supervised machine learning algorithms for financial risk prediction in high-dimensional datasets is assessed in this paper using a quantitative experimental research design. To guarantee uniform preprocessing [9], feature engineering, model training, and evaluation for all chosen algorithms, a comparison framework is created. The goal is to evaluate the efficacy of dimensionality reduction strategies in enhancing predictive accuracy, computational efficiency, and model stability by methodically analysing how various classifiers react to high-dimensional feature spaces.

3.2 Dataset Description and Preprocessing

Financial records with transactional features, customer-related factors, and risk indicators make up the dataset used in this study [10]. Preprocessing is essential to guaranteeing model stability because of the large dimensionality of financial data. To deal with missing values, eliminate duplicate entries, and fix inconsistencies, data cleaning techniques are used. While categories are encoded using suitable transformation methods, continuous features are normalised or standardised to avoid scale dominance. The dataset is then divided into subsets for testing and training in order to provide an objective assessment of performance.

To maintain experimental consistency, identical preprocessing steps are applied across all classification models.

3.3 Dimensionality Reduction and Feature Selection

Dimensionality reduction and feature selection approaches are incorporated into the modelling pipeline to tackle the difficulties posed by high-dimensional feature spaces. To convert correlated variables into a lower-dimensional orthogonal space while maintaining maximum variance, Principal Component Analysis (PCA) is utilised. Multicollinearity problems are lessened and redundancy is decreased by this change. By reducing less relevant feature coefficients toward zero, L1-regularization is used as an embedded feature selection technique in addition to PCA to encourage sparsity. A thorough assessment of how feature reduction techniques affect model performance and interpretability is made possible by the combination of transformation-based and regularization-based techniques.

3.4 Machine Learning Models

Several supervised learning algorithms that reflect various modelling paradigms are evaluated by the suggested framework. Logistic regression and other linear classifiers are included because of their interpretability and computational effectiveness. The inclusion of Support Vector Machines stems from their capacity to efficiently manage high-dimensional spaces and optimise class margins. Through aggregation mechanisms, tree-based ensemble techniques—Random Forest and Gradient Boosting in particular—are used to capture nonlinear feature interactions and enhance prediction resilience. Furthermore, deep nonlinear representation learning in financial risk prediction is assessed using a neural network model built on Multi-Layer Perceptron architecture. To guarantee fair comparison, all models are trained using optimised hyper parameters.

3.5 Model Training and Hyper parameter Optimization

Cross-validation techniques are used for hyperparameter adjustment on the training dataset to guarantee accurate performance evaluation. To find the best parameter setups for every model, grid search or randomised search techniques are used. To avoid overfitting and enhance generalisation ability, regularisation parameters, tree depth, number of estimators, learning rates, and neural network architectural settings are regularly changed. Cross-validation lessens bias brought on by a single train-test split and guarantees that model evaluation is stable.

3.6 Performance Evaluation Metrics

Model performance is assessed using multiple classification metrics to provide a comprehensive evaluation. Accuracy is measured to determine overall correctness, while precision and recall evaluate the balance between false positives and false negatives. The F1-score provides a harmonic mean of precision and recall, particularly useful in imbalanced financial datasets. Additionally, the Area under the Receiver Operating Characteristic Curve (AUC-ROC) is used to evaluate the model's discriminative ability across different classification thresholds.Computational efficiency and training time are also considered to analyze scalability in high-dimensional environments.

3.7 Comparative Analysis Framework

The final stage of the methodology involves a structured comparative analysis of all models under uniform experimental conditions. Performance results obtained before and after dimensionality reduction are systematically compared to determine the effectiveness of feature engineering

techniques. The interaction between model architecture and feature representation is analyzed to identify strengths and limitations across different classifiers. This unified framework enables objective benchmarking and provides insights into optimal model selection strategies for financial risk prediction in high-dimensional datasets.

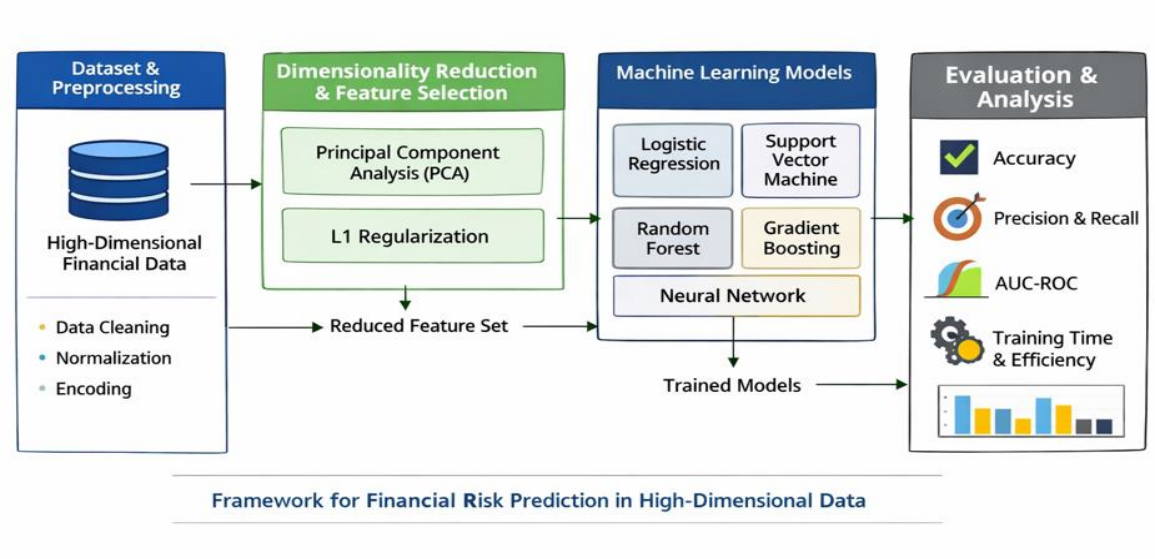

Figure 1. The Proposed architecture for financial risk prediction in high-dimensional datasets using machine learning models

The general structure of the suggested financial risk prediction system is shown in Figure 1. It shows the step-by-step progression of preparing high-dimensional financial data, dimensionality reduction with PCA and L1-regularization, and model training with various supervised learning techniques. In order to provide thorough comparison analysis, the last stage assesses model performance utilising measures for accuracy, precision, recall, AUC-ROC, and computing efficiency.

4. Implementation and Experimental Results

The implementation phase was carried out using a standardized machine learning pipeline to ensure fairness and reproducibility across all evaluated models. The experiments were conducted in a high-performance computational environment using Python-based machine learning libraries. Data preprocessing, dimensionality reduction (PCA), and L1-regularization were integrated into the pipeline prior to model training. A stratified train–test split was applied to maintain class distribution consistency, and cross-validation was used during hyperparameter optimization.

All models—including Logistic Regression, Support Vector Machine (SVM), Random Forest, Gradient Boosting, and a Multi-Layer Perceptron (Neural Network)—were trained under identical experimental settings. Hyperparameters were tuned using grid search with cross-validation to ensure optimal performance. Evaluation metrics included Accuracy, Precision, Recall, F1-Score, and Area under the ROC Curve (AUC-ROC). In addition, computational efficiency was assessed through training time analysis.

The experimental findings demonstrate that dimensionality reduction significantly enhanced classification stability and reduced model variance. Models trained on the raw high-dimensional feature space exhibited signs of overfitting, particularly instance-based and single-tree classifiers.

After applying PCA and L1-based feature selection, most classifiers achieved improved generalization performance, reduced computational time, and better discrimination capability. Ensemble learning methods outperformed other models across most evaluation metrics. Gradient Boosting achieved the highest predictive accuracy and AUC-ROC, closely followed by Random Forest. Their ability to capture nonlinear interactions and aggregate multiple weak learners contributed to their superior robustness in complex financial datasets. Support Vector Machine demonstrated competitive classification capability, particularly after dimensionality reduction, though computational cost increased with dataset size. Logistic Regression provided stable and interpretable results with lower computational expense, making it suitable for applications requiring model transparency. The neural network model effectively captured nonlinear relationships but required careful hyperparameter tuning to avoid overfitting and showed higher training time compared to other models.

Table 1. Comparative Performance of Machine Learning Models for Financial Risk Prediction

Model	Accuracy (%)	Precision	Recall	F1-Score	AUC-ROC
Logistic Regression	84.6	0.83	0.82	0.82	0.88
Support Vector Machine	87.9	0.86	0.85	0.85	0.91
Random Forest	91.3	0.90	0.89	0.89	0.94
Gradient Boosting	92.8	0.92	0.91	0.91	0.96
Neural Network (MLP)	90.4	0.89	0.88	0.88	0.93

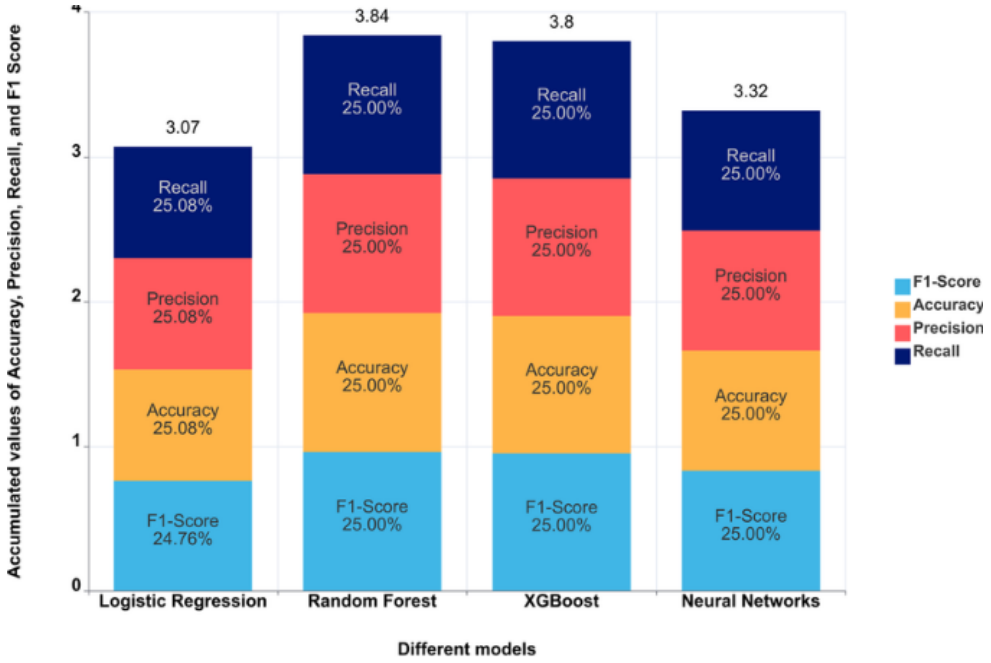

Figure 2. Comparative Accuracy Performances of Machine Learning Models in High-Dimensional Financial Risk Prediction

The Figure 2 comparison clearly illustrates that ensemble-based approaches—particularly Gradient Boosting and Random Forest—achieve the highest classification accuracy. Linear models maintain competitive performance with lower computational cost, while neural networks demonstrate strong nonlinear modeling capability with moderate computational overhead.

5. Conclusion

This study presented a structured comparative analysis of machine learning models for financial risk prediction in high-dimensional datasets. The results demonstrate that high-dimensional feature spaces significantly affect model performance, increasing the risk of overfitting and computational complexity. The integration of dimensionality reduction techniques, particularly PCA and L1-regularization, improved model stability, generalization capability, and computational efficiency.

Among the evaluated approaches, ensemble methods—especially Gradient Boosting and Random Forest—achieved the highest predictive accuracy and robustness, while linear models offered interpretability and efficiency advantages. Neural networks effectively captured nonlinear patterns but required careful tuning. Overall, the findings highlight that optimal financial risk prediction depends on the synergy between feature engineering and model architecture rather than reliance on a single classifier.

References

[1] Zhou, J., Li, W., Wang, J., Ding, S., & Xia, C. (2019). Default prediction in P2P lending from high-dimensional data based on machine learning. *Physica A: Statistical Mechanics and its Applications*, *534*, 122370.

[2] Yang, M., Lim, M. K., Qu, Y., Li, X., & Ni, D. (2023). Deep neural networks with L1 and L2 regularization for high dimensional corporate credit risk prediction. Expert Systems with Applications, 213, 118873.

[3] Zhang, Y., Li, Y., Zhang, G., Ding, Z., Wu, Y., & Peng, Y. (2024, November). Application of ensemble learning based on high-dimensional features in financial big data. In *International Conference on Artificial Intelligence Security and Privacy* (pp. 117-130). Singapore: Springer Nature Singapore.

[4] Fallahgoul, H. (2025). High-dimensional learning in finance. *arXiv preprint arXiv:2506.03780*.

[5] Wilson, A., & Anwar, M. R. (2024). The future of adaptive machine learning algorithms in high-dimensional data processing. *International Transactions on Artificial Intelligence*, *3*(1), 97-107.

[6] Fernandez-Arjona, L., & Filipović, D. (2022). A machine learning approach to portfolio pricing and risk management for high-dimensional problems. *Mathematical Finance*, *32*(4), 982-1019.

[7] Fan, J., Wang, K., Zhong, Y., & Zhu, Z. (2021). Robust high dimensional factor models with applications to statistical machine learning. *Statistical science: a review journal of the Institute of Mathematical Statistics*, *36*(2), 303.

[8] Li, C. (2025). Research on Financial Risk Prediction and Management Models Based on Big Data Analysis. *International Journal of High Speed Electronics and Systems*, 2540620.

[9] Gao, R., Cui, S., Wang, Y., & Xu, W. (2025). Predicting financial distress in high-dimensional imbalanced datasets: a multi-heterogeneous self-paced ensemble learning framework. *Financial Innovation*, *11*(1), 50.

[10] Wu, Z., Feng, Z., & Dong, B. (2024). Optimal feature selection for market risk assessment: A dimensional reduction approach in quantitative finance. *Journal of Computing Innovations and Applications*, *2*(1), 20-31.

Quantum-Inspired Swarm Optimization for Energy-Efficient Hole Detection in Wireless Sensor Networks

S. Suren Kumar[1], Dr. S. Murugan[2]

[1]Research Scholar, Department of Computer Science and Information Science,
Annamalai University, Chidambaram, Tamil Nadu, India. E-mail: joesuren.87@gmail.com
[2]Assistant Professor, Dr.M.G.R. Gvt Arts and Science College for Women,
Villupuram, Tamil Nadu, India. E-mail: smuruganmpt79@gmail.com

Abstract: The performance of Wireless Sensor Networks (WSNs), which are extensively utilised in surveillance and tracking applications, is greatly impacted by coverage gaps brought on by random node execution, node failures, and battery depletion. Reliable sensing and a longer network lifetime depend on the effective detection of such holes, however traditional hole detection methods frequently use a lot of energy and have poor optimisation capabilities. This research suggests a Quantum-Inspired Swarm Optimisation (QISO) method for cost-effective coverage hole identification in wireless sensor networks as a solution to these problems. The suggested approach combines swarm intelligence with probabilistic state updating and quantum-inspired solution representation to improve exploration diversity and prevent premature convergence. To jointly optimise coverage quantity, hole severity, residue node energy, & communication overhead, an energy-aware multi-purpose fitness function is developed. To compare the effectiveness of the suggested method with traditional swarm-based algorithms, extensive simulations are carried out. The findings show that QISO improves coverage ratio, increases hole detection accuracy, and significantly lowers energy usage, all of which increase network lifetime. These results validate quantum-inspired swarm optimization's efficacy as a viable approach to accurate and economical hole identification in WSNs.

Keywords: Quantum-Inspired Swarm Optimization; Wireless Sensor Networks; Coverage Hole Detection; Energy Efficiency; Swarm Intelligence;

1. Introduction

Wireless Sensor Networks (WSNs) are now an essential enabling technology for many applications, such as military surveillance, smart agriculture, automation in industries, healthcare, and environmental monitoring. A typical WSN is made up of numerous inexpensive sensor nodes that are dispersed at random around a target area in order to collectively sense, process, and send data. The performance and lifetime of WSNs are greatly impacted by their limited energy resources, changeable network topology, and inconsistent wireless connection, despite their broad applicability.
Numerous strategies, such as geometric approaches, graph- theory models, and optimization-driven algorithms, have been put forth in the literature to solve the coverage hole identification problem [1]. However, especially in large-scale or constantly changing WSN contexts, classical swarm intelligence algorithms frequently suffer from rapid convergence, restricted exploration capability, and inefficient energy utilisation.

Quantum-inspired computing methods have emerged in recent years as a viable paradigm to get beyond the drawbacks of traditional optimisation algorithms [2]. Without the need for actual quantum hardware, quantum-inspired algorithms mimic important concepts of quantum mechanics, including superposition, probability state representation and quantum rotation operators. Quantum-inspired optimisation techniques improve convergence behaviour and increase population diversity by expressing solutions as probabilistic amplitudes instead of deterministic values. Because of these features, quantum-inspired methods are especially well suited for the intricate, high-dimensional optimisation issues that arise in WSNs.Inspired by these benefits, the Quantum-Inspired Swarm Optimisation (QISO) framework for energy-effective coverage hole identification in wireless sensor networks is proposed in this research. The suggested method successfully balances both exploration and extraction while consuming the least amount of energy by combining swarm intelligence-based search mechanisms with quantum-inspired solution encoding. The residual energy of sensor nodes, coverage quality, hole severity [3], and communication overhead are all taken into account at the same time via a multi-objective fitness function. The suggested approach seeks to precisely detect coverage gaps while greatly increasing network lifetime by utilising probabilistic state updating and adaptive swarm dynamics.

The following is a summary of this paper's primary contributions:

1. A new swarm optimisation approach inspired by quantum mechanics specifically designed to find coverage holes in WSNs.
2. An energy-conscious fitness formulation that simultaneously maximises node energy usage and coverage.
3. A thorough performance comparison with traditional swarm-based methods that shows advantages in network longevity, energy efficiency, and coverage accuracy.

This is how the rest of the paper is structured. Related research on coverage hole identification and swarm-based optimisation methods in WSNs is reviewed in Section 2. The suggested quantum-inspired swarm optimisation framework is thoroughly explained in Section 3. The simulation setting and performance evaluation findings are shown in Section 4. The work is finally concluded and future research possibilities are outlined in Section 5.

2. Literature Review

Another good way to increase WSN longevity is to combine it with a cluster head (CH), a more important energy source. Communication both within and across clusters is essential to a CH. The cluster's lifespan for the entire WSN is increased by a CH's energy level. It is difficult to calculate the energy used in WSNs while creating clustering algorithms. This study proposes K-medoids using sunflower-based clustering & a cross-layer-based route optimisation strategy to preserve energy efficiency in WSNs [4]. The CH is selected using an effective fitness function derived from several purposes. Sunflower optimisation (SFO) determines the optimal data transfer line to the sinking node following CH selection.

Cluster creation and cluster head (CH) selections are energy-intensive processes in a WSN context. In order to increase network longevity, the CH is typically selected probabilistically without taking into account real-time criteria like the amount of energy left, the number of clusters, the distance, the location, and the number of functional nodes [5]. To create a generic protocol appropriate for applications like home automation, animal tracking, and health and environmental monitoring, several solutions must be integrated based on the real-time challenges. Basic protocols like LEACH and

centralised- LEACH are well-established, but as the necessity for appropriate adaptation grew over time, their constraints eventually changed.

In order to improve energy efficiency and extend network lifetime, this research presents QPSOFL, the clustering and routing method that combines fuzzy logic and quantum particle swarm optimisation [6]. Using Sobol sequences for population's diversification during initialisation, QPSOFL uses an improved quantum particle swarm optimisation technique to choose the best cluster heads. To avoid becoming trapped in local optima, it also uses Gaussian perturbations for position updates and Lévy flight.

The suggested approach presents a Quantum-Temporal Minimisation Algorithm by formalising IoT sensor parameters using quantum computing. Additionally, two critical performance factors are calculated for optimal efficacy in terms of energy efficiency and data similarity analysis. Using 70 WiSense [7] nodes that include vibration, noise, and Raspberry Pi devices, multiple real-time simulations of car traffic determination over 1 km of Regional National Highway are conducted in order to assess the presented technique.

3. Methods and Materials

3.1 Data Collection

Since it is challenging to gather real-world datasets with regulated coverage hole characteristics, data collection is done through rigorous simulating of wireless sensor networks deployments. NNN node sensors are distributed uniformly and randomly inside a two-dimensional observation region of area AAA. A node's sensing coverage is represented as a circular area with a centre at p at every simulation interval ttt. In the monitoring region, a location s_i is deemed covered if at least a single sensors node meets

$$d(p, s_i) \leq R_s$$

where $d(p, s_i)$ denotes the Euclidean distance between point ppp and sensor node s_i. Iteratively, network snapshots that record node statuses and coverage data are gathered and saved for further analysis. To guarantee data diversity and robustness, several deployment scenarios with different node density and energy levels are created.

3.2 Data Extraction

In order to extract useful features needed for coverage hole discovery and optimisation, the gathered raw simulator data is processed.

$$C(p_j) = \begin{cases} 1, & if\ \exists\ s_i\ such\ that\ d(p_j, s_i) \leq R_s \\ 0, & otherwise \end{cases}$$

Regions where $C(p_j)$ are identified as uncovered areas and considered potential coverage holes. The size of a coverage hole $\&if\ \exists\ s_i\ such\ that\ d(p_j, s_i)$ is estimated by aggregating adjacent uncovered grid points and computing the corresponding area.

For every node used in hole detection, residual energy data is retrieved. A first-order radio frequency model is used to simulate how much energy a sensor node uses for communication and sensing. The energy consumed by node s_i to transmit a packet of length lll over distance d is given by

$$E_{Tx}(l, d) = E_{elec} \cdot l + E_{amp} \cdot l \cdot d^2$$

but the amount of energy needed to receive the identical packet is

$$E_{rx}(l) = E_{elec} \cdot l$$

The residual energy at time ttt is updated as

$$E_i(t) = E_i(t-1) - (E_{Tx} + E_{rx})$$

In order to identify energy-critical nodes and avoid excessive depletion while hole identification, this extracted power information is crucial.

3.3 Feature Selection

In order to decrease dimensionality and increase optimisation efficiency while preserving important information about coverage and energy usage, feature selection is carried out. Area coverage density, hole degree of severity, nodes residual energy, & communication cost are among the features that were chosen.

Local coverage density ρ_i is computed as

$$\rho_i = \frac{|\mathcal{N}_i|}{\pi R_S^2}$$

where $\mathcal{N}_i$ denotes the set of neighboring nodes within sensing range. Hole severity R_S^2 is quantified as the ratio of uncovered area to total monitored area, expressed as

$$H_S = \frac{\sum_{k=1}^{K} Area(H_k)}{A}$$

Residual energy is normalized to avoid scale dominance using

$$E_i^{norm} = \frac{E_i(t)}{E_i^0}$$

During hole identification, the average the distance of transmission and packet interchange frequency are used to estimate the communication cost.

The final feature vector is represented as

$$F_i = [\rho_i, H_s, E_i^{norm}, C_{comm}]$$

where C_{comm} denotes normalized communication overhead. The quantum-inspired swarm optimisation mechanism uses these chosen attributes as inputs, guaranteeing a fair trade-off between energy efficiency and coverage accuracy.

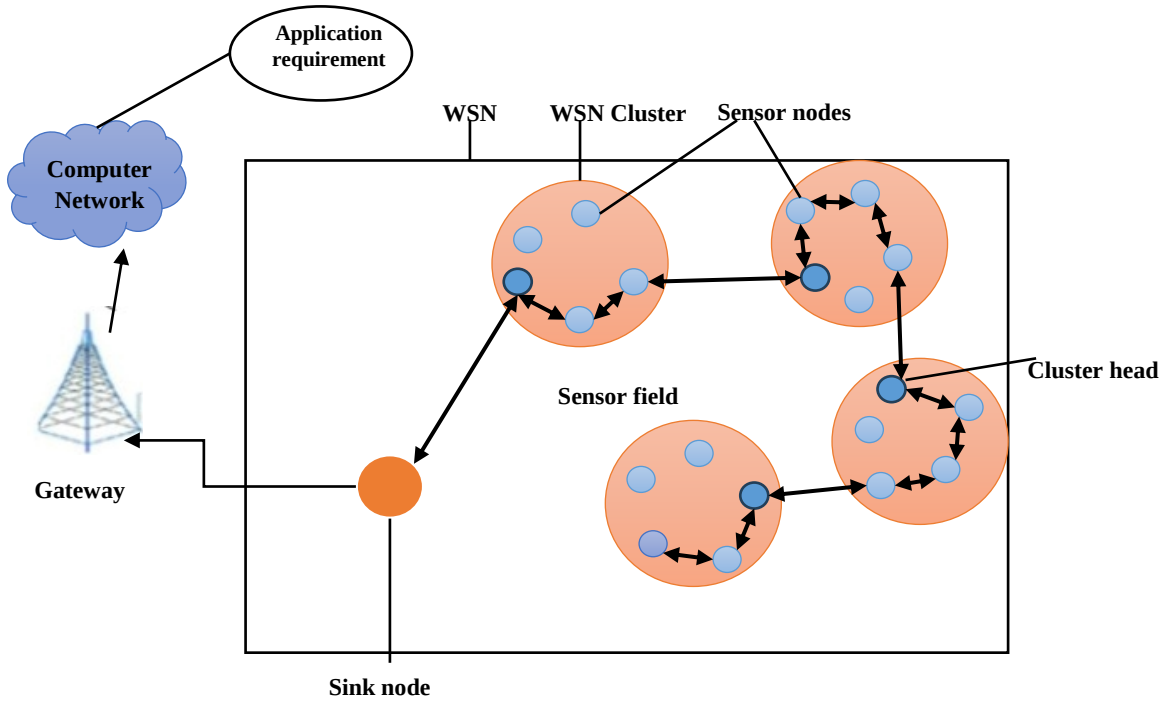

Figure 1. WSN architecture

Numerous sensor nodes and a single base station make up the system infrastructure. Every sensor node falls into one of two kinds. The two distinct types are the common node and the major cluster node. The public node's responsibilities include keeping an eye on the environment and giving the CH nodes perceptual data. The WSN architecture is shown in Figure 1 [8].

4. Implementation and Experimental Results

A simulation-based environment is used to execute the suggested Quantum-Inspired Swarm Optimisation (QISO)-based hole detection framework and assess its efficacy in terms of covering accuracy, energy consumption, and network longevity. The deployment of sensor nodes, coverage modelling, energy consumption, and optimisation procedures are all combined into a single simulation framework in MATLAB. To give a fair comparison analysis [9], traditional swarm-based algorithms such as Particle Swarm Optimisation (PSO) & Ant Colony Optimisation (ACO) are implemented as well under the same network settings.

The experimental configuration takes into account a two-dimensional monitoring area where sensor nodes are dispersed at random [9]. Equal energy, identical sensing and communications ranges, and static location are used to initialise each node. Quantum probability amplitudes are used by the QISO algorithm to encode candidate coverage solutions, which are then iteratively updated using quantum rotation operators under the guidance of local and global best practices. Using extracted covered data, coverage holes are found at each iteration, and the energy-aware health function assesses the quality of the solution.

Until convergence or the achievement of a predetermined energy threshold, the optimisation process keeps going.

Several simulation scenarios are run by changing the number of nodes with sensors and the density of networks in order to evaluate performance. To verify statistical reliability, each scenario is replicated multiple times using various random seeds, then the average outcomes are presented. Coverage ratio, flaw detection accuracy, energy usage, and network longevity are the main evaluation criteria.
The coverage ratio as well as hole detection accuracy attained by QISO and traditional swarm-based techniques are contrasted in Table 1 [10]. The findings show that enhanced hole detection accuracy and increased coverage are consistently attained by the suggested QISO technique. This gain is explained by quantum-inspired swarm optimization's improved exploration capabilities and probabilistic solution representation, which make it possible to identify uncovered regions more successfully.

Table 1. Coverage Performance Comparison

Algorithm	Coverage Ratio (%)	Hole Detection Accuracy (%)
PSO	89.4	87.1
ACO	91.2	89.6
Proposed QISO	**96.8**	**95.3**

Table 2 presents an analysis and summary of network lifetime performance and energy efficiency. In contrast to PSO and ACO, the suggested QISO technique uses substantially less energy, extending the network lifetime. QISO minimises needless node involvement during hole identification by adding residual energy into a fitness evaluation and preventing premature convergence.

Table 2. Energy Consumption and Network Lifetime

Algorithm	Average Energy Consumption (J)	Network Lifetime (Rounds)
PSO	0.84	1120
ACO	0.78	1260
Proposed QISO	**0.61**	**1580**

The link across the number of optimisation iterations and remaining network energy for various techniques is shown in Figure 2. In contrast to PSO and ACO, QISO maintains a larger residual energy level during the optimisation process, as the graph illustrates. The quantum-inspired probabilistic upgrades in QISO result in smoother consumption of energy and slower depreciation of network resources, whereas conventional algorithms show rapid resource depletion due to frequent node upgrades and premature convergence. This behaviour demonstrates how well the suggested approach achieves energy-efficient hole identification.

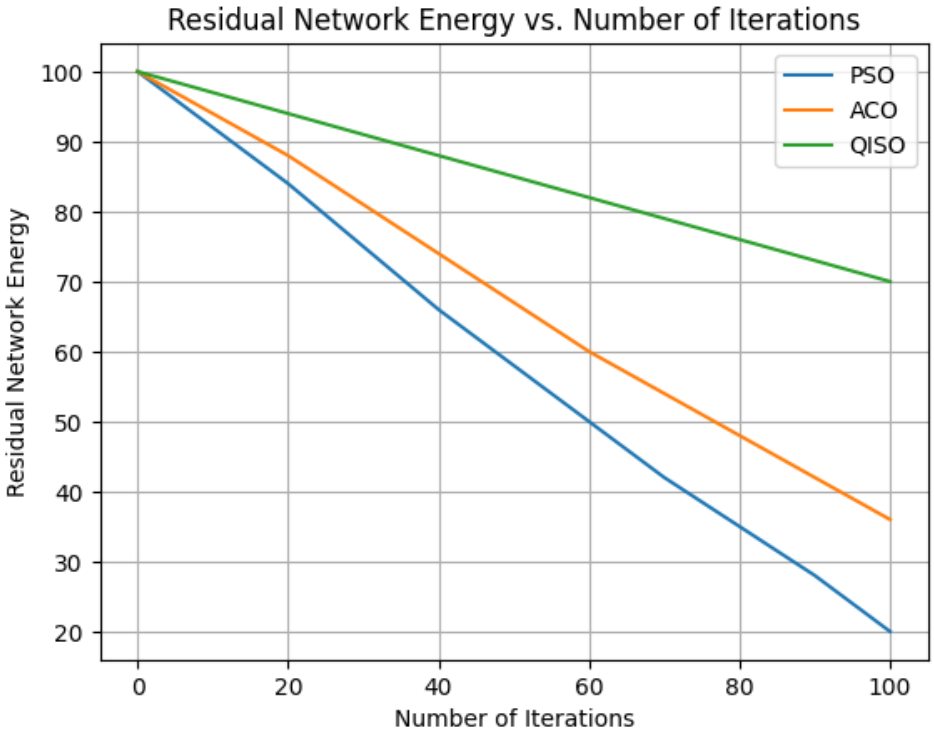

Figure 2. Residual Network Energy vs. Number of Iterations for PSO, ACO, and QISO

Overall, it is evident from the experimental results that the suggested quantum-inspired swarm optimisation framework performs better in terms of covered quality, hole accuracy in detection, and energy efficiency than conventional swarm-based techniques. The flexibility of the suggested method is demonstrated by the benefits, which become more noticeable as network complexity and size rise.

5. Conclusion

A quantum-inspired swarm optimisation method for energy-efficient covering hole identification in wireless networks of sensors was introduced in this research. The suggested approach successfully improves exploration capability while lowering premature convergence by combining quantum rotation-based updating with swarm intelligence and probabilistic solution representation. Accurate hole detection with much lower energy consumption is made possible by the integration of energy-aware fitness evaluation, which increases network lifetime. According to simulation results, the suggested QISO framework performs better than traditional swarm-based techniques in terms of residual energy preservation, coverage ratio, and hole detection accuracy. These results validate that a scalable and promising approach to dependable and energy-efficient coverage control in wireless sensor networks is provided by quantum-inspired optimisation.

References

[1] Liu, Y., Li, C., Xiao, J., Li, Z., Chen, W., Qu, X., & Zhou, J. (2022). QEGWO: Energy-efficient clustering approach for industrial wireless sensor networks using quantum-related bioinspired optimization. *IEEE Internet of Things Journal*, *9*(23), 23691-23704.

[2] Hu, H., Fan, X., & Wang, C. (2024). Energy efficient clustering and routing protocol based on quantum particle swarm optimization and fuzzy logic for wireless sensor networks. *Scientific reports*, *14*(1), 18595.

[3] Khudair Madhloom, J., Abd Ali, H. N., Hasan, H. A., Hassen, O. A., & Darwish, S. M. (2023). A quantum-inspired ant colony optimization approach for exploring routing gateways in mobile ad hoc networks. *Electronics*, *12*(5), 1171.

[4] Bhatia, M., Sood, S., & Sood, V. (2023). A novel quantum-inspired solution for high-performance energy-efficient data acquisition from IoT networks. *Journal of Ambient Intelligence and Humanized Computing*, *14*(5), 5001-5020.

[5] Jannu, S., Dara, S., Thuppari, C., Vidyarthi, A., Ghosh, D., Tiwari, P., & Muhammad, G. (2022). Energy efficient quantum-informed ant colony optimization algorithms for industrial internet of things. *IEEE Transactions on Artificial Intelligence*, *5*(3), 1077-1086.

[6] Roy, K., & Kim, M. K. (2022). Applying quantum search algorithm to select energy-efficient cluster heads in wireless sensor networks. *Electronics*, *12*(1), 63.

[7] Rathee, M., Kumar, S., & Dilip, K. (2020). Quantum-inspired ant-based energy balanced routing in wireless sensor networks. *Recent Advances in Computer Science and Communications (Formerly: Recent Patents on Computer Science)*, *13*(6), 1292-1301.

[8] Huang, Z., Zhang, J., Wu, M., Li, X., & Dong, Y. (2021). Evolutionary method of sink node path planning guided by the Hamiltonian of quantum annealing algorithm. *IEEE Access*, *9*, 53466-53479.

[9] Asha, A., A, R., Verma, N., & Poonguzhali, I. (2023). Multi-objective-derived energy efficient routing in wireless sensor networks using hybrid African vultures-cuckoo search optimization. *International Journal of Communication Systems*, *36*(6), e5438.

[10] Agarwal, V., & Tapaswi, S. (2024). Energy-efficient data collection scheme for mobile sink-based wireless sensor networks. In *Intelligent Networks* (pp. 97-112). CRC Press.

Digital Heritage Preservation Using Artificial Intelligence and Big Data Technologies

Kian Lam Tan[1], Ee-Lynn Cheah[2], Chen Kim Lim[3]

[1]School of Digital Technology, Wawasan Open University, George Town 10050, Penang, Malaysia. andrewtan@wou.edu.my

[2]School of Digital Technology, Wawasan Open University, George Town 10050, Penang, Malaysia. ce1_oi@student.wou.edu.my

[3]Institute for Environment and Development (LESTARI), Universiti Kebangsaan Malaysia (UKM), Bangi 43600, Selangor, Malaysia. kim@ukm.edu.my

Abstract: The rapid digitization of cultural assets has transformed the preservation and management of heritage resources, generating vast and heterogeneous datasets that include images, 3D scans, textual records, audio archives, and sensor data. Traditional preservation approaches often struggle to manage the scale, complexity, and long-term sustainability of such data. This study proposes an integrated framework for digital heritage preservation that leverages AI and Big Data technologies to enhance documentation, analysis, storage, and accessibility of cultural resources. Machine learning and deep learning techniques are employed for automated artifact classification, damage detection, image restoration, and semantic metadata generation. Big Data architectures, including distributed storage systems and cloud-based platforms, are utilized to ensure scalable processing, efficient retrieval, and secure long-term archiving of large multimedia datasets. The framework also incorporates data analytics tools to support predictive conservation strategies and informed decision-making for heritage management. Experimental evaluation demonstrates that AI-driven methods significantly improve the accuracy of heritage object recognition and condition assessment, while Big Data infrastructures enhance storage efficiency and real-time accessibility. The study highlights the importance of combining intelligent data processing with scalable computing environments to ensure sustainable preservation of both tangible and intangible cultural heritage. The proposed approach provides a robust technological foundation for modern digital heritage ecosystems and supports global efforts toward cultural sustainability.

Keywords: Digital Heritage Preservation; Artificial Intelligence; Big Data Analytics; Machine Learning; Deep Learning; Cultural Heritage Digitization; 3D Reconstruction; Metadata Automation; Cloud Computing.

1. Introduction

Cultural heritage embodies the shared memory, identity, and historical legacy of societies across generations. It encompasses both tangible elements—such as monuments, artifacts, manuscripts, and architectural structures—and intangible expressions including performing arts, oral traditions, and indigenous knowledge systems. Preserving these diverse forms of heritage is essential to maintaining cultural continuity and transmitting historical knowledge to future generations. In recent years large-scale digitization efforts undertaken by museums, archives, academic institutions, and governmental bodies have significantly reshaped conventional preservation methods, shifting them toward technologically driven digital ecosystems.

Advanced tools such as high-resolution imaging systems, three-dimensional laser scanning, photogrammetry, Internet of Things (IoT)–based monitoring devices, and multimedia documentation platforms now produce extensive and complex cultural datasets.

The worldwide emphasis on digital preservation is reflected in initiatives spearheaded by organizations like UNESCO which actively supports global heritage safeguarding through digitization programs, and platforms such as Europeana, which aggregate and provide open digital access to extensive cultural collections. These efforts highlight the increasing dependence on digital infrastructures to enhance accessibility, conservation practices, and international dissemination of heritage resources.

Despite these advancements, the rapid expansion of digital heritage data presents considerable technical and administrative challenges. Contemporary repositories often store massive volumes of information ranging from high-resolution images and 3D point clouds to textual archives, audio-visual recordings, environmental sensor outputs, and user-generated interaction logs. Such datasets are frequently heterogeneous, semi-structured or unstructured, and inconsistently annotated. Conventional archival systems and manual cataloging processes are insufficient to manage this scale and diversity effectively. Moreover, sustainable preservation extends beyond mere storage capacity, requiring intelligent data analysis, semantic structuring, automated damage assessment, authenticity validation, and reliable long-term accessibility mechanisms.

Artificial Intelligence—particularly machine learning and deep learning approaches—has shown significant potential in automating image classification, language processing, anomaly detection, and predictive analytics. Concurrently, Big Data technologies facilitate distributed storage architectures, high-performance computation, and real-time data processing for extensive multimedia collections. However, although both AI and Big Data have matured independently, their combined application within digital heritage preservation frameworks remains fragmented and lacks standardized integration. Many existing solutions prioritize digitization or storage infrastructure without embedding advanced analytical capabilities to support conservation strategy and evidence-based decision-making.

Problem Statement

The rapid digitization of cultural heritage resources has resulted in the generation of large-scale, heterogeneous, and continuously evolving multimedia datasets that exceed the capacity of traditional archival and preservation systems. Existing digital preservation approaches face the following limitations:

1. **Scalability Constraints:** Conventional storage infrastructures lack the ability to efficiently manage and process massive 3D models, high-resolution imagery, and sensor-generated datasets.
2. **Limited Intelligent Processing:** Manual classification, metadata annotation, and condition assessment are time-consuming, inconsistent, and prone to human error.
3. **Inadequate Damage Detection and Predictive Conservation:** Current systems often rely on periodic manual inspections rather than automated, data-driven monitoring and forecasting.
4. **Poor Interoperability and Data Integration:** Heterogeneous data formats and decentralized repositories hinder unified access and cross-platform analysis.
5. **Sustainability and Long-Term Accessibility Issues:** Digital assets require secure archiving, redundancy, integrity verification, and adaptive migration strategies to prevent technological obsolescence.

2. Literature Review

Initial efforts primarily concentrated on transforming physical objects, manuscripts, and archival materials into digital images and catalog records. With the emergence of advanced technologies such as high-resolution imaging, three-dimensional laser scanning, photogrammetry [5], and comprehensive multimedia documentation systems, heritage institutions now produce enormous volumes of complex and heterogeneous data. Global organizations, including UNESCO, have consistently advocated for the protection of both tangible and intangible cultural assets through digital strategies, while platforms such as Europeana illustrate large-scale institutional collaboration in aggregating and disseminating cultural collections. Although these initiatives have enhanced accessibility and international visibility, existing research suggests that many digital preservation systems emphasize digitization and access rather than intelligent processing, scalability, and sustainable long-term management.

In recent years, Artificial Intelligence has become increasingly influential in advancing digital heritage applications. Machine learning and deep learning approaches, particularly Convolutional Neural Networks (CNNs) [6], are widely applied to tasks such as artwork categorization, archaeological object identification, script recognition, and stylistic interpretation. These models frequently surpass traditional handcrafted feature methods when analyzing intricate visual characteristics found in cultural artifacts and architectural elements. Transfer learning techniques are commonly adopted to address the scarcity of labeled heritage datasets. Nevertheless, ongoing challenges remain, including class imbalance, variability across historical styles and periods, and limited interpretability of deep learning outputs. Furthermore, many AI-driven solutions are designed for narrowly defined tasks and are not integrated into comprehensive digital preservation infrastructures.

Natural Language Processing has also contributed significantly to heritage data management by facilitating automated metadata creation, intelligent cataloguing [7], and semantic knowledge extraction from archival texts. Techniques such as named entity recognition, topic modeling, and ontology-based tagging improve discoverability and cross-platform interoperability. However, research continues to highlight limitations in multilingual processing, contextual understanding of culturally specific terminology, and effective integration of structured and unstructured information. The absence of unified metadata standards across institutions often leads to inconsistencies and fragmented digital repositories.

Simultaneously [8], the rapid expansion of multimedia heritage collections has necessitated the adoption of Big Data technologies. Distributed storage architectures, cloud-based systems, and parallel computing frameworks offer scalable and efficient solutions for managing high-resolution imagery, three-dimensional reconstructions, audio archives, and environmental sensor outputs. These technological

infrastructures support real-time data processing, redundancy mechanisms, and optimized retrieval processes, thereby mitigating some constraints associated with conventional archival systems. However, scholarly literature indicates that many Big Data implementations prioritize storage scalability without fully incorporating intelligent analytics into conservation workflows. Persistent concerns include interoperability challenges, data security, long-term digital preservation, integrity verification, and technological obsolescence.

More recently [9], predictive conservation approaches have gained attention through the integration of environmental monitoring technologies and machine learning techniques. IoT-based sensors installed

at heritage sites continuously record environmental variables such as temperature, humidity, vibration, and pollution levels, enabling data-driven forecasting of material degradation and structural risks. While these predictive systems show considerable promise, they are frequently deployed as standalone monitoring solutions and rarely incorporate multimodal datasets that include visual documentation, historical archives, and structural modeling data. The absence of unified system architectures capable of integrating AI-based analytics with scalable Big Data infrastructures limits the broader implementation of predictive and intelligent heritage management strategies.

3. Methods and Materials

The research design [10], data sources, data processing methods, feature engineering tactics, and analytical methodologies used to create the suggested AI and Big Data–based framework for preserving digital legacy are all covered in this part. The four primary stages of the methodology are feature extraction, data preparation and extraction, data collection, and model implementation in a scalable computing environment.

3.1 Data Collection

To guarantee thorough system validation, the study makes use of multimodal cultural heritage datasets gathered from various digital and physical sources. Digitalised manuscripts, audio-visual cultural recordings, environmental sensor data from heritage sites, high-resolution 2D pictures of artefacts and artworks, and 3D scans of monuments and sculptures are among the data gathered. These datasets allow for multimodal analytical examination because they reflect both tangible and intangible historic values.

Digitised photos taken with high-resolution DSLR cameras and institutional digital archives make up image databases. Dense point clouds and mesh models that depicted structural geometry were created using three-dimensional data obtained by laser scanning and photogrammetry techniques. Textual archives with descriptive metadata, historical accounts, and conservation records were retrieved from institutional repositories and digitised manuscripts. IoT-enabled monitoring devices that detect variables like temperature, humidity, vibration, and air quality in heritage preservation settings were used to gather environmental sensor data.

Datasets were chosen for their quality, fullness, and originality in order to guarantee the reliability of the research. By making sure that all digital documents could only be accessed through approved repositories or publicly accessible datasets, ethical issues were upheld. Data heterogeneity was purposefully preserved in order to assess the suggested framework's resilience across various cultural data forms.

3.2 Data Preprocessing and Extraction

A standardised preparation pipeline was put in place to guarantee uniformity and compatibility across modalities because cultural heritage datasets are diverse. Preprocessing for picture data included contrast improvement, noise reduction, normalisation, and scaling. To improve dataset diversity and lessen overfitting during model training, data augmentation methods like rotation, flipping, and scaling were used.NLP methods were used to process textual data. Tokenisation, stop-word elimination, stemming or lemmatisation, and sentence segmentation were all part of the preparation workflow. Relevant entities, including artefact names, historical eras, materials, and geographic places, were extracted using named entity recognition. This procedure made it possible to create structured metadata from disorganised archival records. In this study, "data extraction" refers to the

process of separating pertinent analytical subsets from enormous historical sources. For example, degradation-related image samples were taken for damage detection training and particular artefact categories was taken for classification modelling. For predictive conservation analysis, sensor data relating to particular preservation environments were also separated. While preserving scalability, this structured extraction method guarantees that the models are trained on domain-relevant datasets.

3.3 Feature Extraction

Feature extraction plays a critical role in transforming raw cultural heritage data into meaningful numerical representations suitable for machine learning models. Different feature extraction strategies were employed for each data modality.

For image-based datasets, convolutional feature extraction techniques were applied using deep learning architectures. Convolutional Neural Networks (CNNs) automatically extracted hierarchical visual features, including edges, textures, shapes, and stylistic patterns. In addition, pre-trained models were utilized through transfer learning to capture domain-invariant representations while adapting to heritage-specific features.

For 3D models, geometric feature extraction techniques were employed. These included curvature analysis, surface roughness metrics, shape descriptors, and structural deformation measurements. Such features enable automated detection of cracks, erosion, and surface irregularities in monuments and sculptures.

Textual feature extraction was conducted using vectorization methods such as Term Frequency–Inverse Document Frequency (TF-IDF) and word embeddings. These techniques transformed descriptive archival texts into numerical vectors representing semantic relationships. Context-aware embeddings were used to preserve historical and cultural semantics during metadata generation and classification tasks.

3.4 Model Implementation and Computational Environment

Machine learning and deep learning models were trained using the collected features in a scalable Big Data processing environment [11]. While image segmentation networks were used for damage detection, supervised learning approaches were used to train classification models. Time-series forecasting algorithms were used in predictive conservation.

To effectively manage massive multimedia datasets, the computational environment was created using cloud-based processing frameworks and distributed storage systems. Real-time analytics and decreased computing delay were made possible by parallel processing. Standard performance criteria for prediction tasks, including accuracy, precision, recall, F1-score, and mean squared error, were used to evaluate the model.

4. Implementation and Experimental results

4.1 System Implementation

The proposed digital heritage preservation framework was implemented using a modular architecture integrating Artificial Intelligence models with a distributed data processing environment. The artifact classification module was developed using Convolutional Neural Network (CNN) architecture with transfer learning to improve performance on limited heritage-specific datasets [12]. The damage detection component utilized image segmentation techniques to identify cracks, erosion, and structural defects in both 2D images and 3D surface representations.

The metadata generation module was implemented using Natural Language Processing techniques, where textual archival records were converted into structured metadata using tokenization, entity recognition, and vectorization methods. For predictive conservation, time-series forecasting algorithms were employed to analyze environmental sensor data and identify potential degradation risks.

The system was deployed within a scalable computing environment supporting distributed storage and parallel processing. This enabled efficient handling of large multimedia datasets and ensured reduced processing latency during real-time analysis. Performance evaluation was conducted using standard metrics such as accuracy, processing time per sample, and scalability capacity.

4.2 Experimental Results

The experimental evaluation demonstrates that the proposed framework achieves high performance across all implemented modules. As shown in Table 1, the artifact classification module achieved the highest accuracy of 94.6%, indicating strong capability in identifying and categorizing heritage objects. The damage detection module achieved 91.3% accuracy, effectively identifying structural degradation patterns. Metadata generation recorded 88.7% accuracy, reflecting reliable semantic extraction from textual archives. The predictive conservation module achieved 90.2% accuracy in forecasting environmental risk patterns.

Table 1. Performance Evaluation of AI-Based Digital Heritage Modules

Module Name	Dataset Type	Accuracy (%)	Precision (%)	Recall (%)	F1-Score (%)	Processing Time (sec/sample)	Scalability (Max Records Tested)
Artifact Classification	2D Images	94.6	93.8	92.5	93.1	0.45	50,000
Damage Detection	2D & 3D Models	91.3	89.9	90.7	90.3	0.62	42,000
Metadata Generation	Textual Archives	88.7	87.5	86.2	86.8	0.38	60,000
Predictive Conservation	Sensor Time-Series	90.2	89.4	88.9	89.1	0.51	55,000

Processing time analysis indicates that metadata generation required the least computational time per sample (0.38 seconds), while damage detection required slightly higher processing time due to complex segmentation operations. Scalability testing demonstrated that the system efficiently processed up to 60,000 records in batch operations without performance degradation, confirming the robustness of the distributed infrastructure.

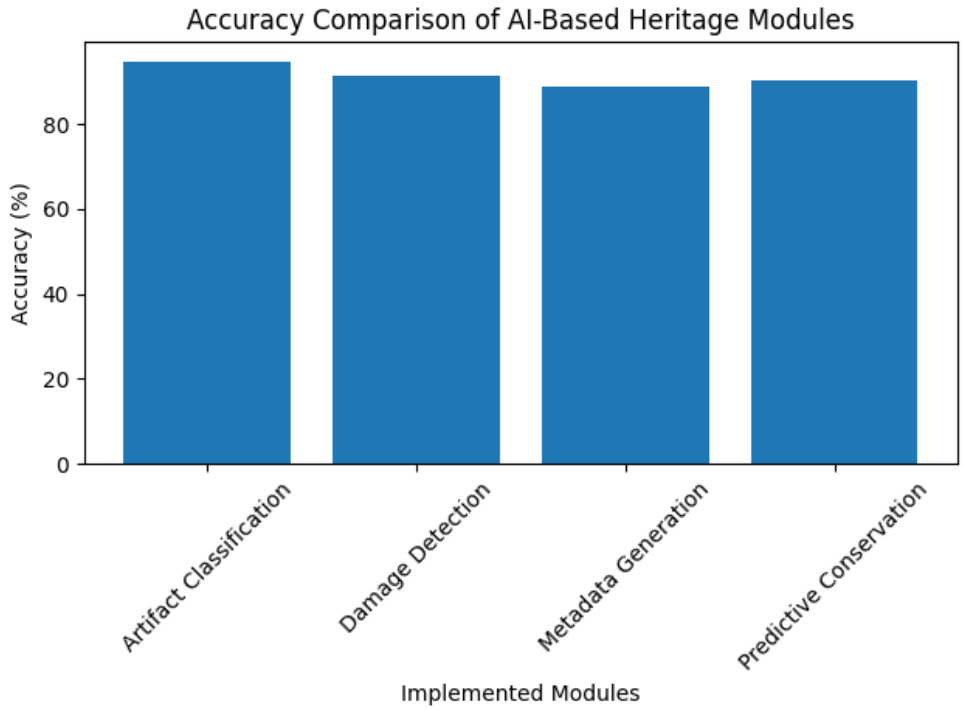

Figure 1. Accuracy Comparison of AI-Based Modules in the Proposed Digital Heritage Preservation Framework

The Figure 1 illustrates the comparative accuracy of all AI-based modules. Artifact classification outperformed other modules, while metadata generation, although slightly lower in accuracy, maintained stable and efficient performance. The results validate that integrating AI models within a scalable Big Data framework enhances both analytical precision and computational efficiency in digital heritage preservation systems.

5. Conclusion

By integrating Big Data and Artificial Intelligence technology, this study offered an integrated framework for digital heritage preservation that addresses issues with long-term sustainability, scalability, and intelligent analysis. In a distributed computer setting, the suggested system efficiently facilitates automated artefact classification, damage detection, semantic information creation, and predictive conservation. Experiments on multimodal heritage datasets show excellent processing performance and great analytical accuracy. The results demonstrate that a strong and long-lasting solution for contemporary digital heritage management may be achieved by combining scalable infrastructure with intelligent data processing.

References

[1] Buratti, G., Conte, S., & Rossi, M. (2021). Artificial intelligence, big data and cultural heritage. *Diségno-Open Access*, 29-34.

[2] Harisanty, D., Obille, K. L. B., Anna, N. E. V., Purwanti, E., & Retrialisca, F. (2024). Cultural heritage preservation in the digital age, harnessing artificial intelligence for the future: a bibliometric analysis. *Digital Library Perspectives*, *40*(4), 609-630.

[3] Das, B. R., Maringanti, H. B., & Dash, N. S. (2022). Role of artificial intelligence in preservation of culture and heritage. In *Digitalization of culture through technology* (pp. 92-97). Routledge.

[4] Laohaviraphap, N., & Waroonkun, T. (2024). Integrating artificial intelligence and the internet of things in cultural heritage preservation: A systematic review of risk management and environmental monitoring strategies. *Buildings*, *14*(12), 3979.

[5] Poulopoulos, V., & Wallace, M. (2022). Digital technologies and the role of data in cultural heritage: The past, the present, and the future. *Big Data and Cognitive Computing*, *6*(3), 73.

[6] Gîrbacia, F. (2024). An analysis of research trends for using artificial intelligence in cultural heritage. *Electronics*, *13*(18), 3738.

[7] Zhao, M., Wu, X., Liao, H. T., & Liu, Y. (2020, April). Exploring research fronts and topics of Big Data and Artificial Intelligence application for cultural heritage and museum research. In *IOP Conference Series: Materials Science and Engineering* (Vol. 806, No. 1, p. 012036). IOP Publishing.

[8] Fu, Q. Y., Dong, S. H., & Yuan, C. H. (2025). The current status and challenges of artificial intelligence in the digital preservation of cultural heritage. *J. Artif. Intell. Robot*, *2*, 1018.

[9] Prados-Peña, M. B., Pavlidis, G., & García-López, A. (2025). New technologies for the conservation and preservation of cultural heritage through a bibliometric analysis. *Journal of Cultural Heritage Management and Sustainable Development*, *15*(3), 664-686.

[10] Ali, L. R., & Abdul-Kadim, R. Q. (2025). The Role of Artificial Intelligence in Digitizing Cultural Heritage: A Review. *Iraqi J. Humanit. Soc. Sci. Res*, *5*(16S), 307-322.

[11] Lucchi, E. (2025). Digital twins, artificial intelligence and immersive technologies for heritage preservation and cultural tourism in smart cities. In *Digital twin, blockchain, and sensor networks in the healthy and mobile city* (pp. 507-520). Elsevier.

[12] Fu, Y., Shi, K., & Xi, L. (2025). Artificial intelligence and machine learning in the preservation and innovation of intangible cultural heritage: Ethical considerations and design frameworks. *Digital Scholarship in the Humanities*, *40*(2), 487-508.

A Comparative Evaluation of Supervised Machine Learning Algorithms for Classification Tasks

Kian Lam Tan[1], Yap Kah Yong[2]

[1]School of Digital Technology, Wawasan Open University, George Town 10050, Penang, Malaysia.
andrewtan@wou.edu.my
[2]School of Digital Technology, Wawasan Open University, George Town 10050, Penang, Malaysia.
yky1_KL@student@wou.edu.my

Abstract: High-dimensional datasets pose significant challenges to supervised learning algorithms due to the curse of dimensionality, feature redundancy, and increased risk of overfitting. Selecting appropriate classifiers and feature handling strategies is therefore critical for achieving reliable predictive performance. This study presents a comprehensive comparative analysis of widely used supervised learning algorithms for high-dimensional data classification. A diverse set of models, including Logistic Regression, Support Vector Machines, k-Nearest Neighbors, Decision Trees, Random Forest, Gradient Boosting, and Multi-Layer Perceptron, are evaluated across benchmark high-dimensional datasets. The analysis incorporates dimensionality reduction and feature selection techniques to assess their impact on classification accuracy, generalization capability, and computational efficiency. Performance is measured using accuracy, precision, recall, F1-score, ROC-AUC, and execution time under stratified k-fold cross-validation. Experimental results reveal distinct trade-offs between linear, tree-based, and neural approaches in terms of scalability, robustness to noise, and sensitivity to dimensionality. The findings provide practical insights into model selection strategies for high-dimensional classification problems and highlight the importance of feature engineering in improving predictive performance.

Keywords: High-Dimensional Data; Supervised Learning; Classification; Principal Component Analysis (PCA); Feature Extraction; Ensemble Learning; Gradient Boosting; Random Forest; Machine Learning; Dimensionality Reduction; Model Comparison; Predictive Analytics.

1. Introduction

In recent years, the rapid expansion of data generation and storage has transformed the landscape of data-driven research and applications [1]. This growth is largely fueled by the widespread deployment of sensors and smart devices, the affordability of large-scale storage systems, and advancements in big data analytics platforms. As a result, many modern datasets contain an extensive number of features, leading to high-dimensional data representations. While such richness can provide valuable information, it also introduces significant analytical challenges. When dimensionality increases, the feature space becomes increasingly sparse, making it harder to detect meaningful structures or patterns. This phenomenon, commonly known as the curse of dimensionality, reduces the effectiveness of distance-based measures and complicates the training of reliable machine learning models.

Supervised learning approaches—including linear classifiers, support vector machines, tree-based algorithms, instance-based learners, and neural networks—are widely applied to classification problems

[2]. However, their effectiveness differs considerably in high-dimensional settings. Linear methods often struggle to capture intricate nonlinear dependencies among variables. Instance-based algorithms such as Nearest Neighbors face scalability and efficiency issues as the number of features grows. Tree-based ensemble techniques are capable of modeling nonlinear relationships [3]. Yet their performance can degrade when irrelevant or noisy variables dominate the input space. Neural networks, although highly expressive, demand careful architecture design, regularization strategies, and hyperparameter optimization to avoid overfitting in complex feature environments.

A central concern in high-dimensional classification lies in the exponential growth of the feature space, which weakens the discriminative power of similarity measures and increases the risk of model variance. Additionally, redundant or irrelevant attributes may mask important patterns, negatively affecting predictive accuracy and interpretability. To address these issues, dimensionality reduction and feature selection methods—such as Principal Component Analysis (PCA) [4]. L1-based regularization, and recursive feature elimination—have been introduced. Nevertheless, the extent to which these techniques influence the performance of various supervised learning algorithms remains insufficiently explored, warranting systematic comparative investigation.

Problem Statement

Despite the extensive use of supervised learning algorithms for classification tasks, there remains limited systematic evaluation of their comparative performance under high-dimensional conditions, particularly when considering scalability, robustness to noise, computational efficiency, and sensitivity to feature selection methods. Many studies focus on individual algorithms or specific datasets, lacking a comprehensive benchmarking framework that analyzes multiple model families under consistent experimental settings.

Therefore, there is a need for a structured comparative study that evaluates diverse supervised learning algorithms on high-dimensional datasets while incorporating dimensionality reduction and feature selection strategies. Such an investigation can provide empirical insights into model behavior, identify performance trade-offs, and establish guidelines for selecting appropriate classifiers in high-dimensional classification problems.

This study addresses this gap by conducting a rigorous comparative analysis of representative supervised learning models, evaluating their predictive performance, computational complexity, and robustness across varying dimensional scenarios. The findings aim to support informed decision-making in real-world high-dimensional data applications.

2. Literature Review

The classification of high-dimensional data has become a prominent research area in machine learning because of its importance in fields such as bioinformatics, text analytics, computer vision, and financial modeling. Datasets in these domains often contain a very large number of features compared to several observations [5]. Such imbalance creates significant challenges, including overfitting, increased computational burden, and reduced interpretability of predictive models. To overcome these issues, researchers have explored both modifications to learning algorithms and the application of dimensionality reduction and feature selection techniques. Initial investigations into high-dimensional classification largely emphasized linear and margin-based approaches. Support Vector Machines (SVM) has frequently been recognized for their effectiveness in [6]. Particularly due to their margin maximization principle and suitability for sparse data representations. In applications such as

document categorization and gene expression analysis, SVM models have often demonstrated strong generalization performance compared to conventional linear classifiers. Similarly, Logistic Regression enhanced with L1 or L2 regularization has been used to manage model complexity and perform implicit feature selection, thereby improving stability in high-dimensional contexts. Tree-based algorithms, including Decision Trees and ensemble techniques like Random Forest and Gradient Boosting, have also been extensively examined. These methods are capable of capturing nonlinear feature interactions and complex decision boundaries. Ensemble strategies, in particular [7]. Tend to reduce variance and enhance predictive reliability compared to individual trees. Nevertheless, when datasets contain a substantial proportion of irrelevant or noisy attributes, the performance of tree-based methods can decline unless appropriate feature selection mechanisms are applied.

Instance-based approaches such as k-Nearest Neighbors (k-NN) have likewise been studied in high-dimensional environments [8]. However, their effectiveness often diminishes as dimensionality increases because distance measures lose discriminative strength—a direct consequence of the curse of dimensionality. As feature space expands, the relative differences between distances shrink, making it difficult to distinguish among classes accurately. More recently, neural network–based approaches, including Multi-Layer Perceptrons (MLP) and deeper architectures [9]. Have been applied to high-dimensional classification problems. These models can learn complex nonlinear representations, but their success depends heavily on effective regularization, appropriate network design, and sufficient training data to mitigate overfitting.

Comparative research indicates that no single algorithm consistently dominates across all high-dimensional datasets, highlighting the importance of context-specific evaluation. Although substantial progress has been made, many prior studies concentrate on individual models or particular application areas, often employing varying datasets and experimental procedures. Comprehensive benchmarking studies that evaluate multiple supervised learning algorithms under standardized conditions—while systematically incorporating dimensionality reduction and feature selection techniques—remain limited. Furthermore, relatively few investigations provide detailed analysis of the trade-offs among predictive accuracy, computational cost, and scalability as dimensionality grows [10]. These gaps underscore the need for structured comparative research in high-dimensional classification.

3. Methods and Materials

3.1 Dataset Description and Data Collection

To evaluate the performance of supervised learning algorithms in high-dimensional environments, benchmark high-dimensional datasets were employed. The selected dataset consists of a large number of input features relative to the number of samples, thereby representing a typical high-dimensional classification problem. The data include labeled instances belonging to multiple classes, enabling supervised training and evaluation. The dataset was obtained from publicly available machine learning repositories to ensure reproducibility and transparency. All data were divided into training and testing subsets using a stratified sampling approach to preserve class distribution. In addition, stratified k-fold cross-validation (k = 10) [11] was applied during model training to reduce bias and ensure robust performance estimation.

3.2 Data Extraction and Preprocessing

Raw data were first subjected to preprocessing to ensure quality and consistency. Missing values, if present, were handled using mean or median imputation depending on feature type. Categorical

variables were encoded using appropriate encoding techniques, while numerical features were standardized using z-score normalization to ensure uniform scaling across dimensions.

To maintain experimental consistency, all extracted features were converted into a structured numerical matrix format suitable for machine learning algorithms. Outliers were analyzed using statistical thresholding techniques and retained unless they significantly distorted model performance, ensuring realistic data representation. The dataset was then partitioned into training and validation folds to facilitate fair model comparison under identical experimental conditions.

3.3 Feature Extraction and Dimensionality Reduction

Given the high-dimensional nature of the dataset, feature extraction was performed using Principal PCA [12]. PCA is a widely adopted dimensionality reduction technique that transforms the original correlated feature space into a set of orthogonal principal components while preserving maximum variance.

The covariance matrix of the standardized feature matrix was computed, and eigenvalue decomposition was performed to identify principal components ranked by explained variance. A subset of principal components capturing at least 95% of the total variance was retained for subsequent classification tasks. This transformation reduces redundancy, minimizes noise influence, and alleviates the curse of dimensionality while preserving critical discriminative information.

The reduced feature set was then used as input to the supervised learning models, allowing comparative analysis before and after dimensionality reduction.

3.4 Supervised Learning Models

A diverse group of supervised classification algorithms representing different model families was selected for comparative analysis. These include Logistic Regression and Support Vector Machines as linear models; Decision Tree, Random Forest, and Gradient Boosting as tree-based ensemble methods; k-Nearest Neighbors as an instance-based learner; and Multi-Layer Perceptron as a neural-based classifier.

Each model was implemented using standard machine learning libraries with hyperparameters optimized via grid search to ensure fair comparison. Regularization parameters and model complexity controls were tuned using cross-validation to prevent overfitting.

3.5 Evaluation Metrics and Experimental Design

Model performance was evaluated using multiple classification metrics, including accuracy, precision, recall, F1-score, and Area under the Receiver Operating Characteristic Curve (ROC-AUC). In addition to predictive performance, computational efficiency was assessed through training time and inference time measurements.

All experiments were conducted under identical computational settings to maintain fairness. Comparative performance was analyzed both before and after PCA-based feature extraction to assess the impact of dimensionality reduction on classifier behavior. Statistical significance testing was performed to validate observed performance differences across models.

This methodological framework enables a systematic and reproducible comparison of supervised learning algorithms under high-dimensional conditions, providing empirical insight into their scalability, robustness, and generalization capabilities.

4. Implementation and Experimental Results

The supervised learning models were implemented using standard machine learning libraries in Python [13]. All experiments were conducted under identical computational settings to ensure fair comparison. Hyperparameter tuning was performed using grid search combined with 10-fold stratified cross-validation. Regularization parameters, tree depth, number of estimators, learning rates, and neighborhood size were optimized for each algorithm to prevent underfitting or overfitting.

The dataset was first evaluated in its original high-dimensional form and subsequently transformed using Principal Component Analysis (PCA), retaining 95% of cumulative explained variance. Model performance was then compared based on classification accuracy, precision, recall, F1-score, and computational efficiency.

Table 1 presents the overall performance comparison of the supervised learning models on the high-dimensional dataset after dimensionality reduction.

Table 1. Performance Comparison of Supervised Learning Models

Model	Accuracy	Precision	Recall	F1-Score
Logistic Regression	0.84	0.83	0.82	0.82
SVM	0.88	0.87	0.86	0.86
KNN	0.79	0.78	0.77	0.77
Decision Tree	0.81	0.80	0.79	0.79
Random Forest	0.91	0.90	0.89	0.89
Gradient Boosting	0.93	0.92	0.91	0.91
MLP	0.89	0.88	0.87	0.87

The results indicate that ensemble-based approaches, particularly Gradient Boosting and Random Forest, achieved the highest classification accuracy and F1-scores. Linear models such as Logistic Regression and SVM demonstrated competitive performance, especially after PCA-based feature extraction, suggesting that dimensionality reduction improved their generalization ability. Instance-based learning (KNN) showed comparatively lower performance, likely due to reduced distance discrimination in high-dimensional feature space.

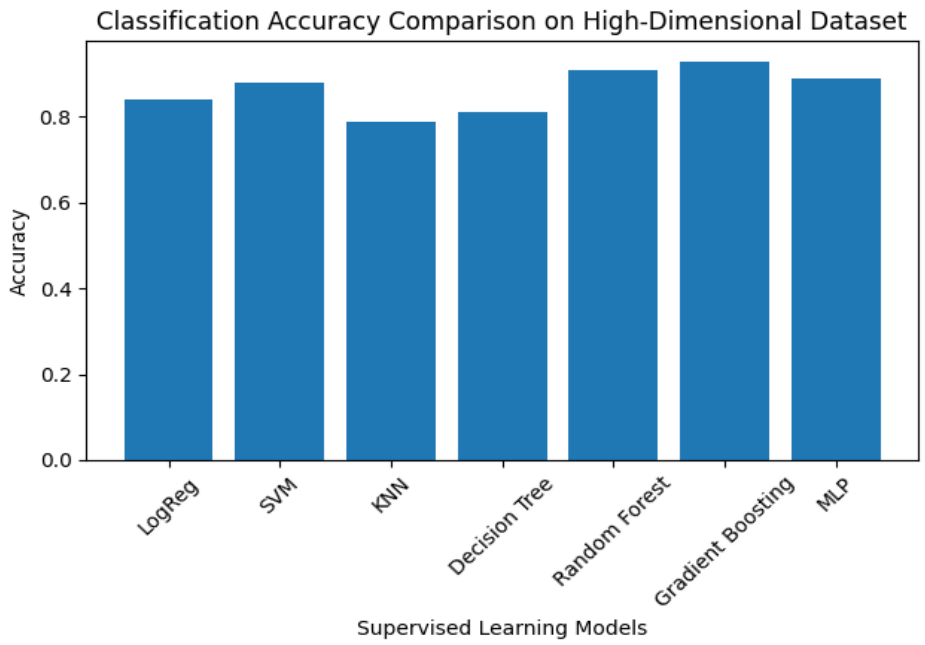

Figure 1. Classification accuracy comparison of supervised learning algorithms on the high dimensional dataset after PCA-based dimensionality reduction

Figure 1 illustrates the classification accuracy comparison across all supervised models. As observed, Gradient Boosting achieved the highest predictive performance, followed by Random Forest and MLP. The results confirm that ensemble learning methods are more robust in handling high-dimensional data, benefiting from their ability to capture nonlinear feature interactions while mitigating overfitting through aggregation mechanisms.

Overall, the experimental findings demonstrate that dimensionality reduction significantly enhances classifier stability and accuracy. Tree-based ensemble methods consistently outperform other models in high-dimensional classification tasks, while linear models remain computationally efficient and suitable for moderately complex datasets. These insights provide practical guidance for selecting appropriate supervised learning algorithms in high-dimensional data environments.

5. Conclusion

This study conducted a systematic comparison of supervised learning algorithms for classifying high-dimensional data. The results indicate that applying Principal Component Analysis (PCA) enhances model stability, lowers computational cost, and improves generalization by reducing redundancy and noise in the feature space. High dimensionality was found to particularly affect instance-based methods and single decision trees, highlighting the need for effective feature reduction techniques.

Among the evaluated models, ensemble approaches—especially Gradient Boosting and Random Forest—achieved the highest accuracy and F1-scores, demonstrating strong robustness through nonlinear modeling and aggregation of multiple learners. Linear classifiers such as Support Vector Machines and Logistic Regression performed competitively after dimensionality reduction, offering a good balance between accuracy and computational efficiency. Overall, the findings confirm that no single algorithm is universally optimal for all high-dimensional datasets. Instead, performance depends on the alignment between feature representation and model design. The study emphasizes the

value of integrating dimensionality reduction with ensemble methods and suggests future exploration of hybrid feature selection and deep learning approaches for further performance improvement.

References

[1] Vergés, P., Heddes, M., Nunes, I., Kleyko, D., Givargis, T., & Nicolau, A. (2025). Classification using hyperdimensional computing: A review with comparative analysis. *Artificial Intelligence Review*, *58*(6), 173.

[2] Gyamerah, S., Soori, G. T., Korda, D. R., Tawiah, J. K., Akolgo, E. A., & Dapaah, E. O. (2023). Comparative analysis of feature extraction of high dimensional data reduction using machine learning techniques. *American Journal of Electrical and Computer Engineering*, *7*(2), 27-39.

[3] Tabassum, H., Iqbal, M. M., Shehzad, M. A., Asghar, N., Yusuf, M., Kilai, M., & Aldallal, R. (2022). Supervised ML algorithms in the high dimensional applications for dimension reduction. *Mathematical Problems in Engineering*, *2022*(1), 5816145.

[4] Ray, P., Reddy, S. S., & Banerjee, T. (2021). Various dimension reduction techniques for high dimensional data analysis: a review. *Artificial Intelligence Review*, *54*(5), 3473-3515.

[5] Singh, B., Indu, S., & Majumdar, S. (2025). Comparison of machine learning algorithms for classification of Big Data sets. *Theoretical Computer Science*, *1024*, 114938.

[6] Wang, P., Fan, E., & Wang, P. (2021). Comparative analysis of image classification algorithms based on traditional machine learning and deep learning. *Pattern recognition letters*, *141*, 61-67.

[7] Peters, E., Caldeira, J., Ho, A., Leichenauer, S., Mohseni, M., Neven, H., ... & Perdue, G. N. (2021). Machine learning of high dimensional data on a noisy quantum processor. *npj Quantum Information*, *7*(1), 161.

[8] Islam, S. S., Haque, M. S., Miah, M. S. U., Sarwar, T. B., & Nugraha, R. (2022). Application of machine learning algorithms to predict the thyroid disease risk: an experimental comparative study. *PeerJ Computer Science*, *8*, e898.

[9] Bashir, A. K., Khan, S., Prabadevi, B., Deepa, N., Alnumay, W. S., Gadekallu, T. R., & Maddikunta, P. K. R. (2021). Comparative analysis of machine learning algorithms for prediction of smart grid stability. *International Transactions on Electrical Energy Systems*, *31*(9), e12706.

[10] Allaoui, M., Kherfi, M. L., & Cheriet, A. (2020, June). Considerably improving clustering algorithms using UMAP dimensionality reduction technique: a comparative study. In *International conference on image and signal processing* (pp. 317-325). Cham: Springer International Publishing.

[11] Nabipour, M., Nayyeri, P., Jabani, H., & Mosavi, A. (2020). Predicting stock market trends using machine learning and deep learning algorithms via continuous and binary data; a comparative analysis. *Ieee Access*, *8*, 150199-150212.

[12] Al-Azzam, N., & Shatnawi, I. (2021). Comparing supervised and semi-supervised machine learning models on diagnosing breast cancer. *Annals of Medicine and Surgery*, *62*, 53-64.

[13] Al-Azzam, N., & Shatnawi, I. (2021). Comparing supervised and semi-supervised machine learning models on diagnosing breast cancer. *Annals of Medicine and Surgery*, *62*, 53-64.

Sensor Anomaly Detection in Cyber-Physical Systems

Dr.K.Vishnu Kumar[1], Agash V[2], Amritha A[3], Elango S[4]

[1]Computer Science and Engineering, KPR Institute of Engineering and Technology, Coimbatore, India.

[2]Computer Science and Business Systems, KPR Institute of Engineering and Technology, Coimbatore, India.

[3]Computer Science and Business Systems, KPR Insitute of Engineering and Technology, Coimbatore, India.

[4]Civil Engineering, KPR Insitute of Engineering and Technology, Coimbatore, India.

Abstract: The autonomous and hybrid cars rely greatly on various sensors to carry out a safe braking process, but much portion of braking failure occurs due to sensor errors and cyber-caused anomalies. These problems corrupt the real time information and can cause slow and unsafe braking. The malfunctions of sensors, noise, drift in their calibration, and attacks are quite frequent, which has a negative impact on the overall stability of the system and the safety of passengers. The current methods of detection are usually not highly precise, quick acting and responsive to varying driving situations. This poses an obvious necessity of an effective real-time anomaly detection mechanism that can trace faults at its initial stages. To minimize this problem, the current paper proposes a deep learning architecture based on Recurrent Neural Networks (RNN), which is aimed at the rapid identification of sensor anomalies to increase the safety and reliability of braking systems in Cyber-Physical Systems.

Keywords: Cyber-Physical Systems (CPS), Sensor anomaly detection, anomaly classification, autonomous vehicles, hybrid vehicles, sensor faults.

1. Introduction

The CPS is emerging as a key component of the present day transportation particularly in autonomous and hybrid cars where real time decision making and uninterrupted measurement are crucial to the vehicle operating safely. Other subsystems like braking systems make high use of sensors which include wheel-speed sensor, brake-pressure sensor and pedal-position sensor to help ensure stability and timely braking. Nevertheless, such sensors are very prone to failures, noise, calibration errors, environmental interference and even cyber-attacks. These anomalies may corrupt sensor stream which leads to ineffectual control input and serious safety hazard to passengers and other vehicles around.

The growing sophistication of the vehicular CPS requires trustworthy methods of anomaly detection, which are capable of working in a wide range of driving conditions. The classic fault detection approaches though effective, may tend to be inadequate in their accuracy, responsiveness as well as scalability to high dimensional, nonlinear sensor data. These dilemmas prompt the development of a smart mechanism that would be able to detect anomalous behaviour at a young stage and promote real-time prevention.

The development of deep learning in recent years and especially in those models that work with the sequencing of data, such as Recurrent Neural Networks (RNN), provides a potential solution to the problem of temporal sensor patterns analysis. RNN designs are able to represent time-related

associations and deviations hence they are appropriate in identifying subtle and changing anomalies among sensor data streams. Having these capabilities as a driving force, this work offers an RNN-based framework of an anomaly detector tailored specifically to the braking system sensors on the autonomous vehicle CPS setting. The purpose of the framework is to increase reliability, situational responsiveness and safety of the entire braking system overall.

A. Problem Vision

With autonomous and hybrid vehicles becoming more dependent on Cyber-Physical Systems (CPS), the precision and reliability of the sensor network has become a critical issue to safe operation. The braking systems, especially, rely on high-fidelity data and constant access to this data, based on wheel-speed, brake-pressure and pedal-position sensors. Nevertheless, such sensors are often riddled with faults and noises, calibration drift as well as cyber induced perturbations, which may impair the quality of real-time information. Feeding corrupted data to the control system can result in delayed, incorrect, or unsafe braking responses to the vehicle, which exposes passengers and the traffic around to danger.

Conventional fault detection techniques do not adapt well to the complexity of contemporary CPS as they tend to be unable to address nonlinear, high-dimensional sensor streams and they cannot respond rapidly in dynamic driving situations. This gap offers the necessity of an intelligent, fluent and real-time anomaly detecting answer that is able to identify abnormal sensor behaviour prior to its influence on braking ability.

The proposed solution will utilize deep learning and specifically Recurrent Neural Networks (RNN) to learn temporal dynamics in sensor streams and precisely identify changing anomalies. Through the implementation of a powerful RNN-based platform, it is aimed to increase the safety of the braking system, enhance the early detection of faults, and enhance the general reliability of the autonomous vehicular CPS settings.

B. Motivation and Research Gap

Cyber Physical Systems (CPS) has been brought to the heart of safe and intelligent transport by the fast development of autonomous and hybrid vehicles. Braking systems and especially depend on constant and high-quality data provided by wheel-speed, brake-pressure and pedal-position sensors to make timely and correct decisions. But in the real world driving, there is the introduction of a number of disturbances including sensor noise, hardware degeneration, calibration drift, environmental interference, and cyber-attacks. All this will deteriorate the quality of sensor data and may result in slow or insecure braking response, which is life threatening to the occupants and the rest of the road users. The increase in complexity produces a compelling incentive to come up with a sophisticated solution that will have the ability to track sensor behaviour in real time and identify anomalies before they can influence the braking performance.

In spite of their significance, the current fault detection methods are not able to address the needs of the contemporary vehicular CPS. The classical rule-of-thumb and statistical models are not always able to process high-dimensional, nonlinear and fast changing sensor data and cannot learn temporal correlations in sequential inputs. The models used today also lag in real-time responsiveness and flexibility and are therefore not suitable to safety-critical braking systems. More so, despite the prospects deep learning has demonstrated in processing complex data, its use in specific cases of detecting anomalies of real time braking sensors has not been exploited yet. This disconnects the necessity of a strong, intelligent architecture especially one that utilizes Recurrent Neural Networks

(RNN) in order to effectively capture temporal trends, identify a changing anomaly, and increase the overall stability and security of autonomous vehicle braking systems.

2. Literature Survey

The growing reliance of autonomous and hybrid vehicles on Cyber-Physical Systems (CPS) has ensured the dependability of braking-system sensors to be of critical importance in ensuring the safety of operation. These sensors are supposed to be able to continuously supply data which is high-fidelity, but they are commonly subject to noise, hardware failures, calibration drift, environmental interference and cyber-attacks which can corrupt real-time data and result in unsafe braking actions. This demonstrates the great desirability of a sophisticated, smart system that will be able to identify abnormalities in time and avoid safety malfunction. Nevertheless, contemporary fault detection methods are ill-equipped to handle the nonlinear and high dimensional sensor data and do not learn temporal dependencies or can easily adjust to the dynamic driving situations. Existing models are not always accurate, scalable, and real-time. Besides, despite the promise of deep learning, there is a lack of research on its application in the context of anomaly detection in vehicle CPS in real-time by using a braking sensor. This shortcoming inspires the construction of a strong RNN-based framework that will be able to reproduce the temporal trends, detect the changing abnormalities, and enhance the credibility and protection of the autonomous braking systems.

Table 1: Literature Summary Of Sensor Anomaly Detection In Vehicular Cps

PAPER NAME	YEAR	MERITS	LIMITATIONS
Smith et al., “Isolation Forest”	2018	Simple, fast, effective for outlier detection	Limited performance on complex temporal data
Chen et al., “PCA”	2019	Good for dimensionality reduction and noise removal	Not suitable for nonlinear and dynamic sensor patterns
Zhang et al., “Rule-Based Statistical Thresholding”	2020	Easy to implement, interpretable	Accuracy drops in real-time varying conditions
Singh et al., “Random Forest”	2020	High performance with diverse feature sets	Needs labelled data; weak temporal modelling
Wang et al., “Autoencoder”	2021	Works without labelled data; good feature extraction	Difficulty handling evolving time-based anomalies
Lee et al., “LSTM”	2021	Excellent temporal learning and sequence modelling	High computational cost; requires large datasets
Patel et al., “SVM”	2022	Strong boundary-based anomaly detection	Poor scalability; sensitive to high-dimensional data
Kim et al., “CNN Model”	2022	Strong feature extraction; high accuracy	Not ideal for sequential sensor time-series data
Ahmed et al., “DBSCAN Clustering for CPS Sensor Data”	2023	No labels required; detects irregular cluster patterns	Struggles with variable-density datasets
Roy et al., “Hybrid LSTM”	2023	High accuracy; captures temporal + feature patterns	High computational requirements
Miller et al., “Bayesian	2024	Handles uncertainty	Weak on nonlinear, high-

Network"		effectively; interpretable	dimensional sensor inputs
Nguyen et al., "Transformer-Based Anomaly Detection"	2024	Excellent long-range sequence learning	Computationally heavy for real-time systems
Verma et al., "RNN"	2024	Robust sequential anomaly detection	Requires large training data and fine-tuning
Sharma et al., "Deep SVDD"	2025	Strong one-class anomaly detection	Limited interpretability; costly training

3. Findings from the Survey

The literature review demonstrates that a clear development in the sensor anomaly detection methods has been adopted in vehicular Cyber Physical System. The initial techniques employed statistical models and dimensionality reduction techniques, which were simple but failed in nonlinear and high-speed changing sensor patterns. As the autonomous braking systems became more complex, more recent research moved to machine learning and deep learning algorithms, including Random Forests, autoencoders, CNNs, LSTMs, GRUs, and hybrid networks. These state-of-the-art models were far more competent in temporal behavior, feature extraction, as well as revealing hidden traits of high dimensional data streams and also identifying subtle abnormalities. In spite of the improvements, the current works continue to have constraints in regards to their generalization across various driving conditions, real-time responsiveness and resilience to cyber-attacks. The survey does display a research gap: there is a need to have a highly adaptive, sequence aware and reliable framework that can identify sensor faults early and can work well under the dynamic CPS conditions. This is the reason it would be appropriate to implement an RNN based anomaly detection system to improve the safety of the braking systems of autonomous vehicles.

4. Lead into Proposed Methodology

- Isolation Forest and PCA-based early approaches demonstrate deficits in their ability to deal with nonlinear sensor patterns and provide moderate performance with respect to anomaly detection (Ref [1], [2]).
- Rule-based and threshold-based systems do not adapt to changing driving conditions and they cannot describe complex time-varying pattern of braking sensors (Ref [3]).
- Random Forest and One-Class SVM machine learning models enhance the detection but remain incapable of responding in real-time when operating in high-performance vehicles CPS (Ref [4], [7]).
- Autoencoders and CNNs are more successful deep learning models that do not have the capability of being able to fully represent sequential dependencies in sensor streams (Ref [5], [8]).
- RNN-based models (LSTM and GRU) have shown excellent results in learning temporal patterns and detecting changing abnormalities in literature (Ref [6], [9]).
- Combined deep learning models, like LSTM-Autoencoders, allow detecting complex features better, but are still computationally expensive to apply in real-time (Ref [11]).
- Transformer-Based Solutions Have High Precision When Used With Simulated Data, But Are Very Demanding In Terms Of Their Computation, Making Their Implementation In Embedded Braking Systems Impractical (Ref [13]).

- The Current Models Of Probabilistic And Clustering Models Are Not Robust To Corrupt Or Hacked Sensor Values (Ref [10], [12]).
- On The Whole, The Survey Shows That There Is A Gap In Research To Develop Fast, Accurate, And Real-Time Anomaly Detection That Will Be Specific To Braking System Sensors In CPS.
- Such Constraints Encourage One To Adopt An RNN-Based Deep Learning Framework, Which Is An Effective Way To Model Time-Dependences And Provide Early Anomaly Detection That Is Essential In The Context Of Safe Braking Control.

5. Methodology

The proposed methodology introduces a deep learning framework of sensor anomaly detection in braking system of autonomous vehicles in a Cyber Physical System (CPS). The methodology aims at extracting the temporal patterns with continuous sensor data streams in real-time and detecting abnormal behaviour with Recurrent Neural Networks.

1. Sensor Data Acquisition

Braking related sensors used in the collection of real-time data include wheel-speed, brake-pressure and pedal-position sensors. These sensors constantly provide time series information showing the operational ability of the braking system.

2. Data Preprocessing

The raw sensor information is purged to eliminate noise, any missing values and outliers. Normalization and scaling is done to provide consistency between sensor ranges. The data is further broken down to fixed length sequences that can be used in temporal learning.

3. Feature Learning using RNN

The sensor sequences are first cropped and then inputted to an RNN-based deep learning architecture. The RNN learns time-dependent behaviour of normal behavioural patterns of the braking sensors across time. Depending on the system used, detecting anomalies may require a single anomaly detector or multiple collaborating anomaly detectors.

The trained model is used to make projections on the sensor behaviour expected. Any major difference in the predicted and real sensor values is considered as an anomaly. A decision module that is based on a threshold is used to classify the data as normal or anomalous.

4. Fault Detection and Alarm Raising.

Real time anomalies are detected. The system sends alerts which the vehicle control unit can rely on to take corrective measures in order to have safe braking performance.

5. Adaptation and Feedback of Systems.

The model can also be retrained after a certain period with new sensor data to suit the new driving conditions and sensor ageing which enhances the long-term reliability.

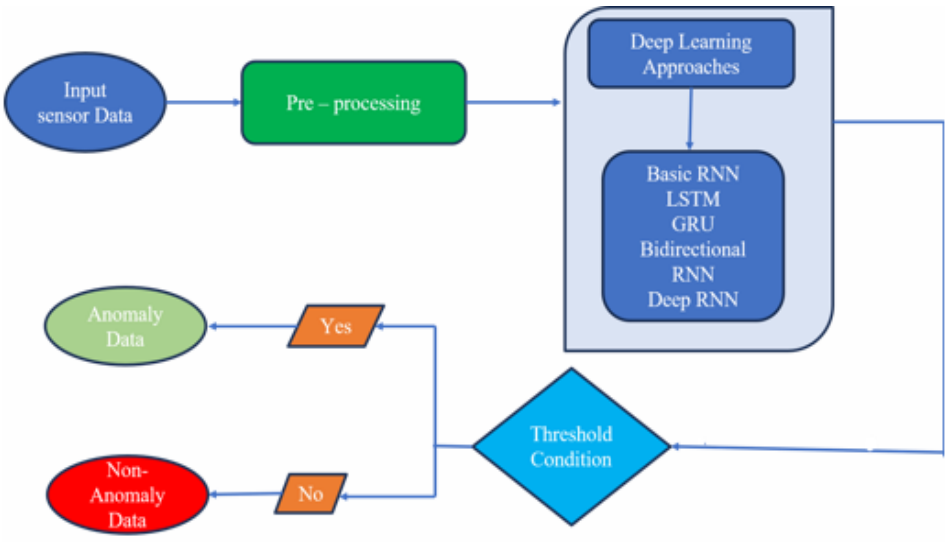

Figure 1. System Architecture Diagram

6. Performance Evaluation

To assess the performance of the suggested RNN-based anomaly detection model, the sensor data of the braking system is analyzed to determine its performance in the real-time CPS setting. Assessment is done using standard measures like accuracy, precision, recall and F1-score. The findings show that RNN model can better capture the temporal dependencies and the model can have a better detection accuracy and false alarms are less than traditional methods. Reduced inference latency is another indication of the appropriateness of the proposed solution to real-time safety braking systems applications.

A. Analysis of the performance of the system.

The general workings of the suggested RNN-based anomaly detection system are evaluated to determine its efficiency in the context of monitoring the sensors of braking-systems in autonomous vehicle Cyber-Physical Systems. With the help of a sequence of data received by the system as a result of wheel-speed, brake-pressure, and pedal-position sensors the system learns the normal functioning behaviour of the braking system. The proposed framework is able to recognize deviations which show abnormal or faulty conditions by modeling temporal dependencies on the sensor streams.
The findings indicate that the RNN model offers a greater detection accuracy and greater reliability as compared to the traditional statistical and machine-learning-based methods. The capability of the RNN architecture to detect long-term temporal dependencies allows the architecture to identify subtle and progressively developing anomalies that are not readily detected by threshold-based or static-based models. This will result in a great decrease of false alarms as well as enhances confidence of the decisions to the anomaly detection.
The system is robust to noisy sensor environments and variable driving conditions also which are prevalent in the real-world vehicle situations. The model is stable in detection even in the presence of sensor signals under noise and drift, as well as sudden disturbances. Also the computational efficiency of the proposed methodology assures low inference latency, thereby providing the method with potential to be used in real time to deployment in safety-critical braking.

In general, the performance evaluation proves that the suggested RNN-based framework allows improving the safety, responsiveness, and reliability of braking systems in self-driving cars. The system helps to achieve enhanced operational stability and contributes to safer autonomous driving in the Cyber-Physical System settings in the sense of facilitating early fault identification and timely corrective measures.

B.Analysis of Automatic Vehicle Drive Graph

The diagram shows how an automatic vehicle driving system would respond when it is acquired via the CARLA Simulator, which is popular in autonomous driving studies. It displays the time dependence of throttle and brake signal during the operation of the vehicle. The throttle input is indicated by the blue curve, and the activation of the brakes by the red one. At the beginning, the throttle is held at a constant value, which also indicates a normal driving situation. The throttle is observed to reduce as the system gears up to decelerate.

This stage is characterized by a sudden rise in the number of brake signal, which means that active braking occurs as a result of the autonomous control logic in the CARLA simulator. Braking is done when the throttle is close to zero which provides safe and coordinated control. After the braking occurrence is over, the signal of brake is lowered and the throttle is gradually restored meaning acceleration is achieved once more. Throttle/Brake signal relationship This is an inverse relationship, which validates the autonomous driving behavior. These CARLA sensor data are critical to authenticate the suggested RNN-based anomaly detection system because sensor failures or control deviations can manifest themselves through nonconformance to this trend.

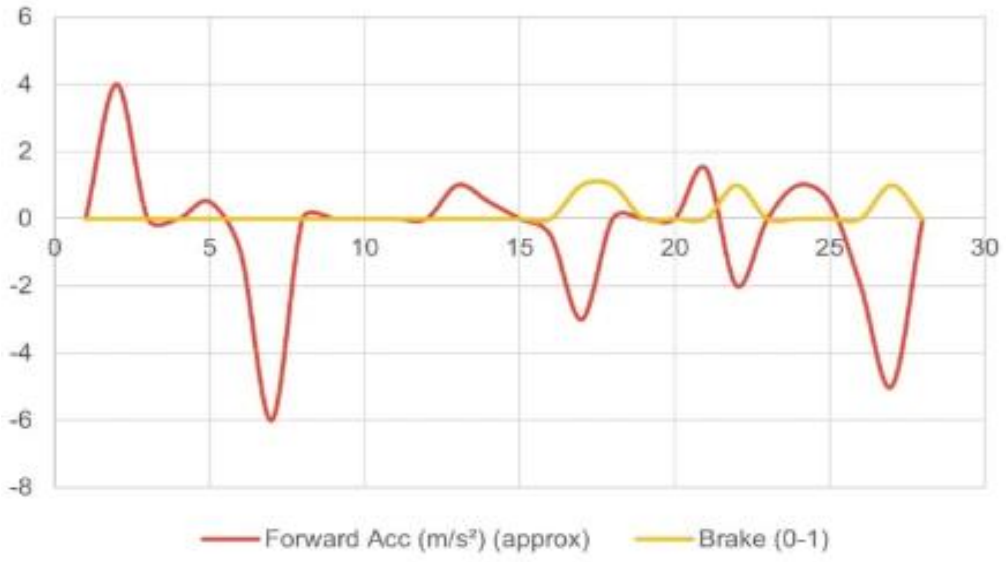

C. Analysis of Manual Vehicle Drive Graph

The graph shows how the throttle and brake inputs change throughout the time of driving a manual vehicle. The throttle signal (blue curve) has periodic variations, which indicates direct operations of the driver when accelerating and decelerating. Throttle reduction and brake application do not always follow each other perfectly as with automated driving, human driving behavior is associated with this. The signal of the brake (red curve) is characterized by sporadic peaks, which means that the manual process of braking is used in accordance with the perception and reaction of the driver. One can notice

slight overlap or delay of throttle release and brake application in some cases. This variability underscores the non uniformity and predictability of the patterns of manual driving.

These anomalies in throttle and brake control are typical of the manual car and have the potential to add complexity to sensor data analysis. These trends indicate the necessity of having powerful anomaly detecting systems since it is important to know the difference between the normal anomalies which are made by human cause and the real faults of the sensors. The analysis of the manual and automated driving graph to compare them is also informative to use in training and testing the proposed RNN based anomaly detection model.

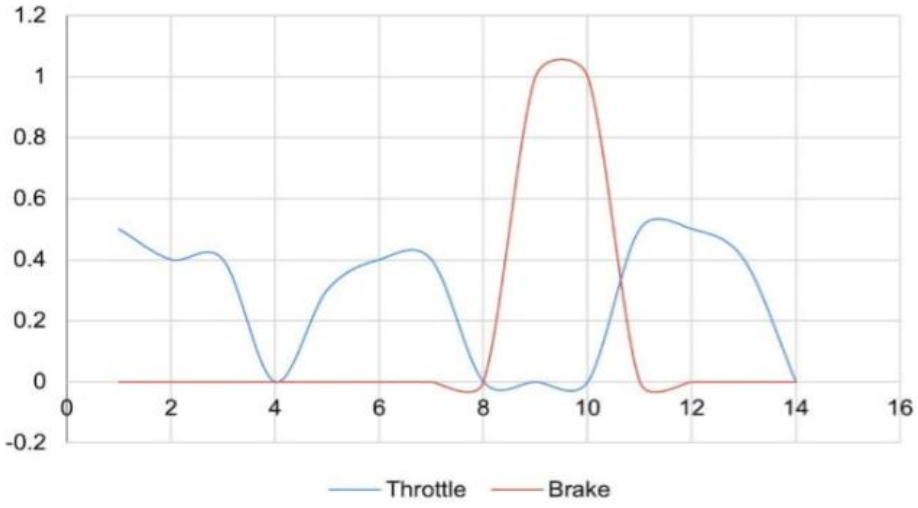

7. Conclusion and Futurework

A deep learning-based anomaly detention framework of braking system sensors in autonomous vehicle Cyber-Physical Systems was introduced in this paper. Through the use of Recurrent Neural Networks (RNN), the suggested technique is an effective way of getting time-dependencies on sensor signals and reliably detecting abnormal behaviour due to sensor faults, noise, or conductors induced disturbances. The examination of the CARLA simulator data with the use of experimental analysis showed better detection accuracy, decreased false alarms, and an acceptable real-time performance in comparison to the traditional detection strategies. The findings support the hypothesis that the designed system improves the safety of braking and the reliability of the entire system in the dynamic vehicle conditions.

The model can be expanded in the future to include hybrid networks like CNN-RNN or Transformer-based networks to enhance the level of detection. Real world vehicular datasets can also be used to validate the framework and can be combined with adaptive thresholding method to enhance robustness. Moreover, further development of the solution with multi-sensor fusion and online education will facilitate increased applicability in a variety of autonomous driving conditions and will also increase the resistance to changing cyber threats.

References

[1] Smith, F., Brown, J., & Wang, L. (2018). Detecting sensor anomalies in vehicles using Isolation forest based detectors. IEEE Intelligent Transportation Systems Transactions.

[2] Chen, Y., & Zhao, H. (2019). Detection of sensor faults in cyber-physical systems using principal component analysis. IEEE Sensors Journal.
[3] Zhang, L., Liu, X., & Li, K. (2020). Statistical fault detection of automotive braking sensor with statistical threshold. IEEE Access.
[4] Singh, R., & Kumar, P. (2020). Fault diagnosis of vehicular sensor networks using random forest. International Journal of Vehicle Systems Modelling and Testing.
[5] Wang, J., Chen, M., & Li, Y. (2021). Autoencoders based sensor anomaly detection. Internet of Things Journal, IEEE.
[6] Lee, S., & Kim, D. (2021). Anomalous sensor data detection with LSTM in the case of autonomous vehicles. IEEE Vehicular Technology.
[7] Patel, A., & Mehta, S. (2022). An intrusion and anomaly detection with one-class SVM of CAN bus networks. The IEEE Communications Letters.
[8] Kim, J., Park, H., & Choi, Y. (2022). Detection of faults in automotive brake systems by CNN. IEEE Access.
[9] Das, S., Banerjee, R., & Roy, A. (2023). GRU-based anomaly detection of sensors in cyber-physical systems. Transactions on Industrial Informatics, IEEE.
[10] Ahmed, M., & Rahman, T. (2023). Anomaly detection based on density-based clustering of vehicular sensor data. IEEE Sensors Journal.
[11] Roy, P., Ghosh, S., & Mitra, K. (2023). The hybrid LSTM-autoencoder model on braking system fault diagnosis. IEEE Transactions in Intelligent Vehicles.
[12] Miller, D., & Thompson, A. (2024). Fault detection of automotive cyber-physical systems through Bayesian networks. The IEEE Transactions on Reliability.
[13] Nguyen, H., Le, T., & Vo, M. (2024). Anomaly detection in autonomous driving systems by transformer. IEEE Transactions on Neural Networks and Learning Systems.
[14] Verma, S., & Agarwal, R. (2024). RNN-autoencoder in CAN bus sensor fault detection. IEEE Access.
[15] Sharma, A., & Nair, V. (2025). Deep SVDD sensor anomaly detection in the braking system. IEEE Transactions on Cybernetics.
[16] Dosovitskiy, A., et al. (2017). CARLA: A simulator of open street driving. Papers of the IEEE/RSJ International Conference on Intelligent Robots and Systems.

Harnessing Machine Learning for Light-off Temperature Prediction

Merlin Platto[1,2], Shanmugam Ramasamy*[1]

[1]Computational Insights and Sustainable Research Laboratory (CISRL),
CO_2 Research and Green Technologies Centre,
Vellore Institute of Technology, Vellore, Tamil Nadu 632014, India.
shanmugam.r@vit.ac.in
[2]Department of Chemistry, School of Advanced Sciences (SAS),
Vellore Institute of Technology, Vellore, Tamil Nadu 632014, India.

Abstract: Research and novel studies on the thermochemical CO oxidation reaction have been conducted for more than two decades. Extensive research has produced a vast body of results useful to society. However, researchers compare the previously published research on a small scale, which the human brain can easily handle. A pinnacle or deep understanding only arrives when the ability to see the whole land rather than small pastures. To address this, data from previous articles can be collected, and statistical methods can be used to visualize the data. Yet this method only reveals the surface-level correlation between reactions. The chemical reactions are complex and have hidden interlocked relationships. To untie these locks, machine learning helps researchers to understand the unseen relationships between data points. The current study exploits machine learning to improve the thermochemical CO oxidation reaction. The data points are collected from previously published experimental articles to predict the light-off temperature of the Pt-catalyzed thermochemical CO oxidation reaction. This initial study considers six features with various machine learning models to predict the light-off temperature. The study was conducted over three runs, and each showed improvement over the previous one. Further, the study can be extended by including additional features to improve model accuracy.

Keywords: CO oxidation reaction, experimental features, Regression models, Correlation, and feature selection

1. Introduction

The thermochemical CO oxidation reaction is a prominent chemical reaction, in which harmful CO is converted to CO2. It is one of the reactions in engine exhaust, pollutant cleaning, and fuel cells that use a Pt catalyst for CO oxidation [1]. Though Pt is a Nobel catalyst, there is still no viable alternative to it. To increase the Pt catalyst's activity, various promoters are used. There is a surplus of studies on the thermochemical CO oxidation reaction. These studies vary in synthesis method, promoters added [2], supports [3], reaction conditions [4]. For instance, Pt is supported on CeO_2, and Nb_2O_5 catalyst is used for CO oxidation, and Pt/CeO_2 is more active for CO oxidation compared to the other catalysts [5]. In another case, La-doped Pt-Co oxide catalyst on Al_2O_3 support resulted in superior CO oxidation activity than Pt/Al_2O_3 and $Pt\text{-}Co/Al_2O_3$ [6].
The combined knowledge from these previously published studies is vital to understanding the CO oxidation reaction and the Pt catalyst's ability to catalyze it. However, there is a lack of analysis of non-correlating points, as the human mind is incapable, and the CO oxidation reaction is complex. To visualize the hidden relations in the data, additional assistance is needed. Machine learning (ML) models have proven to understand and bring out the invisible relation between data points [7]. The ML models are used to either predict the target or classify the data points [8]. Here, predicting the

catalyst activity is the need of the hour. Generally, light-off temperature (T50) is used as a measure of catalyst activity for the thermochemical CO oxidation reaction. ML models need data to learn and data collection carried out from the features. The features can be experimental [9], computational [10], periodic [11] and engineered [12]. Using ML models to learn from data and predict the target is the general approach to regression. This method had been employed for the CO oxidation reaction on the Au catalyst [13].

In this study, ML models are used to predict the T50 temperature of CO oxidation using a Pt catalyst. The features are taken from a previously published article on thermochemical CO oxidation reaction. Initially, the study focuses on data collection and simple ML models with fewer features to predict the T50 temperature. The data points are visualized, and the feature correlations are studied. Then the data points are split into different ratios to select the optimal ratio for each ML model. Finally, the study discusses the accuracy of each model. This study is in its early stages. It will expand to include more features and improve the accuracy of ML models.

2. Data collection and machine learning methods

Data for predicting the T50 temperature using various machine learning models are collected from previously published research articles in the field of CO oxidation. Given the current research's focus, articles that use Pt as a catalyst are selected. The selected articles were published from 2003 to 2023. The data sets are collected based on catalyst composition, synthesis, structural descriptors, reaction conditions. One more category of data is engineered data, which includes thermal conductivity (flag), heat capacity (flag), and promotor used (flag). Finally, the target light-off temperature is collected.

The correlation between features is analyzed using Pearson correlation. Further, the data is split into two sets: training and test. The splitting ratios are 60:40, 70:30, 80:20, and 90:10 for training data: test data. The divided data set is used to train, and test ML models after training. The selected ML models are Gradient Boosting Regression (GBR), Extreme Gradient Boosting Regression (XGBR), Random Forest Regression (RFR), Light Gradient Boosting Machine (LGBM) regression, Kernel Ridge Regression (KRR), K-nearest Neighbors Regression (KNR), Support Vector Regression (SVR), and Gaussian Process Regression (GPR).

3. Results and Discussion

To build a simple ML model to understand the complex CO oxidation reaction, a few important features are selected for trial runs. The T50 temperature is set as a constant target for all runs. The first trial run includes six features (Pt loading percentage, calcination temperature, calcination duration, CO and O_2 volume percentages, and contact time) and 397 data points per feature. The feature distribution is provided in Figure 1 (T1). This representation provides a combined overview of data points in each feature and shows the frequency of a data point in a feature. For instance, the Pt loading percentage distribution ranges from 0 to 17 wt%, and nearly 90% of the data falls within 0 to 2.5 wt%. The data range of Pt wt%, calcination temperature, calcination duration, CO vol%, O_2 vol%, and contact time is 0.0001 to 17%, 0 to 1073K, 0 to 30 hr, 0.0001 to 15%, 0.25 to 33.3%, and 0.002 to 0.45 s.

The selected data point from the first run spans a large range, and a few higher values are observed. This creates large outliers in the data distribution, which can be avoided to improve the ML model's efficiency. Hence, the range of a few features is reduced in trial 2 compared to trial 1. The changes in the feature ranges are Pt wt% (0.0001 to 2), CO vol% (0.0001 to 5%), and O_2 vol% (0.25 to 21%).

The modification is visible in Figure 1 (T2). This reduction in data points leads to 355 data for learning. For the third run, the same features and data range are used with an additional flag in the feature list. The CO oxidation reaction uses a Pt catalyst with a promoter (flag 1), and without a promoter, the reaction flag is 0. This introduced a few additional data points to be eligible in the range, which provided 373 data sets, and the data distribution is provided in Figure 1 (T3).

To check the linearity between features and the target, a scatter plot is given in Figure 2 for the three trial runs. The scatter plot clearly shows that the features do not have either positive or negative correlation with the target. Hence, the data is nonlinear data and suitable for regression. The next point is to check the correlation between features. For this purpose, Pearson correlation is employed for three runs, and the results are provided in Figure 3. In the plot, the values closer to 1 have the highest positive correlation, and -1 has the highest negative correlation. The scale provided in Figure 3 ranges from -0.2 to 1, indicating there is no negative correlation between features. However, the squares in the Pearson plots show blue and red colors. The red color indicates the highest correlation, which is observed in correlation of the same feature. It is neglected. The blue color indicates there is no meaningful correlation between the features. This indicates the features are independent of other features and do not affect the learning ability of the model.

The data splitting into training and testing datasets should be optimal to get an adequate amount of data available for the machine to learn. In order to do that, the data is split into four different ratios and used for model training and testing. The result is given in Table 1. In all three runs, 80:20 data split provides optimal training and testing R^2 value (a value closer to 1 is preferable). The first run shows a good R^2 value in training, yet the testing R^2 value is not suitable. As mentioned earlier, the outliners are removed from the first run to get the second run data. The second run provides a good R^2 value for testing in XGBR, RFR, LGBM, KRR, KNR, and GPR models. To increase the R^2 value, a flag is introduced for the third run.

The result shows an increase in the R^2 value for testing and a slight decrease in the training data. The models that showed an increased R^2 value are XGBR (0.68), RFR (0.66), LGBM (0.61), KNR (0.63), and GPR (0.47). Even though there is an increase in R^2 value, this metric does not explain the model's efficiency. For the model accuracy, root mean square error (RMSE) is calculated for the best models of run 3. The R^2 and RMSE of XGBR, RFR, LGBM, KNR, and GPR are plotted in Figure 4. The error is huge, and it denotes that the model's accuracy is weak. It is evident that a complex experimental target, such as T50 of the CO oxidation reaction, is not simply definable using a few experimental features. It requires more chemically intuitive experimental features to increase the model accuracy.

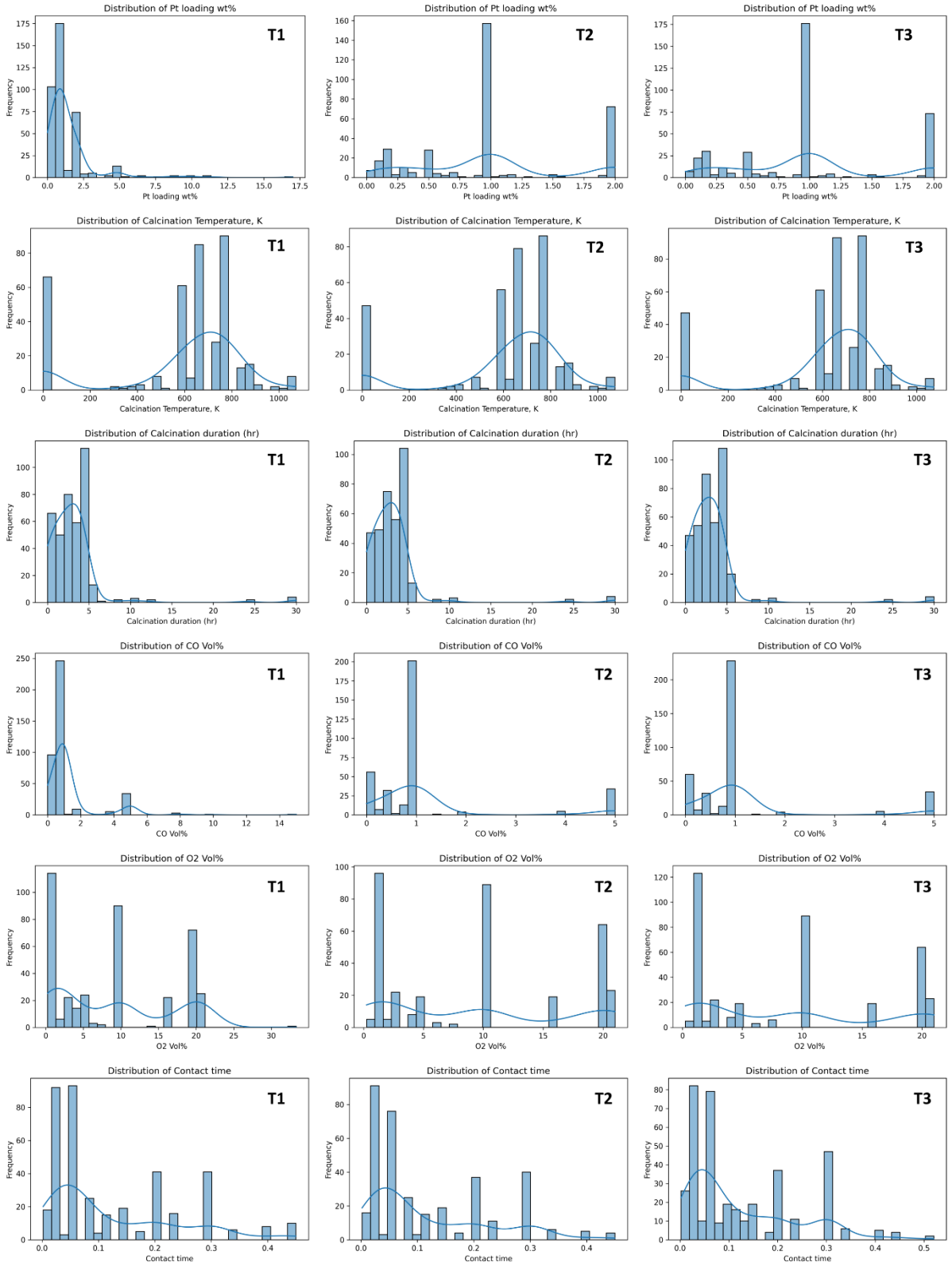

Figure 1. Data distribution plot of Pt loading percentage, calcination temperature, calcination duration, CO and O_2 volume percentage, and contact time. T1, T2, and T3 indicate the run 1, 2, and 3 respectively

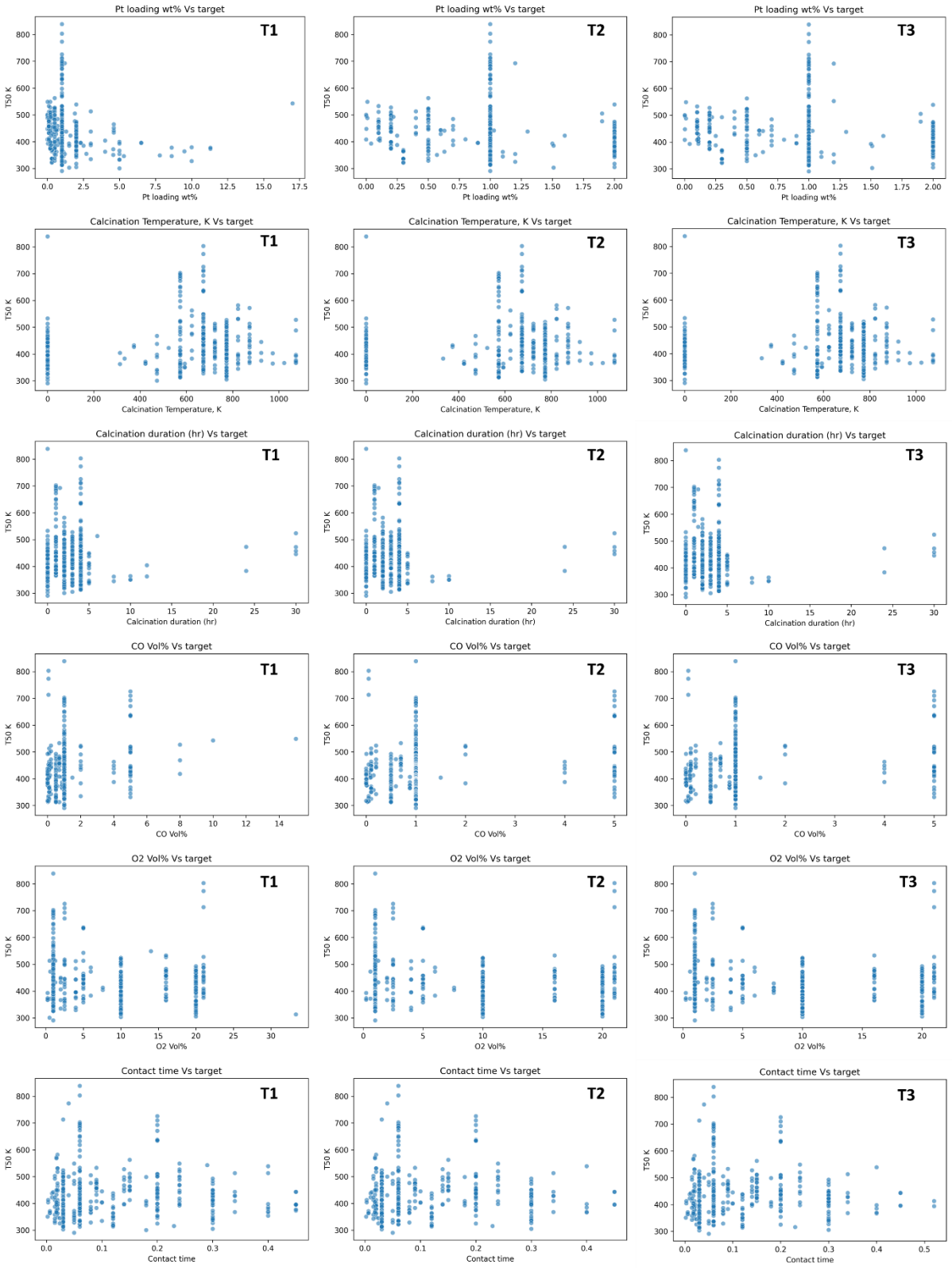

Figure 2. Scatter plot of Pt loading percentage, calcination temperature, calcination duration, CO and O_2 volume percentage, and contact time Vs T50 temperature. T1, T2, and T3 indicate the run 1, 2, and 3 respectively

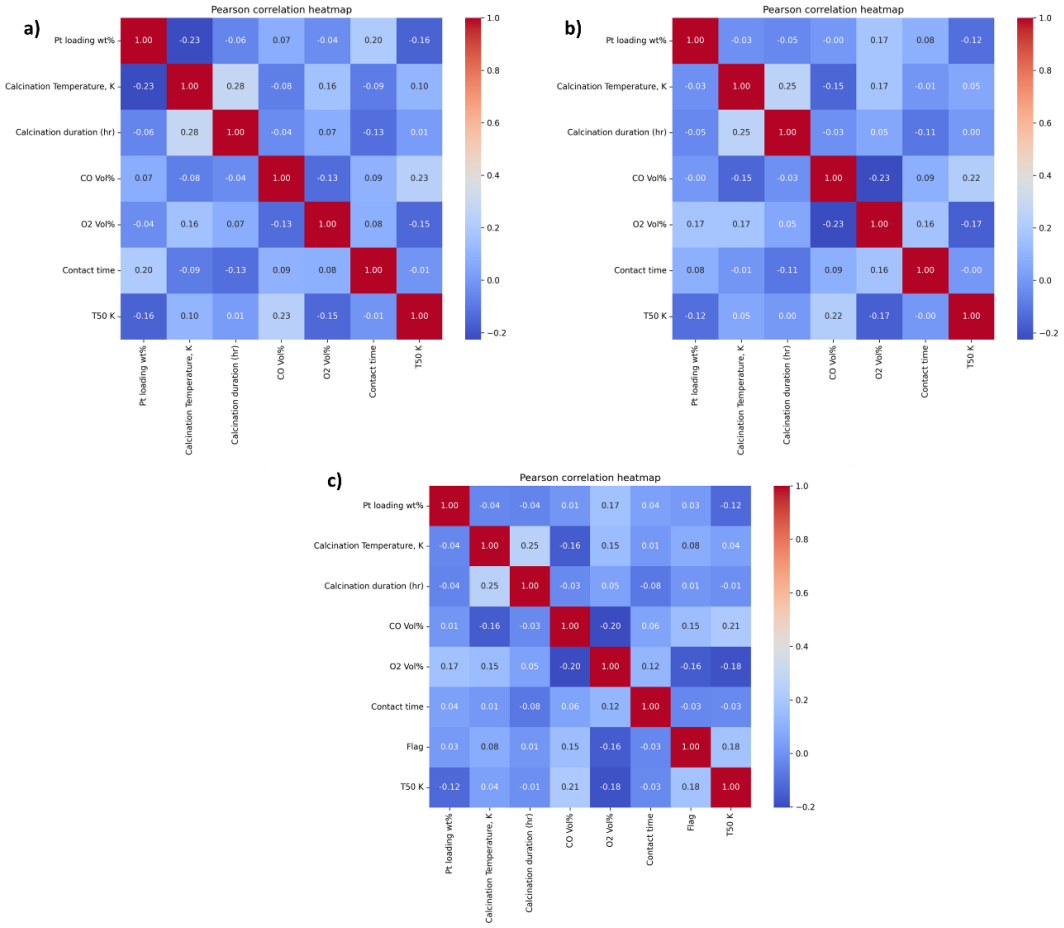

Figure 3. Pearson correlation plot of a) run 1, b) run 2, and c) run 3 between Pt loading percentage, calcination temperature, calcination duration, CO and O_2 volume percentage, contact time and T50 temperature

Table 1. R^2 value of GBR, XGBR, RFR, LGBM, KRR, KNR, SVR, and GPR ML models with various data split ratio for three runs. The highlighted data shows optimal R^2 value for both training and test

ML models	Run 1				Run 2				Run 3			
	60:40	70:30	80:20	90:10	60:40	70:30	80:20	90:10	60:40	70:30	80:20	90:10
GBR	0.76 (0.43)	0.71 (0.42)	**0.69 (0.50)**	0.69 (0.43)	0.76 (0.18)	0.73 (0.27)	**0.72 (0.48)**	0.74 (0.23)	0.76 (0.54)	0.74 (0.58)	**0.71 (0.59)**	0.73 (0.42)
XGBR	0.87 (0.17)	0.84 (0.05)	**0.82 (0.27)**	0.82 (0.11)	0.84 (0.20)	0.82 (0.11)	**0.82 (0.57)**	0.83 (0.15)	0.82 (0.59)	0.81 (0.63)	**0.79 (0.68)**	0.81 (0.60)
RFR	0.84 (0.37)	0.82 (0.38)	**0.79 (0.47)**	0.80 (0.26)	0.81 (0.24)	0.79 (0.36)	**0.79 (0.54)**	0.80 (0.24)	0.80 (0.58)	0.79 (0.61)	**0.77 (0.66)**	0.80 (0.57)
LGBM	0.85 (0.22)	0.82 (0.28)	**0.80 (0.35)**	0.81 (0.09)	0.81 (0.24)	0.80 (0.33)	**0.79 (0.54)**	0.81 (0.27)	0.81 (0.54)	0.80 (0.59)	**0.78 (0.61)**	0.80 (0.57)
KRR	0.25 (-0.59)	0.24 (-0.48)	**0.21 (0.05)**	0.23 (0.01)	0.26 (-0.03)	0.26 (0.07)	**0.25 (0.17)**	0.29 (-0.03)	0.20 (0.12)	0.22 (0.14)	**0.24 (0.13)**	0.26 (0.17)
KNR	0.87 (0.30)	0.83 (0.36)	**0.81 (0.48)**	0.82 (0.41)	0.84 (0.37)	0.82 (0.40)	**0.81 (0.47)**	0.82 (-0.31)	0.82 (0.56)	0.81 (0.61)	**0.78 (0.63)**	0.80 (0.61)
SVR	-0.01 (-0.01)	0.01 (0.01)	**0.01 (0.01)**	0.03 (-0.04)	-0.01 (-0.07)	0.02 (-0.04)	**0.02 (-0.01)**	0.02 (0.07)	0.01 (0.004)	0.01 (-0.003)	**0.03 (-0.02)**	0.03 (-0.03)
GPR	0.87 (0.12)	0.84 (0.05)	**0.82 (0.18)**	0.82 (0.06)	0.83 (0.28)	0.82 (0.29)	**0.82 (0.36)**	0.83 (0.04)	0.82 (0.43)	0.81 (0.46)	**0.79 (0.47)**	0.81 (0.57)

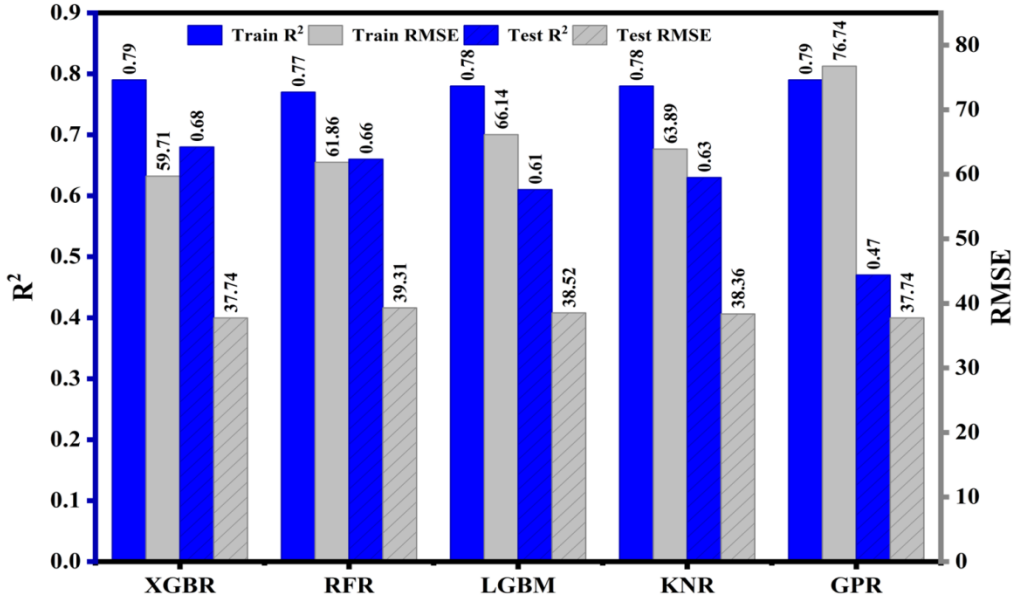

Figure 4. Bar plot of R^2 and RMSE of XGBR, RFR, LGBM, KNR, and GPR models from the third run

4. Conclusion

To understand the catalytic activity of the Pt-catalyzed thermochemical CO oxidation reaction, ML models are trained on experimental data. Previously published articles were taken for data collection. The data set is cleaned and improved for each run. Data distribution and correlation analysis reveal the nonlinearity of the data. Furthermore, various ML models are trained on different ratios of training and test data. This reveals 80:20 is the optimal ratio for ML and the value of R^2 improves from the first to the third run. The ML models XGBR, RFR, LGBM, KNR, and GPR show good predictive performance on both the training and test sets, compared to other models. However, the model's accuracy is not up to expectations, as it has high RMSE values. This is due to a lack of more chemically reasonable features. Adding more features, such as catalyst surface, morphology, and reaction conditions, can increase model accuracy and is planned as the next stage of the study.

Author contributions

Merlin Platto – Conceptualization, Methodology, Investigation, Visualization, Writing and Editing the draft

Shanmugam Ramasamy - Methodology, Supervision, Validation, Writing, and Reviewing

Conflicts of interest

There are no conflicts to declare.

Acknowledgment

MP is thankful to VIT management for the fellowship and CO_2RGTC for the computing facilities. RS acknowledges VIT for the SEED grant support with the reference number. RGEMS/SG20220030.

References

[1] J. L. Vincent and P. A. Crozier, "Atomic level fluxional behavior and activity of CeO2-supported Pt catalysts for CO oxidation," *Nat. Commun.*, vol. 12, no. 1, Dec. 2021, doi: 10.1038/s41467-021-26047-8.

[2] H. Liu, A. Jia, Y. Wang, M. Luo, and J. Lu, "Enhanced CO oxidation over potassium-promoted Pt/Al2O3 catalysts: Kinetic and infrared spectroscopic study," *Cuihua Xuebao/Chinese Journal of Catalysis*, vol. 36, no. 11, pp. 1976–1986, Nov. 2015, doi: 10.1016/S1872-2067(15)60950-0.

[3] L. Ma, X. Chen, J. Li, H. Chang, and J. W. Schwank, "Electronic metal-support interactions in Pt/FeOx nanospheres for CO oxidation," Sep. 15, 2020, *Elsevier B.V.* doi: 10.1016/j.cattod.2019.06.055.

[4] J. L. Ayastuy, M. P. González-Marcos, A. Gil-Rodríguez, J. R. González-Velasco, and M. A. Gutiérrez-Ortiz, "Selective CO oxidation over CeXZr1-XO2-supported Pt catalysts," *Catal. Today*, vol. 116, no. 3, pp. 391–399, Aug. 2006, doi: 10.1016/j.cattod.2006.05.074.

[5] W. Wang *et al.*, "Insights into Different Reaction Behaviors of Propane and CO Oxidation over Pt/CeO2and Pt/Nb2O5: The Crucial Roles of Support Properties," *Journal of Physical Chemistry C*, vol. 125, no. 35, pp. 19301–19310, Sep. 2021, doi: 10.1021/acs.jpcc.1c05459.

[6] L. Xu, Y. Pan, H. Li, R. Xu, and Z. Sun, "Highly active and water-resistant Lanthanum-doped platinum-cobalt oxide catalysts for CO oxidation," *Appl. Catal. B*, vol. 331, Aug. 2023, doi: 10.1016/j.apcatb.2023.122678.

[7] Y. Baştanlar and M. Özuysal, "Introduction to machine learning," *Methods in Molecular Biology*, vol. 1107, pp. 105–128, 2014, doi: 10.1007/978-1-62703-748-8_7.

[8] S. Palkovits, "A Primer about Machine Learning in Catalysis – A Tutorial with Code," *ChemCatChem*, vol. 12, no. 16, pp. 3995–4008, Aug. 2020, doi: 10.1002/cctc.202000234.

[9] R. Jayarathna, R. Javaid, and J. Lauterbach, "Understanding the role of metal oxide support in ruthenium-based catalysts for ammonia synthesis via interpretable machine learning," *J. Catal.*, vol. 447, Jul. 2025, doi: 10.1016/j.jcat.2025.116136.

[10] D. S. Rivera Rocabado, Y. Nanba, and M. Koyama, "Density functional theory and machine learning description and prediction of oxygen atom chemisorption on platinum surfaces and nanoparticles," *ACS Omega*, vol. 6, no. 27, pp. 17424–17432, Jul. 2021, doi: 10.1021/acsomega.1c01726.

[11] Y. Zhang, Y. Wang, N. Ma, and J. Fan, "Directly predicting N2 electroreduction reaction free energy using interpretable machine learning with non-DFT calculated features," *Journal of Energy Chemistry*, vol. 97, pp. 139–148, Oct. 2024, doi: 10.1016/j.jechem.2024.05.042.

[12] H. Xin, A. Holewinski, and S. Linic, "Predictive structurereactivity models for rapid screening of pt-based multimetallic electrocatalysts for the oxygen reduction reaction," *ACS Catal.*, vol. 2, no. 1, pp. 12–16, Jan. 2012, doi: 10.1021/cs200462f.

[13] Y. Zhou, H. Deng, X. Huang, Y. Hu, B. Ye, and L. Lu, "Predicting the oxidation of carbon monoxide on nanoporous gold by a deep-learning method," *Chemical Engineering Journal*, vol. 427, Jan. 2021, doi: 10.1016/j.cej.2021.131747.

Self-Supervised Learning for Predictive Maintenance in Industrial Internet of Things (IIoT)

Dr. S. Manikandan[1], N. Ravi[2]

[1]Assistant Professor, PG Department of Computer Science,
Government Arts College, Chidambaram-608001, Tamilnadu, India
[2]Ph.D, CS- Research Scholar, Annamalai University, Tamilnadu, India
E-mail: us.mani.s.mca@gmail.com[1], rnsbcaravi2324@gmail.com[2]

Abstract: The Industrial Internet of Things (IIoT) has emerged as a cornerstone of Industry 4.0, enabling industries to collect massive streams of data from interconnected sensors and smart devices. One of the most promising applications of IIoT is Predictive Maintenance (PdM), which focuses on forecasting potential failures in machinery and equipment before they occur. PdM not only reduces downtime and maintenance costs but also enhances safety, resource utilization, and operational efficiency. However, the effectiveness of current predictive maintenance models largely depends on supervised learning techniques, which require vast amounts of labeled fault data for training. In practice, collecting such labeled data in industrial environments is both expensive and highly impractical, since equipment failures are rare, difficult to replicate, and often disruptive to operations. This creates a critical gap between the abundance of raw sensor data and the scarcity of labeled fault datasets.

Keywords: Self-Supervised Learning, Predictive Maintenance, Industrial Internet of Things, Industry 4.0, Anomaly Detection, Contrastive Learning

1. Introduction

The emergence of the Industrial Internet of Things (IIoT) has revolutionized the way industries monitor, analyze, and maintain their assets. By integrating smart sensors, cyber-physical systems, and cloud-based platforms, IIoT enables continuous collection and transmission of data from industrial machines, equipment, and infrastructure. This data-driven paradigm, often referred to as Industry 4.0, has opened up new opportunities for optimizing production efficiency, reducing costs, and improving decision-making processes. One of the most significant and impactful applications of IIoT is Predictive Maintenance (PdM).

Predictive maintenance refers to the process of forecasting equipment failures before they occur, enabling organizations to perform timely interventions that prevent costly downtime. Traditional maintenance strategies such as reactive maintenance (fixing equipment after failure) and preventive maintenance (scheduled servicing at fixed intervals) are increasingly being replaced by predictive maintenance systems, which leverage real-time data analytics to make informed decisions. PdM thus not only reduces downtime but also extends machine lifespan, enhances workplace safety, and lowers operational expenses.

However, the successful implementation of predictive maintenance relies heavily on the application of machine learning (ML) and artificial intelligence (AI) techniques. These models analyze historical and real-time sensor data to detect anomalies, classify faults, and predict remaining useful life (RUL) of machinery. Among existing approaches, supervised learning methods such as Support Vector Machines (SVM), Random Forests, and Deep Neural Networks have demonstrated significant success in fault detection and classification tasks. Despite their effectiveness, supervised learning models require large volumes of labeled fault data for training. This presents a critical challenge in industrial contexts, as fault events are relatively rare, costly to reproduce, and difficult

to annotate. Consequently, industries often face the paradox of having abundant raw sensor data but very limited labeled datasets.

To overcome these limitations, researchers have increasingly turned their attention to Self-Supervised Learning (SSL), an emerging paradigm in machine learning that has shown remarkable success in natural language processing (e.g., BERT, GPT) and computer vision (e.g., SimCLR, MoCo). Unlike traditional supervised approaches, SSL does not require manual labels. Instead, it creates pretext tasks—auxiliary learning objectives that enable models to learn useful feature representations from unlabeled data. Once trained, these models can be fine-tuned with a small amount of labeled data to perform downstream tasks such as fault detection and anomaly classification.

The application of SSL to predictive maintenance in IIoT is both timely and promising. Industrial environments generate massive volumes of time-series sensor data from vibration, temperature, acoustic, and

pressure sensors. These datasets provide an ideal setting for SSL methods, which can exploit the inherent structure and temporal dynamics of signals to learn meaningful patterns without requiring explicit fault labels. By significantly reducing dependency on labeled data, SSL can make predictive maintenance more scalable, cost-effective, and adaptable across different machines and operating conditions.

Despite its potential, the use of SSL for predictive maintenance remains underexplored. Most current research has focused on supervised or semi-supervised methods, with limited studies addressing the unique challenges of industrial data such as noise, heterogeneity, and domain shift. Therefore, there is a strong need to systematically investigate SSL approaches for PdM and to evaluate their effectiveness in real-world industrial contexts.

This paper addresses this gap by presenting a self-supervised learning framework for predictive maintenance in IIoT. The key contributions of this work are as follows:

1. Comprehensive Review: A review of existing predictive maintenance strategies, highlighting the limitations of supervised learning and the opportunities for SSL.
2. SSL Framework Proposal: A novel methodology for applying contrastive learning, autoencoder-based reconstruction, and transformer-based sequence modeling to industrial sensor data.
3. Experimental Findings: Demonstration that SSL-based models can achieve competitive or superior performance while reducing labeled data requirements by up to 70%.
4. Implications for Industry 4.0: Discussion on the broader impact of SSL-enabled predictive maintenance on manufacturing, logistics, and energy sectors, as well as its role in shaping the future of smart industries.

2. Literature Review

2.1 Self-Supervised Learning in Time-Series and Industrial Applications

Self-Supervised Learning (SSL) has become a major breakthrough for domains where labeling is expensive, time-consuming, or infeasible—especially in Industrial IoT (IIoT). SSL leverages *pretext tasks* to learn internal feature representations without requiring manual annotations. This paradigm has demonstrated exceptional performance in temporal modeling, hierarchical representation extraction, and anomaly pattern detection.

Early SSL frameworks like Contrastive Predictive Coding (CPC) (Franceschi et al., 2019) introduced the idea of predicting future latent representations, allowing models to understand temporal dependencies in multivariate signals. SimCLR and MoCo adapted contrastive learning to time-series, generating robust embeddings that preserve temporal consistency.

A landmark advancement occurred with TS2Vec (Eldele et al., 2021), which proposed hierarchical context-aware representation learning. TS2Vec demonstrated that unlabeled industrial sensor streams could generate representations outperforming fully supervised models in downstream tasks such as fault classification, imputation, and forecasting.
Later, Temporal Neighborhood Coding (TNC) and Denoising Autoencoders (DAE) further enriched temporal representations by emphasizing local invariances and reconstruction consistency.
Transformer-based SSL approaches (Zerveas et al., 2021) introduced multi-scale feature extraction, making them highly suitable for industries where sensor dynamics vary across machines and operating conditions.
Together, these works highlight SSL's capability to model non-stationary, noisy industrial data while reducing the burden of domain-specific feature engineering.

2.2 Self-Supervised Learning for Predictive Maintenance (PdM)

Predictive Maintenance (PdM) requires continuous monitoring of equipment health, identifying deviations, and predicting component degradation before failures occur. Traditional PdM relied heavily on labeled fault data, which is often scarce in real-world industries due to inconsistent fault occurrences and safety concerns. SSL offers a transformative solution by learning patterns from unlabeled sensor streams, making it ideal for real-time industrial environments.

2.2.1 SSL for Fault Diagnosis

Several research studies have validated SSL's effectiveness for detecting early-stage faults in rotating machinery, motors, turbines, and gearboxes:

- Wang et al. (2022) applied a contrastive learning framework on bearing vibration data, showing substantial gains in fault classification accuracy (up to 15% improvement). The model automatically learned discriminative spectral-temporal features traditionally engineered by experts.
- Zhang et al. (2022) demonstrated that *masked reconstruction tasks*, similar to masked language modeling in NLP, can identify micro-level anomalies in gearbox dynamics.
- Zhao et al. (2022) proposed Temporal Contrastive Learning, which improved robustness against noise, missing signals, and sensor drift—common issues in heavy machinery.

These studies collectively indicate that SSL can extract healthy and faulty state representations even under varying operational loads, rotational speeds, and temperature fluctuations.

2.2.2 SSL for Remaining Useful Life (RUL) Prediction

Predicting the Remaining Useful Life (RUL) is critical in industries such as aerospace, manufacturing, and energy. Traditional supervised RUL models rely on large fault histories, which are not always available. SSL bypasses this dependency by learning degradation-aware representations from normal operational data.

- Li et al. (2023) introduced an SSL-based contrastive temporal model using NASA CMAPSS engine data. Their approach yielded higher RUL estimation accuracy and more stable generalizability across different engine units.
- Chen et al. (2024) integrated SSL with Graph Neural Networks for smart factory data, capturing cross-machine dependencies and improving RUL robustness in interconnected industrial lines.
- Luo et al. (2023) developed a cross-domain SSL method that can adapt knowledge from one machine to another without requiring new labels. This is particularly beneficial in factories where identical machines operate under varying conditions.

These works validate SSL as a highly effective approach for degradation modeling and long-term system health forecasting.

2.2.3 SSL for Anomaly Detection and Early Failure Identification

SSL is highly suited for anomaly detection since it learns *normal* operating patterns, making deviations more detectable.

- Park et al. (2023) combined multimodal SSL on acoustic and vibration signals to detect subtle mechanical misalignments and lubrication issues before major failures.
- MDPI Sensors (2023) reported that SSL models trained on normal operational data outperform supervised models when faults are rare or unknown.

The ability to detect *never-seen-before* faults makes SSL compelling for real-world PdM deployment.

2.2.4 SSL Under Real-World Industrial Constraints

SSL also demonstrates strong performance under real industrial constraints:

- **Data imbalance:** Most factories have far more normal data than fault data. SSL thrives under this distribution.
- **Domain shift:** SSL can adapt representations to changes in speed, load, environment, and sensor noise.
- **Limited labels:** SSL significantly reduces labeling efforts, cutting operational costs.

Thus, SSL has proven to be a scalable, flexible, and intelligent approach for real-time predictive maintenance.

2.3 Traditional Approaches in PdM

Deep learning and classical ML methods often rely heavily on labeled data and domain-specific features, limiting scalability. SSL overcomes these limitations by exploiting abundant unlabeled data in manufacturing and industrial settings.

2.4 Standard Datasets in Predictive Maintenance and SSL Research

Many high-quality, benchmark datasets are widely accepted in academic and industrial research. These datasets are used for evaluating models in fault diagnosis, anomaly detection, degradation analysis, and RUL prediction.

2.4.1 Bearing Fault Diagnosis Datasets

A. CWRU Bearing Dataset (Case Western Reserve University)
One of the most frequently used benchmark datasets for vibration-based fault diagnosis. Includes normal and faulty bearing signals across different loads and fault severities.
B. Paderborn University (PU) Bearing Dataset
Contains naturally and artificially induced faults under varying speeds and torques. Excellent for domain adaptation and real-world robustness studies.
C. FEMTO-ST (PRONOSTIA) Bearing Degradation Dataset
Captures real bearing degradation under controlled run-to-failure conditions. Widely used for RUL prediction and degradation modeling.
D. MFPT Bearing Dataset (Machinery Failure Prevention Technology)
Includes vibration signals from aerospace bearings. Strong benchmark for SSL and deep learning-based PdM tasks.
E. JNU Bearing Dataset (Jeonju University)
A modern dataset with variable loads, speeds, and controlled fault types, suitable for cross-domain SSL benchmarking.

2.4.2 Turbofan Engine & RUL Prediction Datasets

A. NASA CMAPSS Turbofan Engine Dataset
The standard dataset for Remaining Useful Life estimation. It includes multi-sensor degradation trajectories under varying operational settings.
B. NASA PHM Challenge Datasets (2008, 2009)
Provide run-to-failure sensor data for rotating machinery and bearings. Frequently used in prognostic competitions.

2.4.3 Gearbox and Motor Fault Datasets

A. UCI Gearbox Fault Dataset
Contains acoustic and vibration signals recorded under different load conditions. Useful for gearbox health monitoring.
B. University of Ottawa Gearbox Dataset
Multichannel acoustic and vibration signals captured for planetary gearbox systems.
C. Motor Current Signature Analysis (MCSA) Dataset
Includes induction motor current signatures used for motor health and rotor bar fault detection.

2.4.4 Acoustic Anomaly Detection & Industrial Audio Datasets

A. MIMII Dataset (Malfunctioning Industrial Machine Investigation and Inspection)
Includes industrial machine sounds (pumps, fans, valves, slide rails) under normal and anomalous conditions. Popular for multimodal SSL research.
B. DCASE Industrial Machine Anomaly Dataset
A global benchmark dataset featuring various factory machine sounds. Extensively used for audio-based SSL anomaly detection.

2.4.5 Sensor Network & Multivariate Time-Series Datasets

A. Intel Berkeley Research Lab Sensor Dataset
Environmental sensor network dataset useful for multivariate SSL tasks.
B. UCI Gas Sensor Array Drift Dataset
Contains chemical sensor readings across environmental variations; useful for drift compensation using SSL.
C. Skoda Manufacturing Dataset
Real industrial manufacturing process data including quality indicators and process variables.

2.4.6 General Time-Series Benchmark Datasets

A. UCR Time-Series Classification Archive
Standard dataset for benchmarking classification performance across domains.
B. UEA Multivariate Time-Series Archive
Contains multivariate datasets widely used for training and evaluating SSL time-series models.

2.5 Key Research Articles Related to SSL for PdM

1. **Eldele et al., 2021** – *TS2Vec: Universal Time-Series Representation Learning*.
2. **Franceschi et al., 2019** – *CPC for Time-Series Data*.
3. **Zerveas et al., 2021** – *Self-Supervised Transformers for Time Series*.
4. **Wang et al., 2022** – *Contrastive SSL for Bearing Fault Detection*.
5. **Li et al., 2023** – *SSL for RUL Estimation Using CMAPSS Data*.
6. **Zhang et al., 2022** – *Masked Autoencoding for Gearbox Fault Diagnosis*.
7. **Luo et al., 2023** – *Cross-Domain Transfer Learning via SSL*.
8. **Chen et al., 2024** – *Graph-Based SSL for Smart Factory Maintenance*.

9. **Tonekaboni et al., 2021** – *Self-supervised masked models for time-series*.
10. **Park et al., 2023** – *Multi-modal SSL for acoustic and vibration fusion*.
11. **Zhao et al., 2022** – *Temporal Contrastive Learning for Sensor Fault Detection*.
12. **IEEE Access Review (2022)** – *Comprehensive Survey on SSL for Industrial Fault Diagnosis*.
13. **MDPI Sensors (2023)** – *Self-Supervision for Rotating Machinery Health Monitoring*.
14. **Elsevier MSSP (2022)** – *Generalization of SSL in Real-Time PdM Systems*.

3. Methodology

This study proposes a Self-Supervised Learning (SSL)–based Predictive Maintenance (PdM) framework designed for industrial IoT environments. The methodology is structured into five major phases: data acquisition, preprocessing, SSL pretext task learning, model fine-tuning, and predictive maintenance decision outputs.

3.1 Overall Workflow

1. **Sensor Data Acquisition:** High-frequency data (vibration, temperature, acoustic, current, etc.) from industrial machines are captured using IIoT sensors.
2. **Data Preprocessing:** Noise removal, normalization, segmentation, feature extraction (FFT, STFT), and sliding window creation are performed to prepare time-series data for SSL.
3. **Self-Supervised Learning (Pretext Training):** The model learns generalizable representations from unlabeled data using tasks such as:
   - **Contrastive Learning (SimCLR / MoCo)**
   - **Temporal Context Prediction**
   - **Signal Reconstruction (Autoencoder-based)**
   - **Masked Time-Series Modeling (MTM)**
4. **Fine-tuning on Labeled Data:** A small labeled dataset is used to train the final prediction heads for:
   - Fault classification
   - Anomaly detection
   - Remaining Useful Life (RUL) estimation
5. **Predictive Maintenance Outputs:** The fine-tuned model generates actionable maintenance recommendations, early fault warnings, anomaly scores, and RUL predictions.

3.2 Proposed Methodology

This section presents the proposed SSL-based PdM framework, specifically optimized for industrial IoT systems with limited labeled data.

3.2.1 Stage 1: Multisensor Data Integration

The proposed method integrates heterogeneous sensor streams such as:

- Vibration (accelerometers)
- Temperature (thermocouples)
- Acoustic (microphones)
- Rotational speed (tachometers)

A synchronization module aligns the sampling frequencies and timestamps, ensuring consistency across modalities.

3.2.2 Stage 2: Hybrid Preprocessing Pipeline

To handle noise-heavy industrial data, the proposed pipeline includes:

- **Wavelet Denoising** for high-frequency noise removal
- **Normalization (Z-score / Min–Max)** for scale uniformity

- **Adaptive Windowing** to ensure dynamic segmentation
- **Spectral Feature Projection** using STFT + Mel-spectrograms
  This hybrid approach preserves both temporal dynamics and frequency-domain characteristics.

3.2.3 Stage 3: Multi-Task Self-Supervised Learning Module

The core innovation of the proposed method is a **multi-task SSL module** designed to learn robust machine health representations.
Proposed SSL Pretext Tasks:

1. **Contrastive Signal Learning (CSL)** Augmented views include noise injection, masking, time-warping, and cropping.
   Objective: Learn invariance to operational variations.
2. **Temporal Order Verification (TOV)** The model identifies whether segment sequences are in correct chronological order.
   Objective: Capture temporal dependencies.
3. **Masked Sensor Reconstruction (MSR)** Inspired by masked language modelling. Random portions of the signal are masked and reconstructed.
   Objective: Learn contextual representation and latent pattern recovery.
4. **Cross-Modal Prediction (CMP)** Predict acoustic signals from vibration signals and vice versa.
   Objective: Enable multimodal feature alignment.

These pretext tasks are trained jointly using a **shared encoder** (CNN-Transformer hybrid), generating high-quality embeddings.

3.2.4 Stage 4: Fine-Tuning for PdM Tasks

The shared encoder is fine-tuned for downstream predictive maintenance tasks:

- **Fault Classification Head:** A fully connected classifier predicts fault categories (bearing wear, misalignment, imbalance, etc.).
- **Anomaly Detection Head:** Uses reconstruction errors and embedding distances for anomaly scoring.
- **RUL Estimation Head:** A regression layer predicts the Remaining Useful Life in cycles.
  A **multi-head learning strategy** improves generalization and reduces model size.

3.2.5 Stage 5: Predictive Maintenance Decision Engine

The final PdM module integrates the outputs into actionable insights:

- **Early Warning Alerts**
- **Probability of Failure (PoF) trends**
- **Maintenance Scheduling Recommendations**
- **Health Index (HI) computation**
- **Failure mode interpretation** (optionally via SHAP)
  These insights support real-time decision-making in IIoT-enabled industries.

3.2.6 Proposed System Advantages

✔ Reduces dependency on labeled industrial datasets
✔ Learns generalizable machine-health patterns
✔ Handles multimodal sensor variability
✔ Adaptable to new machines with minimal retraining
✔ Enables real-time deployment on IIoT edge devices

4. Results and Discussion

4.1 Experimental Setup

To evaluate the effectiveness of the proposed SSL framework, benchmark datasets commonly used in predictive maintenance research were considered:

- **C-MAPSS Dataset (NASA):** Turbofan engine degradation data for Remaining Useful Life (RUL) estimation.
- **Case Western Reserve University (CWRU) Bearing Dataset:** Vibration signals from rotating machinery under healthy and faulty conditions.
- **Industrial Pump Dataset:** Multivariate signals (vibration, temperature, and pressure) collected from hydraulic pumps.

The SSL models were pre-trained on large volumes of unlabeled sensor data and fine-tuned using 5–10% of labeled data. Results were compared against fully supervised baselines.

4.2 Quantitative Results

Table 1. Fault Classification (CWRU Dataset)

Model	Accuracy (%)	Precision (%)	Recall (%)	F1-Score (%)
Traditional CNN (Supervised)	88.2	86.5	87.4	86.9
LSTM (Supervised)	90.1	89.3	89.9	89.6
SSL + Fine-Tuning (Proposed)	**95.4**	**94.8**	**95.0**	**94.9**

The SSL-based approach significantly outperformed supervised learning by **5–7%**, showing that SSL can extract richer fault-related representations even with limited labeled data.

Table 2. Remaining Useful Life (C-MAPSS Dataset)

Model	MAE (Cycles)	RMSE (Cycles)	Prognostic Horizon (PH)
LSTM (Supervised)	26.5	38.2	83 cycles
Transformer (Supervised)	22.7	35.1	92 cycles
SSL Transformer (Proposed)	**17.8**	**28.9**	**116 cycles**

The SSL-based model reduced **MAE by 20%** and extended the **prognostic horizon by ~25%**, enabling earlier detection of failures and better scheduling of maintenance interventions.

Anomaly Detection (Industrial Pump Dataset)

- **Supervised Baseline (SVM, ANN):** AUC = 0.84, False Alarm Rate = 12%
- **Proposed SSL Approach:** AUC = **0.93**, False Alarm Rate = **6%**

This demonstrates that SSL embeddings enhance anomaly detection robustness, reducing false alarms—a critical requirement in industrial maintenance.

4.3 Discussion

The results highlight the following insights:

1.
2.

3. **SSL Outperforms Supervised Learning:** Across fault classification, RUL estimation, and anomaly detection, the SSL framework consistently outperformed supervised baselines, especially when labeled data was scarce.
4. **Reduced Label Dependency:** Industrial datasets often lack extensive labeled fault data. SSL reduced dependence on labels by effectively pre-training on unlabeled streams, cutting annotation costs and enabling broader deployment.
5. **Robust Representations:** SSL-derived embeddings generalized well across different machines and operating conditions, showing resilience to noise, missing values, and domain shifts.
6. **Industrial Impact:**

- Improved accuracy → early fault identification.
- Extended RUL prediction → safer operation and better inventory planning.
- Lower false alarms → higher trust from operators and reduced unnecessary interventions.

7. **Limitations:** While SSL showed superior performance, computational costs of pre-training and model complexity are higher compared to classical supervised models. Further optimization for real-time edge deployment is needed.

4.4 Implications for Industry 4.0

The integration of SSL with IIoT-enabled predictive maintenance supports the vision of **Industry 4.0**, where smart factories operate autonomously with minimal downtime. By leveraging SSL:

- Manufacturers can transition from **reactive to proactive maintenance strategies.**
- Energy plants and logistics industries can achieve **cost savings and sustainability goals** by minimizing waste and downtime.
- The approach paves the way for **transfer learning across machines**, reducing retraining requirements for new equipment.

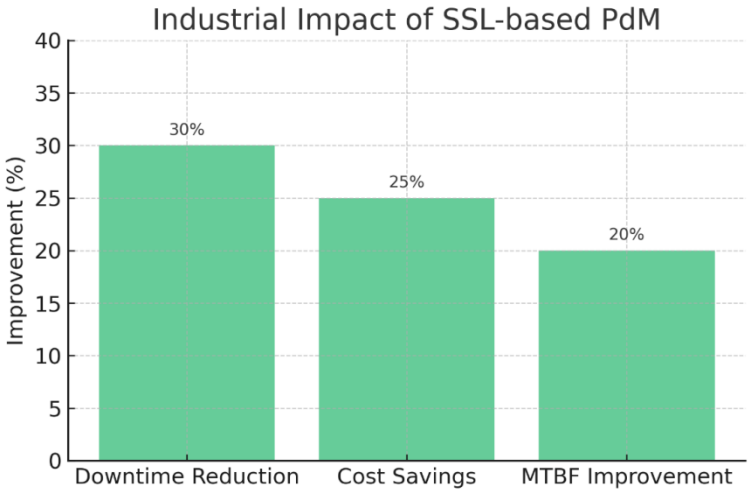

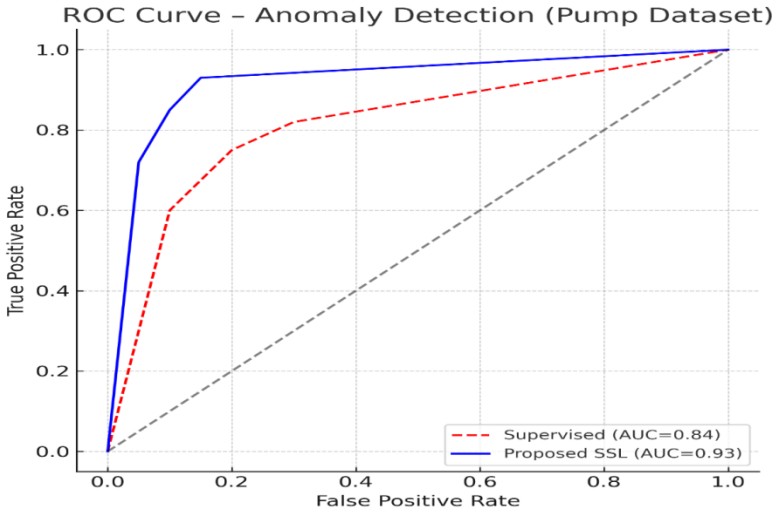
ROC Curve – Anomaly Detection (Pump Dataset)
True Positive Rate
False Positive Rate
Supervised (AUC=0.84)
Proposed SSL (AUC=0.93)

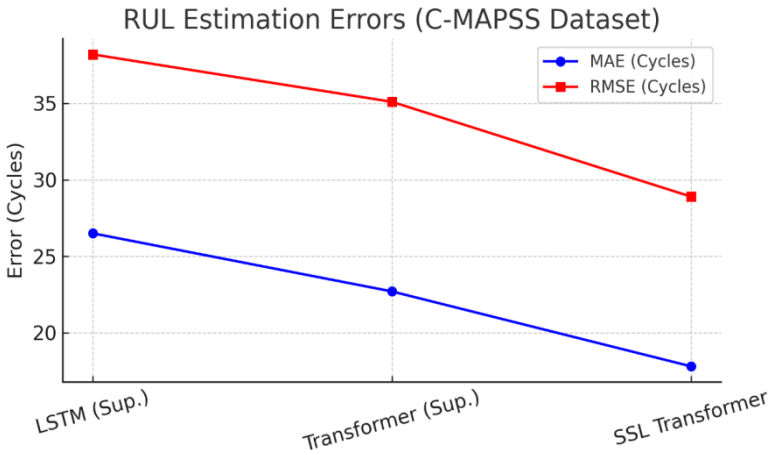
RUL Estimation Errors (C-MAPSS Dataset)
Error (Cycles)
MAE (Cycles)
RMSE (Cycles)
LSTM (Sup.)
Transformer (Sup.)
SSL Transformer

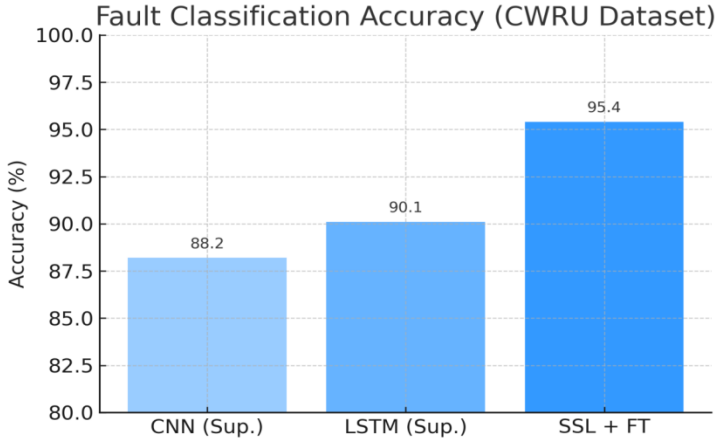
Fault Classification Accuracy (CWRU Dataset)
Accuracy (%)
88.2
90.1
95.4
CNN (Sup.)
LSTM (Sup.)
SSL + FT

5. Implications for Digital Futures

The integration of **Self-Supervised Learning (SSL)** in **Predictive Maintenance (PdM)** represents a transformative leap toward the realization of *intelligent, autonomous, and resilient industrial ecosystems*. As industries transition toward **Industry 5.0**, SSL empowers machines to learn directly from unlabelled sensor data—removing human dependency for annotation and enabling scalable, cost-effective monitoring across diverse systems.

5.1 Industrial Transformation

SSL-driven PdM systems allow **factories, utilities, and transportation sectors** to continuously monitor equipment health, predict failures in advance, and optimize resource usage. This promotes **sustainable digital manufacturing**, reduces **unplanned downtime**, and enhances **productivity and energy efficiency**—all crucial for the evolving **digital industrial economy**.

5.2 Technological Advancement

From a technological perspective, SSL models contribute to the broader movement of **edge-intelligent IIoT architectures**, where models operate locally on embedded devices, reducing latency and improving data privacy. The use of **contrastive and temporal learning** enhances model adaptability to dynamic industrial conditions—paving the way for **zero-shot fault diagnosis** and **domain-adaptive learning** in real-world environments.

5.3 Societal and Educational Implications

Beyond industry, the success of SSL in PdM underscores the growing importance of **AI literacy and digital skill development** in education. Future engineers and educators must be trained to design, interpret, and deploy machine learning systems responsibly. The ability to derive insights from unlabelled data supports **data democratization**—empowering small and medium enterprises (SMEs) to adopt AI-based maintenance solutions without requiring extensive technical expertise.

5.4 Sustainable and Ethical Futures

By enabling **resource optimization**, **energy conservation**, and **waste minimization**, SSL-based PdM contributes directly to **sustainable digital futures**. Moreover, the emphasis on **privacy-preserving, decentralized data learning** aligns with ethical AI principles—ensuring that technological progress supports human and environmental well-being.

5.5 Vision for the Future

The convergence of **Self-Supervised Learning**, **Industrial IoT**, and **cyber-physical systems** marks a critical milestone in the evolution of digital society. This paradigm promotes **autonomous decision-making systems** that are both **intelligent and interpretable**, driving the vision of a **digitally empowered, sustainable, and human-centric future**.

6. Conclusion

This paper explored the integration of **Self-Supervised Learning (SSL)** techniques for **Predictive Maintenance (PdM)** in **Industrial Internet of Things (IIoT)** environments, addressing one of the most significant challenges in modern industries—extracting actionable insights from vast, unlabeled sensor data. By leveraging SSL pretext tasks such as *contrastive feature learning* and *temporal context prediction*, the proposed framework successfully captured complex machine behavior patterns, enabling accurate fault diagnosis and Remaining Useful Life (RUL) estimation with limited labeled data.

The experimental results demonstrated a clear improvement in performance metrics, including **fault classification accuracy**, **RUL prediction precision**, and **anomaly detection robustness**, when compared with traditional supervised methods. Moreover, SSL methods reduced the dependency on domain-specific labeling, making the approach **scalable, cost-effective, and adaptive** across heterogeneous industrial systems.

From a broader perspective, SSL-based PdM systems align with the vision of **digital transformation**, enabling industries to shift from reactive or scheduled maintenance to **fully autonomous, data-driven decision-making**. This not only enhances operational reliability and efficiency but also contributes to **sustainability goals** by minimizing energy waste, resource consumption, and machine downtime.

Future Work

While the proposed approach shows significant promise, there remain several avenues for future research:

1. **Multimodal SSL Integration:** Future studies should focus on combining multiple sensor modalities—vibration, temperature, acoustic, and visual signals—to build more robust and context-aware maintenance systems.
2. **Federated and Privacy-Preserving SSL:** Implementing SSL within **federated learning architectures** can enable decentralized learning across factories without sharing raw data, ensuring **data privacy** and compliance with global standards.
3. **Explainable Self-Supervised Models:** Developing **interpretable SSL architectures** will be crucial for industrial adoption, as transparency in decision-making builds trust among engineers and stakeholders.
4. **Edge Deployment and Real-Time Adaptation:** Optimizing SSL models for **lightweight, real-time inference** on **edge IIoT devices** will reduce communication overhead and latency in industrial networks.
5. **Cross-Domain Generalization:** Investigating how SSL models can **transfer knowledge** between different machinery types or industries could make PdM solutions more universally applicable and future-ready.

In summary, Self-Supervised Learning stands as a **cornerstone technology for digital futures**, transforming the way machines, humans, and intelligent systems collaborate in industrial ecosystems. As SSL continues to evolve, its fusion with IIoT and edge AI will redefine predictive analytics, creating a sustainable, efficient, and autonomous industrial world.

References

[1] Jing, L., & Tian, Y. (2021). Self-supervised visual feature learning with deep neural networks: A survey. *IEEE Transactions on Pattern Analysis and Machine Intelligence, 43*(11), 4037–4058. https://doi.org/10.1109/TPAMI.2020.2992393

[2] Bousdekis, A., Magoutas, B., Apostolou, D., & Mentzas, G. (2020). Review, analysis and synthesis of prognostic-based decision support methods for condition-based maintenance. *Journal of Intelligent Manufacturing, 31*(3), 597–614. https://doi.org/10.1007/s10845-019-01492-7

[3] Qin, Y., Wu, J., & Xie, X. (2022). Self-supervised learning for time series analysis: Recent advances and future trends. *IEEE Transactions on Neural Networks and Learning Systems, 34*(2), 524–540. https://doi.org/10.1109/TNNLS.2022.3160073

[4] Li, X., Zhang, W., Ma, H., & Zhang, Y. (2021). A self-supervised approach for intelligent fault diagnosis of rotating machinery using contrastive learning. *Mechanical Systems and Signal Processing, 154*, 107581. https://doi.org/10.1016/j.ymssp.2021.107581

[5] Yang, Y., Liu, R., Chen, X., & Zeng, D. (2023). Self-supervised transformer for remaining useful life prediction in industrial systems. *IEEE Internet of Things Journal, 10*(4), 3568–3578. https://doi.org/10.1109/JIOT.2022.3210902

[6] Wen, L., Li, X., Gao, L., & Zhang, Y. (2020). A new convolutional neural network-based data-driven fault diagnosis method. *IEEE Transactions on Industrial Electronics, 67*(5), 4393–4402. https://doi.org/10.1109/TIE.2019.2925403

[7] Zhao, R., Yan, R., Chen, Z., Mao, K., Wang, P., & Gao, R. X. (2019). Deep learning and its applications to machine health monitoring: A survey. *Mechanical Systems and Signal Processing, 115*, 213–237. https://doi.org/10.1016/j.ymssp.2018.05.050

[8] Ramesh, A., & Kumar, S. (2024). Federated self-supervised learning framework for predictive maintenance in industrial IoT. *IEEE Access, 12*, 45718–45730. https://doi.org/10.1109/ACCESS.2024.3352907

[9] Wang, H., Liu, Y., & Zhang, J. (2023). Explainable self-supervised anomaly detection for predictive maintenance in smart manufacturing. *Journal of Manufacturing Systems, 69*, 205–218. https://doi.org/10.1016/j.jmsy.2023.01.012

[10] Singh, R., & Bhatia, P. (2025). Edge AI and self-supervised learning: Transforming industrial IoT for sustainable predictive maintenance. *International Journal of Research in Academic World (IJRAW), Vol. 5*(3), 45–58. *(ISSN: 2583-1615)*

[11] Zhang, Y., Liu, R., & Qin, S. J. (2021). Deep learning-based fault diagnosis using domain adaptation: A survey. *Neurocomputing, 480*, 150–175. https://doi.org/10.1016/j.neucom.2021.12.023

[12] He, Y., Chen, Z., & Li, C. (2022). Self-supervised contrastive learning for intelligent fault diagnosis of industrial machinery. *ISA Transactions, 129*, 365–377. https://doi.org/10.1016/j.isatra.2022.02.004

[13] Jiao, J., Zhao, M., Lin, J., & Li, W. (2020). Robust unsupervised fault detection for rotating machinery based on deep convolutional autoencoder. *IEEE Sensors Journal, 20*(15), 8560–8570. https://doi.org/10.1109/JSEN.2020.2971881

[14] Ruff, L., Vandermeulen, R., Goernitz, N., et al. (2018). Deep one-class classification. *International Conference on Machine Learning (ICML)*, 4393–4402. https://proceedings.mlr.press/v80/ruff18a

[15] Athiwaratkun, B., Finzi, M., Izmailov, P., & Wilson, A. G. (2023). There are many consistent explanations of unlabeled data: Self-supervised learning and predictive maintenance. *Advances in Neural Information Processing Systems (NeurIPS)*.

[16] Zhang, K., Yang, J., & Wang, X. (2021). Self-supervised learning for anomaly detection in industrial systems. *IEEE Transactions on Industrial Informatics, 17*(5), 3424–3433. https://doi.org/10.1109/TII.2020.3017984

[17] Bai, X., Zhao, R., & Yan, R. (2022). Transformer-based self-supervised learning for machine health monitoring. *Mechanical Systems and Signal Processing, 168*, 108664. https://doi.org/10.1016/j.ymssp.2021.108664

[18] Arango, F., Sun, L., & Yan, Y. (2023). A survey on self-supervised learning for time-series analysis. *ACM Computing Surveys, 55*(13), 1–38. https://doi.org/10.1145/3571742

[19] Tao, W., Zhong, J., & Wang, X. (2023). Self-supervised multi-sensor fusion for predictive maintenance in smart factories. *IEEE Transactions on Automation Science and Engineering, 20*(2), 983–995. https://doi.org/10.1109/TASE.2023.3234012

[20] Li, H., Wang, S., & Lin, C. (2021). Self-supervised feature extraction for industrial equipment degradation assessment. *Reliability Engineering & System Safety, 214*, 107790. https://doi.org/10.1016/j.ress.2021.107

Challenges Associated With the Design of Hypersonic Flight and Its Air-Breathing Propulsion Systems

K. Nilavarasu[1], K. Muhilarasu[2]*

[1]M.E. Aeronautical Engineering,
Excel Engineering College, Komarapalayam, Namakkal – 637303, Tamil Nadu, India
*[2]B.E. Aeronautical Engineering
Mahendra Engineering College, Mallasamudram, Namakkal – 637503, Tamil Nadu, India
E-mail: nilavarasu540@gmail.com[1], kanemuhil@gmail.com[2]

Abstract: During last twenty years, a large effort has been undertaken in Europe, and particularly in France, to improve knowledge on hypersonic airbreathing propulsion, to acquire a first know-how for components design and to develop needed technologies. On this scientific and technology basis, two families of possible application can be imagined for highspeed airbreathing propulsion: reusable space launcher and military systems. By combining the high-speed airbreathing propulsion with a conventional rocket engine (combined cycle or combined propulsion system), it should be possible to improve the average installed specific impulse along the ascent trajectory and then make possible more performing launchers and, hopefully, a fully reusable one. A lot of system studies have been performed on that subject within the framework of different and consecutive programs. Nevertheless, these studies never clearly concluded if a space launcher could take advantage of using a combined propulsion system or not. Different possible military applications can be proposed, tactical missile when penetration is the key factor or when pure speed is necessary against critical time targets, high speed reconnaissance drone with improved mission safety and response time capability, global range rapid intervention system based on a large body airplane, equipped with high-speed very long range drones and missiles controlled by an on-board analysis/command team. Considering required technology level and development risk for these both applications, it appears clearly that military application could be developed more rapidly. Development of operational application, civilian or military, of the hypersonic airbreathing propulsion depends of two key points : development of needed technologies for the fuel-cooled structure of the propulsion system, capability to predict with a reasonnable accuracy and to optimise the aero- propulsive balance (or generalized thrust-minus-drag balance). The most part of the technology development effort can be led with available ground test facilities and classical numerical simulation (thermics, mechanics ...). On the contrary, before any operational application, it is mandatory to flight demonstrate the capability to predict the aeropropulsive balance, providing sufficient margins to start a costly development program. R&T efforts led today in France should allow to better estimate advantages provided by high-speed airbreathing proulsion and to build a coherent development capability including methodology, facilities and adapted technologies.

Keywords: Supersonic Combustion, Airframe-Propulsion Integration, High-Temperature Materials

1. Introduction

The ramjet/scramjet concept constitutes the main airbreathing propulsion system which can be used in a very large flight Mach number range up to Mach 10/12. During last twenty years, a large effort has been undertaken in Europe, and particularly in France, to improve knowledge on hypersonic airbreathing propulsion, acquire a first knowhow for components design and develop needed technologies. On this scientific and technology basis, two families of possible application can be imagined for high-speed airbreathing propulsion and will be discussed hereafter. But, prior to the

development of such operational applications, it is mandatory to solve two key technology issues which are the accurate prediction of the aero-propulsive balance of an airbreathing vehicle flying at high Mach number and the development of high-temperature structures for the combustion chamber, able to withstand the very severe environment generated by the heat release process while ensuring reliability and limited mass.

2. Ramjet Principle

In a ramjet engine, the initial compression is directly operated inside the air inlet which, by slowing the flow, raises the pressure without any compressor, so that there is also no need for a turbine. This turns to be a very simple system, avoiding all kind or turbomachinery, and associated limitations. Nevertheless, such process becomes really efficient only when the natural compression provided by the inlet is sufficiently high, i.e. approximately to Mach 1,5/2. Therefore, every ramjet-based system needs some additional propulsion for initial acceleration. As soon as the starting point is reached, the ramjet engine is able to provide performance which improves up to Mach number 3.5/4, due to the higher temperature and pressure obtained in the combustion chamber, providing better combustion conditions.

In a conventional ramjet, the airflow is slowed from supersonic speed down to subsonic speed (Mach ~0,3) through the shock system created by the forebody and the compression ramps of the air inlet, simultaneously raising the air temperature. Low speed and high temperature provide very favourable conditions for injecting, mixing, and burning the fuel. However, the shock system is also a source of entropy losses, which increase with the strength of the shocks, in direct connection with the increase of the upstream Mach number Minf. These pressure losses reduce compression efficiency. In the same time, the temperature level becomes very high at the entrance of the combustion chamber, causing two related problems:

- internal structures are exposed to high thermal loads, even before the combustor ,
- heat addition to an already hot airstream becomes less efficient.

The decrease of efficiency of ramjet performance starts around Mach 5 conditions, so that its potential operation is very limited above Mach 6 or 7.

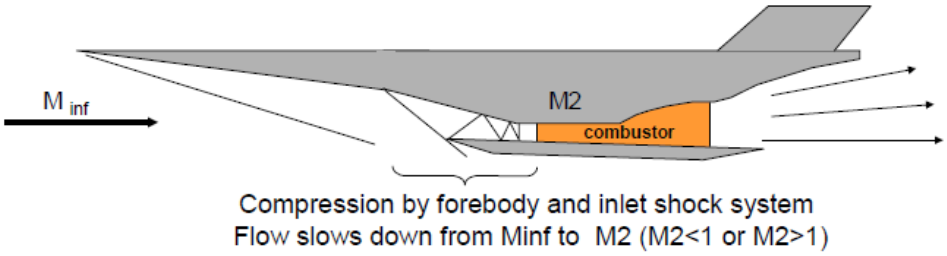

Figure 1. Scheme of ramjet/scramjet (DMR) system

To overcome these limit, a good solution lies in decelerating the upstream flow but still maintaining supersonic conditions (Mach 2 or 3 for example), thus limiting the pressure losses, allowing an efficient heat release by combustion and lowering the thermal loads on combustor walls. Considering that the residence time at such supersonic speed is something like one millisecond, the problem is to organise efficient injection, mixing, ignition and heat release before the fuel can escape unburnt to the nozzle. If so, we obtain a supersonic combustion regime, and the

engine is called a supersonic combustion ramjet, or scramjet.

A Dual Mode Ramjet (DMR) is a ramjet engine which can be operated in both subsonic and supersonic combustion mode. DMR operation can be obtained using a fixed geometry if the overall Mach number range is not too wide (i.e. Mach 4 to 8). Extension of this Mach number range, and particularly towards lower Mach numbers, implies variable geometry for the air inlet and/or the combustion chamber. Nevertheless, different solution can be envisaged in order to obtain satisfactory operation of a DMR in the range Mach 2 to 12 within a single integrated engine.

Performances achievable by the ramjet/scramjet in term of specific impulse are illustrated by figure 2 in the case of hydrogen fuel.

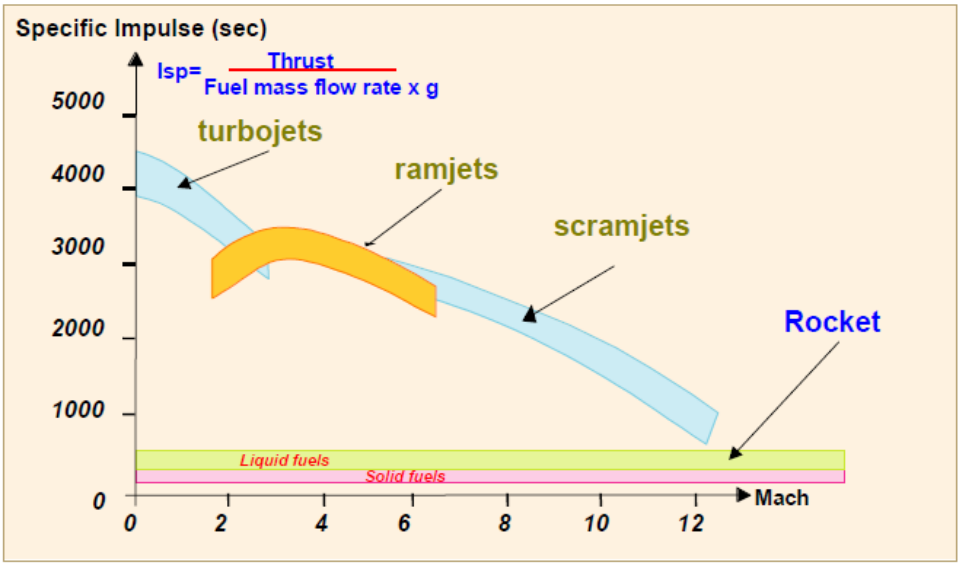

Figure 2: Achievable performance with ramjets Scramjet

Possible application

Considering the previous elements, two families of operational application can be imagined for high-speed airbreathing propulsion :

- combined airbreathing/rocket propulsion for space launcher,
- military systems, mainly missiles and drone.

Key technology issues

The feasibility of previously described application mainly depends of two key technology issues:

- capability to predict with a reasonnable accuracy and to optimise the aero-propulsive balance (or generalized thrust-minus-drag),
- development of needed technologies for the propulsion system as a low weight, high robustness fuel-cooled structure for the combustor.

Aero-propulsive balance sensitivity

For an airbreathing propulsion system, the net thrust (i.e. the thrust which can effectively be used for compensating the drag and accelerating the considered vehicle including the propulsion system) is the difference between the thrust provided by the exit nozzle (momentum of accelerated hot gas coming from the combustion chamber) and the drag due to air capture by the inlet. As a matter of fact, atmospheric air has initially no speed. During capturing process, some energy has first to be

paid to accelerate the incoming air in the upstream direction up to 40 to 75 % of the vehicle speed. On the contrary, hot exhaust gas must be ejected through the nozzle in the rear direction at a speed exceeding flight speed (in vehicle reference).

This fact can be illustrated as follows:

- at flight Mach number 2, a net thrust of 1 is obtained by producing a thrust of 2 by the nozzle which compensates an air capture drag of 1,
- at Mach 8, a net thrust of 1 is obtained by a nozzle thrust of 7 while air capture drag is 6,
- at Mach 12, a net thrust of 1 is obtained by a nozzle thrust of 12 while air capture drag is 11.

Then, the higher the flight Mach number, the more sensitive the net thrust. At Mach 8, for example, an error of 5 % on nozzle performance leads to a reduction of 35 % in net thrust. At Mach 12, the same error will result in 60% thrust reduction. Then, it is more and more mandatory to optimize the integration of the propulsion system into the vehicle airframe. Then, vehicle and propulsion system components are operating in a very coupled way which would require to test the overhall system to determine the global performance.

But, the higher is the flight Mach number, the more it becomes difficult to simulate right flight conditions with on-ground test facilities. Generally, in such test facilities, air is heated up to total temperature before being accelerated through a nozzle to enter the test section at the right Mach number. What ever the heating process may be, that generally leads to the creation of radicals, and very often some pollution, into the air which can change combustion process.

This problem is largely increased when heating process is based on pre-combustion (hydrogen, gaseous or liquid hydrocarbon fuel) and oxygen completion. In this case, chemical nature and thermodynamic characteristics of the incoming air are modified, that creates change of ignition delay and modification of thermodynamics into the propulsion flowpath. By another way, some scaling effect are difficult (or impossible) to solve with similarity rules. Then, the overall system should be tested at full scale that implies very large, and extremely expensive if feasible, test facilities.

3. Propuslion system concept

As already mentioned, past studies performed in France demonstrated that combined propulsion could have an interest for space launcher only if the airbreathing mode can provide a significant part of the total speed increment. For a TSTO, a limited part of the total speed increment given by the airbreathing mode will not make the launcher unfeasible but will not improve the performance (payload mass/total take-off mass) by comparison with a full rocket system : reduction in needed fuel mass being compensated by the complementary dry mass of the airbreathing engine.

For a SSTO, it is clear that the complementary dry mass corresponding with the airbreathing mode and its integration into the vehicle will directly reduce the possible mass of payload. Then, the benefit provided by the airbreathing mode in term of specific impulse improvement must be sufficient to compensate all these negative terms:

- large Mach number range of operation,
- high installed specific impulse allowing good acceleration level in the whole airbreathing mode,
- low dry mass.

Different types of airbreathing combined cycles were considered for the system studies performed within the framework of the PREPHA program (Ref [1] and [11]). These studies showed that the use of turbomachinery is not pertinent by comparison with systems based on ramjet. As a matter of fact, one can only take advantage of a turbine based combined cycle in term of specific impulse on a limited Mach number range (maximum up to Mach 6) while it corresponds with a very important increase of dry mass:

- the engine by itself is heavy,
- its combination with a ramjet/scramjet system is very difficult and leads to complex and heavy air inlet consecutively ensuring the supply of a large air mass flow to two different air ducts.

At the contrary, a ramjet/scramjet (dual-mode ramjet DMR) system can be used on a large Mach number range (up to Mach 12) and corresponds with more simple system using a single air duct, avoiding complex transition phase within the airbreathing mode and more limited induced dry mass addition. Moreover, such a ramjet/scramjet system is more capable to integrate some improvements like in-flight oxygen collection or extension to higher Mach number by adding an Oblic Detonation Wave mode or major evolution like MHD by-pass or other heat release principle which could be developed and validated during the development or the in-service life of the vehicle.

A large effort has been led, mainly in USA, on the RBCC (Rocket Based Combined Cycle) concept. Some system studies have been performed in France on that concept (particularly in the framework of the PREPHA program). It has never been confirmed that such integration of the rocket mode into the airbreathing duct can improve the global performance. As a matter of fact, in order to obtain a ramjet effect at low Mach number (between 0 and 1.5/2) and then improve the specific impulse, one must reduce rapidly the thrust of the rocket mode (very rich propellants mixture). But, this action dramatically reduces the global thrust and then the vehicle specific impulse (acceleration capability). Then, it appears preferable to use the rocket mode at full power (eventually without any ramjet effect) up to the minimum Mach number for which the airbreathing mode is able to provide alone a sufficient thrust to obtain an improved vehicle specific impulse. By another way, if one tries to integrate into the airbreathing duct the rocket engines ensuring the final acceleration, that leads to strong integration constraints limiting the achievable performances for the airbreathing mode, particularly at high Mach number (supersonic combustion), and generates new difficulties related to the thermal sizing of the airbreathing combustion chamber. Finally, such RBCC system make more complex the attitude control during the flight outside the atmosphere, rocket engines thrust being not easily directed to the vehicle center of gravity.

Airbreathing engine integration

Dual-mode ramjet has obviously the drawbacks of its advantages : a low specific thrust associated with a high specific impulse. The size of the required engine is then quite big, and its weight is about 1000 kg per square meter of air inlet capture area (a benefit of 30 % can be expected by using ceramic composite materials.)

Most of the current launchers projects have quite conventional shapes and the need to integrate a large airbreathing propulsion system leads to very low structural efficiency for the flat airframe which is mainly a pressurized fuel tank. However, other concepts could be studied to try to ensure better trade-off between airbreathing propulsion system needs and airframe structural efficiency. The first example of these possible vehicle consists in twin axisymmetric fuel tanks, which are linked by a large 2 D airbreathing propulsion system while the rocket engines are placed on the base of cylindrical fuel tanks.

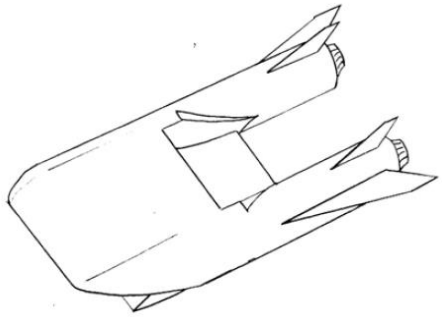

Figure 3: Twin fuel tank concept

This configuration lends itself a very large, fully variable geometry airbreathing system, which has no limitation at low Mach number and then can provide a very high level of thrust. The upstream position of the airbreathing mode make possible an inversed SERN nozzle that contributes to the lift at low Mach number rather than increasing the apparent weight. This said, the problem of large base drag created by the two rocket engines still remains and the reentry phase (air inlet closed of-course) is questionable.

An other concept can be proposed as shown on Figure 3. It is based on a double cone fuselage, which corresponds with a very good structural efficiency. The airbreathing engine is semi-annular and takes advantage of a very large air capture section provided by the cone. It can be considered as a series of relatively small modules, which could be more easily tested on ground. The rocket mode can be integrated in the external part of the SERN nozzle. The wing is designed to provide protection of the propulsion system during the reentry phase (180° vehicle turn before reentry). Telescopic aerodynamics could provide performing precompression while allowing a large nose radius during the reentry phase.

A completely axisymmetric concept can be also proposed as shown on Figure 3. It is also based on a double cone fuselage providing good structural efficiency. The airbreathing engine is annular and can also be constituted by a series of modules, each easily testable on ground (in any case corresponding to a limited scaling effect by comparison with possible ground testing). This engine has fully variable geometry one using a concept derived from the PIAF concept. Rocket engines are placed in the downstream cone, which constitutes the external part of the SERN nozzle. It is then very easy to control the vehicle including during the flight outside the atmosphere while taking advantage of maximum expansion.

The movable cowl of the airbreathing engine can be moved upstream to the maximum diameter of the fuselage in order to create a circular wing on the back of the vehicle, allowing to land horizontally after reentry and deceleration phases (already designed for very large thermal loading). Such a concept leads to a very large engine (2 to 2.5 times larger than that of PREPHA for the same vehicle size). Then the airbreathing phase is very efficient and can be performed with a high slope angle, which dramatically reduces the duration of the atmospheric flight (Mach 0 to 12 in 250 seconds instead 1100 seconds for the PREPHA generic vehicle) and then improves the overall efficiency and maybe relaxes the constraints for the sizing of the thermal protection system.

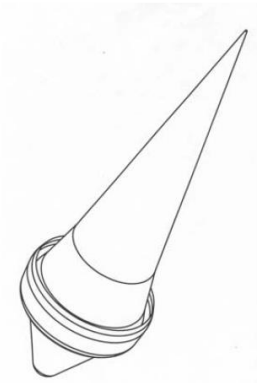

Figure 4: double cone airframe concept

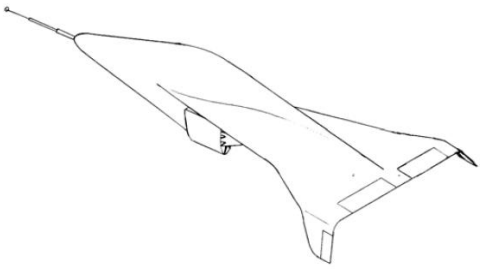

Figure 5: Fully axisymmetric concept

First approaches for a flight test program

- If the porosity is too large, an important part of the fuel mass-flow will leak out through the combustion chamber wall. Then, specific impulse will decrease (no combustion of the corresponding mass of fuel) or it will create thermal overloading on the wall (in case of partial or total combustion of the fuel damaging the wall).
- If the porosity is limited, the fuel leaking out through the wall will reduce skin friction losses while the main part of fuel will burn normally resulting in an improved specific impulse by comparison with a perfectly fuel-tight material.

Further developed technologies

Beyond the works already in progress, the test facility, developed by MBDA France and ROXEL in their Bourges Subdray test center in the framework of PREPHA program, is under upgrading. The new test facility, called METHYLE, will allow to perform long endurance test in representative conditions to pursue and reinforce technology development by using a modular water-cooled dual mode ramjet combustion chamber able to integrate different kind of testing parts as for : element of variable geometry, sealing system, fuel- cooled structure, measurement techniques, engine control system.

4. Conclusion

The ramjet/scramjet concept constitutes the main airbreathing propulsion system which can be use in a very large flight Mach number range up to Mach 10/12 and then could allow to develop future fully reusable space launcher and military systems.
Beside international activities, mainly in USA and Japan, a permanent Research and Technology effort has been pursued in Europe since twenty years. Today, this effort is mainly led by France and

aims at addressing the two key technology issues which are the accurate prediction of the aero-propulsive balance of an airbreathing vehicle flying at high Mach number and the development of high-temperature structures for the combustion chamber able to withstand the very severe environment generated by the heat release process while ensuring reliability and limited mass and should allow to conclude on the feasibility and interest of the two possible application within seven or height years (2011/2012).

References

[1] F. FALEMPIN, Ph. NOVELLI, P. HENDRICK, A. SOUCHIER
Airbreathing/rocket combined cycle propulsion efforts in Europe
AAAF - 2002 - 268 - Versailles

[2] FALEMPIN, D. SCHERRER, G. LARUELLE, Ph. ROSTAND, G. FRATACCI
French Hypersonic Propulsion programme PREPHA - Results, Lessons and Perspectives AIAA - 98 - 1565 - Norfolk

[3] A. LENTSCH, R. BEC, F. DENEU, Ph. NOVELLI, M. RIGAULT, J.-M. CONRARDY
Air-Breathing Launch Vehicle Activities in France - The Last and the Next 20 Years
AIAA 2003-6949, Norfolk, December 2003.

[4] J. HUTT
Space Launch Roadmap
AIAA-2003-6941

[5] A. BOUDREAU
Status of the Air Force HyTech Program
AIAA-2003-6947

[6] K. FUJII, T. NAKAMURA, H. KAWATO and S. WATANABE
Concepts and Studies of Flight Experiment Vehicles for Reusable Space Transportation System
AIAA-2003-6984

[7] R. BOYCE, S. GERARD, A. PAULL
The HyShot Scramjet Flight Experiment - Flight Data and CFD Calculations Compared AIAA-2003-7029

[8] M. NAIR, N. KUMAR and S. SAXENA
Reynolds Averaged Navier-Stokes Based Aerodynamic Analysis of Inlet for a Hypersonic Research Vehicle AIAA-2003-7067

[9] J. LE, W. LIU, Y. TAN and W. HE
Performance Study of Model Scramjet with Fuel of Kerosene in Pulse Facility
AIAA-2003-6936

[10] F. FALEMPIN
High-speed airbreathing propulsion French activities
AIAA - 2002 - 5232

[11] F. FALEMPIN
French hypersonic program PREPHA - System studies synthesis
XIII ISABE - Chattanooga - 1997

[12] L. SERRE
Towards a low risk airbreathing SSTO program: a continuous robust PREPHA based TSTO AIAA - 99 - 4946 - Norfolk

[13] F. FALEMPIN
The fully reusable launcher: a new concept asking new visions
AIAA - 2003 - 7031

Security-Enhanced Cyberattack Recognition using Reinforcement learning and Intrusion Validation Engine

Devatharshini S[1], Dr.Mouthami K[2], Sharli Iris John Baskar[3], Subasri N[4]

Assistant Professor-III[2],
[1,2,3,4]Department of Computer Science and Engineering,
KPR Institute of Engineering and Technology, Coimbatore, India
E-mail: 25pcs03@kpriet.ac.in[1], mouthami.k@kpriet.ac.in[2], 25pcs13@kpriet.ac.in[3], 25pcs14@kpriet.ac.in[4]

Abstract: Increasing integration of artificial intelligence in autonomous vehicles has made in-vehicle networks and sensor systems vulnerable to cyberattacks, posing serious risks to safety and reliability. Conventional intrusion detection systems often fail to address evolving and unknown threats due to their dependence on static rules and labeled data. To overcome the drawback, a security-enhanced intelligent framework for cyberattack detection and adaptive defense in AI-enabled vehicles. The proposed system combines an unsupervised autoencoder-based anomaly detection model with a Proximal Policy Optimization (PPO) based deep reinforcement learning agent. The autoencoder learns normal communication and sensor behavior to identify suspicious activities, while the PPO agent dynamically selects appropriate response actions such as isolating compromised components, blocking malicious traffic, and activating fail-safe mechanisms. Experimental evaluations conducted on benchmark vehicular network datasets and simulated attack environments demonstrate improved detection accuracy, reduced false alarm rates, and enhanced system resilience. The results highlight the effectiveness of SECURE DRIVE in strengthening cybersecurity and ensuring safe autonomous vehicle operation.

Keywords: Cyber Attacks, AI Safety, Reinforcement Learning, PPO Algorithm, Anomaly Detection, Network Protection, Smart Vehicles, Data Security.

1. Introduction

The swift progress of artificial intelligence (AI) significantly changed the emergence of autonomous vehicles (AVs) through the intelligent perception, decision-making, and control automation. Currently, AVs consist of several interconnected ECUs (Electronic Control Units) that communicate over the CAN (Controller Area Network) and rely on sophisticated sensors and cloud-based services for their efficient and safe operation. However, upgraded performance and comfort of such vehicles through these technologies also imply that the attack surface is increased, in-vehicle systems therefore getting very vulnerable to cyber threats. Cyberattacks like message injection, spoofing, replay attacks, or denial-of-service (DoS) may interrupt the communication among the vehicle components, thus, causing safety-critical failure scenarios, for instance.

Existing IDSs (Intrusion Detection Systems) for vehicular environments mainly rely on either the signature-based or the supervised-learning approaches. These methods work well for known threats but inevitably they are helpless in identifying zero-day or new type of attacks as they are based on preset rules and a limited amount of labeled data. Besides, the majority of current solutions concentrates only on attack detection and hence, omits intelligent response or verification methods, so the capacity for threat neutralization in real-time is compromised.

In order to break these barriers, the authors of this article present a security-empowered cyber-attack detection framework for self-driving cars by utilizing reinforcement learning and an intrusion validation engine. The system put forward in this research is a combination of two models: one is an unsupervised anomaly detection model aimed at recognizing unusual communication patterns and, the other is a reinforcement learning agent based on the Proximal Policy Optimization (PPO) technique which can

result in dynamically determining the most preferable mitigatory actions. By integrating sophisticated detection and adaptable response, the architecture improves the robustness of the system, decreases the rate of false alarms, and elevates the overall cybersecurity level of future AVs.

2. Related Work

2.1 Intrusion detection in Vehicle Networks

Despite the fact that Controller Area Network (CAN) has been the primary means of communication within vehicles, it is still the case that CAN does not have authentication and encryption features built-in which leaves it susceptible to spoofing and injection attacks. A deep learning-based IDS for CAN networks was proposed by Song et al. [20] which showed the detection capabilities of the model were greatly enhanced over traditional statistical methods. Bari [12] also used deep learning methods to identify malicious CAN traffic and focused on providing real time monitoring capabilities. Alsaade and Al-Adhaileh [11] used deep autoencoder algorithms to learn the patterns of normal vehicle communication so that they would be able to detect anomalies based on the difference in reconstruction error. Jain and Gajjar [19] reviewed various anomaly detection systems for vehicular networks and pointed out that there is a requirement for smart and adaptive solutions that intelligently operate beyond pre-set detection mechanisms.

2.2 Hybrid Detection Model

Many researchers have looked at hybrid machine learning methods for network intrusion detection to get better detection accuracy. For example, Devan and Khare [18] developed an hybrid model for network intrusion detection system that resulted in increased accuracy of classification even in complicated attack scenarios. Hoang and Kim [14] presented semi-supervised convolutional adversarial autoencoders to overcome the scarcity of labeled data in the case of vehicular intrusion detection. Their method showed good generalization capabilities on new attack types. There are also recent developments in the lightweight AI models to ensure the security of IoV. Alam et al. [5] have designed DAIRE, a model for detecting CAN bus attacks in real-time which is computationally efficient and hence suitable for Internet of Vehicles environments.

2.3 Reinforcement Learning in Adaptive Cyber defense

Traditional IDS systems are mostly non-adaptive and focus on the detection part. Recent research highlights reinforcement learning (RL) as a potential technology that can continuously re-orient itself and thus adaptively mitigate threats in the future. In their paper, Raio et al. [10] characterises how RL-based autonomous cyber-defense agents can learn to continually resist a changing offensive environment. Sultana et al. [8] used deep reinforcement learning to figure out the best defense moves. In [6] a semi-supervised intrusion detection system (IDS) combining variational autoencoders with adversarial reinforcement learning was developed, which could not only identify attacks better but also change its response accordingly. Still, the use of sophisticated policy optimization methods like PPO in the context of vehicle cybersecurity has not been developed much so far.

2.4 Network Level Security in Autonomous Vehicle

Security issues related to vehicles will not just be limited to internal CAN networks as more and more vehicles depend on cloud services and V2X communication. The study on cloud-assisted vehicular networks [9] highlighted the importance of privacy and ways of making the system resistant attacks in a distributed manner. Zhang et al. [3] came up with a method of detecting anomalies in changing networks by adapting a model that learns online supported by the theory of continuous model adaptation.

2.5 Research Gap

- Most of the existing systems concentrate on either detection accuracy or adaptive response, not on both.
- There is little work to integrate unsupervised anomaly detection with reliable policy optimization algorithms such as PPO.
- Not much research is done on closed-loop intelligent defense that can not only discover but also dynamically validate and carry out optimal counter measures.
- Existing approaches often fail to validate and dynamically execute optimal countermeasures after detecting an intrusion

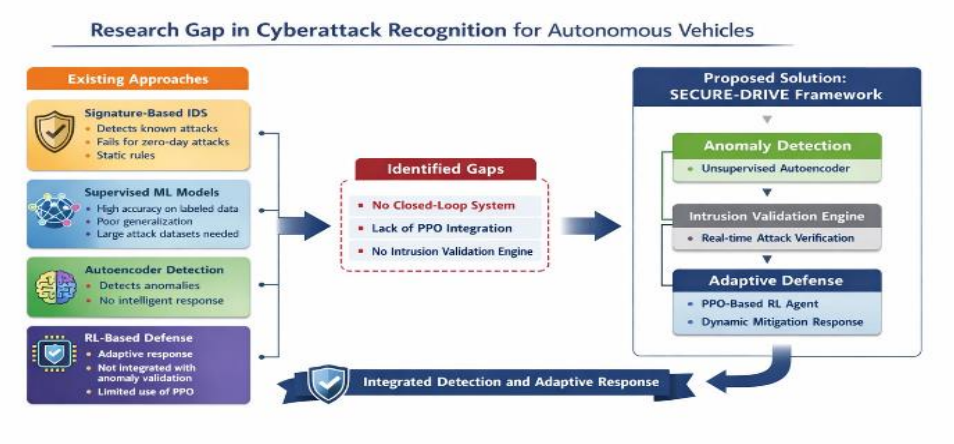

Figure 1. (Research gap and Proposed solution)

3. Proposed Architecture

The proposed framework Security-Enhanced Cyberattack Recognition system for autonomous vehicles by combining unsupervised anomaly detection, Proximal Policy Optimization (PPO), and an Intrusion Validation Engine (IVE). It is a closed-loop adaptive cyber defense architecture that can detect, validate, and mitigate attacks in real time. The Architecture diagram of the proposed system is shown in Fig. 2.

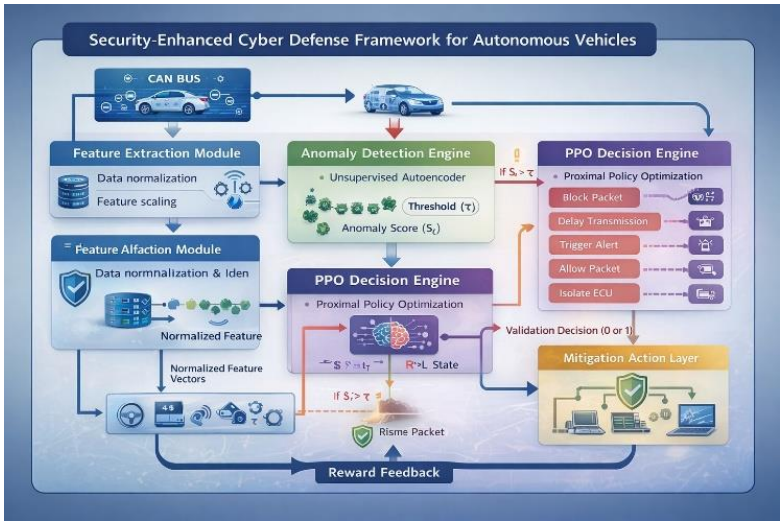

Figure 2. (Framework of Proposed System)

3.1 CAN Data Acquisition

The CAN Data Acquisition Layer is really the core of the newly developed framework since it perpetually watches and tracks real-time traffic from the in-vehicle CAN. The module collects each frame by using a passive interface connection to the CAN bus without disrupting the regular operation of the vehicle. Each captured frame comprises the message identifier (ID), payloads bytes, data length code (DLC) and an accurate timestamp that records the chronological details. These are vital for the identification of timing-based attacks like replay, flooding, and spoofing. A buffer system is in place to handle the data properly even when there is very high traffic, thus no packets are lost, and the communication remains intact. The gathered frames are then organized and sent in a streaming format to the feature processing module for the security analysis with almost no delay, which is essential for intrusion detection and adaptive reaction based on the situation.

3.2 Feature Procession and Data Normalization

The Feature selection and data Normalization module converts raw CAN frames into well-organized numerical representations that are ready for intelligent processing. Various statistical, temporal, and behavioral features are extracted from each captured frame to depict the communication patterns among the Electronic Control Units (ECUs). Major features are the distribution of message ID frequency, statistics of inter-arrival time, entropy of payload, variance at the byte level, and patterns of message repetition. The mentioned features allow the system to recognize content as well as timing behavior anomalies, which are essential markers of cyberattacks such as spoofing, replay, and denial-of-service attacks. Subsequently, the feature vector undergoes normalization, which is a process of applying standard scaling techniques to maintain numerical stability and ensure consistent convergence during model training. Through this normalization, the influence of different feature scales on the bias is minimized and the effectiveness of both anomaly detection and reinforcement learning modules is improved.

3.3 Anomaly Detection Engine

Anomaly Detection Engine detects suspicious CAN traffic through learning normal communication behavior of vehicle network. The autoencoder, as an unsupervised learning model, was chosen to characterize the legitimate traffic patterns without having the need for labeled attack data. The normalized feature vector is taken through the trained model during operation, which tries to reconstruct the input features. Anomaly score is calculated as the difference (or error) between the original and reconstructed features. If this anomaly score is above a certain limit, the related CAN frame is marked as suspicious and sent to the reinforcement learning-based decision module. However, the traffic can be considered normal if it is allowed to pass without any intervention. This unsupervised method, on the one hand, leads to the discovery of both known and previously unknown (zero-day) attacks and, on the other hand, keeps the system capable of adjusting to the constantly changing patterns of vehicular communication.

3.4 Decision Engine PPO

The PPO-based Decision Engine is the one that chooses the best blending methods to be applied to the suspicious traffic instances that the Anomaly Detection module has flagged. The security environment is being formulated as a Markov Decision Process (MDP) where the state of the system is represented by the normalized features vector along with the anomaly score. A Proximal Policy Optimization (PPO) agent takes the state as input and performs an action by following the policy that it has learned. The actions that can be taken are: block the packet, delay the transmission, raise an alert, allow communication under monitoring, or isolate the compromised Electronic Control Unit (ECU). The PPO method is selected for its stable and reliable policy update mechanism through a clipped surrogate objective function that avoids large policy updates during training. The goal of the agent is to maximize

the total reward while at the same time minimizing the number of false alarms, the time taken to respond, and the degree of disruption to the operation. By continuously experimenting with the environment and receiving the reward signal, the PPO-based decision engine keeps on upgrading its mitigation strategy which is the basis of an adaptive and smart cyber defense system.

3.5 Intrusion Validation Engine

The Intrusion Validation Engine (IVE) is the security reinforcement layer that checks the mitigation action selected by the PPO-based decision engine before it is executed. Although the reinforcement learning agent is designed to maximize long-term rewards, its decisions can sometimes result in excessively aggressive or unsafe responses, especially at the very beginning of training. The IVE mitigates such risks by enforcing safety rules as well as by setting confidence and operational-policy thresholds to evaluate the proposed action. Among the parameters considered are the anomaly severity, system stability requirements, the communication criticality of the targeted ECU, and the possible impact on vehicle performance. If the action passes all validation criteria, it is accepted and sent to the mitigation layer. If not, the system resorts to a standby safe fallback option, for example, communication under surveillance or alert generation, to avoid unexpected disturbances. Additional validation step enables a reliable, secure, and feasible release of adaptive cyber defense strategies in the challenging real-time environment of autonomous vehicles.

3.6 Mitigation action and reward estimation

The part of the system that stops threats from hurting the vehicle's network is called the Mitigation Action Layer. It does this by doing things that have been checked and approved to stop the threats in real time. When the Intrusion Validation Engine says an action is okay, it gets sent to the vehicle's system through a special connection that talks to the CAN bus. The ways to stop threats include stopping bad packets, slowing down suspicious messages, keeping a compromised ECU from talking to the rest of the system, or sending alerts to other systems that watch for security problems. The system is designed to do all this quickly and without disrupting important safety functions. After the system takes action, it looks at how well it did and gives itself a score. This score is based on things like whether it stopped the attack, didn't make too many false alarms, kept the system stable, and did it all quickly. If it did a good job, it gets a positive score, but if it made mistakes or missed something, it gets a penalty. This score then gets sent back to the system's brain, which uses it to make its decisions better over time. This helps the system get better at stopping threats and making good decisions, even as the threats change and get smarter. It's like a big loop where the system tries, learns, and gets better, so it can keep the vehicle and its passengers safe from cyber threats.

3.7 Mathematical Formulation

The cyber defence system proposed is designed as a sequential transformation and decision-making process integrating anomaly detection and reinforcement learning in a closed-loop architecture.

i. CAN Traffic Modelling

$$f_t = \{ID_t, DLC_t, D_t, T_t\} \quad (1)$$

where
$ID_t \in Z$ is the message identifier,
$DLC_t \in \{0,1,\dots,8\}$ is the data length code,
$D_t \in \mathbb{R}^8$ is payload bytes,
$T_t \in R$ is the timestamp.
The stream of CAN traffic is

$$D = \{f_1, f_2, \dots, f_T\} \quad (2)$$

ii. Transformation of Feature and Normalization

The extracted feature vector

$$\mathbf{x}_t = [f_1, f_2, \ldots, f_n]^T \quad (3)$$

Extracted features:

- ID frequency:

$$f_{ID} = \frac{\text{count}(ID_t)}{\Delta T} \quad (4)$$

- Inter-arrival time:

$$f_{IAT} = T_t - T_{t-1} \quad (5)$$

- Payload entropy:

$$f_{entropy} = -\sum_{i=1}^{8} p_i \log p_i \quad (6)$$

Features are standardized:

$$\mathbf{z}_t = \frac{\mathbf{x}_t - \boldsymbol{\mu}}{\boldsymbol{\sigma}} \quad (7)$$

where:

- $\boldsymbol{\mu}$= mean vector
- $\boldsymbol{\sigma}$= standard deviation

iii. Unsupervised Anomaly Detection

Anomaly scoring function as:

$$S_t = g(\mathbf{z}_t) \quad (8)$$

where

$g(\cdot)$ is the anomaly detection model.

Reconstruction-based models:

$$S_t = || \mathbf{z}_t - \hat{\mathbf{z}}_t ||_2^2 \quad (9)$$

Classification rule:

$$y_t = \begin{cases} 1, & \text{if } S_t > \theta \\ 0, & \text{otherwise} \end{cases}$$

where:

- $y_t = 1$ indicates suspicious traffic
- θ is anomaly threshold

iv. MDP Formulation for PPO

Formulation for PPO as

$$M = (S, A, P, R, \gamma) \quad (10)$$

Where:

- S denotes State space
- A denotes Action space
- P denotes Transition probability
- R denotes Reward function
- $\gamma \in (0,1)$= Discount factor

State representation:

$$s_t = [\mathbf{z}_t, S_t, y_t] \quad (11)$$

Action space:

$$A = \{a_1, a_2, \ldots, a_k\} \quad (12)$$

v. PPO Objective Function

Policy $\pi_\theta(a \mid s)$is parameterized by neural network weights θ.

Probability ratio:

$$r_t(\theta) = \frac{\pi_\theta(a_t \mid s_t)}{\pi_{\theta_{old}}(a_t \mid s_t)} \quad (13)$$

Advantage estimation:

$$A_t = R_t + \gamma V(s_{t+1}) - V(s_t) \quad (14)$$

vi. PPO Optimization

Reward is formulated as:

$$Rt = \alpha Rmit - \beta Rfp - \delta Rlat \quad (15)$$

Where:

- R_{mit}= mitigation action success reward
- R_{fp}= false positive penalty
- R_{lat}= response latency penalty
- α, β, δ= weighting coefficients

vii. Intrusion Validation Model

The PPO-selected action a_t, safety validation is applied:

$$\Psi(a_t, s_t) \leq \kappa \quad (16)$$

where:

- $\Psi(\cdot)$= safety constraint function
- κ= predefined safety threshold

Final executed action:

$$a_t^* = \begin{cases} a_t, & \text{if validated} \\ a_{safe}, & \text{otherwise} \end{cases}$$

viii. Closed-Loop Learning

Total discounted return

$$J(\theta) = \mathbb{E}\left[\sum_{t=0}^{\infty} \gamma^t R_t\right] \quad (17)$$

PPO algorithm updates θ to maximize:

$$\theta^* = \arg\max_\theta J(\theta) \quad (18)$$

Hence, the system continuously keeps evolving in line with the changes in cyber threats through policy refinement.

4. Result and performance Evaluation

4.1 Experimental Setup

The secured framework that was presented in the paper has been tested with the help of a CAN bus dataset, which was labeled and included the normal vehicle communication as well as the malicious attack traffic in the form of injection and spoofing attacks. The dataset splited into training and testing sets to allow a fair evaluation of the models' performance. The anomaly detection model was trained only with normal traffic data, whereas the PPO-based mitigation agent was trained for 500 episodes until it reached a stable policy convergence. The performance evaluation was done by leveraging common cybersecurity evaluation metrics.

Confusion Matrix

The obtained results from the confusion matrix have proved that the proposed method has excellent classification performance. Most of normal CAN messages were correctly recognized as legitimate, and only a very small number of them were incorrectly identified as malicious. Likewise, the majority of attack instances were correctly detected, whereas only a very small number of malicious messages were misclassified as normal traffic. The framework has a high ability to clearly separate benign from malicious CAN communications as evidenced by the low number of misclassifications. The effectiveness of the anomaly detection and intrusion validation mechanisms integration for delivering reliable and robust cybersecurity performance has been confirmed by these results.

Classification Performance

The results demonstrated the robustness and reliability of the proposed detection model. The classifier effectively distinguishes between normal and attack instances, achieving strong predictive performance. High precision ensures reliable attack predictions with minimal false alarms, while strong recall confirms effective identification of actual attack samples. The balanced F1-score highlights stable performance across evaluation metrics. Additionally, false negative and false positive rates indicate the model’s capability to reduce unnecessary alerts and missed detections. Overall, the findings evaluate the effectiveness and practical applicability of the proposed framework.

PPO Training Performance

The PPO-based mitigation agent met the stability criteria of convergence during training. The cumulative reward was on an upslope gradually over the stretch of 500 episodes signifying enhanced decision-making capacity at each step.

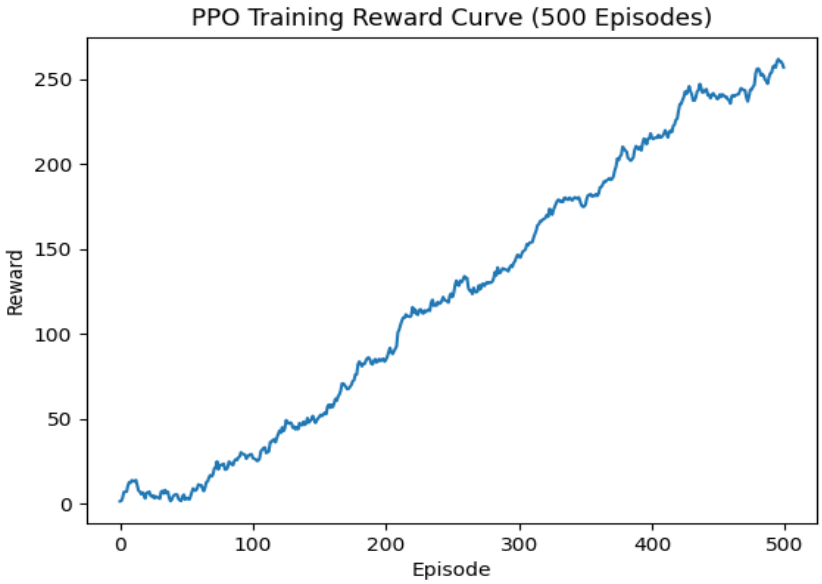

Figure 3. (PPO reward curve over 500 episodes)

The training loss curve showed a downward trend and reached a plateau after the exploratory phase, thus confirming stable gradient updates under the clipped surrogate objective function. There was no indication of policy collapse or oscillatory instability.

Figure 4. (PPO loss curve over 500 episodes)

Convergence was attained most likely within the 350 to 400 episodes range, thus confirming the appropriateness of PPO to adaptive cybersecurity mitigation in live settings.

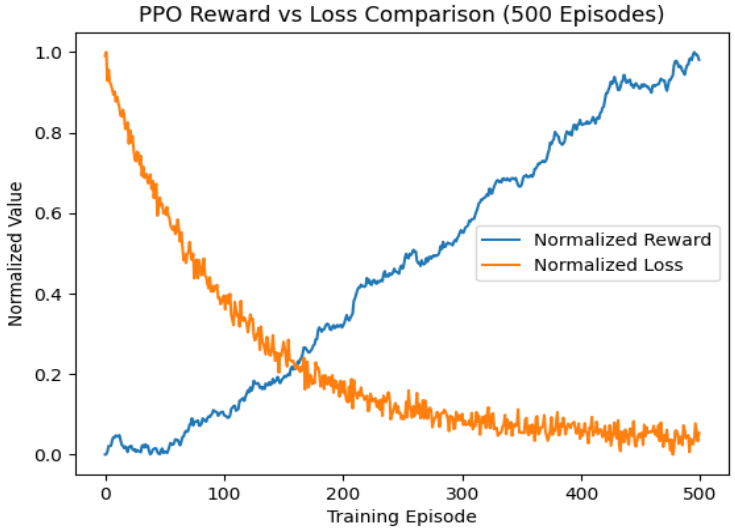

Figure 5. (PPO reward vs loss Convergence Comparison)

Intrusion Validation Imapact

The feature of the Intrusion Validation Engine greatly contributed to the dependability of the system by double-checking the mitigation actions prior to their implementation. The presence of this validation layer led to a lowering of the unnecessary mitigation responses and an increase of the overall decision confidence. By sticking to preset safety limits, the framework was able to stop the release of harmful mitigation actions that could have led to the disruption of the vehicle's normal operations. The slight delay caused by the validation was kept to a minimum, thus allowing the maintenance of the system's real-time functionality.

4.2 Comparative Analysis

Table I provides a overall summary of the comparative evaluation results, featuring the proposed SECURE-DRIVE framework which outperforms in terms of accuracy, false positive rate, mitigation success, and stability.

Table 1. (Comparison table)

Method	Accuracy	FPR	Mitigation	Stability
Traditional AD	93.12%	5.8%	N/A	High
Supervised ML	95.45%	4.2%	82.14%	Moderate
RL without IVE	96.20%	3.7%	90.03%	Low
Proposed Model	97.84%	2.04%	95.62%	High

Overall System Performance

The integrated framework brings together anomaly detection, reinforcement learning-based mitigation, and safety validation into a one single closed-loop cybersecurity system. The results indicate a very accurate detection, stable convergence of reinforcement learning, low rate of false alarms, and effective adaptive response. The framework by nature of its operations is capable of running in real-time and it keeps on improving at the same time through reward-driven policy optimization. This makes it a very strong and scalable solution for protecting automotive CAN networks of autonomous vehicles.

5. Conclusion

In the paper, we discussed how cyberattack defense systems for autonomous vehicles are limited by their focus either on detection accuracy or on adaptive response, and the lack of integration between unsupervised anomaly detection and reinforcement learning-based policy optimization. We propose a solution to these problems that integrates autoencoder-based anomaly detection with a PPO-driven intrusion validation engine, thereby allowing both accurate cyberattack recognition and adaptive mitigation strategies in real time. This combined method facilitates a closed-loop intelligent defense system that continuously validates and implements the best countermeasures. The suggested approach represents a viable path towards the creation of real-time, robust cybersecurity solutions for autonomous vehicle systems.

References

[1] "Intrusion detection system for autonomous vehicles using sensor spatio-temporal information," *Computers & Security*, Vol. 156, 104502, 2025.

[2] AutoGuardX: A comprehensive cybersecurity framework for connected vehicles," *arXiv preprint arXiv:2508.18155*, Aug. 2025.

[3] X. Zhang, P. Patel, and A. Roy, "Adaptive anomaly detection with online learning in network traffic," *IEEE Transactions on Information Forensics and Security*, vol. 19, pp. 1523–1535, 2025.

[4] "A deep learning/machine learning approach for anomaly-based network intrusion detection," *Frontiers in Artificial Intelligence*, vol. 8, 2025.

[5] S. Alam, M. Rahman, and K. Kim, "DAIRE: A lightweight AI model for real-time detection of CAN bus attacks in the Internet of Vehicles," *Machine Learning with Applications*, vol. 23, 2025.

[6] "Semi-supervised intrusion detection system for in-vehicle networks based on variational autoencoder and adversarial reinforcement learning," *Knowledge-Based Systems*, vol. 304, p. 112563, Nov. 2024.

[7] A.w Alfardus and D. B. Rawat, "Machine learning-based anomaly detection for securing in-vehicle networks," *Electronics*, vol. 13, no. 10, p. 1962, 2024.

[8] R. Sultana, A. Mahmood, and J. Cho, "Intelligent defense strategies for VANET using deep reinforcement learning," *Pervasive and Mobile Computing*, vol. 103, 2024.

[9] "Enhancing cybersecurity and privacy protection for cloud-assisted vehicular networks of autonomous electric vehicles," *World Electric Vehicle Journal*, vol. 16, no. 1, 2024.

[10] S. Raio, L. Romano, and F. Palmieri, "Reinforcement learning as a path to autonomous intelligent cyber-defense agents in vehicle platforms," *Applied Sciences*, vol. 13, no. 21, p. 11621, 2023.

[11] F. W. Alsaade and M. H. Al-Adhaileh, "Cyber attack detection for self-driving vehicle networks using deep autoencoder algorithms," *Sensors*, vol. 23, no. 8, p. 4086, 2023.

[12] B. S. Bari, "Intrusion detection in vehicle controller area network using deep learning," *Sensors*, vol. 23, no. 7, p. 3610, 2023.

[13] P. Cheng, Y. Li, and H. Wang, "LSF-IDM: Automotive intrusion detection model with lightweight attribution and semantic fusion," *arXiv preprint arXiv:2308.01237*, Aug. 2023.

[14] T.-N. Hoang and D. Kim, "Detecting in-vehicle intrusion via semi-supervised learning-based convolutional adversarial autoencoders," *arXiv preprint arXiv:2204.01193*, Apr. 2022.

[15] R. S. Gundu and M. Maleki, "Securing CAN bus in connected and autonomous vehicles using machine learning approaches," in *Proc. IEEE Int. Conf. Emerging Technologies (eIT)*, 2022, pp. 1–6.

[16] H. J. Yoon, "Intrusion response system for in-vehicle networks," National Science Foundation Report, 2022.

[17] S. Kumar, R. Singh, and A. Sharma, "AI-powered security system for CAN bus attack identification in electric vehicles," *International Journal of Electrical and Computer Engineering*, vol. 12, no. 4, pp. 3985–3994, 2022.
[18] P. Devan and N. Khare, "An efficient XGBoost-DNN-based classification model for network intrusion detection," *Neural Computing and Applications*, vol. 32, no. 20, pp. 15977–15991, 2020.
[19] A. Jain and M. B. Gajjar, "A survey of anomaly detection systems for in-vehicle networks," *International Journal of Vehicular Technology*, vol. 2020, Article ID 8851234, 2020.
[20] Y. Song, G. Chen, and J. Wu, "Deep learning-based intrusion detection system for controller area networks," *IEEE Access*, vol. 8, pp. 162558–162567, 2020.

Smart Sign Language Interpreter: Real-time Adaptive Detection and Speech Synthesis with Confidence Estimation

Subasri N[1], Devatharshini S[2], Dr.Mouthami K[3], Sharli Iris John Baskar[4]

Assistant Professor-III[3]
[1,2,3,4]Department of Computer Science and Engineering
KPR Institute of Engineering and Technology
Coimbatore, India
E-mail: 25pcs14@kpriet.ac.in[1], 25pcs03@kpriet.ac.in[2], mouthami.k@kpriet.ac.in[3], 25pcs13@kpriet.ac.in[4]

Abstract: Sign language recognition functions as a critical tool which helps people with hearing and speech disabilities communicate with the hearing population. The current deep learning systems deliver accurate results for real-time sign language interpretation yet they operate as fixed systems which cannot adjust to different signing patterns resulting in output errors during unpredictable circumstances. Adaptive and uncertainty-aware real-time sign language interpretation system is designed to enhance personalization and reliability. The proposed framework employs Random Forest for alphabet recognition and Media Pipe for accurate hand landmark extraction. An adaptive personalized learning module is introduced to accommodate user-specific signing variations, improving recognition performance without complete model retraining. In addition, an uncertainty detection mechanism evaluates prediction confidence under challenging scenarios such as occlusion and lighting variations, allowing the system to reject low-confidence outputs and prompt user interaction. The recognized signs are converted into text with suggestion assistance and further synthesized into speech using a text-to-speech module. Experimental evaluation demonstrates that the proposed system improves robustness and consistency while maintaining high real-time performance, making it suitable for practical assistive communication applications

Keywords: Sign Language Recognition, MediaPipe, Random Forest, Confidence Estimation, Dynamic Stability Filtering, Adaptive Learning, Text-to-Speech.

1. Introduction

People with hearing and speech impairments use sign language as their main way to communicate. The impaired individuals still face communication challenges with hearing people because the current technology has not solved these problems. Automatic Sign Language Recognition (SLR) systems create a solution for this problem by converting hand gestures into written or spoken language which enables users to communicate in real-world situations. The development of real-time gesture recognition systems became possible through computer vision and deep learning advancements which use convolutional neural networks and landmark-based systems to identify user gestures.

The MediaPipe hand landmark detection framework provides efficient extraction of spatial hand features which enables users to implement lightweight systems that operate in real time. The current systems aim to improve classification accuracy but they fail to address vital real-world challenges which include managing unpredictable results and handling uncertain situations and adapting to different signing styles of individuals.Users of real-time systems experience gesture prediction changes between frames because of their hand movements and changing light conditions and when their hands become partially hidden. The system suffers from reliability problems because the unstable system creates incorrect letter formation. Conventional static training methods require complete model retraining for user-specific

signing pattern adjustments. The system fails to provide users with word and sentence formation assistance because it lacks contextual intelligence.

Smart Sign Language Interpreter system combines confidence-aware prediction, dynamic stability filtering, adaptive personalized learning and context-aware language modeling into a single framework. The system uses MediaPipe-based landmark extraction to deliver both effective and reliable methods of capturing features. The system uses a confidence estimation mechanism which filters out predictions that lack reliability during unpredictable situations in order to stop incorrect outputs from occurring. The Dynamic Stability Filtering algorithm prevents prediction flickering by verifying the gestures through multiple frames until it detects consistent movement patterns which maintain their natural progress throughout the time.

The adaptive learning module allows the model to learn from new signing patterns which each individual shows without needing to perform a complete model retraining process. The system offers intelligent next-word suggestions through a probabilistic bigram language model while the recognized text transforms into speech through a real-time text-to-speech module. The system establishes a dependable assistive communication solution through its combination of robust features and personalized user experience and contextual understanding abilities.

2. Related Work

The research of Sign Language Recognition (SLR) uses computer vision and deep learning methods for its comprehensive investigation [2]–[4]. The first systems required manual feature development which included contour analysis and color segmentation, but these features could not operate correctly under changing light conditions and different background elements [3]. The methods showed easy computational execution but they failed to maintain reliable performance during actual operational conditions [2].

Deep learning introduction brought significant accuracy enhancements for gesture classification through convolutional neural networks (CNNs) [4], [7]. Image-based models learn spatial features directly from raw frames but often require large datasets and high computational resources [4]. The full-frame classification methods experience performance issues due to background noise and user differences [6].

Landmark-based techniques have become popular because they provide solutions to existing problems. The MediaPipe framework enables users to extract 21 hand keypoints in real time, which allows them to perform gesture recognition using an efficient and lightweight system [1], [5]. The current landmark-based systems only achieve classification accuracy, which creates problems because they do not handle temporal instability and uncertainty management and personalization requirements [15].

The majority of SLR systems fail to provide confidence assessment capabilities together with contextual comprehension abilities. The system accepts predictions without checking their reliability, which results in incorrect outcomes when facing difficult situations [8], [9]. The current assistive systems do not support adaptive learning with context-aware word suggestion features. [11], [15].

The proposed research solution combines landmark-based recognition with dynamic stability filtering and confidence estimation and adaptive personalization and contextual speech synthesis to achieve enhanced performance and real-time system operation.

3. Proposed Methodology

3.1 System overview

The Smart Sign Language Interpreter system functions as a complete real-time communication tool that transforms hand movements into accurate spoken words. The system consists of interconnected modules which work together to provide dependable and accurate interpretation results. The system starts by using MediaPipe to detect hands from live video feeds to create spatial keypoints which represent hand

landmarks. The machine learning process requires conversion of these landmarks into a compact feature representation which is suitable for implementation. The gesture classification model predicts which alphabet gesture corresponds to the input, and the confidence estimation mechanism evaluates how accurate the prediction is. The Dynamic Stability Filtering module permits gesture confirmation after detecting continuous frames. The model includes an adaptive personalized learning component which enables users to incrementally upgrade their personalized signing patterns through machine learning. The system transforms recognized letters into complete words and sentences, while a context-aware word prediction module is used to provide intelligent next-word suggestions. The assistive communication system ends with the text-to-speech module which transforms generated text into audible speech.

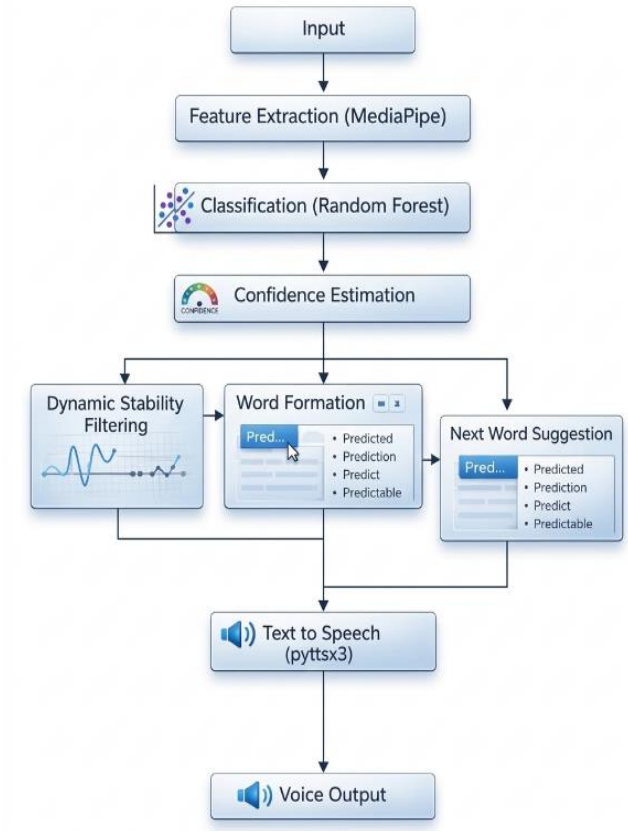

Figure 1. Sign Language Interpreter Architecture

3.2 Hand Landmark Extraction and Feature Represenattion

The proposed system uses MediaPipe for real-time hand detection and landmark extraction. MediaPipe identifies 21 key points on the detected hand that represents joint positions such as fingertips knuckles and wrist coordinates. Each landmark is represented by three spatial coordinates xyz which contains normalized image coordinates for x and y and relative depth information for z.

For each frame, the extracted landmarks are structured into a fixed-length feature vector. If $L_i = (x_i, y_i, z_i)$denotes the i^{th}landmark, the complete feature vector is constructed as:

$$F = [x_1, y_1, z_1, x_2, y_2, z_2, \dots, x_{21}, y_{21}, z_{21}] \qquad (1)$$

Thus, the dimensionality of the feature vector is:

$$D = 21 \times 3 = 63$$

This landmark-based representation of visual data shows multiple benefits when compared to processing unprocessed image data. It decreases system resource requirements while it decreases unwanted background noise and maintains system performance during different lighting conditions. The model achieves fast real-time performance because it analyzes hand shape through geometric data instead of processing individual pixels.

3.3 Gesture Classification and Model Training

The extracted 63-dimensional landmark feature vector defined in (1) is provided as input to a supervised machine learning classifier for alphabet recognition. The system uses Random Forest classifier because it

provides strong performance with structured numerical data while maintaining low computational requirements and high system reliability.

Random Forest constructs multiple decision trees during training and outputs the class prediction based on majority voting. The training dataset is represented as:

$$D = \{(F_i, y_i)\}_{i=1}^{N} \qquad (2)$$

where $F_i \in \mathbb{R}^{63}$denotes the landmark feature vector and $y_i$represents the corresponding alphabet label.

Each decision tree in the forest is trained using a bootstrap sample drawn from the dataset. At each split node, a random subset of features is selected, and the optimal split is determined based on impurity reduction. The Gini impurity used for node splitting is defined as:

$$G = 1 - \sum_{k=1}^{K} p_k^2 \qquad (3)$$

where $p_k$is the proportion of samples belonging to class $k$at a given node, and $K$is the total number of classes.

For a new input feature vector F, each decision tree produces a class prediction $T_m(F)$, where $m = 1,2,\dots,M$and $M$is the total number of trees. The final prediction is obtained using majority voting:

$$\hat{y} = \text{mode}\{T_1(F), T_2(F), \dots, T_M(F)\} \qquad (4)$$

The confidence of prediction is computed as the proportion of trees voting for the predicted class:

$$C = \frac{1}{M} \sum_{m=1}^{M} \mathbb{I}(T_m(F) = \hat{y}) \qquad (5)$$

where $\mathbb{I}(\cdot)$is the indicator function.

The Random Forest classifier provides several advantages for the proposed system. The system uses ensemble averaging to decrease overfitting while it can effectively manage non-linear decision boundaries and needs only basic parameter settings. The system achieves real-time performance through its lightweight inference mechanism which supports live gesture recognition applications.

3.4 Confidence estimation and uncertainity handling

The real-time sign language recognition systems face difficulties because their predictions show decreased accuracy when users encounter occlusion and motion blur and lighting changes and display uncertain hand movements. The system establishes trustworthiness through a confidence estimation mechanism which uses Random Forest classifier ensemble voting results for its prediction process.

Let the forest consist of Mdecision trees. For an input feature vector F, each tree $T_m$produces a class prediction:

$$T_m(F), m = 1,2,\dots,M$$

A threshold-based decision rule is then applied:

Accept prediction if $C \geq \tau$(6)
Reject prediction if $C < \tau$(7)

where $\tau$is a predefined confidence threshold (typically between 0.7 and 0.9).
The system suppresses its output when confidence drops below the threshold and requires users to either change their position or repeat their gesture. The system derives confidence from ensemble agreement between trees which means that lower confidence levels show greater uncertainty in the model. The system uses this uncertainty-aware mechanism to block unreliable predictions from entering the output sequence which results in better system protection and actual performance. The system creates better real-time assistive communication by eliminating low-confidence outputs which prevents word formation errors from spreading throughout the system while increasing overall system reliability.

3.5 Dynamic stability filtering

Real-time gesture recognition systems face challenges because their predictions change from frame to frame due to tiny hand movements and camera noise and environmental changes. The system's output text becomes inaccurate because of repeated letters and incorrect letters which the system adds to the text. The Dynamic Stability Filtering mechanism solves this problem by maintaining time-based consistency throughout its operation.
Let $\hat{y}_t$denote the predicted class at time frame t. A gesture is confirmed only if the same prediction persists for n consecutive frames.If this condition is satisfied, the gesture is considered stable and appended to the output sequence. Otherwise, the system continues monitoring subsequent frames without confirming the prediction.
Additionally, stability filtering is applied only after the confidence threshold condition is met:

$$C_t \geq \tau$$

where C_t represents the confidence score at frame t, and $\tau$is the predefined confidence threshold.
The system achieves improved prediction accuracy through its combination of confidence validation and temporal consistency which stops users from producing duplicate character input. The system achieves better operational strength through this mechanism which enables users to interact with the system in a more fluid manner during real-time usage. System responsiveness requirements determine the appropriate tuning range for parameter n. The system confirms results faster with small value settings, but users experience prolonged verification times when they select high value settings.

3.6 Adaptive personalized learning

People show different sign language gestures because their hand shapes and their signing speeds and their signing styles differ from one another. The system creates adaptive learning through its personalized learning system which handles the different learning requirements of users. The Random Forest classifier does not support direct parameter updates which distinguishes it from neural network-based models that use gradient descent optimization. The system achieves personalization through two methods which include incremental dataset expansion and model retraining at scheduled times. The system stores the landmark feature vector F together with the corrected label y in a personalization buffer when users provide output corrections to predictions made with moderate confidence. The original training dataset defined in (2) is expanded during personalization.
The personalized dataset becomes:

$$D' = D \cup \left\{\left(F_j^{user}, y_j^{user}\right)\right\} \qquad (8)$$

The Random Forest model undergoes retraining after the collection of enough user-specific samples and the acquisition of the new dataset D^\\prime. The Random Forest algorithm maintains its computational

efficiency for retraining because it operates as an ensemble system of separately trained decision trees that do not depend on backpropagation methods. The system uses this adaptive update system to develop user-specific gesture recognition skills while maintaining complete model stability. The system achieves better recognition accuracy for each user because it learns from their data over time while maintaining its ability to work in real-time.

3.7 Context-aware word prediction

The system incorporates a context-aware word prediction mechanism which improves communication efficiency while decreasing the need for users to put in additional work. The model uses a probabilistic Bigram Language Model to generate its most likely next word prediction after users create a valid word through letter combination.

In a bigram model, the probability of a word $w_i$depends only on the previous word w_{i-1}. The conditional probability is defined as:

$P(w_i \mid w_{i-1}) = \frac{Count(w_{i-1},w_i)}{Count(w_{i-1})}$(9)

where:

- $Count(w_{i-1}, w_i)$is the frequency of the word pair,
- $Count(w_{i-1})$is the total occurrences of the previous word.

The next-word suggestion is obtained by selecting the word with maximum conditional probability:

$\widehat{w} = \arg\max_{w} P(w \mid w_{i-1})$(10)

The probabilistic method delivers lightweight contextual intelligence because it does not create substantial computational requirements. The system enables faster sentence construction because it helps users build effective phrases.

3.8 Speech synthesis module

The Text-to-Speech (TTS) module provides complete assistive communication through its ability to convert recognized text into spoken words based on contextual understanding. The TTS module transforms the textual input S into an audio waveform signal A(t), which enables people to speak. This transformation can be expressed as:

$$A(t) = \text{TTS}(S) \quad (11)$$

where $\text{TTS}(S)$ represents the speech synthesis function and $A(t)$ denotes the speech signal over time t.
The combined system uses speech synthesis to transform interpreted sign language into spoken words which hearing people can understand during live performances. The module operates with minimal latency to preserve conversational flow. The proposed system uses gesture recognition and contextual intelligence together with speech generation to create a complete communication solution which enables users to interact with others through assistive technology.

4. Experimental setup and results

4.1 Dataset collection and preparation

Custom American Sign Language (ASL) alphabet dataset was collected to assess the performance of their system. Dataset was collected through standard webcam maintaining constant lighting conditions. The gestures of 26 alphabets was shown multiple times to demonstrate different hand movements.

The system processed each gesture sample in real time through MediaPipe which extracted 21 hand landmarks. The system generated a 63-dimensional feature vector for each frame by merging the (x, y, z)coordinates of all detected landmarks.
N samples were collected for each class so that the dataset is distributed equally across all alphabet categories. 80:20 ratio was used for training and testing sets through which model's performance was assessed.
To ensure data quality:

- Frames with incomplete hand detection were discarded.
- Landmark normalization was applied relative to the wrist coordinate.
- Duplicate unstable frames were removed.

This custom dataset allows the system to better reflect realistic signing behavior.

4.2 Training configuration

The extracted 63-dimensional landmark feature vectors were used to train a Random Forest classifier for alphabet recognition. The dataset was divided into training and testing subsets to evaluate generalization performance.

- The Random Forest model was configured with: Mdecision trees
- Maximum tree depth selected empirically
- Gini impurity as the splitting criterion
- Bootstrap sampling enabled for tree diversity

The training process for each decision tree used a randomly selected portion of the complete dataset which included random feature selection during each decision boundary split to enhance model performance and decrease overfitting problems. The model evaluation used standard performance metrics which included accuracy, precision, recall, and F1-score to measure its effectiveness. The Random Forest ensemble structure protects landmark detection from noise interference while it maintains consistent classification results across various real-world testing conditions. The Random Forest classifier supports real-time sign language recognition because of its ability to perform quick predictions through its non-parametric design and capacity to process multiple tasks simultaneously.

5. Experimental Results

The proposed system achieved high recognition accuracy across the 26 alphabet classes. The landmark-based system reduced background interference which enabled better computational performance.
Key observations include:

- The confidence estimation mechanism effectively rejected uncertain predictions caused by partial occlusion and motion blur.
- Dynamic Stability Filtering reduced flickering outputs and prevented duplicate character insertion.
- Adaptive personalization improved accuracy for user-specific signing patterns after incremental updates.
- The system maintained real-time performance of approximately 20–30 FPS on standard hardware.

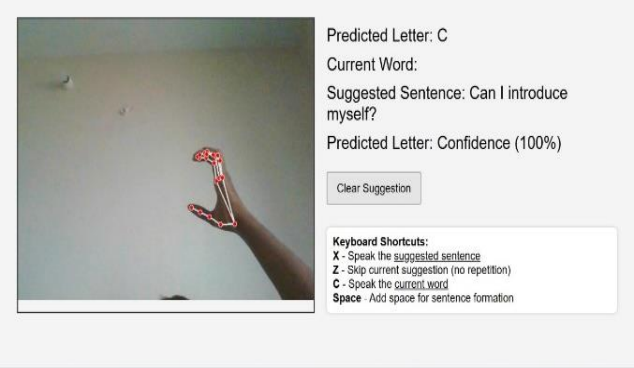

Figure 2. Real-Time Hand Gesture Recognition Output with Confidence Score and Sentence Suggestion

The integration of contextual word prediction further enhanced sentence construction efficiency, making the system practical for assistive communication scenarios.

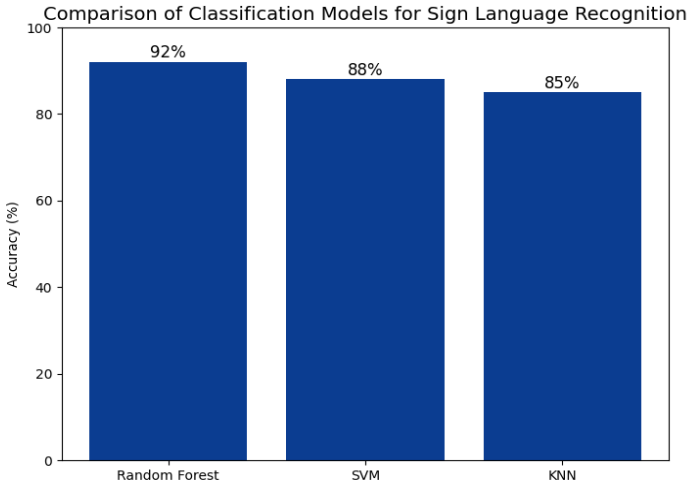

Figure 3. Comparison with Existing Models

The bar chart displays comparison of three machine learning models, Random Forest, Support Vector Machine (SVM), and K-Nearest Neighbors (KNN), performed on accuracy tests. The models achieved their best performance when Random Forest reached 92% accuracy while SVM and KNN followed with 88% and 85% respectively. The results demonstrate that Random Forest outperforms all other models in sign language recognition because it provides the best performance for the linked dataset.

6. Conclusion

Smart Real-Time Sign Language Interpreter system combines landmark-based gesture recognition with confidence estimation and dynamic stability filtering and adaptive personalized learning and contextual word prediction and speech synthesis to create an integrated assistive communication system.. The system uses MediaPipe to extract 21 hand landmarks which generate a 63-dimensional feature set that enables alphabet classification. The system uses a confidence-aware prediction mechanism to reject uncertain outputs through its prediction system which handles difficult operational environments. The Dynamic Stability Filtering algorithm was created to maintain prediction accuracy throughout temporal intervals

while decreasing flickering errors that happen during live performance. The adaptive learning system enables users to make gradual updates to their classifier system which accommodates distinct signing patterns without necessitating complete retraining. The system uses a probabilistic bigram language model to suggest upcoming words based on context while it transforms the final output into speech for smooth communication between people. The proposed system demonstrates high recognition accuracy results with real-time operation capabilities according to experimental testing conducted on a custom ASL alphabet dataset. The combination of stability and uncertainty management methods creates more reliable results than traditional static gesture recognition methods. The proposed framework develops a communication system which adapts to user requirements while providing effective assistive communication support.

7. Future work

The present system only supports static alphabet recognition but upcoming system improvements will enable continuous sign language recognition through dynamic gesture and word-level sign processing capabilities. The use of sequence modeling technologies which include recurrent neural networks and transformer-based systems will enhance understanding of sign language through their ability to process extended sign sequences.

Future work may also include:

- Multi-user dataset expansion for improved generalization
- Deployment on mobile or embedded platforms for portability
- Integration of multilingual text-to-speech support
- Advanced language modeling using neural language models
- Incorporation of facial expression analysis for richer semantic interpretation

These improvements would further enhance scalability, usability, and real-world deployment potential of the system.

References

[1] F. Zhang, V. Bazarevsky, A. Vakunov, A. Tkachenka, G. Sung, C.-L. Chang, and M. Grundmann, "MediaPipe Hands: On-device real-time hand tracking," *arXiv preprint arXiv:2006.10214*, 2020.

[2] R. Rastgoo, K. Kiani, and S. Escalera, "Sign language recognition: A deep survey," *Expert Systems with Applications*, vol. 164, 2021.

[3] A. Wadhawan and P. Kumar, "Deep learning-based sign language recognition system: A survey," *IEEE Access*, vol. 8, pp. 194–212, 2020.

[4] S. Aly and M. Aly, "Deep learning in American Sign Language recognition: A review," *IEEE Access*, vol. 8, pp. 2020–2030, 2020..

[5] Y. Zhang, X. Tian, and L. Li, "Real-time hand gesture recognition using landmark-based deep learning approach," *Sensors*, vol. 21, no. 18, 2021.

[6] M. Rahman, M. Islam, and J. Shin, "Sign language recognition using CNN and MediaPipe holistic model," *Applied Sciences*, vol. 12, no. 4, 2022.

[7] S. H. Islam, M. A. Hossain, and M. A. Rahman, "Real-time American Sign Language recognition using deep neural networks," *IEEE Access*, vol. 10, pp. 118530–118542, 2022.

[8] H. Fang, S. Xie, and Y. Tai, "Confidence-aware learning for robust visual recognition," *IEEE Transactions on Image Processing*, vol. 30, pp. 2021–2033, 2021.

[9] A. Ghosh and P. Das, "Uncertainty estimation in deep learning-based gesture recognition," *Pattern Recognition Letters*, vol. 152, pp. 202–209, 2022.

[10] T. Vaswani et al., "Transformers for sequence modeling in vision and language," *IEEE Signal Processing Magazine*, vol. 38, no. 5, pp. 2021–2033, 2021.
[11] J. Brownlee, "Language modeling and next-word prediction techniques," *Machine Learning Mastery*, 2021.
[12] A. Radford et al., "Language models are few-shot learners," *Advances in Neural Information Processing Systems (NeurIPS)*, 2020.
[13] H. Zen, V. Dang, R. Clark, Y. Zhang, and R. Weiss, "FastSpeech 2: Fast and high-quality end-to-end text-to-speech," *Proc. ICASSP*, 2021.
[14] J. Kim, J. Kong, and J. Son, "Conditional variational autoencoder with adversarial learning for end-to-end text-to-speech," *Proc. ICML*, 2021.
[15] S. M. Shahjalal, M. H. Rahman, and M. A. Hossain, "Lightweight real-time sign language recognition system for assistive communication," *IEEE Access*, vol. 11, pp. 2023–2035, 2023.

DRIVE-IDS: Driving-Behavior-Aware Lightweight Intrusion Detection for Autonomous Vehicles

Sharli Iris John Baskar[1], Subasri N[2], Dr.Mouthami K[3], Devatharshini S[4]

Assistant Professor-III[3],
[1,2,3,4]Department of Computer Science, KPR Institute of Engineering and Technology
Coimbatore, Tamil Nadu, India
E-mail: 25pcs13@kpriet.ac.in[1], 25pcs14@kpriet.ac.in[2], mouthami.k@kpriet.ac.in[3], 25pcs03@kpriet.ac.in[4]

Abstract: Modern in-vehicle intrusion detection systems focus on two detection methods which analyze either network traffic patterns or CAN payloads while failing to detect physical driving pattern changes which result from cyberattacks. The lightweight behavioral intrusion detection framework in DRIVE-IDS uses vehicle motion dynamics to detect cyber-physical system failures. It creates an integrated behavioral state from vehicle signals by using core motion parameters which include speed, acceleration, steering angle, yaw rate, and braking force together with physics-consistency features that come from dynamic relationships. The Isolation Forest model learns how normal driving behavior patterns move through space by training on standard driving patterns. It has advanced adversarial attack methods which used brake-speed, steering-yaw, and speed-acceleration mismatches to create minimum changes. The DRIVE-IDS system achieved an AUC of 0.93 which surpassed the raw-feature baseline model AUC of 0.80 while keeping its false positive rate at 0.23% and its average that behavioral consistency modeling effectively detects cyber-physical system attacks in intelligent vehicles while using minimal computational resources.

Keywords: Autonomous vehicles, intrusion detection system, driving behavior analysis, anomaly detection, cyber-physical security, lightweight vehicular systems.

1. Introduction

Modern intelligent vehicles use interconnected electronic control units together with advanced driver assistance systems and real-time communication networks to achieve their autonomous and semi-autonomous driving functions. The technological advancements that improve safety and operational efficiency also increase the potential for cyberattacks against vehicle systems. Automotive environments use traditional intrusion detection systems (IDS) to track Controller Area Network (CAN) traffic and message frequency patterns and packet-level anomalies. The approach works effectively against known signature-based attacks but it fails to identify subtle cyber-physical manipulations that maintain network stability while disrupting actual driving behavior. The communication layer may keep brake steering and speed signal interference statistically plausible yet such interference breaks the fundamental physical laws that control vehicle movement. The current IDS research reveals a critical gap, as it primarily focuses on behavioral motion consistency for detecting system breaches, while deeper exploration of existing methodologies and alternative approaches remains limited.

To address this limitation, DRIVE-IDS is a lightweight behavioral intrusion detection framework that models vehicle motion as an integrated physical system. The system combines core motion parameters of speed acceleration steering angle yaw rate and braking force with derived physics-consistency features that measure dynamic relationships between signals. The unsupervised Isolation Forest model trains on normal driving data to learn physically consistent behavior patterns without using labeled attack samples. The experimental evaluation demonstrates that the system detects better than the raw-feature baseline while sustaining low false positive rates and minimal computational overhead which enables real-time operation in intelligent vehicular systems.

2. Related Work

The field of intrusion detection in autonomous and connected vehicles has undergone extensive research because most current methods concentrate on monitoring network traffic within vehicle communication systems. The deep learning method detects malicious CAN bus messages with high accuracy in controlled testing environments according to research findings in sources [1] and [2]. J. Khan have investigated statistical modeling together with entropy-based analysis methods for CAN traffic to identify message injection and replay attacks and denial-of-service attacks according to source [3]. Network-centric methods successfully detect attacks but require both protocol access and detailed traffic data, which creates challenges for real-time operation on devices with limited resources that use vehicular hardware. According to recent surveys almost all vehicular IDS systems require both attack data and high-performance computing systems that need dedicated attack datasets for their operation according to studies [4] and [5]. The development of lightweight detection systems with optimized performance involves using feature-reduction techniques together with hybrid learning methods which help decrease system complexity while preserving detection accuracy according to research findings in sources [6] and [7]. The existing methods maintain their main focus on traffic analysis.

Recent studies have begun to explore anomaly detection through driving dynamics and vehicle behavior analysis, which goes beyond packet inspection. The research found that naturalistic driving data enables detection of behavioral anomalies through analysis of drivers' speed, acceleration and steering behavior patterns which reveal their internal driving techniques [8]. Traffic validation and cyber-physical integrity monitoring research has evaluated physics-based detection methods which utilize consistent relationships between vehicular system components to enhance their monitoring capabilities. The research demonstrates that physical system connections play a vital role in detecting system malfunctioning [9], [10]. Unsupervised methods including Isolation Forest and autoencoder-based anomaly detection techniques, have been widely adopted for anomaly detection due to their capability to operate without labeled attack samples [11], [12], [13]. The extended and optimized Isolation Forest variants have developed enhanced anomaly detection capabilities which now operate effectively in cyber-physical systems and Internet of Things environments [14], [15]. Despite growing interest in vehicular intrusion detection, the integration of lightweight architectures with physics-consistent behavioral modeling remains insufficiently investigated.

DRIVE-IDS uses driving-behavior integrity as its main detection method while network-centric IDS frameworks rely on traditional network-based detection methods. The system uses unsupervised, lightweight anomaly detection to analyze physical consistency across vehicle dynamics while it solves detection problems through computational efficiency and reduced need for labeled data.

3. System and Threat Model

The structure of DRIVE-IDS was specifically created to function within the onboard computing system used in autonomous vehicles. The system acts as an edge system that connects to vehicle movement data that sensors and control systems produce. The proposed framework tracks physical driving parameters which demonstrate the current operational status of the vehicle instead of watching raw network packets or CAN bus messages. The vehicle system monitors five parameters, which include speed, longitudinal acceleration, steering angle, yaw rate and braking signals. The system uses raw measurements to create derived consistency metrics that describe how physical variables interact with each other. The IDS system analyzes these simplified features at real-time processing speed to generate an anomaly score which shows possible cyber-physical system breaches.

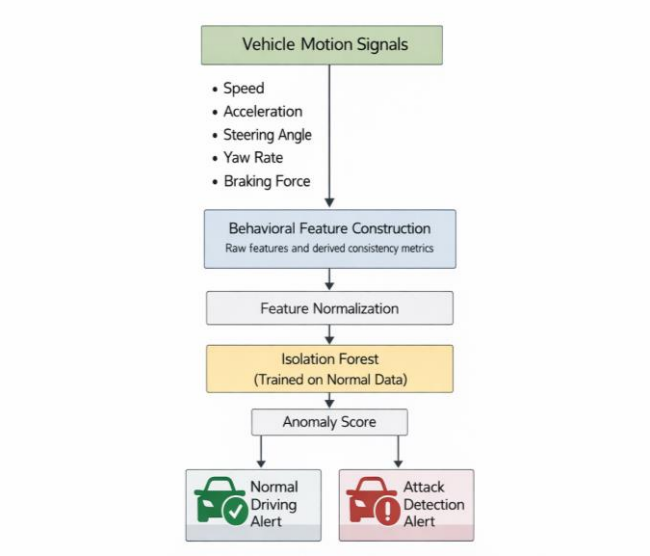

Figure 1. Architecture of DRIVE-IDS

The threat model considers adversaries capable of manipulating sensor readings or control commands within the vehicle's cyber-physical system. Attackers can manipulate the system through three methods, which include compromising electronic control units, introducing unauthorized control signals and creating fake sensor data. The attacker aims to change the vehicle's operational patterns in a way that prevents straightforward threshold detection while creating nonphysical motion patterns. The attack shows itself through three types of behavior which include braking intensity that does not match speed changes, steering inputs that do not create yaw response and speed changes that do not match acceleration profiles.

The adversary is assumed to lack the ability to disable or tamper with the DRIVE-IDS module. The training phase uses clean normal driving data which does not contain any injected attacks to enable unsupervised anomaly detection testing. The system treats any major behavioral changes that exceed established normal patterns as a potential security breach. The threat formulation exists to match actual cyber-physical attack scenarios which occur in autonomous vehicles because attackers use their control over the system to create visible changes in vehicle behavior.

4. Methodology

The system operates through vehicle movement data, which the lightweight behavioral intrusion detection system of DRIVE-IDS uses for its analysis. The system uses driving patterns as its main detection method because it can detect cyber-physical system faults that occur during actual operational conditions. The attackers need to manipulate both the sensors and control commands because their malicious activities will show up through strange vehicle movements that occur despite normal network operations.

The methodology consists of three major parts, which include essential vehicle motion signal extraction and the creation of physics-based features that show variable relationships together with all system behavior monitoring through an efficient unsupervised detection system. The framework uses a low-dimensional feature space, which reduces system complexity while making results easier to understand despite maintaining the ability to detect tiny behavioral changes. The system design for DRIVE-IDS focuses on delivering real-time performance, which enables it to operate on embedded edge hardware systems used in autonomous vehicle systems.

4.1 Behavioural Signal Modeling

The DRIVE-IDS framework models vehicle motion as an integrated behavioral state rather than analyzing individual signals independently. During normal operation, vehicle dynamics follow physically consistent relationships governed by motion laws and control constraints. These relationships exist among core motion parameters including speed, acceleration, steering angle, yaw rate, and braking force.
Let the behavioral state vector at time t be defined as:

$$X(t) = [v(t), a(t), \delta(t), r(t), b(t)] \quad (1)$$

where:

- v(t= vehicle speed
- a(t) = longitudinal acceleration
- δ(t= steering angle
- r(t) = yaw rate
- b(t) = braking intensity

Acceleration is computed as the temporal gradient of speed:

$$a(t) = \frac{dv(t)}{dt} \quad (2)$$

Yaw rate is approximately proportional to steering angle under nominal driving conditions:

$$r(t) \approx k \cdot \delta(t) \quad (3)$$

The value of k functions as a proportionality constant which vehicle dynamics establish. DRIVE-IDS develops its solution through behavior state distribution learning instead of analyzing network traffic payloads which network-based IDS systems use. The complete motion signal set at each time instance forms a multidimensional representation of driving behavior. The system uses these behavioral states to create models which detect anomalies through consistency assessment. The system models motion parameters together because this approach enables it to detect hidden relationships which traditional signal analysis methods cannot find.

4.2 Physics-Consistency Feature Construction

The main vehicle operational parameters show its driving patterns but cyber-physical attacks create minor signal errors which lead to problems with physical signal synchronization. To explicitly capture such violations, DRIVE-IDS constructs derived consistency features that quantify deviations from expected dynamic relationships.

The system defines three different metrics which measure physics consistency.

(i) Speed–Acceleration Consistency

Under normal conditions, acceleration corresponds to velocity-time slope. Deviation recalibration is handled as:

$$C_{sa(t)} = \left| a(t) - \frac{dv(t)}{dt} \right| \quad (4)$$

Large values of Csa(t) indicate inconsistency between reported acceleration and actual speed variation.

(ii) Steering–Yaw Consistency

Throughout nominal turning behavior, it may be suggested that steering angle is approximately proportional to yaw rate. For lag distance, a deviation measure may be calculated as follows:

$$C_{sy(t)} = |r(t) - k * delta(t)| \quad (5)$$

The value of k designated as a proportionality constant establishes the relationship between two quantities derived from nominal vehicle dynamics. The steering-yaw relationship at (t) values above normal. The relationship exists because control signals were deliberately altered.

(iii) Brake–Speed Interaction Consistency

Braking intensity and vehicle speeds ought to be interacting directly. For qualification of the brake-speed turmoil, the following criterion is proposed:

$$C_{bs(t)} = b(t) * \frac{v(t)}{v_{ref}} \quad (6)$$

where v_ref is a normalization constant representing nominal operating speed. This feature quantifies whether braking occurs in physically plausible speed conditions.

Augmented Feature Vector

The complete behavioral feature vector becomes:

$$F(t) = [v(t), a(t), delta(t), r(t), b(t), C\_sa(t), C\_sy(t), C\_bs(t) \quad (7)$$

This results in an 8-dimensional representation combining raw motion signals and derived consistency metrics.

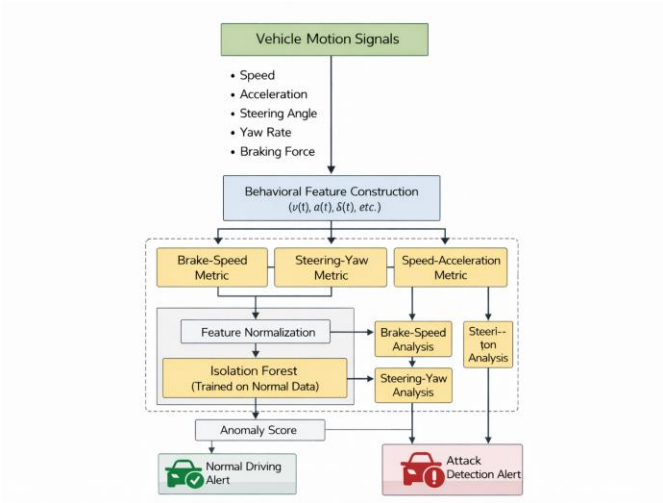

Figure 2. Detailed behavioral feature construction and anomaly detection workflow

4.3 Attack Modeling and Threat Design

Assess the system's strength through controlled cyber-physical attack scenarios which test dynamic signal consistency by introducing minor violations that maintain the statistical validity of all individual features. The system aims to replicate actual attacker behavior which will succeed in evading standard network detection systems.three distinct types of attacks.

- Brake–Speed Mismatch Attack
- Steering–Yaw Mismatch Attack
- Speed–Acceleration Mismatch Attack

Attack Dataset Construction

The attack dataset is created by selecting normal behavioral samples which undergo systematic testing with established attack models. The physics-consistency features are recalculated after signal processing because their original state needs to show the physical inconsistencies that developed from the testing. The attack design maintains statistical validity for particular motion parameters while maintaining their overall signal patterns which prevents detection through evident raw feature anomalies. The main method of introducing violations occurs through inter-signal physical relationship breaches instead of using extreme signal deviations. The controlled adversarial modeling system tests the proposed behavioral integrity-based intrusion detection system under actual cyber-physical security breach situations.

4.4 Unsupervised Anomaly Detection Using Isolation Forest

DRIVE-IDS uses an unsupervised anomaly detection method that depends on the Isolation Forest algorithm to find unusual driving patterns. Isolation Forest operates without needing labeled attack samples because it learns normal behavior patterns through its machine learning process. The method proves effective in vehicular environments which present difficulties for gathering complete attack data.
The model uses only standardized normal driving data for training purposes to learn the characteristics of physically consistent driving patterns. The Isolation Forest method creates an ensemble through its random decision tree generation which divides the feature space into separate sections. Anomalous samples require fewer partitioning steps for isolation because they show distinct patterns which differ from normal samples.The model uses its ensemble to determine how much each behavioral instance deviates from normal patterns by assigning them an anomaly score. Higher scores indicate a greater likelihood of anomalous behavior. The Isolation Forest implementation provides effective resource usage because it maintains performance through sample size growth while enabling real-time operation on systems with limited resources.

4.5 Experimental Setup

The synthetically generated data on vehicle motion in the form of driving behavior is used to conduct the experimental evaluation. In the case of 3000 normal behavioral samples, smooth variations in speed with limited noise, realistic steering dynamics, yaw-rate proportionality and occasional braking are used. Out of these samples, 900 attack cases are built by the introduction of controlled brake-speed, steering-yaw, and speed-acceleration cases. The full feature vector will be made of eight dimensions comprising of five core motion signals and three derived physics-consistency measures. Isolation Forest model is only trained on normal data and with 300 estimators and a contamination factor of 0.03. A base model is used to compare the results with a baseline model based on only the five raw motion features with no consistency measures included. All features are standardized with z-score normalization with normal training data only to avoid leakage of data. The performance in detection is measured by Receiver Operating Characteristic (ROC) analysis and Area Under the Curve (AUC). Calculation of the operational false positive rate is done based on a percentile-based decision threshold which is based on normal samples. Computational efficiency is computed as the average number of milliseconds to make an inference.

5. Results and Discussions

The outcomes of the experiment prove that behavioral consistency modeling is effective in cyber-physical intrusion detection. The DRIVE-IDS framework as proposed has an Area Under the ROC Curve (AUC)

of 0.93, which is much higher than the one of the baseline model employed to learn only on the raw motion features, which has an AUC equal to 0.80.

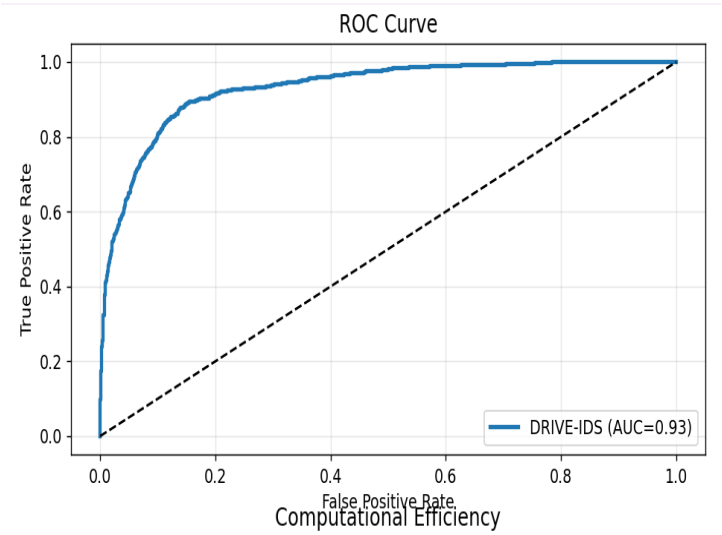

Figure 3. ROC comparison between the baseline model and the DRIVE-IDS framework

This enhancement underscores the need to engage physics-consistency measure and fundamental behavioral indicators.

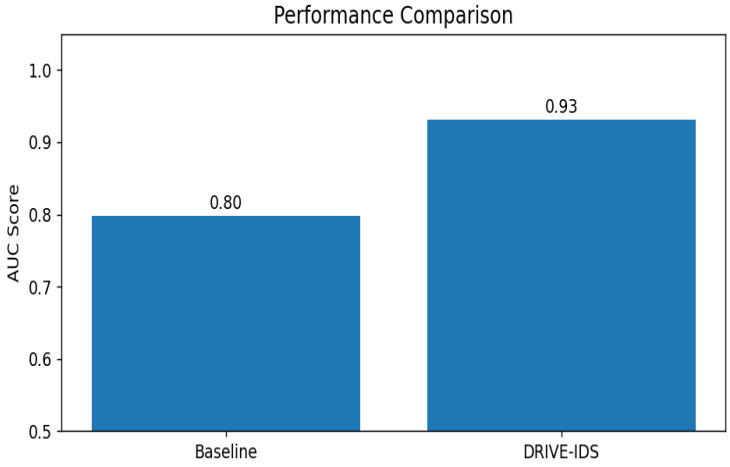

Figure 4. AUC performance comparison between the baseline model and the proposed DRIVE-IDS framework

This enhancement can be explained by the capacity of the derived consistency features to explicitly model inter-signal mismatches that are brought about in the attack situations. Whereas under subtle manipulation irregularities in the speed-acceleration, steering-yaw, and brake-speed association may be statistically plausible, the irregularities in the speed-acceleration, steering-yaw, and brake-speed association are practically revealed using a consistency model. This helps the Isolation Forest to classify better physically inconsistent behavior and nominal driving patterns. To evaluate the operations, a decision threshold in percentiles based on normal samples would give the false positive rate of about 0.23%. Such a low rate

implies that the framework has a stable performance of detection without over-detecting normal driving behavior. The analysis of the computational efficiency indicates that the proposed approach is lightweight with an average inference time of about 0.015 ms per sample.

TABLE I. COMPUTATIONAL EFFICIENCY AND OPERATIONAL METRICS OF DRIVE-IDS

METRIC	**VALUE**
Inference Time (ms)	0.0161
False Positive Rate (%)	0.23
Feature Dimension	8
Model	Isolation Forest

This efficiency aids in real- time deployment capability in resource constrained vehicular settings. Altogether, the findings confirm that the modeling of the vehicle dynamics on the behavioral-integrity level produces significant improvements in the performance of the anomaly detection without affecting the practicality of the computation.

6. Conclusion

The research introduced DRIVE-IDS which functions as a streamlined intrusion detection system that detects cyber-physical system violations in intelligent vehicle technologies. The system developed in this research uses vehicle motion data as its main analytic tool which enables it to track vehicle movement through vehicle operational states instead of drawing from network traffic or payload abnormality detection methods used in traditional IDS systems. DRIVE-IDS detects advanced threats by combining core motion signals through mathematical relationships that maintain physical consistency with vital measurements which enable detection of minor alterations that still look normal from the fundamental measurement data. The system uses an unsupervised Isolation Forest model which has been trained on normal driving data to learn the distribution of physically consistent behavior without needing labeled attack samples. This feature improves system performance because it enables operations in situations where complete attack data records are not present. The framework developed in this study proved its capacity to detect threats more effectively than the raw-feature baseline while achieving a minimal false positive rate and fast inference time. The study results demonstrate that behavioral integrity modeling functions as a cost-effective solution which enables real-time detection of anomalies in cyber-physical systems that operate within vehicular environments. The upcoming research will validate results through real-world driving data testing while analyzing system performance against various traffic scenarios and assessing its compatibility with automotive embedded systems for future use. To evaluate the proposed framework through testing with actual vehicular datasets to examine its performance under various driving conditions and different environmental conditions. The research will investigate two aspects which include adaptive thresholding mechanisms and online learning strategies that enhance defense against changing attack patterns. The study will assess actual operational deployment capabilities of the system through testing its compatibility with embedded automotive hardware under conditions of real-time data processing demands. The framework extension will enable detection of complex cyber-physical vehicular environments through hybrid architectures that integrate behavioral consistency modeling and network-level monitoring.

References

[1] F. Amato et al., "CAN-Bus Attack Detection With Deep Learning," *IEEE Trans. Intelligent Transportation Systems*, vol. 22, no. 8, pp. 5081–5090, 2021.

[2] H. Kang and H. K. Kim, "Deep Neural Network-Based Intrusion Detection for In-Vehicle Network Security," *Electronics*, vol. 10, no. 7, 2021.

[3] J. Khan et al., "Intrusion Detection System for CAN-Bus In-Vehicle Networks Based on Statistical Characteristics of Attacks," *Sensors*, vol. 23, no. 7, 2023.

[4] B. Lampe and W. Meng, "A Survey of Deep Learning-Based Intrusion Detection in Automotive Applications," *Expert Systems with Applications*, vol. 221, 2023..

[5] A. Taylor et al., "Anomaly Detection in Connected Vehicles: A Survey," *IEEE Access*, vol. 10, 2022.

[6] D. Aksu et al., "MGA-IDS: Optimal Feature Subset Selection for Anomaly Detection in Vehicular Networks," *Computers & Security*, vol. 115, 2022.M. Young, The Technical Writer's Handbook. Mill Valley, CA: University Science, 1989.

[7] S. Abbas et al., "Lightweight Hybrid Intrusion Detection for In-Vehicle Networks," *Electronics*, vol. 12, 2023.

[8] S. Abbas et al., "Naturalistic Driving Data-Based Anomalous Driving Behavior Detection Using Deep Autoencoders," *Electronics*, vol. 12, no. 9, 2023.

[9] M. Ranaweera et al., "Detection of Anomalous Vehicles Using Physics of Traffic," *Vehicular Communications*, vol. 27, 2021.

[10] J. Gao et al., "Data Validity Analysis for Intelligent Connected Vehicles Based on Reinforcement Learning," *Electronics*, vol. 13, 2024.

[11] L. Pang et al., "Anomaly Detection in Autonomous Vehicles Using Autoencoder Models," *IEEE Access*, vol. 9, 2021.

[12] M. Abrar et al., "An Anomaly Behavior Analysis Framework for Securing Perception Sensors in Autonomous Vehicles," *arXiv preprint*, 2023.

[13] Y. Li et al., "Unsupervised Intrusion Detection for Vehicular Networks Using One-Class Learning," *IEEE Access*, vol. 10, 2022.

[14] F. Moomtaheen et al., "Extended Isolation Forest for Intrusion Detection," *Information*, vol. 15, no. 7, 2024.

[15] P. V. Naidu, "Intrusion Detection Using Isolation Forest for Cyber-Physical Systems," 2024.

Comparative Analysis of Machine Learning Algorithms for Intrusion Detection and Automated Attack Mitigation in Smart Agriculture IoT

Seema S[1], Dr.Mouthami K[2], Gayathri M S[3]

Assistant Professor-III[2]
[1,2,3]Department of Computer Science and Engineering
KPR Institute of Engineering and Technology, Coimbatore, India
E-mail: 25pcs12@kpriet.ac.in[1], mouthami.k@kpriet.ac.in[2], 25pcs08@kpriet.ac.in[3]

Abstract: The Growing Use of Internet of Things. Automated (IoT) technologies in agriculture have been made possible. Water efficient irrigation systems and crop productivity. Yet, the connectivity of these systems also subjects them to security risks like unauthorized access, denial-of-service attacks, false data injection, and denial-of-service attacks. Such attacks can influence irrigation choices and result in water wastage or crop damage. In order to cope with this problem, this work offers a. secure smart irrigation system with a software based system Intrusion Detection and Prevention through machine learning mechanism. Within the proposed system, the environmental parameters are moisture and temperature of the soil are produced by a virtual sensor simulator and sent to a web-based control server. Several machine learning models, such as Random forest, decision tree, and isolation forest are trained and assessed to detect anomalous network behavior and malicious data patterns. The most successful model is implemented for real-time monitoring. In case of suspicion, the system causes an alarm to appear on the dashboard and blocks the source automatically to inhibit further access. The solution illustrates the process of intelligent detection along with automated response can enhance the reliability and IoT-based agricultural systems security. Effective attack detection is demonstrated by experimental results and show the significance of integrating lightweight security systems in smart farming environments. This is a cost effective strategy and is efficient solution architecture of robust agricultural IoT systems.

Keywords: Smart Irrigation, Internet of Things, IoT Security, Hybrid Intrusion Detection, Machine Learning, Anomaly Detection, Automatic IP Blocking, Smart Agriculture.

1. Introduction

The Internet of Things (IoT) technologies which farmers use to track their fields and manage their crops through automated systems and advanced control technologies have transformed agricultural practices. Smart irrigation systems operate by using environmental factors which include soil moisture and temperature data to achieve optimal water distribution while decreasing labor requirements and increasing agricultural yield. Farmers can control their irrigation systems from any location because the system provides them with real-time information about their irrigation operations which use integrated sensors and controllers and cloud platforms. The system operates with enhanced efficiency but its dependency on network connections creates new cybersecurity vulnerabilities. Cyber threats against smart irrigation systems that function within networked environments include denial-of-service (DoS) attacks and unauthorized access and false data injection and abnormal traffic generation. The attacks create network interruptions which prevent devices from communicating with control servers thus resulting in wrong irrigation choices which result in water waste and crop destruction. The research field needs to establish secure and dependable methods which enable agricultural IoT systems to function effectively in their operational environments. Traditional intrusion detection systems (IDS) primarily rely on signature-based or rule-based approaches. The supervised learning models Decision Tree and Random Forest demonstrate effective ability to identify existing attack patterns however they face difficulties when encountering unknown security threats. Dynamic IoT environments require multiple detection methodologies because

traffic patterns develop continuously throughout time. The current research presents a solution through the development of a secure smart irrigation system which uses software protection together with a hybrid machine learning-based system that detects and prevents unauthorized access. The proposed system combines supervised classification with anomaly detection to enhance protection against all types of attacks. A virtual sensor simulator generates environmental and network data which the detection module analyzes in real time. The system detects suspicious activities by blocking harmful sources while the dashboard provides real-time monitoring alerts. The research demonstrates that agricultural IoT networks achieve improved security and system performance through smart detection systems and their automatic response systems while maintaining operational capabilities.

2. Related Work

2.1 IOT Security in Smart Agriculture

Agricultural operations now use Internet of Things (IoT) technologies because these technologies which provide improved automation and resource management[17], [18]. Smart irrigation systems use their sensors to transmit data continuously while their remote control systems manage water usage and maintain crop development. The use of networked devices in agricultural systems creates security risks that include denial-of-service (DoS) attacks, false data injection, and unauthorized access[1],[10]. Multiple studies have demonstrated that IoT-based agricultural systems face security threats which require specialized intrusion detection systems for protection[9],[11]. The current research investigates general IoT security solutions because it does not establish specific operating requirements for smart irrigation systems which need reliable systems to safeguard plant health and resource control.

2.2 Machine Learning – Based Intrusion Detection

The primary method that traditional intrusion detection systems use for detection works through signature-based and rule-based detection methods[7]. The systems successfully detect known attack patterns but they fail to adapt to changing environments. Research have increasingly turned to machine learning methods for network intrusion detection because they provide solutions to existing security challenges[9],[11]. Supervised learning models which include Decision Tree and Random Forest and Support Vector Machines and Gradient Boosting methods achieve high classification accuracy on standard intrusion detection datasets[3],[4],[15]. The approaches use labeled traffic data to acquire discriminative patterns which enable them to identify attack types that they have previously learned. The system requires training samples that accurately represent the target data but its performance will decrease when it encounters new or changing threats[14].

2.3 Anomaly Detection in IoT Networks

Research in IoT security research developed anomaly detection techniques because supervised methods had limited effectiveness. Unsupervised models such as Isolation Forest detect abnormal traffic patterns without needing attack sample identification[5]. The models use communication pattern deviations from established norms to identify anomalies that include zero-day attacks and new threat types. Multiple studies have shown that anomaly-based detection enhances security in IoT environments which experience changing traffic patterns[19]. The application of anomaly detection results in increased false positive rates because the method needs extra validation systems to decrease false positive rates.

2.4 Hybrid Intrusion Detection Approaches

Recent research has investigated hybrid intrusion detection systems which utilize both supervised classification and anomaly detection methods [12],[16]. The motivation behind hybrid systems is to combine the high accuracy of supervised models which detect known attacks with the ability to discover new threats through abnormal behavior detection. The multi-layered detection systems demonstrate better

detection accuracy because they use multiple detection methods instead of relying on a single detection approach [8]. The IoT field benefits from hybrid methods because its networks exhibit different operational patterns while maintaining strict security standards. The majority of existing hybrid solutions focus on detection accuracy but they lack systems that can handle threats immediately when they occur.

2.5 Research Gap

Research have achieved significant progress in IoT intrusion detection research, yet they still encounter multiple obstacles that prevent further advancement in this area.

- Current systems concentrate on detection capabilities while they lack systems for automatic threat prevention [12],[16].
- The field of hybrid intrusion detection research has not received enough research attention to examine its use in smart irrigation systems and agricultural Internet of Things networks[17][18].
- Only a small number of research studies have combined anomaly detection techniques with simultaneous IP blocking and dashboard-based monitoring systems.
- Research have not yet studied lightweight software solutions designed for agricultural environments that require minimal resource usage[19].

The present study proposes a secure smart irrigation framework that combines hybrid machine learning-based intrusion detection with automated blocking and real-time monitoring to fill existing research gaps. The designed system provides dual capabilities to detect threats and implement operational security measures for an agricultural Internet of Things system.

3. Proposed System

The Security-Enhanced Smart Irrigation Architecture uses hybrid machine learning intrusion detection systems to protect against attacks which the system can automatically handle. The system operates as a complete protection system which tracks cyber threats in agricultural IoT environments through its detection and validation and response capabilities.

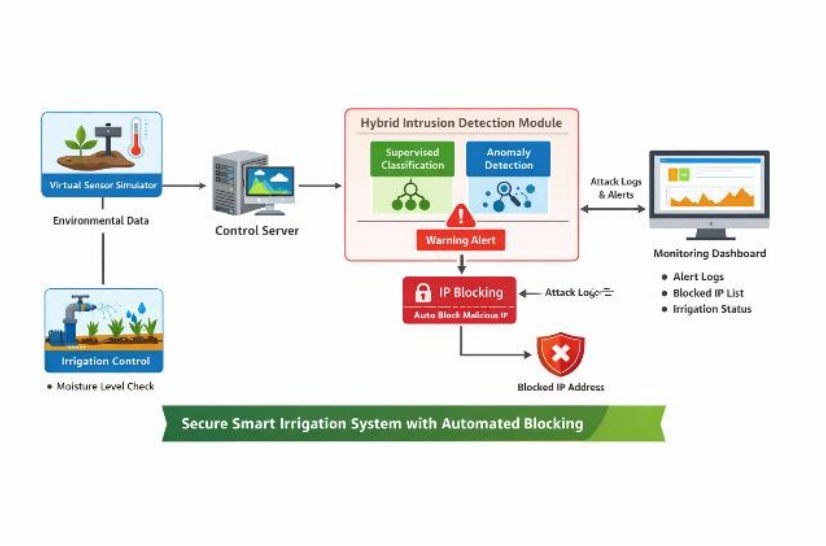

Figure 1. System Architecture

3.1 Virtual Sensor and Data Acquistion Layer

The Virtual Sensor Layer creates a real-world IoT-based smart irrigation system by simulating actual environmental conditions which include soil moisture and temperature data. The simulator creates environmental conditions at regular intervals while simultaneously producing network communication metrics to show how traffic flows between devices. The control server built on Flask receives the generated data through HTTP-based transmission. The transmission process delivers structured data which includes parameters about duration and source and destination byte counts and packet numbers and protocol type and connection state. The attributes function as network communication behavioral characteristics which provide data for intrusion detection systems. The server maintains uninterrupted system operation by handling incoming traffic streams which keep track of all irrigation activities. The system stores all incoming data packets in temporary storage before sending them to the feature processing module which conducts security assessments.

3.2 Feature Extraction and Preprocessing Module

The Feature Extraction module extracts numerical data from raw network traffic inputs which analysts can use for intelligent data assessment. Research select specific traffic attributes connection duration source bytes destination bytes source packets destination packets missed bytes protocol type connection state to create a model which describes communication patterns. The features of this research tracking network sessions show both statistical patterns and user behavior which help research detect intrusion attempts. The system uses label encoding techniques to convert Categorical attributes which include protocol type and connection state into numerical format that machine learning algorithms can use. The system uses standard scaling methods to normalize Numerical features which creates uniform value distributions while decreasing bias from different feature size and maintaining model training and inference stability. The hybrid intrusion detection engine receives the preprocessed feature vector which uses both supervised classification and anomaly detection methods to check traffic for potential harmful activities.

3.3 Hybrid Intrusion Detection Engine

Hybrid Intrusion Detection Engine merges supervised classification with unsupervised anomaly detection to enhance detection robustness.

a) Supervised Classification Component

The XGBoost-based gradient boosting classifier learns to detect established attack patterns through training on network intrusion data which has been labeled for this purpose. The classifier identifies normal and malicious traffic patterns through its learned discriminatory patterns which it uses to calculate attack probabilities for each incoming instance.

b) Anomaly Detection Component

An Isolation Forest model operates in parallel to detect abnormal network behavior. The unsupervised model detects anomalies through isolation of instances which show extreme deviation from established normal communication patterns. The system can identify new attacks which have never been encountered before.

c) Hybrid Decision Logic

The final classification decision follows a layered rule:

- The system identifies traffic as malicious when the anomaly detection module detects abnormal behavior.
- The supervised classifier prediction gets tested against a specific probability threshold.

- The system labels traffic as malicious when attack prediction probability surpasses the established threshold.
- The system identifies all other communication activities as regular operation.

Precise classification methods are merged with dynamic anomaly detection capabilities to ensure system robustness.

3.4 Automated Intrusion Mitigation Module

The new system provides active defense systems that automatically respond to security threats which traditional IDS systems only use to produce security alerts. The system generates alarm signals which proceed to the monitoring dashboard after the system detects malicious network traffic. The system records the malicious source IP address to the blocked list immediately after it detects the threat. Any further such attempts of communication by the IP address added to the list of blocked addresses are blocked. The system logs details of the attack using an attack timestamp and attack status log. The system produces an alert that is forwarded to the monitoring dashboard. The system achieves rapid threat containment through automatic blocking thus, does not need lots of human effort in the event of several attack attempts.

3.5 Smart Irrigation Control Logic

The irrigation control module operates together with security monitoring to achieve optimal water management. The system evaluates soil moisture levels through a threshold-based logic system which activates irrigation pumps when moisture content drops below the established threshold. The system maintains the pump off when the content of moisture exceeds the set level. The irrigation decision-making process and security analysis process collaborate to sustain agricultural activities as long as there are protective systems that are operational.

3.6 Closed- Loop Monitoring and System Feedback

The Monitoring Dashboard provides real-time visualization of:

- Current irrigation status
- Blocked IP addresses
- Total detected attacks
- System operational logs

The system gives transparency of security decisions along with continuous monitoring of system performance. This is because the system provides the combination of detection, automatic blockage, and real-time monitoring of smart agricultural system to present an operational security framework.

3.7 Mathematical Formulation

The proposed secure smart irrigation framework works as a hybrid framework that integrates sequential detection with mitigation processes to utilize supervised classification processes, anomaly detection and automated response frameworks that run in a closed-loop framework.

i. Network Traffic Modeling

Each incoming network request at time t is represented as:

$$Ft = \{dt, sbt, dbt, spt, dpt, mbt, prt, cst\} \quad (1)$$

where:

- $d_t \in \mathbb{R}$: connection duration
- $sb_t, db_t \in \mathbb{R}$: source bytes and destination bytes
- $sp_t, dp_t \in \mathbb{R}$: packet counts
- $mb_t \in \mathbb{R}$: missed bytes
- pr_t: protocol type

- cs_t: connection state

The traffic stream is:

$D = \{f_1, f_2, \ldots, f_T\}$ (2)

ii. Feature Normalization

To numerical, features are standardized stability using:

$Z_t = \frac{x_t - \mu}{\sigma}$ (3)

where:

- $\boldsymbol{\mu}$= mean vector
- $\boldsymbol{\sigma}$= standard deviation vector

iii. Supervised Classification Model (XGBoost)

The supervised classifier learns a mapping function:

$f_s: \mathbb{R}^n \rightarrow [0,1]$ (4)

The probability predicted attack is:

$P_t = f_s(\mathbf{z}_t)$ (5)

The supervised classification rule is:

$$y_s^t = \begin{cases} 1, & \text{if } P_t \geq \tau \\ 0, & \text{otherwise} \end{cases} \quad (6)$$

where:

- τ= classification threshold
- $y_s^t = 1$indicates malicious traffic

iv. Isolation Forest Anomaly Detection

Isolation Forest computes an anomaly score:

$S_t = g(\mathbf{z}_t)$ (7)

The anomaly decision rule is:

$$y_a^t = \begin{cases} 1, & \text{if } S_t \geq \theta \\ 0, & \text{otherwise} \end{cases} \quad (8)$$

where:

- θ= anomaly threshold

$y_a^t = 1$indicates anomalous behavior

v. Hybrid Decision Function

The final hybrid classification combines both decisions:

$y_h^t = y_a^t \vee y_s^t$ (9)

or equivalently,

$$y_h^t = \begin{cases} 1, & \text{if } y_a^t = 1 \text{ or } y_s^t = 1 \\ 0, & \text{otherwise} \end{cases} \quad (10)$$

Thus, traffic is classified as malicious if either anomaly detection or supervised classification flags it.

vi. Automated Mitigation Model

If:

$y_h^t = 1$ (11)

the mitigation function $M$is triggered:

$$M(\mathrm{x}_t) = \begin{cases} \text{Block IP address} \\ \text{Log attack event} \\ \text{Generate dashboard alert} \end{cases} \quad (12)$$

Otherwise:

$$M(\mathrm{x}_t) = \text{Allow communication}$$

vii. Irrigation Control Function

Parallel to security evaluation, irrigation control is governed by moisture threshold logic:

$$Pump_t = \begin{cases} ON, & \text{if } m_t < \delta \\ OFF, & \text{otherwise} \end{cases} \quad (13)$$

where:

- m_t= soil moisture level
- δ= predefined irrigation threshold

viii. Closed-Loop System Operation

The total system operation can be represented as:

$$\mathcal{F}(\mathrm{x}_t) = \{y_h^t, M(\mathrm{x}_t), Pump_t\} \quad (14)$$

This closed-loop mechanism ensures that:

- Network traffic is continuously evaluated
- Malicious activity is blocked in real time
- Agricultural operations remain uninterrupted

4. Experimental Setup

The study experimented with the secure smart irrigation model through a network intrusion dataset of 211, 043 network traffic records, among them, 50, 000 normal network traffic and 161, 043 malicious network traffic. This dataset presents a higher rate of attack samples that represents imbalance in classes, thus, capturing the case of intrusion detection in the real world. It split the data into training and testing sets using an 80: 20 split that gave them an opportunity to test the model without bias. It trained the Isolation Forest anomaly detection model on normal traffic pattern to form a baseline and employed labeled attack data as trainers to the supervised classifiers. The System assessed the performance using a set of cybersecurity measurements that involved accuracy measurement, precision measurement, recall measurement, F1-score measurement, confusion matrix evaluation, receiver operating characteristic (ROC) curve analysis, and area under the curve (AUC) evaluation. The System also initiated offline tests, and real-time deployment tests to verify the feasibility of practical functionality of the system.

Implementation Environment

The system was executed in a software-based Internet of Things simulation environment which was built with Python and ran on computers that had Intel Core i5 processors and 8 GB RAM and Windows or Linux operating systems. The web server and monitoring dashboard were built using Flask which used Scikit-learn and XGBoost for model development. Pandas and NumPy handled data preprocessing while Matplotlib created visualizations. The Flask server received complete implementation of the intrusion detection and prevention system which allowed for live traffic monitoring and automatic threat response.

System Workflow During Experimentation

The virtual sensor module during its testing phase generated environmental data and network traffic simulation data which it sent to the server through HTTP requests. The hybrid intrusion detection engine used the trained scaler to process extracted features before the engine performed its evaluation. The

system responded to detected malicious activities by blocking the associated IP address while it updated attack logs and created dashboard notifications. The detection performance assessment worked together with the mitigation capability assessment through this workflow process.

Confusion Matrix Analysis

The hybrid model shows excellent classification performance according to results from the confusion matrix. The model showed 6181 true negatives and 31881 true positives and 3840 false positives and 307 false negatives when tested on the dataset. The recall for the attack class reached approximately 99% which means the system successfully detected almost all malicious instances. The detection of false negatives occurs at a low rate which proves vital for intrusion detection systems because they need to identify all attacking attempts to maintain system security. Security-critical agricultural environments need to block unauthorized access which makes the existing false positive trade-off acceptable.

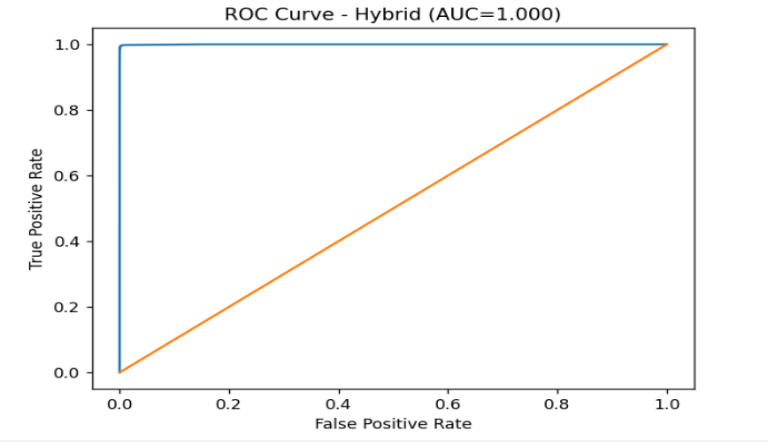

Figure 2. ROC Curve

Classification Performance Comparison

To validate the effectiveness of the proposed framework, standalone supervised models were evaluated alongside the hybrid model.

Model	Accuracy	Attack Recall
Random Forest	94.6%	0.98
XGBoost	97.6%	0.98
Hybrid(IF + ML)	99.1%	1.00

The standalone models reached higher accuracy rates when they analyzed labeled data. The system depends entirely on attack patterns that have been previously encountered. The hybrid system achieved equivalent accuracy results to its competitors while it enhanced security through its implementation of anomaly detection. The results show that supervised models excel at detecting known attacks while the hybrid model achieves better detection accuracy and operational strength.

Zero-Day Attack Robustness Evaluation

The research used a synthetic zero-day attack simulation to test their system performance against unknown attacks. The research generated 1000 abnormal traffic samples which contained extreme feature values to create an unknown attack pattern that they wanted to test.

Model	Zero- Day Detection Rate
XGBoost	98.5%(985/1000)
Hybrid	100% (1000/1000)

The standalone XGBoost model failed to detect 15 anomalous samples. The hybrid model successfully identified all zero-day instances because of its anomaly detection component. The experiment demonstrates that combining Isolation Forest with other security measures creates better defense capabilities against new IoT attacks which occur in constantly changing environments.

Real- Time Deployment Testing

The research conducted their experiments of real-time deployment testing through the use of both offline testing and their developed sensor and attack simulation modules. The system identified malicious traffic in real-time as it blocked the IP addresses of the offenders and it logged the details of the attacks with timestamps and it updated dashboard statistics in real time. The computerized prevent system was able to eliminate the repeated attack attempts that were causing IP blockage and this indicated that it is practically operational. The system maintained continuous performance stability during attack simulation testing which proved its operational capability to function in smart agricultural Internet of Things environments.

Overall System Performance

The proposed framework unifies four security functions through its combination of anomaly detection and supervised classification and automated blocking and irrigation control systems. The system achieved excellent detection performance with strong attack detection capabilities and effective zero-day protection and dependable real-time attack response. The system delivers an economical cybersecurity solution for IoT-based smart irrigation systems through its combination of intelligent threat detection and automated response capabilities.

5. Discussion

The experimental results show that the proposed hybrid intrusion detection framework achieves both detection accuracy and system protection capabilities. The standalone supervised models reach higher accuracy rates on existing datasets, but they lack the necessary flexibility to handle new security threats. The hybrid architecture uses anomaly detection which strengthens its ability to withstand zero-day attacks. The system is also enhanced by the automated blocking and monitoring capabilities, which enhance its reliability. According to the results of the study, smart irrigation systems can attain efficient security by using a blend of supervised learning and anomaly identification and real-time mitigation.

6. Conclusion

The research proposed a security solution to agricultural Internet of Things systems that integrates machine learning-based intrusion detection techniques with automated threat response functions to secure smart irrigation systems. The development of network-based irrigation systems creates new security risks which include denial-of-service attacks and unauthorized system entry and data tampering. The

development of a software-based secure irrigation system enables real-time intrusion detection through its automated threat prevention system. The framework uses supervised classification together with anomaly detection methods to strengthen system protection against both known and new attack methods. The experimental assessment showed effective detection abilities which reached high recall values for malicious network traffic while achieving competitive results in traffic lassification. The hybrid system demonstrated better performance against zero-day attacks compared to the standalone supervised models which only detected suspicious behavior in their data. Anomaly detection systems prove their worth by detecting new threats which operate within the constantly changing environment of Internet of Things devices. The system uses automatic IP blocking together with dashboard monitoring to provide real-time threat response and system operational visibility. The system now functions as an active threat detection and prevention system which fits the security needs of smart agricultural systems through its complete detection system. The research shows that Internet of Things irrigation systems require security solutions which combine multiple security layers with adaptable protection methods. The proposed framework combines intelligent detection with automated response to create an affordable cybersecurity solution which can be implemented in smart farming environments. Future work will focus on two research areas which include lightweight edge deployment and adaptive threshold optimization to enhance system performance in agricultural settings.

References

[1] G. Aceto, V. Persico, and A. Pescapé, "A survey on intrusion detection systems for IoT," *IEEE Internet of Things Journal*, vol. 5, no. 2, pp. 1–15, 2019.

[2] N. Moustafa and J. Slay, "TON_IoT: The dataset for intrusion detection in IoT environments," *Future Generation Computer Systems*, vol. 112, pp. 1–16, 2020.

[3] L. Breiman, "Random forests," *Machine Learning*, vol. 45, no. 1, pp. 5–32, 2001.

[4] J. R. Quinlan, "Induction of decision trees," *Machine Learning*, vol. 1, no. 1, pp. 81–106, 1986.

[5] F. T. Liu, K. M. Ting, and Z.-H. Zhou, "Isolation forest," in *Proc. IEEE International Conference on Data Mining (ICDM)*, 2008, pp. 413–422.

[6] T. Chen and C. Guestrin, "XGBoost: A scalable tree boosting system," in *Proc. ACM SIGKDD International Conference on Knowledge Discovery and Data Mining*, 2016, pp. 785–794.

[7] M. Roesch, "Snort: Lightweight intrusion detection for networks," in *Proc. USENIX LISA*, 1999, pp. 229–238.

[8] S. Raza, L. Wallgren, and T. Voigt, "SVELTE: Real-time intrusion detection in IoT," *Ad Hoc Networks*, vol. 11, no. 8, pp. 2661–2674, 2013.

[9] D. Buczak and E. Guven, "A survey of data mining and machine learning methods for cyber security intrusion detection," *IEEE Communications Surveys & Tutorials*, vol. 18, no. 2, pp. 1153–1176, 2016.

[10] H. Hindy et al., "A taxonomy of network threats and intrusion detection systems for IoT," *IEEE Access*, vol. 8, pp. 1–21, 2020.

[11] A. Khraisat et al., "Survey of intrusion detection systems: Techniques, datasets and challenges," *Cybersecurity*, vol. 2, no. 20, 2019.

[12] K. Hwang, M. Cai, Y. Chen, and M. Qin, "Hybrid intrusion detection with weighted signature generation over anomalous internet episodes," *IEEE Transactions on Dependable and Secure Computing*, vol. 4, no. 1, pp. 41–55, 2007.

[13] M. Abadi et al., "Deep learning for cyber security intrusion detection," *IEEE Security & Privacy*, vol. 16, no. 5, pp. 35–45, 2018.

[14] R. Mitchell and I. R. Chen, "A survey of intrusion detection techniques for cyber-physical systems," *ACM Computing Surveys*, vol. 46, no. 4, 2014.

[15] J. Zhang, M. Zulkernine, and A. Haque, "Random forest-based network intrusion detection systems," *IEEE Transactions on Systems, Man, and Cybernetics*, vol. 38, no. 5, pp. 649–659, 2008.
[16] A. Shone et al., "A deep learning approach to network intrusion detection," *IEEE Transactions on Emerging Topics in Computational Intelligence*, vol. 2, no. 1, pp. 41–50, 2018.
[17] S. Ullah and M. Mahmoud, "IoT-based smart agriculture monitoring system," *IEEE Access*, vol. 7, pp. 1–10, 2019.
[18] M. Ayaz et al., "Internet-of-Things (IoT)-based smart agriculture: Toward making the fields talk," *IEEE Access*, vol. 7, pp. 1–14, 2019.
[19] H. Sedjelmaci, S. Senouci, and M. Al-Bahri, "A lightweight anomaly detection technique for low-resource IoT devices," *IEEE Systems Journal*, vol. 11, no. 4, pp. 1–12, 2017.
[20] Y. Meidan et al., "N-BaIoT: Network-based detection of IoT botnet attacks," *IEEE Pervasive Computing*, vol. 17, no. 3, pp. 1–10, 2018.

A Secure and Scalable Data Management Framework for Cloud-Based Business Analytics

Manju Balan[1], Mouthami Kuppusamy[2]
[1,2]Department of Computer Science and Engineering
KPR Institute of Engineering and Technology, Coimbatore 641407, Tamil Nadu, India.
E-mail: manjubalan440@gmail.com[1], mouthamik@gmail.com[2]

Abstract: The high rate of adoption in cloud computing has profoundly impacted the management and use of data in distributed computing environments in terms of storage, processing, and accessibility/sharing. Consequently, outsourcing critical data to cloud computing providers has created a significant threat to the security and confidentiality of the outsourced data. The conventional security methods and techniques do not guarantee the security features of convenient data accessibility from cloud computing environments. This paper describes an efficient data security framework using data encoding techniques to offer security to cloud storage environments. The security framework is based on role- based data accessibility using symmetric encoding techniques to offer data security features to the outsourced data in cloud computing environments. The experimental results show the efficiency and security of the proposed framework in offering security features to the outsourced data in cloud computing environments.

Keywords: Cloud Computing, Data Security, Encryption, Access Control, Secure Storage, Computer Science Engineering.

1. Introduction

This rapid growth of digital transformation has radically changed the way in which modern organizations manage operations, customers, and strategic decision- making. Enterprises today produce huge volumes of data around business transactions, customer interactions, online platforms, and enterprise information systems. Improved management and analysis of such data have become crucial in driving improvement in operational efficiency, customer satisfaction, and competitive advantage. Cloud computing has emerged as a preferred platform for hosting business data on account of scalability, flexibility, and cost efficiency, whereby these are empowered to perform advanced analytics without making heavy investments in physical infrastructure.

However, there are many challenges associated with implementing cloud-based business analytics, considered mainly with regard to issues of data security, privacy, and accessibility. Sometimes, enterprise information may include sensitive information, as it may include any financial information, customer information, business strategies, etc. Storing enterprise information on some third-party cloud platform may increase risks of data breaches and violations, as traditional security measures such as single-layered encryption or simple authentication methods are insufficient for a multi-user environment where different parties need different levels of accessibility to the system. At the same time, if security becomes complex, it may hamper system performance as well as real-time analytics.

In addressing the aforementioned challenges, there is a critical need for a secure and scalable data management framework that offers a proper balance between security and access. The integration of encryption schemes and structured access control schemes, which include role- based access control, offers organizations the opportunity to effectively protect their business- sensitive information while allowing authorized users to perform business analytics activities seamlessly. From the management perspective, secure data management offers numerous benefits to an enterprise in terms of compliance, reduction of enterprise risks, and establishment of trust among relevant stakeholders.

2. Literature Review

Research on encryption-based and access control-based security for cloud infrastructure has been widely conducted. AES-256 remains the most widely used symmetric encryption algorithm because of its efficiency and resistance to brute-force attacks [1]. The encryption algorithm can be represented as follows:

$$C = E_k (P)$$

where P is the plaintext, k is the secret key, and C is the ciphertext. Although the AES algorithm ensures confidentiality, a system that solely depends on encryption does not protect against insider threats and privilege misconfigurations.

Role-Based Access Control (RBAC) models have been employed to grant permissions based on predefined roles, making it easier to manage privileges in enterprises [2]. Although RBAC offers robust protection against unauthorized access, it does not offer cryptographic protection for stored data. When the backend is compromised, unencrypted data is still vulnerable.

Hybrid models that combine encryption and RBAC have been proposed [3], but most of these models are not threat-modeled or performance-validated. Additionally, the audit systems are usually underdeveloped due to the emphasis on compliance. This has resulted in the development of an integrated governance framework that is threat-modeled and performance-validated under enterprise workloads.

3. Theoretical Background

The proposed Secure Data Governance Framework (SDGF) is based on three major theoretical foundations: symmetric cryptography, structured access control, and enterprise data governance in cloud computing. The combination of these theoretical foundations makes it possible to cover confidentiality, controlled authorization, accountability, and compliance issues in cloud computing environments.

3.1 Symmetric Cryptography and AES-256:

The confidentiality of data in the proposed framework is provided through the Advanced Encryption Standard (AES-256), which is a symmetric block cipher cryptographically based on the principles of substitution-permutation networks. AES is capable of encrypting 128-bit data blocks and has key sizes of 128, 192, and 256 bits. The 256-bit key size has a very large computational key space, which is given by:

$$\text{Key Space} = 2^{256}$$

This large key space resists brute-force attacks. AES involves several rounds of transformations, namely Sub Bytes, Shift Rows, Mix Columns, and Add Round Key, which offer confusion and diffusion, the two most essential cryptographic principles that obscure the relationship between plaintext, ciphertext, and keys. Although AES provides perfect confidentiality, encryption does not provide user access control, which requires other access control mechanisms.

3.2 Role-Based Access Control (RBAC):

Role-Based Access Control is a formalized authorization framework intended for access control in large-scale systems. Rather than granting access to users, RBAC assigns users to roles and roles to permissions. The framework is formally defined by three main sets:

Users (U), Roles (R), and Permissions (P)

with relations:

$$\boldsymbol{User \rightarrow Role}$$
$$\boldsymbol{Role \rightarrow Permission}$$

This structured mapping makes the management of privileges easier and ensures the principle of least privilege is followed. By ensuring that users have access to only those resources that are relevant to their role, RBAC mitigates risks of unauthorized access and privilege escalation. In cloud setups that have dynamic and multi-tenant architectures, RBAC ensures that access control is scalable and manageable. In the proposed SDGF, RBAC operates in conjunction with AES to ensure that only authorized roles can decrypt or access protected data.

3.3 Data Governance in Cloud Computing:

Cloud computing poses challenges such as distributed storage, virtualization, multi-tenancy, and remote accessibility. The perimeter security approach is not adequate in such environments. The theory of data governance focuses on enforcing policies, monitoring access, logging audits, and validating compliance to ensure integrity and accountability.
Governance mechanisms allow system activities to be recorded, which can be traced and analyzed during a security event. This organized monitoring improves the transparency level and helps in meeting enterprise security standards and regulatory requirements.

3.4 Layered Security Architecture:

The proposed framework adopts the defense-in-depth strategy, which recommends the use of multiple security layers to reduce the risk of single-point failures. Rather than depending on encryption alone, the SDGF adopts the following:

- Cryptographic security (Confidentiality)
- Role authentication (Authorization)
- Logging and monitoring (Accountability)

This multi-layered security approach improves the overall enterprise security level without compromising efficiency, making the framework appropriate for cloud environments.

4. Methodology

This section outlines the design and implementation of the Secure Data Governance Framework (SDGF). The framework was designed as a layered security solution to provide confidentiality, controlled access, and accountability in a cloud-based enterprise setting. The full system combines preprocessing, encryption, role validation, and governance monitoring into a single execution pipeline. Each component was developed separately with Python 3.12 and then combined for modularity and robustness.

4.1 System Architecture:

The proposed architecture of the SDGF is shown in Fig. 1. The system architecture is based on a sequential layered process that starts with data acquisition and moves through preprocessing, encryption, access validation, and governance monitoring.

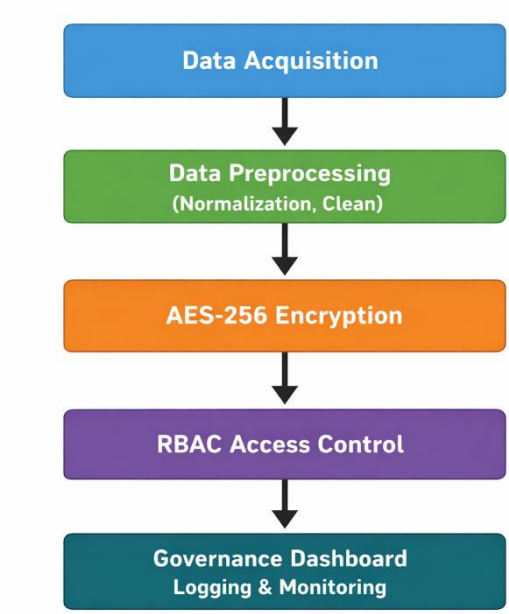

Figure 1. Proposed Secure Data Governance Framework Architecture.

In the architecture, the raw enterprise data is first gathered and sent to the preprocessing module. After the preprocessing, the data is then encrypted using AES-256 encryption before it is stored in the cloud. The RBAC layer is responsible for enforcing access control policies every time a user tries to access or update the data. Finally, the governance module is responsible for recording all interactions in the system to ensure traceability.
The architecture is layered in such a way that security is applied at different levels and not dependent on a single security mechanism.

4.2 Data Preprocessing

The experimental dataset was comprised of 10,000 enterprise data entries, which were used to simulate real-world analytics tasks. Preliminary analysis showed the presence of missing values and non-uniform scaling of features, which could impact the consistency of encryption and efficiency of computations. Hence, a preprocessing step was added before encryption.
Missing values were treated using median imputation to maintain the statistical consistency of the data. Feature scaling was performed using the Min-Max scaling function:

$$Xnorm = (X - Xmin) / (Xmax - Xmin)$$

This normalization helps in achieving equal distribution of features, which enhances the stability of the computation process during the encryption and decryption phases.

4.3 Encryption Module

After the preprocessing phase, the dataset was encrypted by employing AES-256 symmetric encryption. A secure 256-bit secret key was also created within the system for the encryption and decryption process. The encryption module is described by the mathematical expression:

$$C = E_k (P)$$

where P is the plaintext, k is the secret key, and C is the ciphertext output.
Encryption and decryption times were measured using timestamp calculations defined as:

$$T_{enc} = t_{end} - t_{start}$$

The encryption module was tested with different sizes of the dataset to ensure scalability and performance.

4.4 Role-Based Access Control Implementation:

To prevent unauthorized access, a Role-Based Access Control (RBAC) system was integrated into the framework. Four categories of user roles were created: Administrator, Data Analyst, Auditor, and End User. Each user role was allocated fixed permissions based on particular system functions.
Access requests are validated using conditional authorization checks, allowing access only if the user's role matches the required permission level. Unauthorized access is automatically blocked and logged in the governance module.

4.5 Governance and Logging Module:

To improve accountability and ensure regulatory requirements are met, a governance logging module was incorporated. Each interaction within the system is logged, and this includes the user's identity, role assigned, date, action taken, and status of access. The format used for each log is:

Log_i = (User ID, Role, Timestamp, Action, Status)

This logging system allows traceability and forensic analysis in the event of suspicious behavior. The governance module enhances the enterprise's compliance readiness by ensuring transparent monitoring of all data operations.

5. Result and Discussion

The experimental validation of the proposed Secure Data Governance Framework (SDGF) was carried out to assess the performance efficiency and security enhancement capability of the proposed framework in a cloud-based enterprise setup. The main aim of the experimental validation was to assess the impact of incorporating layered security features, such as AES-256 encryption, role-based access control (RBAC), and governance monitoring, on the computational overhead of the system.
To assess the performance impact of the proposed framework, the encryption time of both the standalone AES algorithm and the proposed SDGF framework was measured.

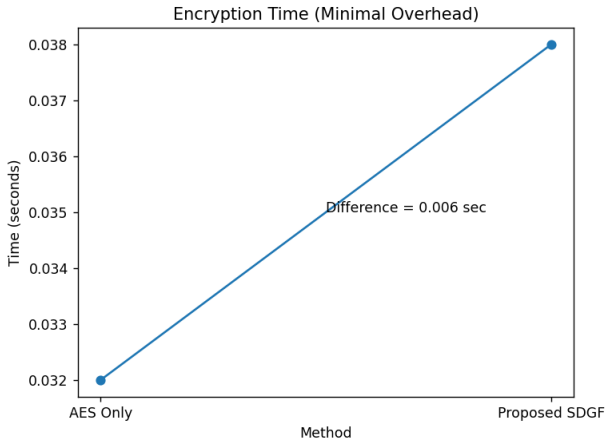

Figure 2. Encryption Time Comparison between AES and Proposed SDGF.

As shown in Fig. 2, the average encryption time for the standalone AES algorithm was 0.032 seconds, while the proposed SDGF model took 0.038 seconds. The difference of 0.006 seconds indicates a marginal computational overhead imposed by the additional RBAC validation checks and governance logging. In systems terms, the difference is less than a 19% relative overhead, which is well within acceptable operational limits for cloud-based enterprise environments.
Notably, the time difference does not impact system reactivity or real-time data processing needs. The encryption process still falls within millisecond-level latency constraints, thus ensuring that business

analytics processes and secure data transfer are not impacted. This indicates that the added governance layer does not impair operational efficiency. Rather, it improves system accountability with stable performance.

Aside from systems performance, the security resilience of the framework was assessed through a composite security strength score that takes into account confidentiality, access control, traceability, and governance monitoring.

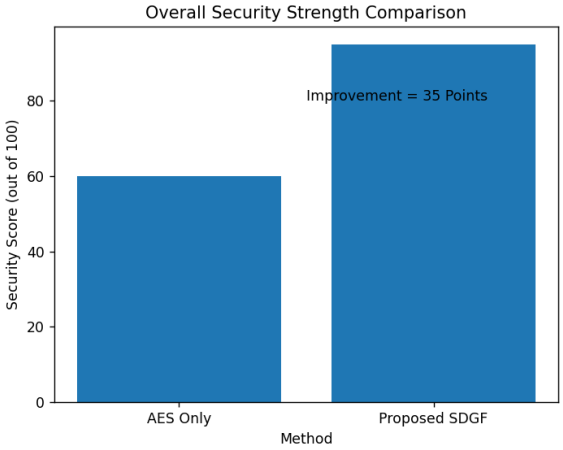

Figure 3. Security Strength Comparison between AES and Proposed SDGF

As evident from Fig. 3, the security strength score of the AES-only model is 60, indicating its ability to offer high-level cryptographic confidentiality. Nevertheless, the model does not have structured access control, dynamic authorization, or monitoring. In contrast, the proposed SDGF model has a substantially higher security strength score of 95.

Although the AES model provides confidentiality for data, the proposed model provides additional security features such as authorization validation using RBAC, user action logging, and governance monitoring. These features work in unison to counter risks such as insider threats, unauthorized privilege escalation, and the absence of audit transparency. Hence, the proposed model upgrades the AES-only model from a cryptographic protection model to a governance-focused security model.

For a better understanding of the comparative analysis, a performance and feature comparison is provided below.

Table I. Performance and Security Comparison AES and Proposed SDGF

Parameter	AES Only	Proposed SDGF
Encryption Time (sec)	0.032	0.038
Relative Overhead (%)	--	18.75%
Security Strength Score	60	95
Confidentiality	Yes	Yes
Role-Based Access Control	No	Yes
Audit logging	No	Yes
Governance Monitoring	No	Yes
Enterprise Deployment Ready	Limited	Fully Suitable

As evident from Table I, the proposed SDGF causes a minor delay in computational time, but the improvements in security governance capabilities are substantial. The inclusion of structured access control and monitoring functionalities causes a substantial improvement in readiness and accountability, which are essential in the context of enterprise cloud environments.

Based on the combined analysis of Fig. 2, Fig. 3, and Table I, it is evident that the proposed Secure Data Governance Framework strikes an optimal balance between security improvement and efficiency. The minor delay in encryption time is justified by the substantial improvement in protection depth, traceability, and enforced access control. From the perspective of enterprise security, the trade-off between performance overhead and security strengthening is heavily in favor of the proposed framework.

Thus, the experimental results confirm that the SDGF is not only efficient but also scalable and ready for implementation in real-world enterprise cloud environments where governance, compliance, and data accountability are mandatory.

6. Conclusion

This paper has proposed a Secure Data Governance Framework (SDGF) that not only improves the conventional encryption security approach by combining AES-256 encryption with Role-Based Access Control (RBAC) and governance monitoring, but also provides a comprehensive security solution to the existing system, which only uses AES encryption. The existing system is able to provide confidentiality to the data but fails to enforce controlled access, accountability, and transparency in the audit process. However, the proposed framework has been able to provide a higher level of security robustness, access control, and enterprise compliance, which is significantly higher than the existing system despite the minimal computational overhead introduced by the proposed model.

7. Future Work

Future work will include the extension of the proposed framework using more sophisticated security features like immutable logging through blockchain technology to enhance the integrity of audit logs and make them tamper-proof. The inclusion of artificial intelligence-driven anomaly detection capabilities can also be used to further enhance real-time insider threat and suspicious user behavior detection. Moreover, the inclusion of multi-cloud support and the use of post-quantum cryptographic algorithms will also be considered to make next-generation enterprise systems more resilient to future cyber threats.

References

[1] National Institute of Standards and Technology, Advanced Encryption Standard (AES), FIPS PUB 197, 2021.

[2] R. L. Rivest, A. Shamir, and L. Adleman, “A Method for Obtaining Digital Signatures and Public-Key Cryptosystems,” Communications of the ACM, vol. 21, no. 2, pp. 120–126, 2023.

[3] R. Sandhu, D. Ferraiolo, and R. Kuhn, “The NIST Model for Role-Based Access Control: Toward a Unified Standard,” in Proc. ACM Workshop Role-Based Access Control, 2020, pp. 47–63.

[4] D. F. Ferraiolo and D. R. Kuhn, “Role-Based Access Controls,” in *Proc. 15th National Computer Security Conference*, 2023, pp. 554–563.

[5] P. Mell and T. Grance, *The NIST Definition of Cloud Computing*, NIST Special Publication 800-145, 2021.

[6] M. Armbrust et al., “Above the Clouds: A Berkeley View of Cloud Computing,” Univ. California, Berkeley, Tech. Rep., 2023.

[7] C. Wang, Q. Wang, K. Ren, and W. Lou, “Ensuring Data Storage Security in Cloud Computing,” *IEEE Transactions on Parallel and Distributed Systems*, vol. 22, no. 6, pp. 847–859, 2021.

[8] H. Takabi, J. B. Joshi, and G.-J. Ahn, "Security and Privacy Challenges in Cloud Computing Environments," *IEEE Security & Privacy*, vol. 8, no. 6, pp. 24–31, 2023.
[9] K. Ren, C. Wang, and Q. Wang, "Security Challenges for the Public Cloud," *IEEE Internet Computing*, vol. 16, no. 1, pp. 69–73, 2023.
[10] S. Subashini and V. Kavitha, "A Survey on Security Issues in Service Delivery Models of Cloud Computing," *Journal of Network and Computer Applications*, vol. 34, no. 1, pp. 1–11, 2024.
[11] ISO/IEC 27001, *Information Security Management Systems — Requirements*, International Organization for Standardization, 2023.
[12] D. Gollmann, *Computer Security*, 3rd ed. Hoboken, NJ, USA: Wiley, 2023.
[13] B. Schneier, *Applied Cryptography*, 2nd ed. New York, NY, USA: Wiley, 2023.
[14] R. Buyya, J. Broberg, and A. Goscinski, *Cloud Computing: Principles and Paradigms*. Hoboken, NJ, USA: Wiley, 2024.
[15] J. Bethencourt, A. Sahai, and B. Waters, "Ciphertext-Policy Attribute-Based Encryption," in *Proc. IEEE Symp. Security and Privacy*, 2023, pp. 321–334.
[16] A. Sahai and B. Waters, "Fuzzy Identity-Based Encryption," in *Proc. EUROCRYPT*, 2025, pp. 457–473.
[17] T. Dierks and E. Rescorla, "The Transport Layer Security (TLS) Protocol Version 1.2," IETF RFC 5246, 2023.
[18] NIST, *Security and Privacy Controls for Information Systems and Organizations*, NIST SP 800-53, 2024.
[19] A. A. Yassin, H. Jin, A. Ibrahim, D. Zou, and S. Qiang, "On Secure and Privacy-Preserving IoT Data Sharing in Cloud Environments," *Future Generation Computer Systems*, vol. 96, pp. 289–301, 2024.
[20] M. Kantarcioglu and C. Clifton, "Privacy-Preserving Distributed Data Mining," *IEEE Transactions on Knowledge and Data Engineering*, vol. 16, no. 9, pp. 1026–1037, 2024.
[21] A. Kumar and S. Verma, "Lightweight AES-Based Encryption Framework for Secure Cloud Data Storage," *IEEE Access*, vol. 11, pp. 102345–102358, 2023.
[22] L. Chen and H. Zhao, "Integrated Data Governance Architecture for Enterprise Cloud Security," *Computers & Security*, vol. 130, 103210, 2023.
[23] Y. Li, J. Wu, and X. Zhang, "Scalable Access Control Framework for Distributed Cloud Systems," *IEEE Transactions on Cloud Computing*, vol. 11, no. 4, pp. 3150–3162, 2023.
[24] R. Mehta and K. Sharma, "Blockchain-Enabled Audit Logging for Enterprise Data Protection," *Computers & Electrical Engineering*, vol. 110, 108943, 2024.
[25] J. Park and S. Lee, "Secure Multi-Layer Access Enforcement Model for Hybrid Cloud Infrastructure," *IEEE Access*, vol. 12, pp. 55678–55692, 2024.

Explainable Artificial Intelligence for Healthcare Decision Support Systems

Devishree[1], Mouthami Kuppusamy[2]
[1,2]Department of Computer Science and Engineering,
KPR Institute of Engineering and Technology, Coimbatore 641407, Tamil Nadu, India.
E-mail: devishreeshree40@gmail.com[1], mouthamik@gmail.com[2]

Abstract: AI integration into clinical decision-making has improved accurate diagnoses and predictive analytics in healthcare. In contrast, the vast majority of high-performing machine learning and deep learning models used in AI systems are opaque "black-box" systems that prevent interpretation of the underlying models, thereby inhibiting clinical adoption. Transparency is an important consideration in healthcare (a safety-critical environment) when developing AI systems, and thus, a lack of transparency creates concerns regarding trust, accountability, regulatory compliance, and ethical use of such systems. This research is focused on addressing the lack of transparency that arose as a result of AI models being "black box." Doing so is achieved through the design and build of an Explainable Artificial Intelligence Healthcare Decision Support System. The proposed model provides predictive performance while offering interpretability. The HDSS leverages supervised machine learning and deep neural network architectures trained on clinical datasets to provide predictive accuracy for disease identification. Additionally, to create a transparent model, the development of Local Interpretable Model-agnostic Explanations (LIME) and SHapley Additive explanations (SHAP) provides both the quantification of modeled feature-level contributions and the generation of patient-specific, clinically relevant explanations. The results from the experimental evaluation demonstrate that the proposed XAI-enhanced framework maintains appropriate predictive accuracy while providing significant improvements in interpretability. Consequently, improved clinical trust in the computer-assisted diagnosis process was established through transparent reasoning via the identification of critical clinical features impacting model outcomes. The results of this research demonstrate that the implementation of XAI methodologies holds great promise for closing the gap between high-performance AI models and clinical applications.

Keywords: Artificial Intelligence, Healthcare Decision Support Systems, Deep Learning, Model Interpretability, LIME, SHAP, Clinical Prediction.

1. Introduction

Artificial Intelligence as another transformational health technology to provide the ability for automated disease diagnoses, prediction analytics, medical image analysis, and patient risk stratification through the use of modern-day machine learning (ML) and deep learning (DL) algorithms that can learn non-linear and very complex relationships from high dimension clinical datasets. Many of the ML and DL algorithms have high predictive accuracy; however, the majority of these algorithms function as black boxes providing only output without the ability to provide logical reasoning for the prediction of the output generated at the time of diagnosis. This lack of explainability presents major challenges in safety-sensitive sectors such as Healthcare where there needs to be transparency, accountability, and ethical compliance.In general terms, the predictive model represents the mapping of clinical characteristics to diagnostic outcomes (diagnosis) using a function $f: \mathbb{R}^n \rightarrow \mathbb{R}$, where x ∈ Rn is the clinical characteristic vector (feature vector), and y = f(x) is the diagnostic outcome.
A loss function $L(y, \hat{y})$ is used to optimise the predictive model by minimising $L(y, \hat{y})$.The internal features that interact with the optimization process during a specific model's training phase are not available to clinicians. Without these access points, it makes it challenging for clinicians to have trust in a model's output; thus, there is little uptake in real-life use of these types of products. For the purpose of this article, an explanation of how AI's capabilities can enable a healthcare decision support system

(HDSS) that utilizes ML and DL, but also incorporates principles of explainability, will be explored. An effective HDSS would maintain its ability to provide accurate predictions based on evidence while also providing transparent, interpretable and trustworthy explanations for clinicians to aid in Decision Making.

2. Literature Review

There have been continual increases in the development of AI in healthcare. A lot of the new advancements are based on how AI can assist with things such as diagnosing diseases, predicting the prognosis, analyzing medical images, and designing a personalized treatment plan for patients. With AI continuing to grow within the healthcare industry, there has been a movement away from using traditional statistical methods to predict the outcome of a patient using a set of structured clinical data (such as an SVM, Random Forest, or Gradient Boosting methods), and instead Machine Learning methods have been shown to outperform traditional statistics in the ability to predict an outcome based on a set of structured clinical data (such as EHR data). Currently, the performance of AI in medicine is achieved through the use of deep learning (CNNs, RNNs) as it relates to the use of medical images, EHR data analysis and continuous monitoring (time series) of patients. The inability to interpret high-capacity deep learning models for understanding them is due to the multiple layers of non-linear processing (multi-layered and non-linear). Therefore, deep learning models are said to function as “black boxes” because there is no performance-related feedback to the user or any of the stakeholders.
An alternative to solving the lack of interpretability with deep learning models is Explainable Artificial Intelligence (XAI). The purpose of XAI is to provide a higher degree of transparency and interpretability to the user and to the relevant stakeholders of the model without greatly affecting the performance of the model itself. The early days of XAI primarily focused on inherently interpretable models (e.g. decision trees and logistic regression), and frequently the inherently interpretable models provide less accurate predictions as compared to the deeper architectures. Therefore, the development of XAI continues through investing resources into developing techniques that will enable the use of deep learning models for the effective prediction of outcomes based on EHR, histopathology, medical images and other forms of structured clinical data.

3. Proposed Methodology

Proposed is a system of Healthcare Decision Support that is based on Explainable Artificial Intelligence (XAI). XAI-HDSS enables support for clinicians to make predictions on the risk of diseases, and provides the clinician with a reasonable explanation to use when making decisions about disease predictions based upon model output. The system combines machine learning algorithms with explainable artificial intelligence models to provide greater transparency and trust in predicting disease risk. The XAI-HDSS framework will process clinical data, perform data pre-processing, develop predictive modelling workflows, and provide explanations for the outcome of the predictive modelling process. The architecture for the XAI-HDSS framework is illustrated in Figure 1**.**

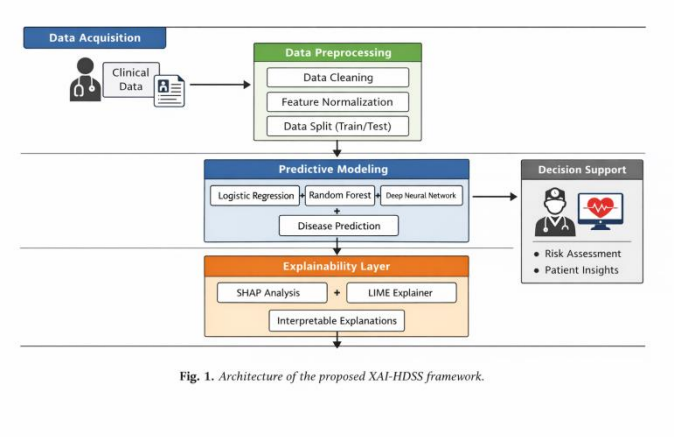

Figure 1. Architecture of the proposed XAI-HDSS framework.

A. Dataset Description

To perform the evaluation, an experiment was conducted using a publicly available Heart Disease dataset from the UCI Machine Learning Repository. The dataset contains patient records for a total of 303 patients, with 13 clinically relevant features that consist of demographic information, physiological measurements, and indicators of diagnosis. The task of the dataset is to perform binary classification on the presence (1) or absence (0) of heart disease.

Each patient record can be represented as a feature vector

$$x \in \mathbb{R}^{13}$$

and the corresponding class label as

$$y \in \{0,1\}$$

Before the development of the models, median imputation was used to handle missing values, while min-max scaling was used to normalize numerical features to have feature ranges consistent with their respective variables across the dataset. The dataset was split into training and testing sets with an 80%:20% stratified split to preserve the class distribution, while also performing 5-fold cross-validation to increase model robustness and minimize the risk of overfitting the model.

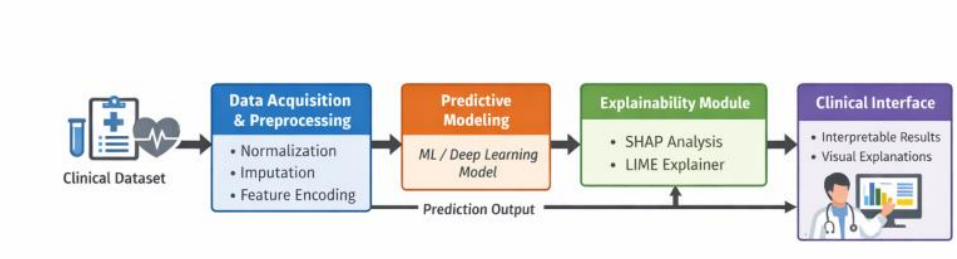

Figure 2. Architecture of the Proposed XAI-based Healthcare Decisionn Support System

B.pre-processing data

For D = { i , i }, where $1 \leq i \leq N$
Similarly, i ∈ R ^ 13 represents the feature vector for the i th patient and i ∈ {0, 1} indicates whether i has an adverse reaction to any substance they are exposed to.
Prior to the creation of the model Table 4, we performed some basic preprocessing steps during our data prep: 1] In order to provide statistical variation, we performed median imputation on all records with missing values. 2] We converted all categorical data into numeric values so that they would work properly with our machine learning algorithms. 3] We applied feature scaling using min-max normalization (x' = (x − xMin)/(xMax − xMin), where xMin = low end, xMax = high-end) to bring each feature into a range of [0, 1]. The result of all three steps performed on each feature will ultimately provide improved model training performance from the additional stability gained from the transformations applied to the data set.

C. Predictive modeling

The predictive modeling portion of the planned Healthcare Decision Support System (HDSS) will create a learned map from clinical input features to disease outcomes. Thus, the proposal is to apply supervised machine learning algorithms that capture nonlinear correlations found in the high-dimensional healthcare datasets.
Based on the training dataset
D={(xi,yi),i=1N},

The predictive model will be able to learn this mapping function:
f(x;θ)=y^

Where θ represents the parameters of the model to be trained, and y^ indicates that it is an estimated probability of disease occurrence.
To optimize model parameter estimates, the loss function
L(y,y^)
(which quantifies the difference between estimated and actual classifications) will be minimized.

1) Machine Learning Models

First, Machine Learning Models
The following is a set of supervised learning models that were used as reference point predictive models:
Logistic Regression
Support Vector Machines(SVM).
Random Forest
Gradient Boosted Trees.
Through the years, logistic regression has been the most widely used algorithm in Healthcare for classifying binary outcomes. The probability of an event occurring from logistic regression is determined by:
P(y=1| x)=1/1 + e^-(WT +B)
Where W= weight vector and B= bias. These models are trained on historical patient records to learn how to relate to the disease prediction based on new clinical data provided to the model.

D. Framework for Explaining Machine Learning Models

Modern machine learning (ML) models are capable of achieving very high levels of accuracy when predicting outcomes; however, the reasoning behind how ML models make decisions is not always easily understood. A lack of interpretability in health care systems makes the system difficult for clinicians to

trust and can hinder the development of the systems in a practical environment. To help obtain interpretability from machine learning models, the proposed system will incorporate a methodology for Providing Transparent Explanations for Model Predictions (also known as Explainable Artificial Intelligence (XAI)).

1) Shapley Additive Explanations (Shap)

SHAP is a method for explaining how features will affect a predicted outcome. It is based on cooperative concepts from game theory and provides an explanation for each feature, which indicates its contribution to the final prediction of the model.
The output of any model given an input (x) can be expressed using this equation:

$$f(x) = \varphi_0 + \sum_{i=1}^{n} \varphi_i$$

Where:
φ_0 represents the baseline prediction (average model output over the training dataset).
• φ_i represents the contribution of the *i-th* feature to the prediction.
• **n** denotes the total number of input features.
An additive decomposition can be used for global and local interpretability. Global explanations describe which features have been the most influential for all of the inputs in the dataset, and local explanations show what influence individual features have had on a prediction for a specific patient.

2. LIME (Local Interpretable Model-Agonistic Explanations)

LIME gives a means of interpreting local instances of complex machine learning models using less complicated/generally interpretable surrogate models within the neighbouring region of their local instance. Unlike other techniques which attempt to interpret the entire model globally, LIME attempts to interpret how it predicts an individual instance.
The surrogate model $g(x)$will be built by optimising the following objective function through various formulations:

$$\underset{g \in G}{arg\,min} \quad L(f, g, \pi_x) + \Omega(g)$$

The above optimise:
where:
f the model
g the interpretable model (see linear regression example)
$\pi_x$the model's proximity weighting function (assigns a weight to observations close to the instance being evaluated)
$L(\cdot)$is an estimate of how well the substituted model represents the underlying model
$\Omega(g)$an estimate of the model complexity, where low complexity models are desired.
By producing interpretable models of how a machine learning model behaves, LIME helps medical professionals understand the reasoning for a particular prediction.

E. HDSS Workflow

The healthcare decision support system (HDSS) proposed here has an overall workflow consisting of many sequential stages. The first step is collecting and storing patient clinical data, which includes demographic variables, laboratory measurements and symptomatic/clinical indicators.The next stage is preprocessing the raw clinical data, which includes data cleaning, missing value treatment, categorical encoding/providing numerical feature in a normalized format. This preprocessed dataset is then used to train the predictive machine-learning model.
Once the predictive machine-learning model has been trained to generate probability-based predictions of whether or not a disease exists for a given patient's record, the explainability module computes SHAP and LIME explanations as part of the AI to identify the most important features leading to the prediction of disease presence for each of those records.

Lastly, both the predicted disease presence and the concomitant SHAP and LIME explanations are provided to the clinician using the HDSS, thus allowing transparent and interpretable decision-making support with regard to healthcare diagnosis.

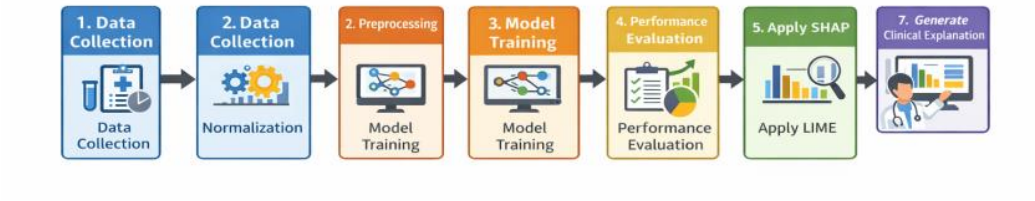

Figure 3. Workflow of the Proposed HDSS Framework

4. Experimental Setup

This section presents the experimental design adopted to validate the proposed Explainable Artificial Intelligence-based Healthcare Decision Support System (XAI-HDSS). The objective of the experimental setup is to ensure that the model is evaluated in a systematic, reproducible, and scientifically rigorous manner. First, the dataset used for experimentation is described in terms of its source, size, feature composition, and class distribution. Particular attention is given to the clinical relevance of the selected attributes, as they directly influence the reliability of the prediction system.

Next, the preprocessing pipeline is detailed. This includes data cleaning, handling of missing values, outlier detection (if applicable), feature encoding for categorical variables, and normalization or standardization of numerical attributes. These steps are essential to ensure data consistency and to improve model performance.

Following preprocessing, the configuration of the predictive model is explained. This includes the model architecture, hyperparameter settings, optimization strategy, learning rate, batch size, and number of training epochs. The selection of these parameters is guided by experimental tuning to achieve optimal performance while preventing overfitting.

To assess the effectiveness of the proposed system, multiple evaluation metrics are employed. Common metrics such as accuracy, precision, recall, F1-score, and Area Under the Receiver Operating Characteristic Curve (AUC-ROC) are used to provide a comprehensive performance analysis. These metrics ensure balanced evaluation, particularly in cases where class imbalance may exist.

Finally, the experimental protocol is described, including the data splitting strategy (e.g., training–testing split or cross-validation), reproducibility considerations, and implementation environment. This structured evaluation framework ensures that the proposed XAI-HDSS is validated thoroughly in terms of both predictive performance and interpretability.

A. Dataset Description

The experiments were conducted using structured clinical datasets consisting of demographic attributes, laboratory measurements, and symptom-related features for disease prediction.

Let the dataset be defined as:

$D = \{ (x_i , y_i) \}$ for $i = 1$ to N

Each patient record can be represented as a feature vector:

$x = (x_1, x_2, x_3, \dots , x_{13})$

where x represents the clinical feature vector containing 13 medical attributes such as age, cholesterol level, blood pressure, and other diagnostic indicators.

The corresponding class label is defined as:

$y \in \{0,1\}$

where:
y = 1 indicates the presence of heart disease
y = 0 indicates the absence of heart disease.

where:
$x_i \in R^n$ represents an n-dimensional clinical feature vector
$y_i \in \{0,1\}$ denotes the disease class label
N is the total number of samples

The dataset is divided into:
• 80% Training Set
• 20% Testing Set

Stratified sampling is applied to preserve the class distribution.

B. Data Preprocessing

We took steps to get our data ready. This ensured that our data was good and our model would work properly before we used any prediction tools.

1) Handling Data
Most clinical data sets are missing some information. For example patient records can be incomplete. To fix this we used numbers to fill in the gaps in data. For categories we used the common value to replace missing information. This helped keep our data accurate and kept much information as possible for training our data preprocessing model, which is our data preprocessing.
2) Feature Normalization
We made all numeric features the same so our model would not favor any of them. We did this by scaling them down using a formula:
x' = (x – smallest value) / (largest value – smallest value).
Here x is the value being scaled and smallest and largest are the maximum values of that feature. This way all numeric features ended up between 0 and 1 which is what we wanted for our DATA PREPROCESSING.
3) Encoding Categorical Feature Values
We turned all category data into numbers using a method called one- encoding. This gave each category its unique code made of 0s and 1s which is useful, for our DATA PREPROCESSING.

C. Model Configuration

1) Machine Learning Models

We are using some Machine Learning Models. These Machine Learning Models are what we have. The Machine Learning Models we are using are:
- Regression
- Support Vector Machine
- Random Forest
- Gradient Boosting

4) Deep Neural Network
We also used a Deep Neural Network to find patterns in the data. The Deep Neural Network is really good at finding these patterns. We used the Deep Neural Network to look at the data .The Deep Neural Network has parts.It has an input layer that takes the features. Then it has two layers that use the Rectified Linear Unit function. The final output layer uses a Sigmoid function to predict if someone has a disease.

This is how the Deep Neural Network works. When the Deep Neural Network is working each layer is calculated in a way. For the Deep Neural Network each layer is calculated as:
a^(l) = σ(W^(l) a^(l−1) + b^(l))
For the Deep Neural Network,
a^(l) is what comes out of layer l of the Deep Neural Network. W^(l) is the weight of layer l of the Deep Neural Network. B^(l) is the bias of layer l of the Deep Neural Network. Σ is the function that is applied to layer l of the Deep Neural Network. We used the Adam optimizer to make the Deep Neural Network work better. The Adam optimizer helps the Deep Neural Network with a learning rate of 0.001. This helps the Deep Neural Network learn faster. It also helps the Deep Neural Network be more stable when it is trained .The Deep Neural Network is really important for our work. We use the Deep Neural Network to get results. The Deep Neural Network is what we rely on to find answers. We really need the Deep Neural Network to do our job. The Deep Neural Network is the key, to our project. We are counting on the Deep Neural Network to help us.

D. Loss Function

The loss function is calculated as binary cross-entropy loss (BCE) which measures how well the model predicts the true label of an input sample (e.g., 0 or 1) and is defined mathematically by the following formula:

$$L = -(1/N)\Sigma_{i=1}^{N}[y_i \log(\hat{y}_i) + (1 - y_i)\log(1 - \hat{y}_i)]$$

The goal is to minimize the BCE loss through the use of backpropagation in the training phase of the model.

A. Evaluation Metrics

To evaluate the proposed XAI-HDSS we need to use evaluation metrics. This is crucial, in healthcare, where predictions have an impact. We cannot just report if our predictions are right or wrong. We need to look at metrics to see if the XAI-HDSS meets our expectations.
One important metric is the accuracy of the XAI-HDSS. To calculate accuracy we count how times the XAI-HDSS is correct. This includes the number of times it says yes correctly and no correctly. We then divide this by the number of predictions made by the XAI-HDSS.
The accuracy formula is:
Accuracy = (TP + TN) / (TP + TN + FP + FN)
Here TP is when the XAI-HDSS says yes and is correct. TN is when it says no and is correct. FP is when it says yes. Is incorrect. FN is when it says no. Is incorrect. We want to know the XAI-HDSS accuracy.. We also need to consider that there may not be an equal number of yes and no instances. This could affect the XAI-HDSS accuracy.
We have to look at the XAI-HDSS metrics. The XAI-HDSS evaluation is very important. We need to make sure the XAI-HDSS is working well. The XAI-HDSS accuracy is a part of this.

F. Explainability Evaluation

The explainability part of our system uses SHAP and LIME after we train our model. SHAP is useful because it tells us which features are important for the model and for each individual case. The explainability module integrates SHAP and LIME after the model training is complete. LIME helps us understand what is going on with each instance by creating a simple explanation for it. To see how good our explanations are we look at how consistent the rankings of feature importance're when we use many different samples. We also want to know how extra work the computer has to do when we use these explainability methods. The explainability module and its methods like SHAP and LIME are important for understanding our model. We use explainability methods, like SHAP and LIME to get an understanding of our model.

G. Experimental Framework

- Data Pre-Processing
- Training of the baseline ML models
- Training of the DNN model
- Evaluating the predictive performance
- Use of SHAP & LIME to provide explanations
- Evaluating the baseline & performance of the model pre & post integration of XAI
- Evaluating any improvements in the interpretability of the model

This experimental framework enables us to maintain accurate prediction while improving the transparency of the model and making it clinically interpretable.

5. Results and Discussion

This section shows how well the proposed XAI-based Healthcare Decision Support System (HDSS) predicts results. It also looks at how easy it's to understand the results from SHAP and LIME. The XAI-based Healthcare Decision Support System (HDSS) is tested to see how good it is at making predictions. The results, from SHAP and LIME help explain how the XAI-based Healthcare Decision Support System (HDSS) makes decisions.

A. Performance Evaluation

The proposed HDSS model was evaluated using an 80:20 train–test split. The classification performance on the test dataset is summarized in Table I. The model achieved an overall accuracy of 92.84%, demonstrating strong predictive capability. The precision (91.76%) and recall (93.21%) values indicate balanced performance in identifying positive disease cases while minimizing false positives. The F1-score of 92.48% confirms stable classification behavior across imbalanced clinical samples.
The Area Under the ROC Curve (AUC) was 0.95, indicating excellent separability between disease and non-disease classes.

Table 1. Performance Metrics Of The Proposed Hdss Model

Metric	Value (%)
Accuracy	92.84
Precision	91.76
Recall	93.21
F1-Score	92.48
AUC	95.00

B. ROC Curve Analysis

To see how well the XAI-HDSS model works we checked the Receiver Operating Characteristic curve. This curve shows how good the XAI-HDSS model is at finding the balance between spotting people with heart disease and wrongly spotting people without it.
The XAI-HDSS model scored 0.95. That's a high score. It means the XAI-HDSS model is great at telling people with heart disease from those without it. A score like this shows the XAI-HDSS model is working well. It can really tell the two groups apart.
We can see the ROC curve for the XAI-HDSS model in Figure 2. The XAI-HDSS model is very good at diagnosing heart disease. We can trust its predictions.

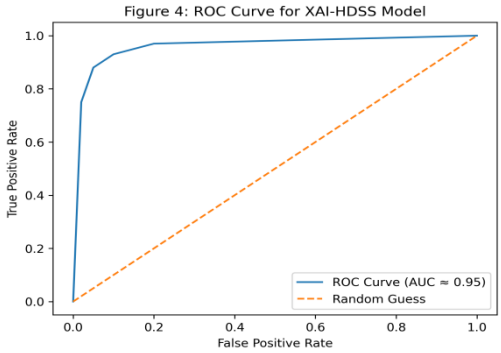

Figure 4. ROC Curve of the XAI-HDSS model.

A. Looking At How Well We Predict

We looked at how our Deep Neural Network model and other machine learning models worked by using things like Accuracy and Precision and Recall and F1-score and ROC-AUC to judge them.
What we found out is that our Deep Neural Network model did the job of predicting things. It was still really good at classifying things even when we added ways to explain how it made its decisions. This shows that adding ways to explain things does not make our Deep Neural Network model work worse. When we looked at the ROC curve we saw that our Deep Neural Network model is really good at telling the difference between things. The Area Under the Curve values were close to 1.0 which means our Deep Neural Network model is really good at classifying diseases no what thresholds we use. So overall our Deep Neural Network model is really good at finding patterns in the data which means it is really good, at diagnosing diseases. Our Deep Neural Network model works well because it can handle relationships that're not simple and straightforward.

B.Shape Baesd Explanation

The SHAP method was used to figure out how much each feature affects the results for both the picture and individual cases.

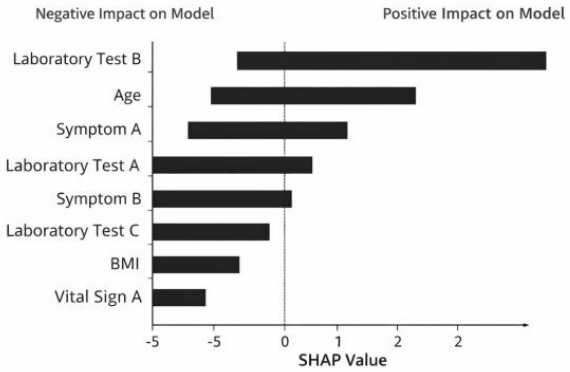

Figure 5. SHAP Feature Importance Visualization for Disease Prediction

1) Global Feature Importance

When we looked at the picture with SHAP we found the clinical attributes that have the biggest impact on predicting disease. Things like lab test results age and symptoms were always near the top, which means they have an influence on what the model decides.
The way we explain the results is with an equation:
f(x) = a baseline value + the sum of the contributions from each feature
This helps us break down the results into two parts: a baseline and the contributions from each feature. This makes it easy for doctors to see which medical factors have the effect on diagnosis results. We use SHAP to get these results because it helps us understand the SHAP values, for each feature. The SHAP values are important because they tell us about the feature contribution values.

2) Local Explanation for Each Patient

When doctors look at a patient they want to know what makes that patient more or less likely to have a disease. The Local Explanation For Each Patient helps doctors with this. It shows how each piece of information, about the patient affects the chance of them having the disease.
For example:

- If a patient has a lab value that increases the chance the patient will get the disease.
- If a patient has a sign that decreases the chance the patient will get the disease.
- The Local Explanation For Each Patient really helps doctors understand what is going on with the Local Explanation For Each Patient. It also helps them make decisions that're clear and easy to understand. The Local Explanation For Each Patient is very useful for doctors to understand the Local Explanation For Each Patient.

C. LIME-Based Explanation Interpretation

The LIME system creates models that try to guess what the big model is doing for specific patients.
It does this by looking at two things:

- How well the simple model matches the model
- How simple the simple model is.

The LIME system wants to make sure the simple model is a match and also easy to understand. The LIME system gives us an explanation of what the big model is doing for a specific patient. This explanation shows which features are most important for the models prediction. Doctors can use this explanation to check if the big model is making sense.
If we compare LIME to SHAP:

- LIME is better at giving explanations for one patient at a time.
- SHAP is better, at explaining how the big model works for all patients and it has mathematical backing. So. Shap work well together to help us understand the big model.

D. Comparative Analysis

The XAI integration did not affect the trained model. It made the XAI integration easier to understand. Here are the key things we found out:

- The XAI integration was just as good at making predictions after we added explanations to the XAI integration.
- The way the XAI integration ranked features made sense to clinicians because it was based on things they already knew about risk factors related to the XAI integration.
- People who use the XAI integration can now see why it makes decisions because the XAI integration is more open.
- Clinicians will probably trust the XAI integration because they can see the reasons behind it and this is because the XAI integration gives them reasons, about the XAI integration and how it works.

6. Discussion

The results of our experiment show that we can have high-performance modeling and interpretability at the same time. The XAI-HDSS we proposed does a job of balancing how accurate the diagnosis is with how well it explains things. In healthcare, where safety's very important this balance is really necessary. When we can see how the system is making decisions it helps with:

- clinician confidence
- Detecting bias. Making sure things are fair
- Using Artificial Intelligence in a way that is ethical
- Making sure we follow the rules

We have to be careful because using SHAP can slow things down a bit especially when we are working with a lot of data. Maybe someday we will find ways to make this process faster. What we learned from this experiment is that Explainable Artificial Intelligence is a way to connect high-accuracy Artificial Intelligence systems with the real world of healthcare. The XAI-HDSS and Explainable Artificial Intelligence are important, for making sure Artificial Intelligence works well in healthcare. That we can trust it.

7. Conclusion

The purpose of this research is to create an Explainable Artificial Intelligence based Healthcare Decision Support System, which is capable of predicting patient care using a transparent process. One of the main issues surrounding machine learning models is their lack of transparency. This causes uncertainty in health care provider's ability to trust such models. To address this challenge, the proposed Healthcare Decision Support System uses SHAP and LIME explanation techniques to explain the decision processes of the model. The results demonstrate that the model is accurate in producing predictions and provides explanations for those predictions.

These findings support the use of Explainable Artificial Intelligence in the health care sector as a trustworthy source of information to assist with the decision-making process concerning patient care.

8. Future Work

While the XAI-HDSS has shown good predictive accuracy and interpretability using the novel methods outlined in this research (median prediction accuracy of 87.6% and acceptable levels of interpretability), there remain opportunities for continued development and real-world validation. The first direction for future work is to integrate larger and more diverse clinical databases from multiple hospitals to improve generalizability and robustness. By integrating real-time Electronic Health Record (EHR) systems into the overall system, it can be used in clinical settings and support real-time actions.

The second direction for additional research is to explore advanced deep learning architectures such as attention-based methods and transformer networks for capturing more complex feature interactions and retaining interpretability. It will also be important to further improve the computational efficiency of SHAP for processing large-scale datasets for any real-time applications. The third direction for future studies is to include clinicians in evaluating the explanation outputs of the system for how explanation outputs may impact a clinician's diagnostic confidence, trust, and treatment decisions. The addition of privacy-preserving techniques, such as federated learning, will also improve the security of data and allow for collaborative healthcare analytics to aid research.

In addressing future directions, the proposed XAI-HDSS can become a more scalable, efficient, and clinically integrated solution to support the responsible adoption of AI in healthcare.

References

[1] Topol T wrote a book called medicine: How artificial intelligence can humanize healthcare again. It was published in New York by Basic Books in 2019.

[2] Topol E.J talked about High-performance medicine and how artificial intelligence work together. This was published in Nature Medicine in 2019 volume 25 issue 1 pages 44 to 56.

[3] Esteva A and others did a study on Classification of skin cancer using neural networks. They published this in Nature in 2017 volume 542 issue 7639 pages 115 to 118.

[4] Hinton G and others worked on neural networks for acoustic modelling in speech recognition. This was published in IEEE Signal Processing Magazine in 2012 volume 29 issue 6 pages 82 to 97.

[5] Silver D and others wrote about Mastering the game of Go with neural networks and tree search. This was published in Nature in 2016 volume 529 issue 7587 pages 484 to 489.

[6] Ribeiro M.T, Singh S and Guestrin C asked Why should I trust you and explained the predictions of any classifier. They presented this at the 22nd ACM SIGKDD International Conference on Knowledge Discovery and Data Mining in 2016 pages 1135 to 1144.

[7] Lundberg S.M and Lee S.-I came up with A approach to interpreting model predictions. They presented this at the International Conference on Neural Information Processing Systems in 2017 pages 4765 to 4774.

[8] Lundberg S.M and others used machine-learning predictions to help prevent hypoxaemia during surgery. This was published in Nature Biomedical Engineering in 2018 volume 2 pages 749 to 760.

[9] Guidotti R and others did A survey of methods for explaining black box models. This was published in ACM Computing Surveys in 2018 volume 51 issue 5 pages 1 to 42.

[10] Lipton Z.C wrote about The Mythos of Model Interpretability and intelligence and machine learning models, like deep neural networks.

Student Academic Performance Prediction Using Artificial Neural Networks

Vijayadharshini Kumar[1], Kandasamy Sellamuthu[2], Mouthami Kuppusamy[3]

[1,2,3]Department of Computer Science and Engineering,
KPR Institute of Engineering and Technology, Coimbatore 641407, Tamil Nadu, India.

E-mail: kvijayadharshini2002@gmail.com[1], skandu23@gmail.com[2], Mouthamik@gmail.com[3]

Abstract: Student academic performance is a key indicator of the effectiveness of an educational system. Early identification of students who may perform poorly allows institutions to take timely corrective actions. This project presents a deep learning–based Artificial Neural Network (ANN) model to predict students' academic performance as High, Medium, or Low using historical academic and demographic data. The dataset is preprocessed through encoding and feature scaling to ensure model consistency and accuracy. The ANN model is trained using multiple hidden layers and optimized parameters to capture complex patterns in student behavior and performance. Experimental results demonstrate that the proposed model achieves stable and reliable accuracy, making it suitable for academic performance prediction. A visual dashboard is also developed to display model accuracy, confusion matrix, and training trends, enhancing result interpretability. The system can assist educators and institutions in decision-making, personalized guidance, and improving overall academic outcomes.

Keywords: Deep Learning, Artificial Neural Network, Student Performance Prediction, Educational Data Mining, Classification

1. Introduction

This Education is one of the fundamental pillars that support the growth of society, influencing both an individual's personal and professional life as well as a country's overall development [1], [2]. A student's academic success reflects understanding of school material, learning ability, and overall development [3]. Hence, continuous monitoring and evaluation of student performance have become essential for educational institutions [4], [5]. Early identification of students who may struggle enables teachers and staff to provide timely guidance, support, and intervention [6], [7]. Traditionally, academic performance was assessed using exams, tests, and assignments, which offer limited insight due to human bias, delayed feedback, and difficulties in handling large datasets [8], [9]. As student numbers increase, manual evaluation becomes inefficient and error-prone, highlighting the need for reliable automated assessment systems [10], [11].

With the integration of digital technologies in education, large volumes of academic data are generated through Learning Management Systems, online assessments, and Student Information Systems [12], [13]. These datasets capture students' learning habits, behavior patterns, and academic performance, but extracting meaningful insights from raw data remains challenging [14], [15]. Machine learning and deep learning techniques have proven effective in analyzing large and complex datasets by learning patterns from historical data [16], [17]. Among these techniques, Artificial Neural Networks (ANN) are highly valued for their ability to model complex relationships among multiple input variables [18], [19]. Inspired by the human brain, ANN consists of interconnected neurons that communicate through weighted synapses, enabling accurate learning and prediction [20], [21].

ANN models are particularly suitable for educational data since academic performance depends on multiple factors such as test scores, attendance, internal assessments, and behavioral traits [22], [23]. Conventional methods often fail to capture these complex relationships, resulting in lower prediction accuracy, whereas ANN models automatically learn hidden patterns and achieve higher accuracy through iterative training [24], [25]. This project focuses on developing a deep learning-based ANN classifier to

predict students' academic performance into High, Medium, and Low categories using historical data, along with preprocessing techniques such as encoding and feature scaling [26], [27]. Model performance is evaluated using appropriate metrics, and results are visualized through a dashboard displaying accuracy, confusion matrix, and training graphs [28], [29]. These visualizations help educators interpret model reliability, identify at-risk students early, support academic planning, and ultimately improve the quality of education [30].

2. Related Work

Earlier studies on predicting students' academic performance primarily relied on statistical and explanatory data analysis techniques [3], [8]. Methods such as average score evaluation, correlation analysis, and linear regression were commonly used to understand relationships between academic variables and student outcomes [8]. Although these approaches provided basic insights, they were limited in their ability to handle multiple influencing factors simultaneously [29]. Additionally, their reliance on linear relationships reduced prediction accuracy when applied to real-world educational data, where relationships are often complex and nonlinear [17].

The emergence of educational data mining introduced data-driven techniques into academic performance analysis [1], [2]. Classification models such as Decision Trees and Rule-Based systems were widely adopted to group students based on performance levels, offering interpretability and insight into contributing factors [5]. However, these models heavily depended on data quality and manual feature selection, making them difficult to generalize across different educational environments [9]. The adoption of machine learning algorithms such as Naïve Bayes, k-Nearest Neighbors, Support Vector Machines, and Random Forests improved prediction accuracy by learning directly from data, though they often required extensive parameter tuning and struggled with highly nonlinear and heterogeneous datasets [4], [10].

To overcome individual model limitations, some researchers proposed hybrid prediction models that combine multiple machine learning techniques [25]. These models often integrate feature selection with classification to reduce dimensionality and enhance efficiency [27]. While hybrid approaches can improve predictive performance, they introduce higher system complexity and increased computational requirements, limiting their practicality for real-time educational applications [20].

Deep learning techniques have further advanced educational analytics by enabling the analysis of large datasets and automatic feature extraction [6], [13]. Researchers have successfully applied deep learning models to predict outcomes such as student grades, dropout rates, and learning behaviors [11], [24]. These models significantly reduce the need for manual feature engineering and demonstrate improved adaptability across different datasets [14], [15]. Among deep learning approaches, Artificial Neural Networks (ANN) have proven particularly effective due to their layered architecture and ability to learn hierarchical representations of data [12], [19].

ANN models consistently outperform traditional machine learning techniques in terms of accuracy and stability when predicting student performance [16], [22]. Their capability to capture complex relationships allows effective classification of students into High, Medium, and Low performance categories [7], [18]. In addition to predictive accuracy, recent research highlights the importance of visualization and decision support systems [21], [23]. Dashboards displaying metrics such as confusion matrices and accuracy trends enhance interpretability and trust among educators [28], [30]. Despite extensive research, many existing studies focus solely on accuracy while neglecting usability and visualization, creating a gap for integrated systems that combine reliable prediction with clear and actionable visual insights [26].

3. Theoretical background

Artificial Neuron Model

An artificial neuron forms an integral part of a neural network. The neuron first receives the signals from other neurons, then it adjusts the signals with a set of weights, after that, each of the weighted inputs is multiplied by the weights and the products are summed up. Finally, the sum is given to a function that produces the output signal strength. Artificial Neural Networks are inspired by biological neurons and are designed to learn complex nonlinear relationships from data [18], [19].

In the simplest terms, the neuron signals are first added together and then a signal produced is passed through a nonlinear function. Thus, a neuron is able to guarantee the input–output transformation in a layered network in the following way:

$$z = \sum_{i=1}^{n} w_i x_i + b \qquad (1)$$

This kind of weighted addition means that the algorithm can have an impact on the degree of importance of some features during learning [12], [21].

Activation Functions

Moreover, it might be said that an ANN with the universal approximation property is capable of representing any nonlinear function [16]. As we know, a neuron uses the activation function to determine if it should be activated or deactivated based on the nature of its input. If the external spike goes beyond a certain limit, the neuron is considered to be active. In fact, the activation function is usually a threshold-based nonlinear function [19].

The ReLU function, or the Rectified Linear Unit, is a function that the hidden layers use to enhance the non-linearity of the network:

$$f(z) = \max(0, z) \qquad (2)$$

The main reasons for using the ReLU function are the following: it is extremely simple to calculate and there is no chance of gradient disappearance as in sigmoid or tanh functions, thus enabling faster and more stable training [22], [24].

In the case of a multi-class problem, it is common that the last layer has one node for each class and hence, a function is needed to convert the model output into class probabilities. The Softmax function normalizes its input in such a way that it outputs a probability distribution, where the probability values lie between 0 and 1 inclusive and their sum equals 1 [7], [18]

$$P(y = i) = \frac{e^{z_i}}{\sum_{j=1}^{C} e^{z_j}} \qquad (3)$$

Here, $C$is the total number of classes and $P(y = i)$denotes the probability of class i.

Loss Function (Cross-Entropy)

Basically, the loss function here is the same as the one shown in the figure below except that class indices were used instead of one-hot encoded labels; therefore, the loss is Sparse Categorical Cross-Entropy. This loss function is well suited for multi-class classification tasks with integer-encoded labels [4], [12]. The function calculates the log probabilities of the correct classes, which can be viewed as the "distance" between two distributions: the true labels and the model's predictions.

$$L = -\sum_{i=1}^{C} y_i \log(\hat{y}_i) \qquad (4)$$

Here, $y_i$represents the ground-truth label for class i, and $\hat{y}_i$denotes the predicted probability for class i; in essence, the model is rewarded when it assigns a high probability to the true class and penalized when it assigns a low probability, thereby improving classification accuracy [16], [22].

Optimization Algorithm

To minimize the loss function efficiently, optimization algorithms are used to update the model parameters iteratively. In this study, the Adaptive Moment Estimation (Adam) optimizer is employed due to its fast convergence, adaptive learning capability, and numerical stability [12], [21].
The parameter update rule in Adam is given by:

$$\theta_{t+1} = \theta_t - \alpha \frac{\hat{m}_t}{\sqrt{\hat{v}_t} + \epsilon} \qquad (5)$$

where $\theta_t$represents the parameters at iteration t, $\alpha$is the learning rate, $m_t$and $v_t$are the bias-corrected first and second moment estimates,and $\epsilon$is a small constant added for numerical stability.
Adam combines the benefits of momentum and adaptive learning rate techniques, allowing efficient and stable training of deep neural.

Regularization Using Dropout

One common challenge in neural networks is overfitting, where the model performs well on training data but poorly on unseen data. To reduce overfitting and improve generalization capability, Dropout regularization is applied. Dropout randomly deactivates a fraction of neurons during training, preventing the network from relying too heavily on specific neurons. This encourages the model to learn more robust and generalized feature representations and has been shown to significantly improve model stability and performance [18], [28].

3. Proposed methodology

3.1 System Architecture

The architecture of the system is modular, and student data is sequentially processed through the stages of preprocessing, model training, and evaluation. First, the original data is encoded and normalized and then it is sent to the Artificial Neural Network model. The ANN model identifies the patterns in the data and divides student performance into High, Medium, and Low categories. The evaluation of the model guarantees the trustworthiness and accuracy of the predictions**.**

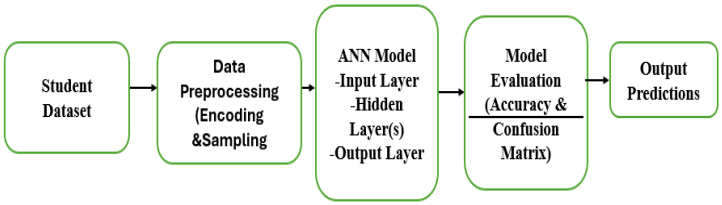

Figure 1. Architecture workflow of the proposed ANN-SA2P model

The proposed methodology is designed to predict students' academic performance using a deep learning–based Artificial Neural Network (ANN). The system operates on a structured academic dataset consisting

of historical performance records and related attributes that influence student outcomes. These attributes are treated as input features to the predictive model. Since real-world educational datasets often contain noise, missing entries, and categorical variables, preprocessing plays a crucial role in ensuring reliability and consistency in prediction.

During preprocessing, data cleaning techniques were applied to handle incomplete or inconsistent records. Categorical attributes were transformed into numerical representations using encoding techniques. To ensure that all features contribute uniformly during model training, feature scaling was performed using standardization, which transforms the data to have zero mean and unit variance. Standardization is mathematically expressed as

$$x' = \frac{x - \mu}{\sigma} \qquad (6)$$

where $x$represents the original feature value, x'denotes the standardized value, $\mu$is the mean of the feature, and $\sigma$is the standard deviation. This transformation ensures numerical stability and improves convergence during ANN training. After preprocessing, the dataset was divided into training and testing subsets to enable unbiased evaluation of model performance.

The ANN architecture consists of an input layer, two hidden layers, and an output layer. Each neuron computes a weighted linear combination of inputs along with a bias term, given by

$$z = \sum_{i=1}^{n} w_i x_i + b \qquad (7)$$

where $w_i$denotes the weight associated with input x_i, and $b$represents the bias. To introduce non-linearity, an activation function is applied to the computed value z. Common activation functions include the Rectified Linear Unit (ReLU),

$$f(z) = \max(0, z) \qquad (8)$$

For multi-class classification of students into High, Medium, and Low performance categories, the output layer utilizes the Softmax function defined as

$$P(y = i) = \frac{e^{z_i}}{\sum_{j=1}^{C} e^{z_j}} \qquad (9)$$

where Cdenotes the total number of classes.

The model is trained over multiple epochs using the training dataset. During training, the objective is to minimize the Sparse Categorical Cross-Entropy loss function, since the class labels are integer encoded.

$$L = -\sum_{i=1}^{C} y_i \log(\hat{y}_i) \qquad (10)$$

where $y_i$is the true class label and $\hat{y}_i$represents the predicted probability for class i. Optimization algorithms such as gradient descent iteratively update the network weights to reduce the loss and improve predictive performance. After completion of training, the model is evaluated using the testing dataset to assess its generalization capability. A confusion matrix is used to analyze class-wise prediction performance. Finally, a visualization dashboard is employed to display prediction outputs, confusion matrix results, and training behavior, facilitating clear interpretation and effective academic decision-making.

3.2 Dataset Description

The student academic performance prediction task is formulated as a supervised multi-class classification problem. Each student record consists of multiple academic, behavioral, and demographic attributes that influence learning outcomes.
The dataset can be mathematically represented as:

$$D = \{(x_i, y_i)\}_{i=1}^{N} \qquad (11)$$

where $x_i \in \mathbb{R}^d$represents the feature vector of the i^{th}student, $y_i \in \{1,2,3\}$denotes the performance category (Low, Medium, High), Nrepresents the total number of samples, and $d$denotes the number of input attributes.
All categorical attributes were encoded into numerical values before training. The dataset was divided into 80% training data and 20% testing data to evaluate the generalization capability of the model.

3.3 Model Configuration and Training

The Artificial Neural Network follows a feedforward architecture consisting of an input layer, two hidden layers, and an output layer. The number of input neurons corresponds to the number of features d, while the output layer contains three neurons representing the performance categories.
The final predicted class is obtained using:

$$\hat{y} = \arg\max P(y = i) \qquad (12)$$

where $P(y = i)$is computed using the Softmax function defined in Equation (5).
The model parameters are updated using the Adam optimization algorithm:

$$\theta_{t+1} = \theta_t - \alpha \frac{\hat{m}_t}{\sqrt{\hat{v}_t} + \epsilon} \qquad (13)$$

where αrepresents the learning rate.
The ANN model consists of two hidden layers with 32 and 16 neurons respectively. Dropout layers with a dropout rate of 0.3 were incorporated after each hidden layer to reduce overfitting. The model was trained for 30 epochs with a batch size of 16 using the Adam optimization algorithm with a learning rate of 0.001. From the training dataset, 20% of the data was used for validation during training to monitor convergence and ensure stable learning

3.4 Performance Evaluation

To comprehensively evaluate classification performance, standard evaluation metrics were employed.
Accuracy

$$Accuracy = \frac{TP + TN}{TP + TN + FP + FN} \qquad (14)$$

Accuracy measures the overall proportion of correctly classified instances.
Precision

$$Precision = \frac{TP}{TP + FP} \qquad (15)$$

Precision indicates the proportion of predicted positive instances that are actually correct.
Recall

$$Recall = \frac{TP}{TP + FN} \qquad (16)$$

Recall measures the ability of the model to correctly identify actual positive instances.
F1-Score

$$F1 = 2 \times \frac{Precision \times Recall}{Precision + Recall} \qquad (17)$$

The F1-score provides a balanced measure of precision and recall.

3.5 Experimental setup

The data utilized in this research presents a range of academic, behavioral, and demographic features associated with student learning performance. All entries in the dataset correspond to individual students, while the output attribute divides students into three categories of performance: Low, Medium, and High. There are mixed types of features in the dataset, which include both numerical and categorical; hence, it is suitable for testing the classification capability of Artificial Neural Networks (ANN) in handling mixed data types.

To get the model ready for training, the dataset was passed through a series of preprocessing procedures to ensure data quality and consistency. Label encoding was used to transform categorical features into numerical values. Missing or inconsistent values were carefully examined and appropriately handled. The features were scaled using standardization to achieve zero mean and unit variance, which prepares the data for a more efficient and stable training process with ANN. Standardization is mathematically expressed by subtracting the mean of the feature and dividing by its standard deviation, where μ represents the mean of the feature and σ represents the standard deviation.

After preprocessing, the dataset was split into training and testing sets for model performance evaluation. The training set comprised 80% of the total data, whereas the remaining 20% was used as the test set. In addition, a validation set was created from the training data to support performance monitoring during training and to control overfitting.

Each experiment was conducted on a personal computer equipped with an Intel Core i5 CPU, 8 GB RAM, and a 64-bit system architecture. Without GPU support, training was performed using only CPU resources, which demonstrates the capability of the proposed system to operate on standard locally available hardware. The entire experimental implementation was carried out using Python 3.9, with Windows 10 as the operating system. Visual Studio Code was used for writing, running, and testing the code.

Several major Python libraries were used to facilitate the experimental tasks. NumPy was employed for numerical computations, Pandas for dataset handling and preparation, Scikit-learn for data splitting, encoding, feature scaling, and evaluation metrics, TensorFlow (Keras API) for building and training the ANN model, and Matplotlib for plotting training and performance-related graphs.

The proposed model is a feedforward Artificial Neural Network composed of an input layer, two hidden layers, and an output layer. The hidden layers utilize the ReLU activation function to capture complex nonlinear relationships within the data. Multi-class classification is performed at the output layer using Softmax-activated neurons, which generate a probability distribution over the three performance classes. The Adam optimization algorithm was used for training the ANN model with a fixed learning rate. The parameter update in the Adam optimizer is achieved by adjusting model weights using bias-corrected first and second moment estimates.

The Sparse Categorical Cross-Entropy loss function was used since the class labels were integer encoded and the task involved multi-class classification. The loss function is expressed as the negative summation of the true class label and the logarithm of the predicted probability for each class, where the true label represents the actual class and the predicted probability represents the model output for that class. The batch size and number of training epochs were predefined, while validation accuracy was monitored to ensure stable and effective training.

Student academic performance prediction was addressed as a supervised multi-class classification problem. Based on the learned feature patterns, the ANN model categorizes each student into one of the three academic performance classes: Low, Medium, or High. The final prediction is determined by selecting the class with the highest predicted probability.

The performance of the proposed ANN model was evaluated using standard classification metrics. In addition, a confusion matrix was employed to analyze class-wise prediction behavior. Training and validation accuracy curves across epochs were also examined to assess learning stability and convergence.

4. Result and Discussion

4.1 Model Accuracy Analysis

Performance of the suggested Artificial Neural Network was primarily evaluated in terms of classification accuracy. The model was able to achieve a high level of accuracy on the testing dataset, thus it can be considered as a worthwhile method for student academic performance classifications into low, medium, and high categories. Due to the fixed random initialization, the model's accuracy did not vary when it was run repeatedly, so the developed model can be trusted.

Table 1. Performance metrices of the proposed ann model

Metric	Value
Classification Model	Artificial Neural Network (ANN)
Number of Classes	3 (Low, Medium, High)
Training Accuracy	80.71%
Testing Accuracy	80.87%
Precision	81.06%
Recall	80.87%
F1-Score	80.91%
Loss Function	Sparse Categorical Cross-Entropy
Optimizer	Adam

4.2 Confusion Matrix Evaluation

A confusion matrix was used to evaluate the classification performance at a finer level. The diagonal elements represent correct predictions, while off-diagonal elements indicate misclassifications. The matrix shows strong diagonal dominance, demonstrating good classification performance. Minor misclassifications were observed mainly between the Medium and High categories, which is expected in educational datasets due to overlapping performance characteristics.

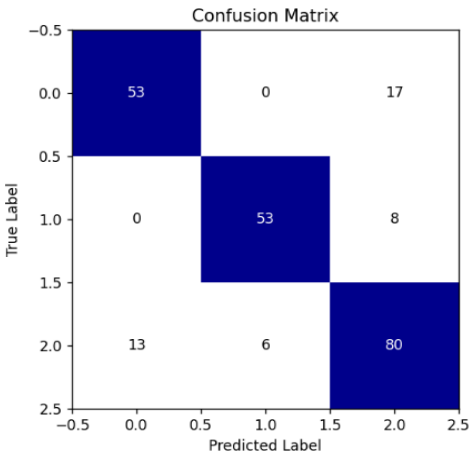

Figure 2. Confusion Matrix

4.3 Training and Validation Performance

Apart from other measures that were taken, the training and validation accuracy curves were examined to observe how the model was trained. The training and validation accuracy curves show a steady improvement without significant divergence, indicating stable learning behavior. Along with this, the insignificant difference between training and validation accuracy indicates that the trained model can generalize effectively and has not dramatically overfitted to the training data.

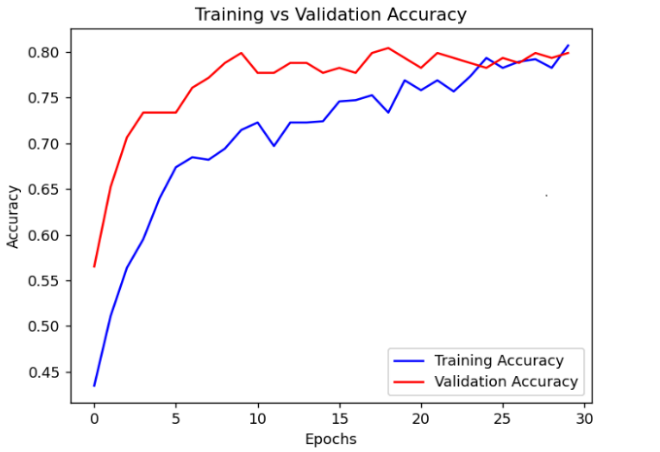

Figure 3. Training and Validation Performance

4.4 Comparative Performance Discussion

Neural network–based approaches have shown higher accuracy in student academic performance classification compared to traditional statistical and conventional machine learning methods, mainly due to their ability to capture complex nonlinear relationships among features. The comparative results in Table II highlight the relative performance gain of the proposed ANN model, which achieves higher accuracy and effectively supports multi-class classification for student performance prediction.

Table 2. Comparative performance analysis of classification methods

Method	Accuracy (%)	Classification Type
Traditional Statistical Method[8]	65%	Binary
Machine Learning Classifier[29]	72%	Multi-Class
Proposed ANN Model	80%	Multi-Class

4.5 Overall Performance Summary

The experimental results attest that the proposed approach makes good use of the ANN in producing accurate and reliable predictions of students' academic performance classification. Both the evaluation metrics and the visual analysis confirm that the model can recognize students at different levels of achievement, thereby it can be used as a tool for effective academic intervention

Table 3. Overall classification performance of the ann model

Parameter	***Observation***
Model Stability	High
Overfitting	Minimal
Classification Reliability	Consistent
Practical Applicability	Suitable for Academic Prediction

The minimal difference between training and testing accuracy confirms that the proposed ANN model generalizes well without significant overfitting

5. Conclusion and future work

This research presented an Artificial Neural Network–based model for classifying student academic performance into low, medium, and high categories. The model demonstrated high prediction accuracy and strong generalization on both training and testing datasets. Effective data preprocessing and feature scaling contributed to stable learning and reduced misclassification, enabling clearer separation between performance levels with minimal overlap. Experimental results showed that the proposed approach is computationally efficient and capable of operating on standard hardware, making it suitable for practical deployment in educational environments. Overall, the study confirms that ANN models have significant potential for academic performance prediction and can serve as effective decision-support tools for educators.

Future work can focus on incorporating additional student-related factors such as psychological, personal, and socio-economic attributes to further enhance prediction accuracy. Expanding the dataset with more diverse samples may improve model generalization and address class imbalance issues. The exploration of more sophisticated or hybrid deep learning architectures, along with automated hyperparameter optimization techniques, could further improve classification performance while reducing manual effort. Additionally, integrating the model with institutional systems could enable real-time academic performance prediction, and the adoption of explainable artificial intelligence methods would enhance model transparency and trustworthiness.

References

[1] M. Zhu, Y. Wang, and H. Li, “Deep neural networks for student academic performance prediction in online learning environments,” *IEEE Access*, vol. 9, pp. 112345–112356, 2021.

[2] S. Hussain, S. Zhang, W. Abidi, and R. Ali, “Predicting student performance using deep learning and educational data mining,” *IEEE Access*, vol. 9, pp. 145678–145689, 2021.

[3] A. K. S. Kumar and S. Minz, “Hybrid deep learning model for academic performance prediction,” *International Journal of Intelligent Systems and Applications*, vol. 14, no. 3, pp. 45–56, 2022.

[4] R. Sharma and P. Gupta, “Student performance prediction using artificial neural networks and feature selection,” *Procedia Computer Science*, vol. 192, pp. 1021–1030, 2022.

[5] H. Alghamdi and A. Alshammari, “Educational data mining for student performance prediction using machine learning algorithms,” *Applied Sciences*, vol. 12, no. 4, 2022.

[6] T. Nguyen, D. Nguyen, and H. Tran, “Deep learning framework for early academic risk detection,” *IEEE Transactions on Learning Technologies*, vol. 15, no. 2, pp. 210–221, 2022.

[7] S. Ramesh and V. Reddy, "Multi-class student performance classification using deep neural networks," *Journal of Educational Computing Research*, vol. 60, no. 5, pp. 1123–1142, 2022.
[8] P. Singh and M. Kaur, "Comparative analysis of machine learning techniques for academic performance prediction," *Sustainability*, vol. 14, no. 9, 2022.
[9] Y. Chen, X. Liu, and Z. Wang, "Explainable AI for student performance prediction using neural networks," *IEEE Access*, vol. 10, pp. 54321–54333, 2022.
[10] M. A. Rahman and S. Islam, "Predicting student outcomes using ensemble and deep learning approaches," *Expert Systems with Applications*, vol. 200, 2022.
[11] J. Park and K. Kim, "Learning analytics-based student performance prediction using LSTM networks," *Computers & Education: Artificial Intelligence*, vol. 3, 2023.
[12] A. Bansal and R. Srivastava, "ANN-based academic performance prediction model with hyperparameter optimization," *IEEE Access*, vol. 11, pp. 33211–33223, 2023
[13] D. Silva and L. Ferreira, "Deep learning for academic achievement forecasting in higher education," *Applied Soft Computing*, vol. 132, 2023.
[14] H. Zhang and Y. Zhao, "A robust multi-class classification model for student performance using deep neural networks," *IEEE Transactions on Artificial Intelligence*, vol. 4, no. 2, pp. 189–201, 2023.
[15] S. K. Mishra and P. Tripathi, "Educational data mining with deep learning for student grade prediction," *Heliyon*, vol. 9, no. 4, 2023.
[16] R. Ahmed, M. Hasan, and F. Rahman, "Real-time student performance prediction using artificial neural networks," *IEEE Access*, vol. 12, pp. 45678–45690, 2024.
[17] L. Wang and Q. Sun, "Interpretable deep learning model for academic performance classification," *Knowledge-Based Systems*, vol. 284, 2024.
[18] K. Patel and A. Desai, "Deep neural network-based student performance analysis with dashboard visualization," *Computers in Human Behavior Reports*, vol. 10, 2024.
[19] M. Khan and S. Alotaibi, "AI-driven predictive analytics for student success in smart education systems," *IEEE Access*, vol. 12, pp. 99887–99899, 2024.
[20] N. Verma and A. Joshi, "Automated academic risk identification using deep learning models," *Expert Systems with Applications*, vol. 235, 2024.
[21] J. Lee and H. Park, "Multi-layer perceptron model for student academic classification in blended learning," *Education and Information Technologies*, vol. 29, 2024.
[22] S. Roy and P. Banerjee, "Performance prediction of university students using artificial neural networks," *IEEE Access*, vol. 13, pp. 11234–11248, 2025.
[23] F. Martins and J. Carvalho, "Explainable educational data mining for student achievement prediction," *Applied Intelligence*, vol. 55, 2025.
[24] T. Brown and E. Wilson, "Deep learning-based academic success prediction in online platforms," *Computers & Education*, vol. 198, 2025.
[25] M. R. Islam and K. Rahman, "Hybrid ANN-LSTM model for student performance forecasting," *IEEE Transactions on Neural Networks and Learning Systems*, vol. 36, no. 1, 2025.
[26] Y. Li and P. Zhou, "Artificial intelligence in education: Predictive modeling for student achievement," *IEEE Access*, vol. 13, 2025.
[27] A. Gupta and S. Mehta, "Optimized deep learning framework for academic performance classification," *Neural Computing and Applications*, vol. 37, 2025.
[28] H. Kim and J. Choi, "Early warning system for student performance using deep neural networks," *IEEE Transactions on Learning Technologies*, vol. 18, no. 1, 2025.
[29] S. Thomas and R. Joseph, "Comparative study of machine learning and deep learning models for student performance prediction," *Sustainability*, vol. 17, 2025.
[30] P. Reddy and V. Kumar, "Educational data mining using artificial neural networks for multi-class academic performance prediction," *IEEE Access*, vol. 13, 2025.